DOT/FAA/PM-83/20
DOT-TSC-FAA-82-6

Program Engineering and
Maintenance Service
Washington DC 20591

AWOS Sensor Evaluation: Transmissometer, Forward-Scatter Meter and Lidar Ceilometer

David C. Burnham
Dennis F. Collins Jr.

Transportation Systems Center
Cambridge MA 02142

January 1984
Final Report

This document is available to the public through the National Technical Information Service, Springfield, Virginia 22161.

U.S. Department of Transportation
Federal Aviation Administration

NOTICE

This document is disseminated under the sponsorship of the Department of Transportation in the interest of information exchange. The United States Government assumes no liability for its contents or use thereof.

NOTICE

The United States Government does not endorse products or manufacturers. Trade or manufacturers' names appear herein solely because they are considered essential to the object of this report.

Technical Report Documentation Page

1. Report No. DOT/FAA/PM-83/20	2. Government Accession No.	3. Recipient's Catalog No.
4. Title and Subtitle AWOS SENSOR EVALUATION: TRANSMISSOMETER, FORWARD-SCATTER METER AND LIDAR CEILOMETER		5. Report Date January 1984
		6. Performing Organization Code DTS-52
7. Author(s) David C. Burnham, Dennis F. Collins, Jr.		8. Performing Organization Report No. DOT-TSC-FAA-82-6
9. Performing Organization Name and Address U.S. Department of Transportation Research and Special Programs Administration Transportation Systems Center Cambridge MA 02142		10. Work Unit No. (TRAIS) FA315/R3119
		11. Contract or Grant No.
12. Sponsoring Agency Name and Address U.S. Department of Transportation Federal Aviation Administration Program Engineering and Maintenance Service Washington DC 20591		13. Type of Report and Period Covered Final Report August 1980 - July 1982
		14. Sponsoring Agency Code APM-340
15. Supplementary Notes		

16. Abstract

Ceiling and visibility measurements are included in an Automatic Weather Observing System (AWOS) which is intended to satisfy the needs of aviation. The performance of one ceilometer and two visibility sensors was examined to determine whether they can meet the requirements of AWOS systems. The visibility sensors employed two different principles of operation: a transmissometer and a forward-scatter meter. The sensors were field tested at Arcata CA, Sterling VA, and Otis Air National Guard Base MA. During the last portion of the field testing the sensors were interfaced to a commercially available AWOS system to verify the sensor interfaces. The results of the evaluation indicate that the laser ceilometer and the transmissometer were generally satisfactory, but that the forward-scatter meter required additional development and testing because of electronic defects in the units tested. A major goal of the study was to develop and evaluate acceptance test procedures for AWOS ceilometers and visibility sensors. Accuracy and maintenance requirements, standard reference sensors, and test methods were examined.

17. Key Words Automatic Weather Observing System Ceilometer Visibility Transmissometer Forward-Scatter Meter	18. Distribution Statement DOCUMENT IS AVAILABLE TO THE PUBLIC THROUGH THE NATIONAL TECHNICAL INFORMATION SERVICE, SPRINGFIELD, VIRGINIA 22161		
19. Security Classif. (of this report) UNCLASSIFIED	20. Security Classif. (of this page) UNCLASSIFIED	21. No. of Pages 224	22. Price

Form DOT F 1700.7 (8-72) Reproduction of completed page authorized

METRIC CONVERSION FACTORS

Approximate Conversions to Metric Measures

Symbol	When You Know	Multiply by	To Find	Symbol
		LENGTH		
in	inches	2.5	centimeters	cm
ft	feet	30	centimeters	cm
yd	yards	0.9	meters	m
mi	miles	1.6	kilometers	km
		AREA		
in^2	square inches	6.5	square centimeters	cm^2
ft^2	square feet	0.09	square meters	m^2
yd^2	square yards	0.8	square meters	m^2
mi^2	square miles	2.6	square kilometers	km^2
	acres	0.4	hectares	ha
		MASS (weight)		
oz	ounces	28	grams	g
lb	pounds	0.45	kilograms	kg
	short tons (2000 lb)	0.9	tonnes	t
		VOLUME		
tsp	teaspoons	5	milliliters	ml
Tbsp	tablespoons	15	milliliters	ml
fl oz	fluid ounces	30	milliliters	ml
c	cups	0.24	liters	l
pt	pints	0.47	liters	l
qt	quarts	0.95	liters	l
gal	gallons	3.8	liters	l
ft^3	cubic feet	0.03	cubic meters	m^3
yd^3	cubic yards	0.76	cubic meters	m^3
		TEMPERATURE (exact)		
°F	Fahrenheit temperature	5/9 (after subtracting 32)	Celsius temperature	°C

Approximate Conversions from Metric Measures

Symbol	When You Know	Multiply by	To Find	Symbol
		LENGTH		
mm	millimeters	0.04	inches	in
cm	centimeters	0.4	inches	in
m	meters	3.3	feet	ft
m	meters	1.1	yards	yd
km	kilometers	0.6	miles	mi
		AREA		
cm^2	square centimeters	0.16	square inches	in^2
m^2	square meters	1.2	square yards	yd^2
km^2	square kilometers	0.4	square miles	mi^2
ha	hectares (10,000 m^2)	2.5	acres	
		MASS (weight)		
g	grams	0.035	ounces	oz
kg	kilograms	2.2	pounds	lb
t	tonnes (1000 kg)	1.1	short tons	
		VOLUME		
ml	milliliters	0.03	fluid ounces	fl oz
l	liters	2.1	pints	pt
l	liters	1.06	quarts	qt
l	liters	0.26	gallons	gal
m^3	cubic meters	35	cubic feet	ft^3
m^3	cubic meters	1.3	cubic yards	yd^3
		TEMPERATURE (exact)		
°C	Celsius temperature	9/5 (then add 32)	Fahrenheit temperature	°F

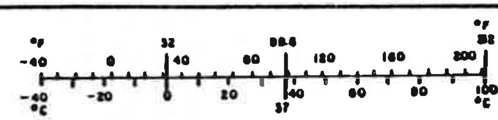

PREFACE

Automatic Weather Observing Systems (AWOS) can be used to replace present observations, with a resulting cost reduction, and to provide weather data for locations having no observations at the present time. The work presented in this report will assist in the development of specifications for the purchase of AWOS systems by the government and in the certification of commercially available AWOS systems.

The study reported here represents the efforts of many organizations:

The work was sponsored by the Federal Aviation Administration (FAA) Systems Research and Development Service (SRDS). Dave Floyd managed the Arcata tests with assistance from Jack Dorman. Ray Colao was the program manager for the Otis tests. Valuable oversight of the project was supplied by Al Thomas, Ray Johnson and Frank Coons. The pass/fail criteria for the tests were adopted from the Automatic Weather Observation Systems (AWOS) achievable sensor accuracy specifications prepared by the FAA Airways Facilities Service. In FY83 these two organizations were merged to form the Program Engineering and Maintenance Service and the responsibility for reviewing this report passed to Leo Gumina, manager of the Weather Sensors Program.

The National Weather Service (NWS) Test and Evaluation Division provided the ceilometer evaluation for the tests. Jim Bradley, Steve Imbembo, and Richard Lewis carried out the work.

The Air Force Geophysics Laboratory (AFGL) made their Weather Test Facility (WTF) at Otis Air National Guard Base (ANGB) available for the visibility sensor and AWOS processor field tests. The cooperation and advice of AFGL personnel, Gene Moroz, Leo Jacobs, and Ralph Hoar, were valuable. Clyde Lawrence provided the intensive maintenance for the standard visiblity sensor and assisted in data collection and equipment repair.

A number of Transportation Systems Center (TSC) personnel made major contributions to the project. Ed Spitzer provided oversight and advice and helped design and implement the data acquisition equipment. Andy Caporale carried out the installation of the sensors and data collection facilities. Bruce Ressler designed the signal conversion and interface electronics for the tests. The electronics were built by Bill Murphy and Irving Golini. Paul Alciere developed the new data display options for the evaluation. Marie Carleton put the report on a word processor. The TSC in-house data service contractor, SDC, along with subcontractors, programmed the AWOS data recording system (Steve Kovner and John Winkler) and assisted in the analysis of the AWOS ceilometer (Richard Daesen) and AWOS visibility (Bob Crosby) data.

The equipment manufacturers played an important role in supplying, installing and repairing the equipment under test. Tasker loaned the RVV-700 system and a stripchart recorder for the tests. Impulsphysics allowed the LD-WHL ceilometer to be used beyond the end of its rental period. In lieu of upgrading the FAA's Weathercheck® AWOS system for the tests, Artais supplied the same system tested at Arcata.

The Arcata, CA test site was managed by Humbolt County. Jim Wilkerson was the test site operator.

TABLE OF CONTENTS

TABLE OF CONTENTS (CONT.)

TABLE OF CONTENTS (CONT.)

LIST OF ILLUSTRATIONS

LIST OF TABLES

LIST OF TABLES (CONT.)

1. SUMMARY

Automatic Weather Observing Systems (AWOS) require visibility and ceiling information to meet the needs of aviation. This report describes a methodology which was developed to evaluate visibility sensors and ceilometers for use with AWOS systems. The methodology was applied to two visibility sensors, one transmissometer: the Tasker RVV-700 and one forward-scatter meter (FSM): the Wright & Wright FOG-15; and to one ceilometer, the Impulsphysics LD-WHL. In addition to evaluating sensor performance, the interface of the sensors to a commercially available AWOS, the Artais Weathercheck ® was examined. Pass/fail criteria for the tests were based on the "Achievable AWOS Sensor Accuracies" recently developed by the FAA Airways Facilities Service.

The selection of sensors to be tested was based on prior field testing in 1981 at Arcata, CA. Those tests also identified needed sensor modifications which have been implemented. Two test sites were employed for the current field tests which began in early 1982. The ceilometer was tested at the National Weather Service (NWS) Test and Evaluation Division site in Sterling, VA. The visibility sensor and AWOS interface tests were conducted at the Air Force Geophysic Laboratory (AFGL) Weather Test Facility (WTF) at Otis Air National Guard Base (ANGB).

The field tests used the current operational sensors for visibility (Tasker RVR-500 transmissometer on a 1000-foot baseline) and ceiling (Rotating Beam Ceilometer, RBC) as standards of comparison. Both sensor accuracy and operational problems were examined in the evaluation.

2. CONCLUSIONS AND RECOMMENDATIONS

2.1 TASKER RVV-700 TRANSMISSOMETER

Table 2-1 summarizes the progress toward successful testing and deployment of the RVV-700 transmissometer, manufactured by the Tasker Systems Division of the Whittaker Corporation. It should be noted that the Otis evaluation period lasted only two months, one of which was plagued with problems. Detailed conclusions are contained in the following Sections.

2.1.1 Performance

The RVV-700 meets the AWOS pass/fail criteria for these tests when data points from rapidly varying events are excluded. The 100-foot separation between the RVV-700 and the standard RVR-500 baselines was large enough to allow significant differences in visibility when the fog was patchy.

The following changes are needed to assure satisfactory sensor performance:

1) An effective baseline 9 percent smaller than actual should be used in the visibility calculations.
2) The background errors should be reduced.
3) A more intensive maintenance schedule should be adopted (see next section).
4) Tower vibration should be damped.

The RVV-700 1000-foot baseline measurements correlated well with those of the parallel 1000-foot RVR-500 baseline, but indicated a visibility biased approximately 9 percent higher than the RVR-500. A similar difference was also observed during the Arcata tests. The physical or instrumental effect producing this difference could not be

TABLE 2-1. RVV-700 PROGRESS

ARCATA PROBLEMS

RVV-700 READ HIGHER VISIBILITY THAN RVR 500 WHICH WAS LOCATED AT MUCH GREATER HEIGHT

ARCATA RECOMMENDATIONS	IMPLEMENTED AT OTIS?	SUCCESSFUL AT OTIS?
INSTALL AT SAME HEIGHT AS REFERENCE	PARTIALLY	NO
USE BACKGROUND CHECKS	YES	YES
RAISE ELEVATION TO 8 FEET	YES	PARTIALLY
USE 1000-FOOT BASELINE	YES	YES
REDUCE BACKGROUND LEVEL	NO	NO
LONGER PROJECTOR HOOD	YES	YES
LET WINDOWS REACH EQUILIBRIUM CONTAMINATION LEVEL	YES	YES

ADDITIONAL OTIS PROBLEMS

FOUNDATIONS UNSTABLE FOR MONTH AFTER INSTALLATION

WATER LEAK AFFECTED ELECTRONICS

identified. Although this difference can be readily corrected for operational use, it would be desirable to identify its source in order to assure that it remains fixed under all conditions. If possible, the RVV-700 should be compared with the FAA laser calibrator at its next installation site.

Because the background light level of the RVV-700 was high (4 percent), measuring the background only once per hour can introduce significant errors when the background level is rapidly changing. Reducing the period between background checks to 15 minutes and increasing the lamp current would eliminate this error. The optimum trade-off between accuracy and lamp life has yet to be determined.

The RVV-700 towers were observed to vibrate during windy conditions. Although no measurement errors were attributed to the vibrations, the performance of the sensor would be more certain if the amplitude of the vibrations could be reduced.

2.1.2 Maintenance

The RVV-700 experienced two instrumental failures during the tests:

1) The first pulse amplifier card showed a large diurnal variation and had to be replaced.
2) The background level of the receiver became erratic because of moisture which had leaked into the pulse amplifier housing through a faulty seal.

These failures represent quality control problems which should be corrected at the factory. The lightning protection circuits of the instrument were successful in maintaining system operation when most of the other equipment at the test site had been disabled by lightning surges.

The receiver alignment was unstable during the first month of operation. The problem appeared to be due to shifts in the receiver foundation rather than any problem with the 8-foot mounting posts. Heavy rains caused the foundation to settle. The alignment required only small adjustments during the second month.

A 30-day calibration schedule is marginal for maintaining acceptable accuracy, at least during the initial operation of the instrument. The windows were cleaned at the beginning of the test period and then allowed to develop an "equilibrium" level of contamination. The loss in the 100-percent calibration was 6 percent in the first month but virtually nothing in the second. However, the most severe window contamination conditions at the site did not occur during the test period.

The calibration and maintenance schedule for the RVV-700 should be at least weekly for the first three months at a new site. A longer maintenance interval could then be introduced at a particular site if no significant changes are noted from week-to-week. More frequent maintenance should be resumed for any season of the year where increased window contamination or foundation instability (e.g., frost heaves) could be expected.

2.1.3 Interface to Artais AWOS

The transfer of data from the RVV-700 computer to the Artais processor was verified. Although the RVV-700 computer is not strictly compatible with the National Weather Service (NWS) visibility reporting algorithm, an examination of actual data showed that this incompatability does not result in any significant reporting errors. Thus, one can conclude that the RVV-700 interface to the Artais AWOS is satisfactory.

Some software anomalies were noted in the RVV-700 visibilty reports. However, the NWS has validated the current Artais software in July 1982 factory tests. AWOS systems should provide an indication of which software version is installed.

2.2 WRIGHT & WRIGHT FOG-15 FORWARD-SCATTER METER

Table 2-2 summarizes the progress toward achieving satisfactory performance from the FOG-15 forward-scatter meter which is manufactured by Wright & Wright. The modifications which were tested at Otis solved some problems but introduced others.

2.2.1 Performance

The FOG-15 sensor underwent substantial modifications during the beginning of the test period. The final version showed some improvement over the EG&G 207 forward-scatter meter on which it was based. However, the extinction coefficient response was not as linear as the EG&G 207 or the earlier versions of the FOG-15. The noise level and zero instability were significantly less, however.

A non-linear response correction was found to be needed for the spring 1982 version of the FOG-15. The intrinsic measurement accuracy of the FOG-15 is then sufficient to meet the test pass/fail criteria for single events, but not for a week of measurements. Under conditions of rapidly varying visibility the FOG-15's point measurement does not agree well enough with the line average of the standard transmissometer to pass the accuracy test. The analysis of data from two EG&G 207 FSM's showed that averaging two separated FSM's did not give much better agreement with the reference transmissometer when the visibility was changing very rapidly. The FOG-15 calibration remained stable over many months. However, a change of calibration was noted during one daytime event.

TABLE 2-2. FOG-15 PROGRESS

ARCATA PROBLEMS

VARIABLE RESPONSE CAUSED BY LINE VOLTAGE DEPENDENCE--ELIMINATED AT OTIS

UNSTABLE ZERO LEVEL--IMPROVED BUT STILL EXISTING AT OTIS

OTIS PROBLEMS

1) NONLINEAR RESPONSE
2) TEMPERATURE AND LIGHT DEPENDANCE OF RESPONSE
3) BOTH CAUSED BY "SOFT" CLIPPING CIRCUIT

At the very end of the test period it was discovered that the response of the FOG-15 decreased at high temperatures. The problem was traced to leakage in the diodes used in the current version for "soft" clipping of the input signals to prevent false signals on sunny days. Since this part of the FOG-15 circuitry is also responsible for the observed nonlinear response and the change in response due to sunlight, additional testing must be done after the problem is corrected to validate the performance of the FOG-15.

2.2.2 Maintenance

One failure was experienced during the test period. Two units were operated, one for three months and one for two. The zero setting potentiometer of one unit developed a poor wiper contact. It is recommended that the manufacturer install a higher reliability component in future units.

The FOG-15 suffered from the lack of an absolute calibration method throughout most of the test period. Each unit had its own calibration level which could be used to detect changes in calibration, but not to set the proper relationship between the sensor response and the atmospheric extinction coefficient. The manufacturer established an absolute calibration standard during July 1982, which will be used for future installations.

The FOG-15 suffered one outage due to lightning surges. The standard voltage output has lightning protection and was not damaged. The modulated output used for the Artais AWOS interface was not protected and was damaged during one storm. Lightning protection should be added to that output also.

2.2.3 Interface to Artais AWOS

The FOG-15 interface showed indications of unstable gain and a saturation at high signal levels. A thorough factory evaluation should be carried out.

2.3 IMPULSPHYSICS LD-WHL LASER CEILOMETER

Table 2-3 summarizes the progress of the LD-WHL lidar ceilometer, manufactured by Impulsphysics, toward meeting the aviation needs for cloud height measurements.

2.3.1 Performance

The LD-WHL ceilometer performed satisfactorily up to its maximum range of 5000 feet. The LD-WHL was as sensitive to clouds as the rotating beam ceilometer. Its accuracy and resolution were satisfactory. Its performance was found to be satisfactory for AWOS use. Three faults were observed. They were not, however, considered to be severe enough to make the sensor unusable. As the ceilometer state of the art advances, these problems are expected to be resolved.

One fault observed in the sensor was excessive cloud detection sensitivity at low altitudes (200-400 feet). This sensitivity results in reports of nonexistent low cloud layers during fog and precipitation, which could lead pilots to avoid an airport at which they could safely land. Discussions with the manufacturer suggest that the sensitivity could be reduced if the amount of reduction could be specified. A possible method for defining the needed reduction is outlined in Section 2.4.2. This reduction would eliminate the false layer reports. When this modification is defined and implemented all LD-WHL units previously installed should be upgraded.

The LD-WHL performance fails on sunny days when the sun angle is high. It is recommended that the sensor windows be shaded from direct sun exposure at high sun angles. This problem becomes severe at low latitude sites.

The LD-WHL is equipped with self-check features which monitor all functions except window clarity. The only window problem observed

TABLE 2-3. LD-WHL PROGRESS

ARCATA PROBLEMS		CORRECTED?
1)	EFFECTIVE RANGE OF ONLY 2000 FEET INSTEAD OF THE NOMINAL 5000 FEET--CAUSED BY WEDGED WINDOWS	YES
2)	DIRECT MODE DISABLED	YES
3)	60 SECONDS BETWEEN MEASUREMENTS INSTEAD OF NOMINAL 15 SECONDS	YES
4)	FALSE LOW-LEVEL LAYERS	NO
STERLING PROBLEMS		
5)	WATER DROPLETS ON WINDOW	

during the test occurred in a light drizzle when water beads formed on the windows and destroyed the sensitivity to clouds. Although this problem is likely to be rare, it would be desirable to devise a solution for it.

2.3.2 Maintenance

Although the LD-WHL was equipped with lightning protection circuitry, its output drive was destroyed twice by lightning surges. The problem may have been due to inadequate grounding of the unit.

2.3.3 Interface to Artais AWOS

The Artais interface performed properly. The AWOS processor tested in the field did not incorporate a necessary software correction identified at the beginning of the project. However, factory tests under NWS supervision verified proper functioning of the NWS cloud layer algorithm in the current Artais software.

2.4 SYSTEM SPECIFICATIONS

2.4.1 Visibility Sensor Acceptance Criteria

The FAA and NWS have not defined a set of visibility sensor acceptance criteria which can be met by commercially available sensors. Appendix A describes two approaches for defining visibility accuracy specifications. Sufficient information on sensor performance is now available from the Arcata, Otis, and Sterling sites to begin defining and negotiating acceptance criteria which are both feasible and operationally acceptable. The acceptance criteria definition should include a cost-benefit analysis in order to take advantage of current sensor technology.

Because no standardized acceptance criteria have been established for visibility sensors, pass/fail criteria had to be adopted specifically for these tests. The pass/fail criteria adopted proved to be inconvenient to apply to massive amounts of data because the criteria are very sensitive to unusual events and to occasional errors in the recording and processing of the data. Criteria which depend upon the bulk of the measurements rather than outlying data points would be more practical. Future criteria definitions should consider this sensitivity.

2.4.2 Improved Ceilometer Acceptance Testing

The current methodology used by the FAA and NWS for acceptance testing of ceilometers is difficult and time consuming. An improved testing methodology is required for timely procurement of ceilometers. The use of attenuated beam measurements on real clouds appears to provide a practical pass/fail test of cloud detection sensitivity for laser ceilometers. This method was successfully tested at Sterling by the FAA and the NWS. The results of the test indicate that some additional testing is needed to establish this method.

A realistic selection of the range response of a laser ceilometer may be possible using the scattered signal from a large solid target. A manufacturer could measure the signal response as a function of range and adjust the cloud hit threshold to give equal cloud hit sensitivity at all ranges under clear weather. The maximum-range cloud response would then be set to pass the attenuated-beam test. This approach should be tested.

2.4.3 Reporting Algorithm Issues

The AWOS visibility reporting algorithm has not reached the point of general agreement. The first issue is the visibility values to be reported. For example, the AWOS "achieveable accuracy" standard in Appendix A includes a value (3-1/2 miles) never used previously. A second issue is the averaging time, currently set at 10 minutes. The aviation requirments for averaging time (as well as comments such as "variable," "increasing," and "decreasing") have not been defined.

The NWS is presently rethinking the details of the cloud layer algorithm which were included to deal with the problems of rotating-beam ceilometers. Algorithm modifications appropriate to laser ceilometers will be developed.

Because of possible future changes in the current algorithms, AWOS systems should be configured to allow algorithm updating.

2.5 SYSTEM INSTALLATION

The Otis AWOS installation had several operational problems. Although many of the problems were due to the "one of a kind" nature of the installation, some of the difficulties could just as easily arise in an operational system. Many of the problems can be traced to two sources:

1) A tight implementation schedule, and
2) Lack of understandings among participants.

The test schedule forced all those involved in the installation to minimize desirable preinstallation checkouts. The installation plan for an operational AWOS should include the scheduling of adequate checkout periods both before and after the actual installation. The Otis installation suffered from a number of misunderstandings among the sensor manufacturers, the processor manufacturer, and the site operators. It would be highly desirable to install an AWOS as a turn-key system with the processor manufacturer directly responsible for all the details of the installation, including sensor installation and associated interfaces. The responsible agent should specify, coordinate, and check all phases of the installation.

2.5.1 Transmissometer Foundations

The settling of the RVV-700 foundations could have been prevented or mitigated by more careful backfilling or by a different foundation design. Nevertheless, the alignment sensitivity of a long-baseline transmissometer, such as the RVV-700, will necessitate careful monitoring at any site where the ground is at all unstable.

2.5.2 Lightning Protection

Inadequate lightning protection in the Otis installation was perhaps the best example of the coordination problems mentioned above. An abnormally stormy month of June resulted in numerous sensor and interface failures and pointed out the importance of properly protecting against lightning surges.

3. BACKGROUND

Automatic Weather Observing Systems (AWOS) require visibility and ceiling sensors in order to meet the needs of the aviation community. The current standard airport sensors (transmissometers and rotating beam ceilometers) are too expensive in both initial cost and required maintenance to be used in low cost AWOS systems designed to meet the weather needs of small airports. Less expensive sensors, some based on different operating principles, have recently become available to make these measurements. The AWOS sensor project reported here was designed to aid certification of these new sensors by

1) developing recommended testing criteria for AWOS visibility and ceiling sensors, and
2) using the methods developed to establish the performance of commercially available visibility and ceiling sensors.

In order to provide timely information to those specifying AWOS Systems, this project was designed to be finished in August 1982.

Figure 3-1 shows a generalized block diagram of an AWOS system. Each sensor measures a desired property of the atmosphere. It sends its measurement via an interface to the AWOS processor. The AWOS processor generates a weather report by means of processing algorithms which analyze the raw sensor measurements and convert them into the appropriate report. The weather reports are then disseminated by means of voice and/or data links.

3.1 ARCATA TESTS

The FAA visibility test site in Arcata CA has been used for many studies of visibility sensors in the last four decades. Its climate is characterized by coastal fog in the summer and fall, and rain in the winter.

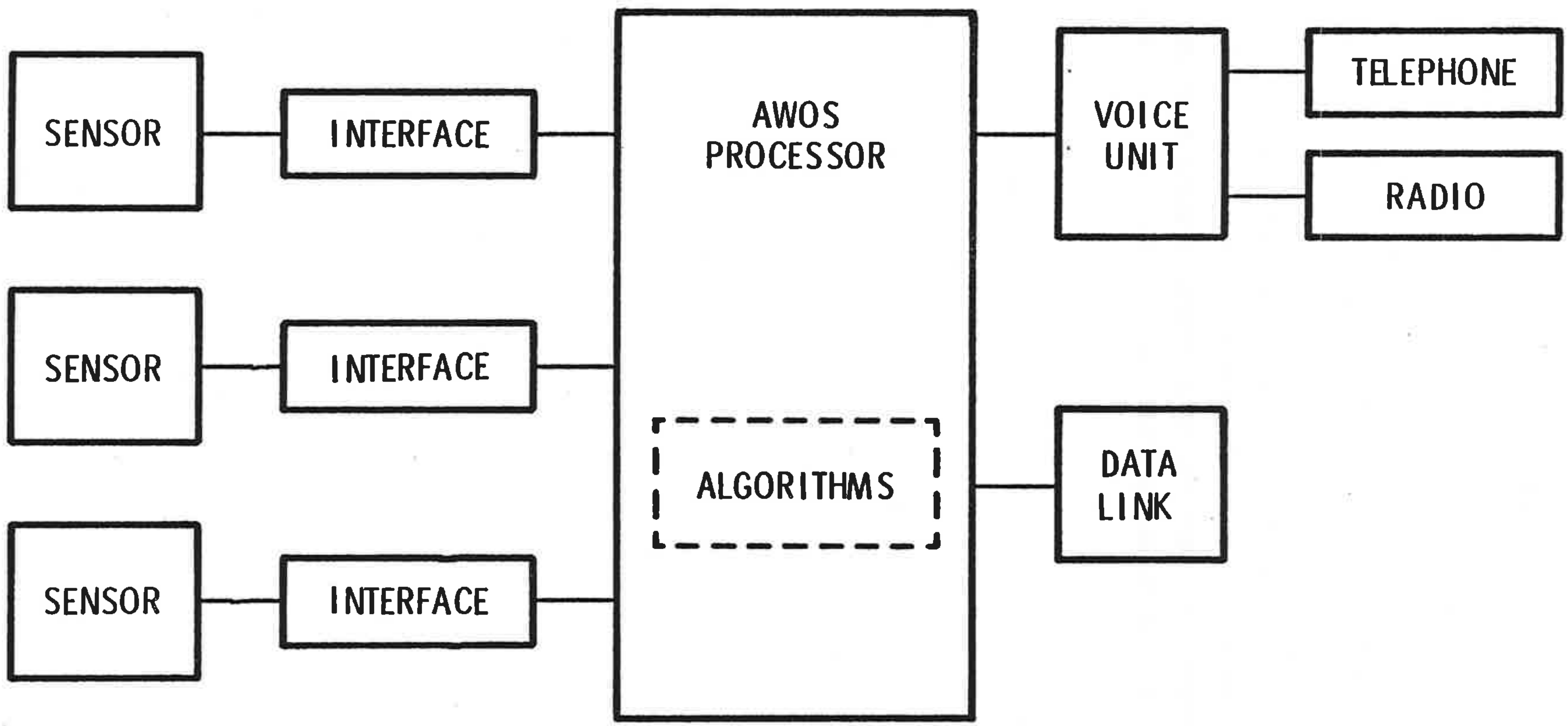

FIGURE 3-1. AWOS BLOCK DIAGRAM.

The Arcata site was reactivated for the period between August 1980 and December 1981 for testing visibility sensors and ceilometers, and for demonstrating their operation with a commercially available Automatic Weather Observing System (AWOS). The FAA supervised the site activities while the DOT Transportation Systems Center (TSC) was responsible for data recording and analysis. Most of the analysis methods used in this report were developed in support of the Arcata Tests.

Table 3-1 lists the weather sensors and their periods of operation at the Arcata site. A variety of sensors became available during the course of the tests. Some of them were modified in response to observed problems. Simultaneous testing was carried out on several of the forward-scatter meters (FSM) at the Air Force Geophysics Laboratory (AFGL) Weather Test Facility (WTF) at the Otis Air National Guard Base (ANGB). The outputs from the various sensors were recorded on magnetic tape and stripcharts. The sensor evaluation made use of comparisons between sensors; recorded human observations were used to identify the weather conditions.

A number of configurations of the Artais Weathercheck® AWOS system were operated at Arcata during the spring of 1981. The purpose of the test was to validate the Artais system for reporting visibility and ceiling from a number of sensors, in particular the Tasker RVV-700 transmissometer and the Impulsphysics LD-WHL ceilometer. It was intended to record the sensor input data along with the AWOS output in order to verify proper operation of the AWOS processor. Because of signal incompatibility, simultaneous recording was unsuccessful.

On the basis of their performance at Arcata the most cost-effective sensors of three types were selected as candidates for certification for use with the Artais AWOS processor:

1. Transmissometer: Tasker RVV-700
2. Forward-Scatter Meter: Wright & Wright FOG-15
3. Ceilometer: Impulsphysics LD-WHL

Each of the sensors showed some problems which needed resolution before certification could be recommended. The problems encountered with the RVV-700 were relatively minor while those of the FOG-15 and LD-WHL were serious. These three sensors and their Arcata performance will be discussed in turn.

TABLE 3-1. ARCATA SENSOR TEST PERIODS

	VISIBILITY SENSORS	BASELINE* (feet)	DATES
(1)	RVR-500	720	Aug. 1980 - Dec. 1981
(2)	NBS Transmissometer	250	Aug. 1980 - Feb. 1981
(3)	FS-3 (version 1)	FSM	Aug. 1980 - Nov. 1980
(4)	EG&G 207	FSM	Aug. 1980 - Sep. 1981
(5)	Touch Down RVR	250	Sep. 1980 - June 1981
(6)	Roll Out RVR	250	Sep. 1980 - June 1981
(7)	RVV-700	720	Mar. 1981 - July 1981
(8)	FS-3 (version 2)	FSM	Mar. 1981 - Apr. 1981
(9)	Skopograph (dual-baseline)	1200	Mar. 1981 - June 1981
(10)	Skopograph (dual-baseline)	164	Mar. 1981 - Aug. 1981
(11)	FS-3 (version 3)	FSM	May 1981 - June 1981
(12)	Wright & Wright FOG-15	FSM	June 1981 - Dec. 1981
(13)	RVR-500 (dual-baseline)	250	June 1981 - Dec. 1981
(14)	RVR-500 (dual-baseline)	40	July 1981 - Dec. 1981
(15)	FS-3 (version 4)	FSM	July 1981 - Aug. 1981
(16)	Skopograph	720	July 1981 - Aug. 1981
(17)	Skopograph (modified)	164,720	Aug. 1981 - Dec. 1981
(18)	FS-3 (version 5)	FSM	Sep. 1981 - Dec. 1981
	CEILOMETERS		
(19)	Impulsphysics LD-WHL		Jan. 1981 - Apr. 1981
(20)	Rotating Beam		Mar. 1981 - Dec. 1981
(21)	Weathertronics		June 1981 - Dec. 1981

*For transmissometers.

3.1.1 Tasker RVV-700 Transmissometer

A transmissometer operates by projecting a narrow beam of light horizontally through the atmosphere. The light intensity is detected by a receiver located a distance b (the baseline) away. When the visibility is reduced, the amount of light reaching the receiver decreases. The receiver field of view is very narrow 1) in order to avoid detecting any light which has been scattered out of the projector beam, and 2) to minimize the detection of background sunlight. A transmissometer with a given baseline can only measure over a certain range of visibilities. If the visibility is too high, the loss of light from the beam is too small to be measured. Conversely, if the visibility is too low, no light will reach the receiver. Because AWOS systems need to measure higher visibilities (5 miles) than currently measured at airports (1 mile maximum), they must use much longer baselines than the 250 feet now used at airports for measuring Runway Visual Range (RVR).

The Tasker RVV-700 transmissometer (see Figure 3-2) is a value-engineered version of the Tasker RVR-500 transmissometer which is currently employed by the FAA to measure RVR. An RVV-700 transmissometer was installed at the FAA sponsored test site in Arcata, CA between March and June of 1981. A 720-foot baseline was employed and the projector and receiver were installed on 5-foot posts. As a reference standard, an RVR-500 transmissometer was installed on a parallel 720-foot baseline at a height of 16 feet.

Automatic background light measurements were performed on the RVV-700 during its first month's operation. They were then discontinued because of incompatibility with the preliminary AWOS interface being used. Later in the tests the proper digital interface described in Section 4.4.1 was tested. Manual background measurements on both the RVR-500 and RVV-700 were made in conjunction with the maintenance (window cleaning) and calibration operations which were scheduled every four days.

The Arcata data showed reasonable agreement between the two transmissometer models. However, the absolute accuracy of the RVV-700 could not be assessed because the major sources of error (window contamination and background light) were strongly correlated for the two instruments. The Arcata installation and results were examined by the test team, with Charles Douglas as a consultant, and five modifications to the RVV-700 were recommended:

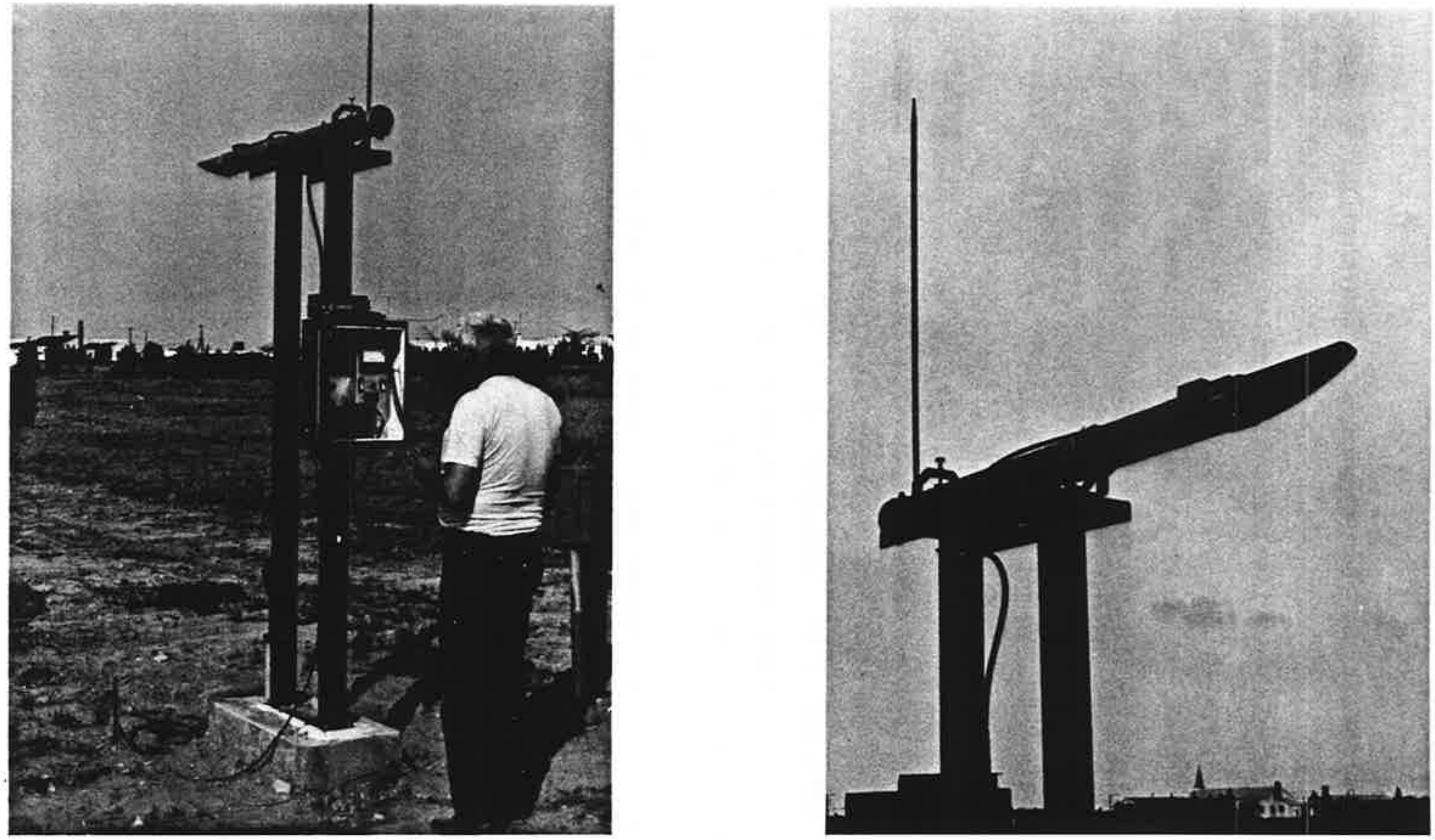

a.   b.

FIGURE 3-2. RVV-700 TRANSMISSOMETER: (a), (b) RECEIVER; (c), (d) PROJECTOR.

c.

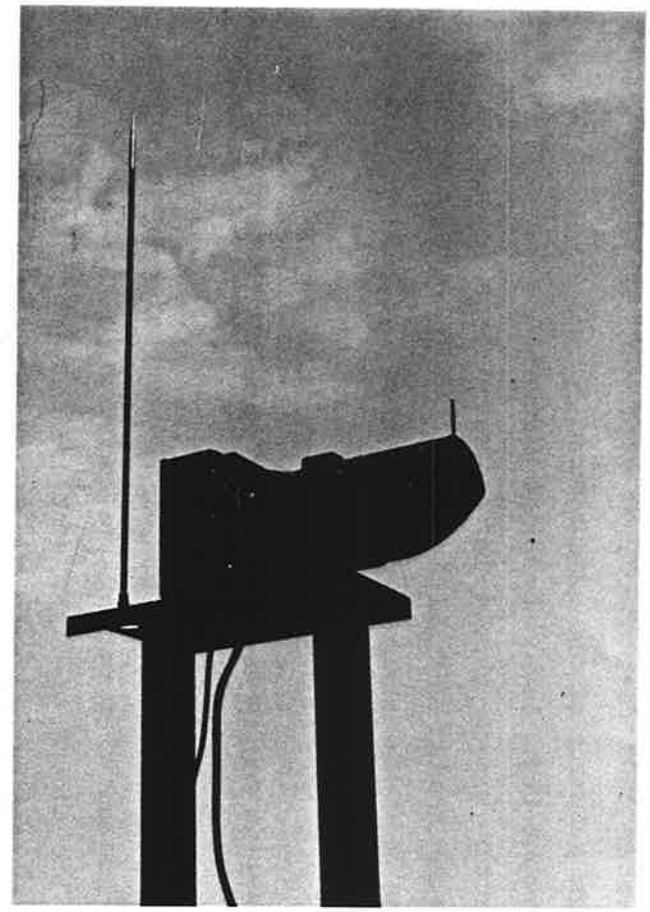

d.

FIGURE 3-2. (concluded)

1) The elevation of the unit should be raised to 8 feet above the ground to give a more representative measurement.
2) A baseline of 1000 feet should be employed, if possible, to improve the accuracy of the measurement.
3) The background light level should be reduced.
4) The projector window should be protected from contamination with a longer hood.
5) The window surfaces should not be cleaned but rather allowed to reach an "equilibrium" level of contamination.

3.1.2 Wright & Wright FOG-15 Forward-Scatter Meter

Forward-Scatter Meters (FSM) operate on a different principle from transmissometers. Instead of measuring the amount of light lost from a beam, they measure the amount of light scattered out of a beam into a specific range of scattering angles. If the light scattered into all angles were collected, the two measurements would be equivalent (neglecting absorption). Since collecting light from all angles has proved to be impractical, forward-scatter meters select a range of angles (typically 20 to 50 degrees) which gives reasonably consistent results no matter what type of particle is causing the scattering.

Forward-scatter meters have many practical advantages over transmissometers:

1) They can measure a larger range of visibilities.
2) They are less affected by window contamination.
3) They can be mounted on a single inexpensive post.
4) They are less expensive to buy and maintain.

All of these advantages come at the cost of two disadvantages:

1) The FSM calibration may depend upon the obstruction to vision (e.g., rain, snow, or fog).
2) A FSM averages over a smaller portion of the atmosphere and thus may at times provide a less representative measurement of visibility for a given averaging time.

The Wright & Wright FOG-15 forward-scatter meter (FSM) (see Figure 3-3) was developed as a low-cost simplified version of the EG&G 207 FSM, which has been used by the Air Force as a research instrument for the last decade. It functions in much the same way, using a chopped incandescent light source and a similar scattering geometry.

Two types of FOG-15 instrument deficiencies were identified in the 1981 Arcata Tests:

1) An excessive variation in the response of the instrument compared to a colocated EG&G 207 FSM (later traced to a severe variation of calibration with line voltage).
2) An instability in the zero level of the sensor output.

In addition to instrumental problems the FOG-15 is also subject to the two generic limitations where the response of a forward-scatter meter may be inferior to that of a transmissometer:

1) For the same averaging time, the spatial average measured by the transmissometer may yield somewhat more representative values of visibility. Two or more FSM's may be needed to produce a comparable spatial average.
2) Forward-scatter meters tend to read lower visibility in rain than a transmissometer by as much as a factor of two. Calculations of the effect of rain on human vision indicate that the transmissometer response is more appropriate. (See Appendix F.)

The operational significance of these limitations has not been assessed.

3.1.3 Impulsphysics LD-WHL Ceilometer

The Impulsphysics LD-WHL ceilometer (See Figure 3-4) measures the distance to a cloud with a short infrared light pulse from a diode laser. It processes the return signal in two ways:

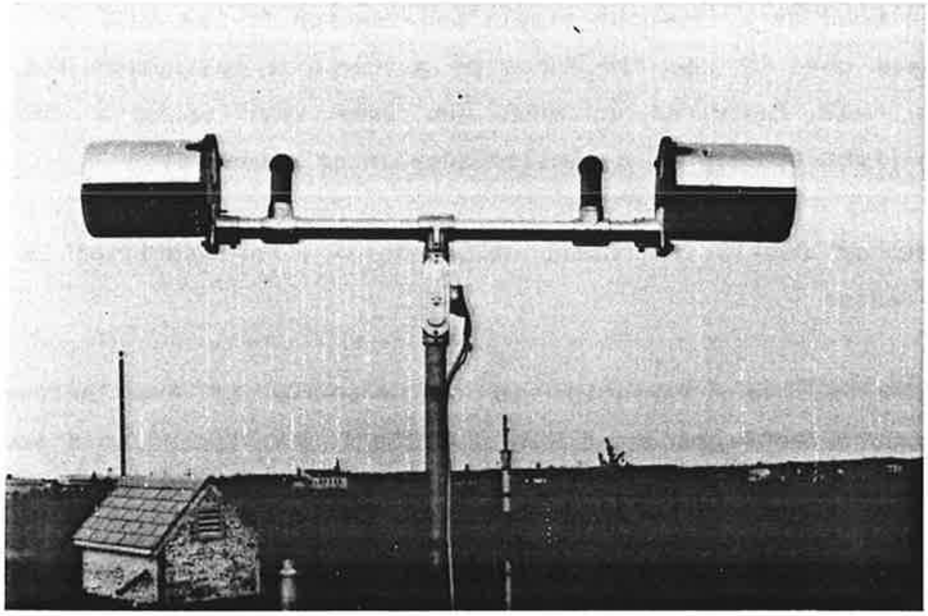

a.

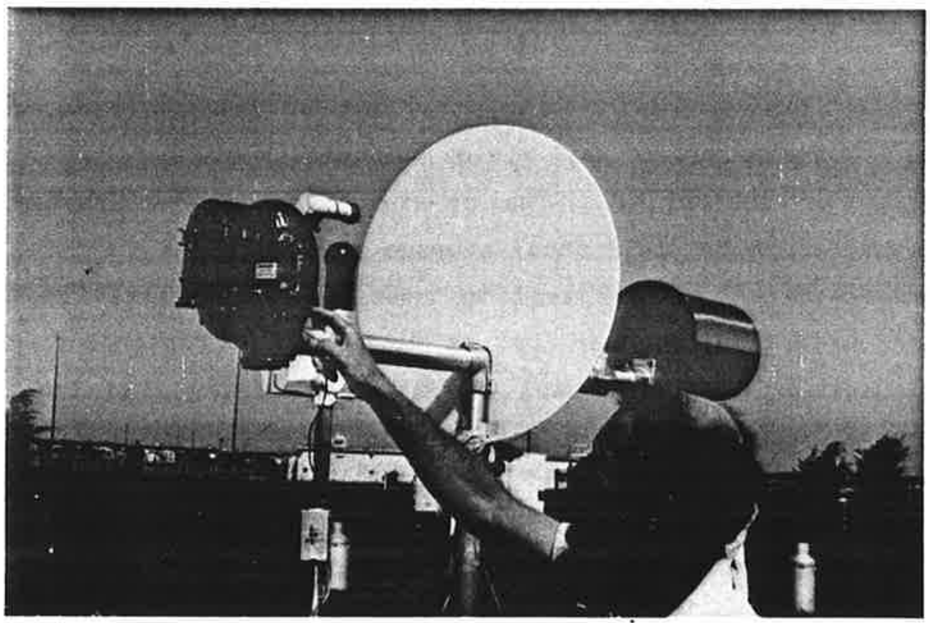

b.

FIGURE 3-3. WRIGHT & WRIGHT FOG-15 FORWARD -SCATTER METER
(a) FOG-15
(b) FOG-15 with CALIBRATOR DISK INSTALLED
(c) PROJECTOR
(d) RECEIVER

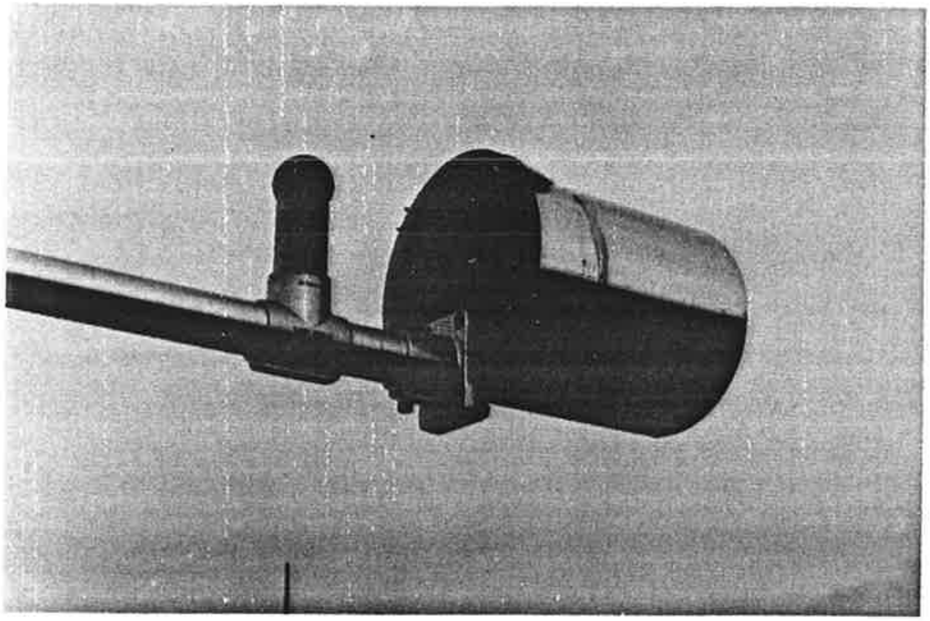

c.

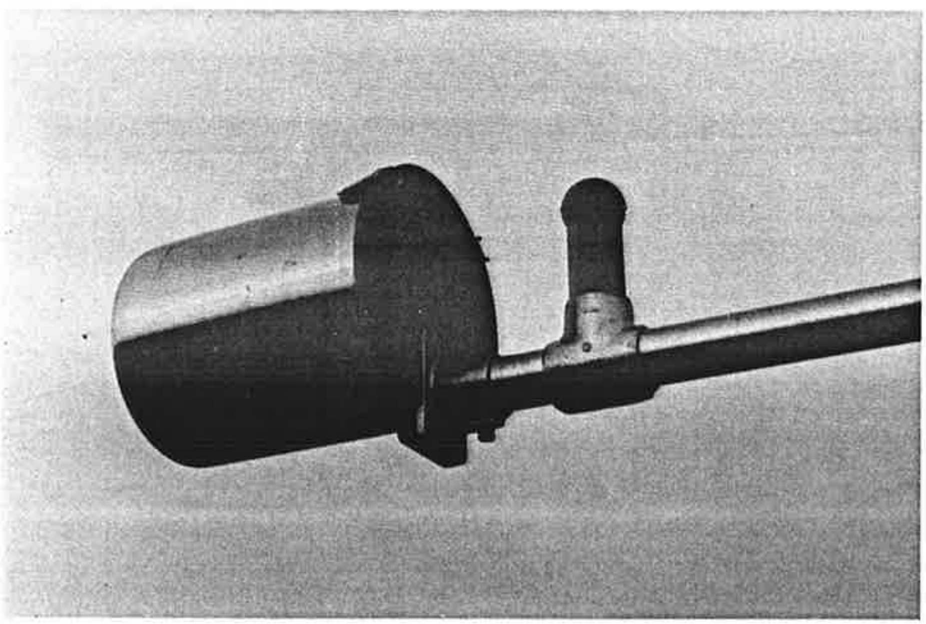

d.

FIGURE 3-3. (concluded)

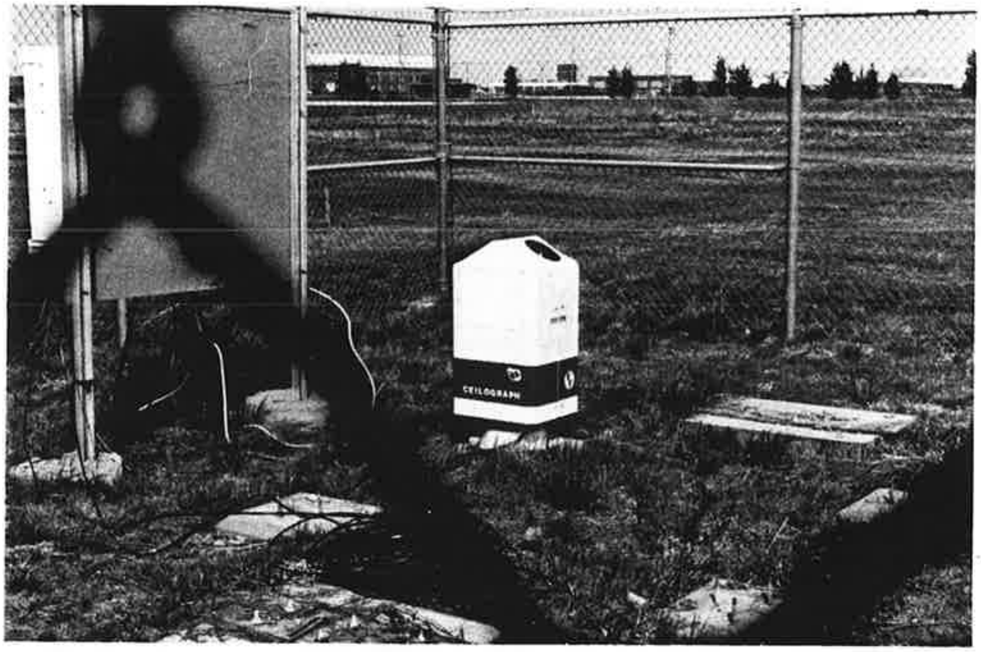

a.

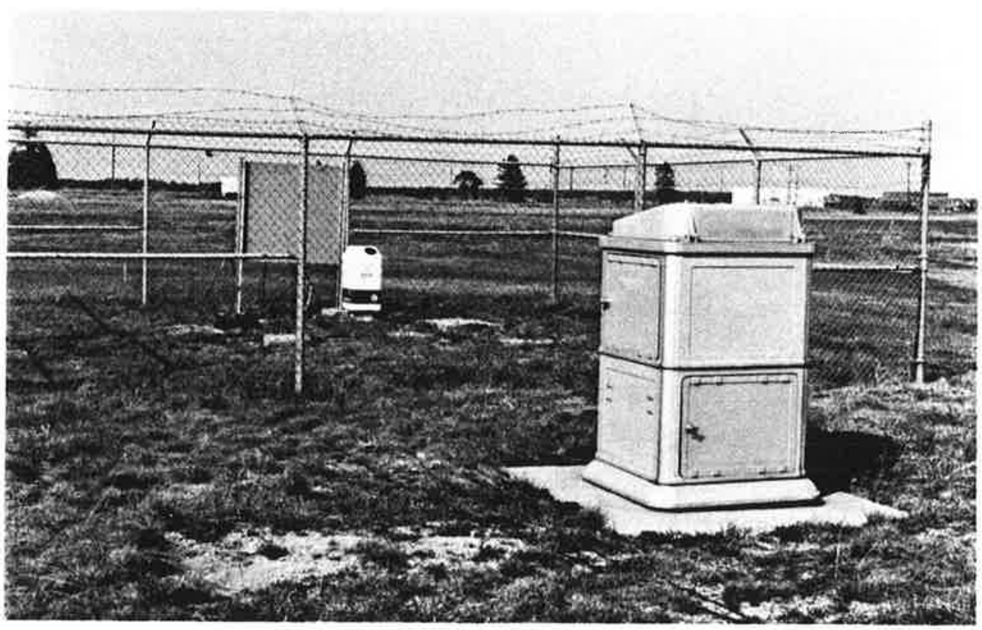

b.

FIGURE 3-4. IMPULSPHYSICS LD-WHL CEILOMETER
(a) ALONE
(b) WITH ROTATING BEAM
CEILOMETER RECEIVER IN FOREGROUND

1) Direct Mode: by clocking the time until the return pulse, and
2) Averaged Mode: by averaging the return signal during a specified range gate which is slowly scanned over the range of the instrument (5000 feet). Each scan lasts for 15 seconds.

The performance of the LD-WHL unit tested at Arcata was found to be satisfactory only to a range of 2000 feet, rather than the maximum range of 5000 feet. This degradation in performance was subsequently traced to beam misalignment caused by wedged windows. The Arcata unit was also programmed for nonstandard sensor operation:

1) One rather than four measurements per minute, and
2) Direct mode disabled.

Standard operation is required.

3.2 1982 AWOS SENSOR TESTS

As a result of the Arcata Tests, the following sensor modifications were made:

1) Flat windows (not wedged) were installed in the LD-WHL to improve reduced sensitivity above 2000 feet. The standard sensor operation (direct mode and four measurements per minute) was restored.
2) The RVV-700's projector shield and mounting height were modified and the use of a longer base line (1000 feet) was adopted to improve resolution.
3) The FOG-15 was modified to reduce inherent instabilities and sensitivity to RFI.

The goals of the 1982 AWOS sensor and system tests were to validate the performance of the modified sensor to verify that the ARTAIS Weather-Check ® system will operate satisfactorily with either of two visibility sensors, the Tasker RVV-700 and the Wright & Wright FOG-15, and with the Impulsphysics LD-WHL ceilometer.

In addition to establishing sensor performance and operational verification, the interface of the sensors to the Artais AWOS processor was also to be verified. Although the sensor reporting algorithms contained in the processor software were not to be examined directly, it was anticipated that they would be checked in factory tests and in the evaluation of the field measurements.

The primary focus of the 1982 tests was to fill in the information not available from the earlier Arcata tests. In particular, the adequacy of sensor modifications in eliminating earlier problems was to be assessed. Data missing from the earlier tests were recorded, specifically the output of the Tasker RVV-700 computer and all the inputs to the Artais AWOS processor.

In order to take advantage of existing test data from Arcata, Otis, and Sterling and to meet the short time frame of the evaluation, the test responsibilities were divided between the National Weather Service (NWS) Test and Evaluation Division at Sterling VA and DOT/TSC in Cambridge, MA. The ceilometer testing was conducted by the NWS at Sterling while the visibility sensor testing was conducted by TSC at the nearby AFGL Otis test site. The Artais AWOS field verification was also conducted at Otis, using one of the ceilometers tested at Sterling. The factory tests of the Artais software were performed by the NWS.

3.3 ACCEPTANCE CRITERIA

3.3.1 Visibility Sensors

Appendix A presents the issues involved in developing realistic acceptance criteria for visibility sensors. Because the 1980 accuracy standards are unattainable, an alternative set of "achievable accuracies" has been proposed for AWOS systems. These AWOS "achievable accuracies" have been adopted, with minor changes, as the pass/fail criteria for these tests. The following AWOS visibility reporting values (miles) are specified: 1/4, 1/4, 1/2, 3/4, 1, 1 1/4, 1 1/2, 2, 2

1/2, 3, 3 1/2, 4, 5, 5. The basic accuracy requirement is that the reported visibility from the test sensor be within one reporting increment of the "standard" sensor at least 90 percent of the time. During precipitation (e.g., rain or snow) readings two increments low are allowed.

In the pass/fail evaluation of the current tests two changes were made in the "achievable accuracy" standards:

1) The reporting value of 3-1/2 miles was eliminated.
2) A different standard sensor was used.

The reporting value of 3 - 1/2 miles has never been required previously. This value also produces the most stringent requirement on sensor accuracy as is shown in Appendix A. The elimination of the 3-1/2 mile value thus leads to a more easily achieved standard that is consistent with current operational practice. Table 3-2 shows the effect of eliminating the 3-1/2 mile value on the required sensor error for two error models. It shows the sensor accuracy needed to meet the requirement that 90 percent of the sensor reports lie within one reporting increment of the report from standard sensor. The numbers in Table 3-2 allow sensor accuracy measurements to be related to the pass/fail criteria even when the amount of data is too small to produce satisfactory statistical information. For example, if the 100-percent calibration of a 1000-foot transmissometer drifts more than 5.0 percent, the sensor will fail the accuracy test no matter whether the 3-1/2 mile value is included or not. Because other sources of error (e.g., background light) add to the error due to calibration drift, the amount of calibration drift allowed is actually less than the value in Table 3-2.

Defining a high visibility "standard" has proved to be a fundamental problem in evaluating visibility sensors. The AWOS achievable accuracy standards specify a laser transmissometer as the standard. Unfortunately, the FAA laser transmissometer used to calibrate transmissometers cannot operate on a 1000-foot baseline

TABLE 3-2. EFFECT OF THE 3-1/2 MILE REPORTING VALUE ON REQUIRED SENSOR ACCURACY

ERROR MODEL	INCLUDE	REMOVE
FRACTIONAL STANDARD DEVIATION	< .14	< .19
TRANSMISSOMETER 100 PERCENT CALIBRATION DRIFT:		
1000-FOOT BASELINE	< 3.6%	< 5.0%
750 FOOT BASELINE	< 2.7%	< 3.7%

without major modifications. Instead, the standard United States transmissometer, the Tasker Model RVR-500, mounted on a 1000-Foot baseline was adopted as the "standard" sensor. Originally it was planned to use an EG&G 207 forward-scatter meter to correct the 100-percent setting of the "standard" transmissometer on a daily basis. Such an approach appeared to be feasible on the basis of earlier studies. Instead it was decided to use the 1000-foot baseline RVR-500 directly while relying on daily window cleaning and calibration checks to maintain accuracy. This approach is simpler and avoids concerns about the response of forward-scatter meters at high visibilities.

3.3.2 Ceilometers

The AWOS ceilometer pass/fail criteria are taken from the same AWOS sensor "achievable accuracy" specification document adopted for visibility sensors. The requirements are:

1) Measure up to 5000 feet for visibility greater than 3 miles with no precipitation.
2) Accuracy of ± 100 feet up to 1500 feet.
3) Accuracy of ± 10 percent to 5000 feet.
4) Capable of measuring to 3000 feet (with a 50 percent cloud detection probability) in moderate rain.

The natural reference "standard" for ceilometers is the rotating beam ceilometer (RBC) which is currently deployed at airports. Any ceilometer performing as well as the RBC would be considered acceptable.

The cloud-height measurement accuracy is not a real issue for laser ceilometers. Because they rely on electronic timing to determine the height, their range accuracy should be limited only by how well the cloud base is defined. Thus, the intrinsic height accuracy of a laser ceilometer is better than that of the RBC. Measuring the range to hard targets could be used to check the timing accuracy of a laser ceilometer.

The cloud detection sensitivity is the primary evaluation question for laser ceilometers. The NWS reporting algorithm relies on the cloud detection probability to determine whether a layer is scattered, broken, or overcast. If the ceilometer misses clouds, the resulting layer report can mislead a pilot by telling him that cloud conditions are better than he will actually experience.

3.3.3 Interfaces

The following requirements were defined for AWOS interface acceptance criteria.

1) The interface shall not degrade the sensor accuracy.
2) The interface must pass on all sensor self-check and failure information.
3) Interface failures must be detectable by the AWOS processor.

4. TEST DESCRIPTION

The decision to proceed with the final portion of the test program was made at the beginning of February 1982. This chapter of the report describes the final six months of the project. The data collection effort reported here was terminated in mid July. The test site layout is shown in Figure 4-1.

4.1 VISIBILITY SENSORS

The AFGL Weather Test Facility (WTF) at Otis Air National Guard Base (ANGB) was selected for several reasons:

1) The Air Force routinely collects data from a large number of weather sensors including many EG&G 207 forward-scatter meters and two transmissometers with RVR-500 electronics (300- and 500-foot baselines).
2) Three of the five participants have offices nearby in Massachusetts.

The routine data collection at the Otis WTF consists of one minute sensor averages (stored on the Modular Automatic Weather System (MAWS) magnetic tapes) and 24 hour surface observations taken at the Otis tower which is one mile from the test site. The MAWS tapes are recorded simultaneously at Otis and via telephone link at the AFGL home office at Hanscom Air Force Base. The Otis tapes serve as a back up and were furnished to TSC for analysis.

The visibility sensor data on the MAWS tapes are sampled every 12 seconds and averaged for one minute. This data recording format was not completely compatible with all the needs of the AWOS sensor tests. Consequently, two additional data recording systems were installed for specific purposes. Nevertheless, the MAWS tapes furnished the primary data for evaluating visibility sensors.

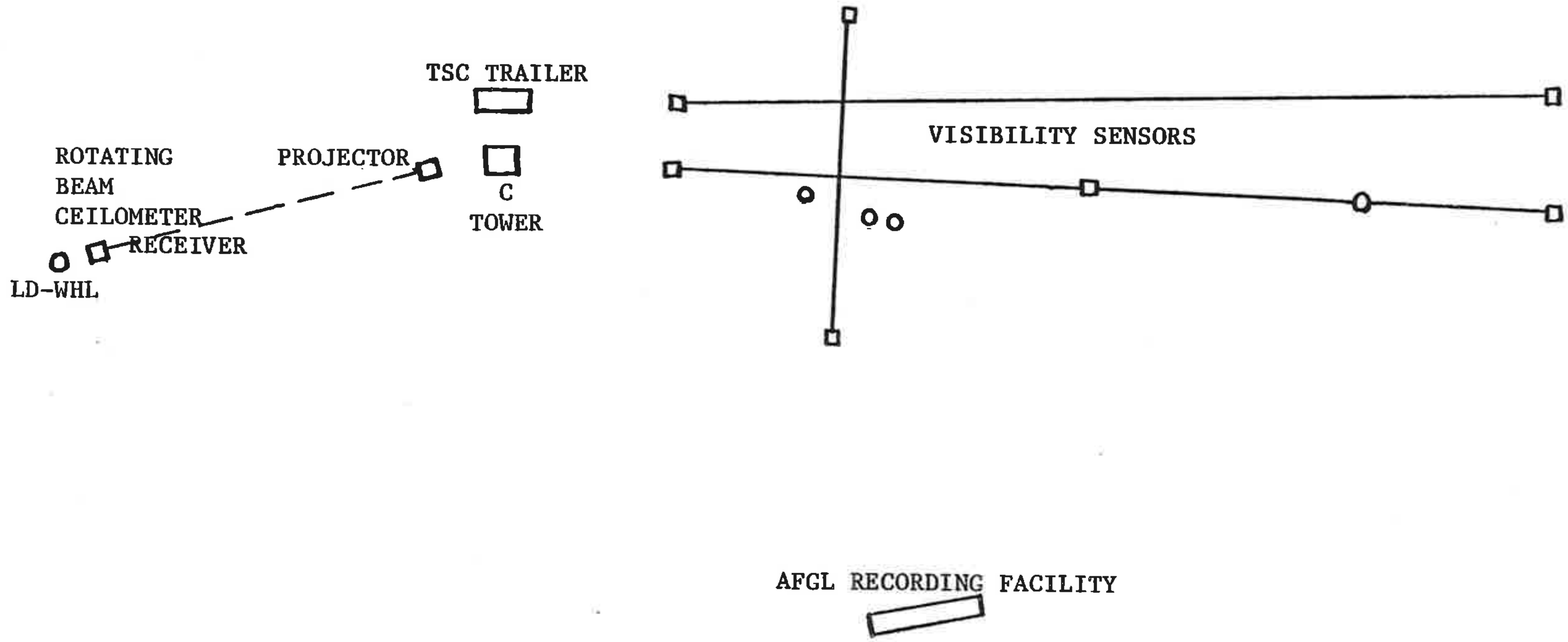

FIGURE 4-1. OTIS TEST LAYOUT

4.1.1 Tasker RVV-700 Transmissometer

The RVV-700 visibility system consists of a projector, a receiver, and a computer. The receiver signal consists of a pulse rate proportional to the detected light intensity (4000 pulses per minute corresponds to 100-percent transmittance). The computer counts the signal pulses for 45 seconds and converts the count to a reporting visibility value by means of look-up tables. A day/night detector is used to select the proper table. The visibility value is output as four parallel bits. Table 4-1 shows the reporting values supplied in the test unit along with the breakpoints between the values and the corresponding extinction coefficient (See Section 5.1). One should note that the Tasker computer reports an extra value (1-3/4 miles) not included in the AWOS "achievable accuracy" standard. The RVV-700 computer checks the background signal by turning the projector lamp off for about a minute every hour. The last background count is subtracted from the data count before the reporting visibility value is generated.

4.1.1.1 Installation

Tasker RVV-700 and RVR-500 transmissometers were installed on parallel 1000-foot baselines (actually 960 feet to eliminate underground cable splices). Figure 4-2 shows the sensor layout. Table 4-2 shows the height above ground level of all sensors and the measured transmissometer baselines. The RVR-500 baseline was produced by adding an additional receiver to the existing 500-foot baseline. The RVV-700 was displaced about 100 feet to the side in order to secure a clear path past small trees, bushes, and the other sensors.

The 1000-foot RVR 500 receiver was mounted on a standard Air Force tower of approximately 12-foot height, which was installed on a foundation consisting of four 18-inch diameter concrete columns resting on a six-foot square, one-foot thick concrete slab buried five feet below the ground. The RVV-700 foundations were much less massive. Tasker recommends that the foundation be produced by using an auger to

TABLE 4-1. RVV-700 REPORTING VALUES AND BREAK POINTS

CODE	VISIBILITY (mi)	VIS. BREAK PT.	σ (day)	σ (nite)
0000	< 1/4			
		7/32	82.4	205.0
0001	1/4		72.1	176.0
		3/8	48.1	110.6
0010	1/2		36.0	79.4
		5/8	28.8	61.3
0011	3/4		24.0	49.6
		7/8	20.6	41.4
0100	1		18.0	35.4
		1 1/8	16.0	30.8
0101	1 1/4		14.4	27.2
		1 3/8	13.1	24.3
0110	1 1/2		12.0	21.9
		1 5/8	11.1	19.9
0111	1 3/4		10.3	18.2
		1 7/8	9.61	16.8
1000	2		9.01	15.5
		2 1/4	8.01	13.5
1001	2 1/2		7.21	11.9
		2 3/4	6.55	10.6
1010	3		6.01	9.52
		3 1/4	5.54	8.64
1011	3 1/2		5.15	7.89
		3 3/4	4.81	7.25
1100	4		4.50	6.69
		4 1/2	4.00	5.79
1101	5		3.60	5.08
		5 1/2	3.28	4.51
1110	> 5			
1111	Overrange			

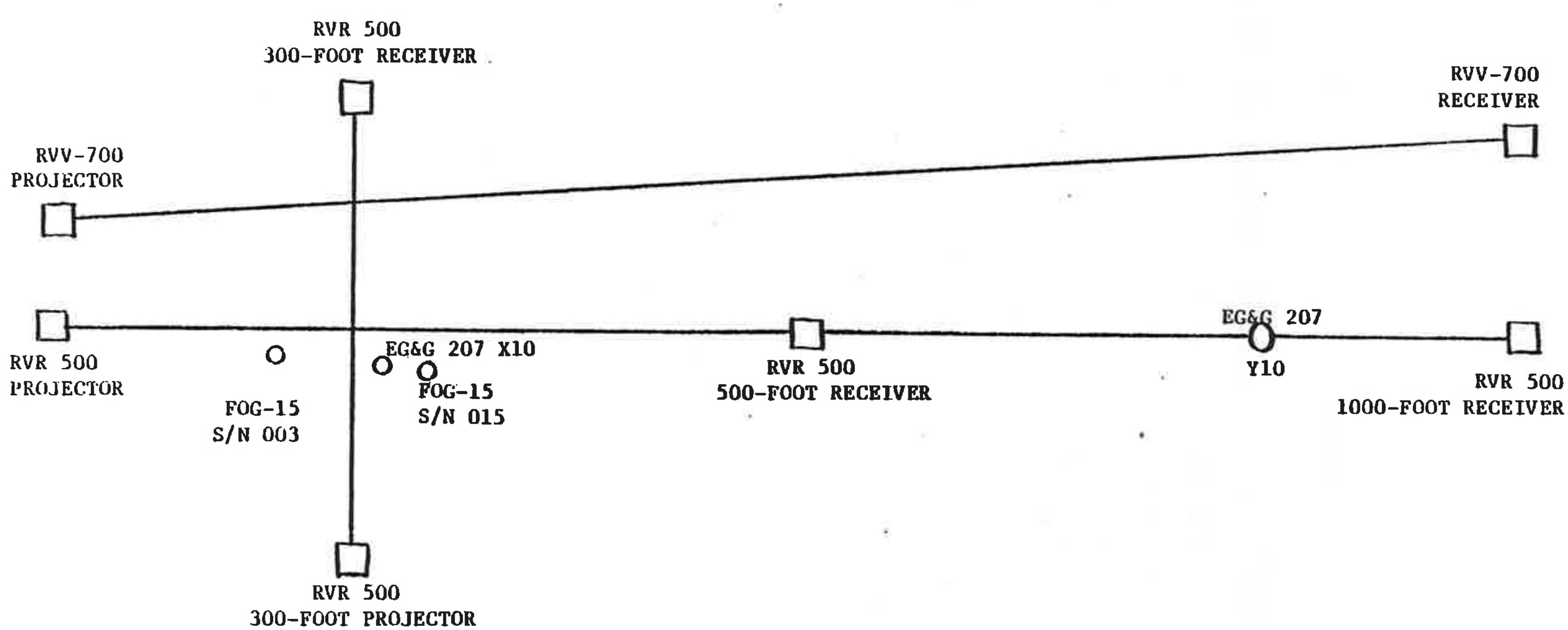

FIGURE 4-2. VISIBILITY SENSOR LAYOUT

TABLE 4-2. SENSOR HEIGHTS AND BASELINES

SENSOR	COMPUTER NAME	HEIGHT (ft.)		BASELINE (ft.)
1000-Foot RVR 500	RVR5	11.5*	13.0**	975
500-Foot RVR 500	T500	11.5*	12.3**	498
300-Foot RVR 500	T300	11.5*	11.0**	297
1000-Foot RVV-700	RVV7	8.7*	8.7**	962
EG&G 207	X10	9.9		
EG&G	Y10	9.5		
FOG-15 (SN 015)	FG15	11.3		
FOG-15 (SN 003)	FG16/FG15***	9.8		

* Projector

** Receiver

*** Fluke "Trailer" Data

drill two 18-inch diameter holes down to two feet below the frost line. The soil between the holes is to be broken out and the holes filled directly with concrete. Securing a contractor to install the sensor foundations was difficult; only one company, located approximately 80 miles away, was found to be willing to take on the job. Since the contractor did not have access to an auger, he used a back hoe to dig the foundation. A hole six-foot deep with a single bucket width (24-inches) was dug. One end was approximately vertical and the other sloped. The top four feet of the foundation were defined with a two-foot by three-foot plywood form which was removed after the concrete had hardened. The bottom of the foundation was cast directly against the soil which was kept as undisturbed as possible.

The sensor signals were connected to two Data Acquisition Systems (DAS) which record signal voltages. The first, the AFGL MAWS system, samples its inputs every 12 seconds and records one-minute averages. The second, a Fluke Model 2240B was synchronized with the counting gates of the RVV-700 computer. It records 45-second averages of the sensor signals listed in Table 4-3. The transmissometer data pulses are converted to dc voltages by a circuit which counts for a specified time (12 or 45 seconds respectively for the two systems) and then latches the count into a digital-to-analog (D/A) converter. The digital output signals (4 visibility bits, day/night, data valid, and failure) from the RVV-700 computer are recorded on the Fluke DAS by using a D/A converter.

All the transmissometers were operated with automatic background measurements. The background checks for the RVR-500 transmissometers were synchronized with that of the RVV-700. Because the standard 45-second background duration is too short to allow measurement with the MAWS DAS, the background duration was increased to 3.4 minutes. This extension of the RVV-700 background check causes the RVV-700 computer to report a failure for a period after each background check. The voltage indicating a background check was recorded on both data acquistion systems.

TABLE 4-3. CHANNEL ASSIGNMENT FOR FLUKE DATA ACQUISITION SYSTEM

CHANNEL	SENSOR
0	1000-Foot RVR 500
1	1000-Foot RVV-700
2	RVV-700 Computer
3	FOG-15 (SN 003)
4	Background Check Voltage

4.1.1.2 Maintenance Strategy

The usefulness of a visibility sensor for an unattended AWOS requires a long period between maintenance and calibration visits. As recommended by Tasker, a 30-day calibration cycle was established. Instead of cleaning the windows, they were allowed to reach an equilibrium level of contamination. After each thirty day period the 100-percent transmittance level was reset on the basis of the observed maximum transmittance on a stripchart recorder. In particular, the transmittance should read 100 percent just after a frontal passage with precipitation.

In contrast, the 1000-foot baseline RVR-500 was maintained intensively as a standard. The windows were cleaned daily and the calibration adjusted whenever it appeared to be necessary.

4.1.1.3 Chronology

The RVV-700 was installed in April. Installation was delayed by a misdirected air freight shipment and a freak April snow storm. When first installed the RVV-700 performed poorly. Setting up the metering circuit of the unit was not possible because of improperly installed lightning protection circuitry. The measured transmission exhibited a 40-percent diurnal variation. Tasker personnel cleared up the problems the week of May 12 by changing the lightning protection, repairing a poor lamp connection, and swapping in a new pulse amplifier card in the receiver.

The installation of the RVR-500 1000-foot baseline was delayed by missing pieces in the receiver tower. The problems experienced with the RVV-700 allowed both transmissometers to begin test operation at the same time (May 17). On May 14, the RVR-500 lamp was changed to correct a severe overshoot which followed each background check. The initial transmissometer calibration was performed on May 17, 1982. The calibration was based on an estimate of 15 mile visibility which corresponds to 96 percent transmittance on a 1000-foot baseline (98 percent on a 500-foot baseline). The transmissometers were set to read the appropriate count rate plus the measured background rate. The RVV-700 windows were cleaned for the last time.

The alignment of the RVV-700 was observed to have shifted on May 31. The system was realigned three times during the first month of the test period. The observed loss in transmittance due to misalignment was 35%, 39% and 12% on June 2, 9 and 18 respectively. The misalignments occurred during a period of heavy rains after a two month spell of very dry weather. The area of backfill around the RVV-700 receiver settled a number of inches during the rainy period. The direction of the foundation shift was toward the sloping side of the hole, which had to be backfilled to the full six-foot depth.

At its time of first recalibration (and realignment) on June 18 the RVV-700 had lost 6 percent in its 100-percent transmittance setting, when compared to the RVR-500 which was calibrated several times and had its windows cleaned every day. Five percent of this loss had occurred by May 25.

Just before the recalibration on June 18, the RVV-700 began to exhibit a background level instability which was traced to moisture which had leaked into the receiver electronics housing through an inadequate seal. The problem was rectified on June 23 when the seal was repaired and a bag of dessicant was installed in the housing. The second recalibration of the RVV-700 was done on July 21 on a very clear day following a storm. The recalibration was made difficult by the failure of the meter in the projector electronics package. No change in the 100-percent setting was needed. The receiver was realigned with a gain in 100-percent setting of less than one percent. Midway during the second month's operation the RVV-700 projector was realigned and gave a 3 percent gain in 100-percent setting.

The 1000-foot baseline RVR-500 needed no changes of alignment during the first month's operation, apart from projector adjustments when the lamp was changed. The July 21 calibration showed that the

1000-foot baseline RVR-500 receiver had finally drifted out of alignment. Realignment produced an increase of 6 percent in the 100-percent setting. Since the alignment had been checked frequently, it is likely that the rainy period preceeding the realignment was responsible for this shift.

4.1.2 Wright & Wright FOG-15 Forward-Scatter Meter

At the beginning of the final six month test period an unmodified FOG-15 unit (SN 003) was operating at Otis. The unit tested at Arcata (SN 004) was returned to the Manufacturer for modifications to correct two deficiencies.

1) An excessive variation in the response of the instrument compared to a colocated EG&G 207 FSM.
2) An instability in the zero level of the sensor output.

4.1.2.1 Modifications

The excessive signal variation was traced to a severe line voltage dependence in the calibration of the instrument. Factory tests showed a factor of two variation in the calibration as the line voltage was changed from 100 to 130 VAC. The source of this variation was the voltage dependence of the light chopping frequency which is generated by an induction motor. The change in frequency leads to phase shifts in the synchronous detector used to extract the chopped signal from the background noise. This problem was solved by introducing identical phase shifts into the reference signal for the synchronous detector. A unit (SN 004) with this modification was installed at Otis on 2/23/82.

The unstable baseline problem persisted in this modified unit and was traced to radio frequency interference (RFI) at the Otis site, a problem which does not exist at the Wright & Wright factory in Oak Bluffs, MA. On 3/12/82 an RFI power line filter was installed and a signal line exhibiting minimum RFI was selected. The zero stability was notably improved although it still exhibited some problems.

On 4/13/82 a new unit (SN 015) was installed which had a number of additional modifications. The cable input to the instrument was modified to permit proper installation of the power line RFI filter. The internal components of the instrument were grounded and bypassed to minimize the sensitivity to radiated RFI. In addition, the chopping frequency was increased to improve the rejection of background light signals. This unit was operated for the duration of the test period except for two weeks at the beginning of May when it was removed for testing at the Calspan environmental chamber because of a prior Air Force commitment. After it was brought back to Otis it developed a zero instability for two weeks. The zero level was adjusted on May 26. The instability persisted until May 27 when the unit stabilized with a zero offset of 36 mV which remained constant until July 9 when the unit was returned to the factory for evaluation. The problem appeared to be caused by poor wiper contact on the zero potentiometer. The manufacturer plans to switch to a higher quality component for this critical adjustment. The observed zero shift corresponds to a 50-percent error at 3-mile daytime visibility, which is unacceptable. An additional FOG-15 unit (SN 003 with the same modifications as SN 015) was installed on May 25. In addition to the usual voltage output, this unit was also equipped with a frequency modulated current output for interface to the Artais AWOS system.

4.1.2.2 Calibration

The FOG-15 units constructed to date are equipped with a rotating filter wheel in front of the detector. The calibration procedure consists of installing a translucent-plastic scattering disk into the scattering volume and rotating a neutral density filter (N.D. 3.0; i.e., x1000) in front of the detector in order to reduce the signal to a manageable level (see Figure 3-3). If the scattering disk and the neutral density filter are stable in time, any drift of the unit can be checked.

This FOG-15 calibration procedure does not allow a unit's calibration to be referenced to a standard because of variations in the actual attenuation of nominally identical neutral density filters. Late in the test program the internal neutral density filter was referenced to a standard filter which can be installed in any unit. The absolute calibration of the standard disk and filter is obtained by measuring the output of a unit which has been calibrated against a transmissometer.

On July 9 the calibrations of three FOG-15 units (SN 3, 4, 15) at Otis were checked with the standard disk and filter as well as an older disk and the internal filters. The results are shown in Table 4-4. Both voltage and frequency outputs were checked. Enough measurements are included to test the consistency of the calibration technique. The ratio of the signals from the two scattering disks should be the same for all units and filters. Likewise, the ratio of the signals from the internal and standard filters should be the same for both scattering disks. The results in Table 4-2 show a calibration consistency of about 6 percent.

On July 16 the calibration of unit SN 015 was rechecked at the factory and found to show a 25-percent higher voltage. This change was traced to a decreased response at high temperatures because of leakage in the diodes used to clip noise in the signal processing electronics. The problem was corrected and unit SN 015 was reinstalled on July 22. This change could conceivably affect the noise rejection capability of the unit. The rain response may also be affected since the large signal spikes from individual rain drops may have been suppressed by the soft clipping. No data from this unit have been analyzed since additional sensor changes are pending.

The calibration data in Table 4-4 for SN 003 and 015 were measured on a hot day with strong solar heating, and may therefore be affected by the temperature problem. The SN 004 measurements were made inside the WTF building and are probably valid. Calibrations made under cool conditions (and with the new clipping for SN 015) on July 22 or 23 are also shown in Table 4-4. The calibration for SN 003 was consistent at

TABLE 4-4. ABSOLUTE CALIBRATION OF FOG-15 (7/9/82)

SN=		003		004		015
DISK	FILTER	V	f(Hz)	V	f(Hz)	V
OLD	INTERNAL	0.349 0.346* 0.351**	 400	1.121	1148	0.450 0.543**
OLD	STD.	0.369			538	0.225
STD.	INTERNAL	0.902		2.72	2663	1.028
STD.	STD.	0.926			1256	0.493
ZERO		0.001 0.005* 0.005**	 94.8*	0.019 0.020**	38.1	0.036 0.005**
DISK RATIO: STD./OLD						
	INTERNAL	2.59		2.45	2.36	2.40
	STD.	2.51			2.44	2.42
FILTER RATIO: STD./INTERNAL						
	OLD	1.06			0.45	0.46
	STD.	1.03			0.46	0.49

*July 16, 1982

**July 22 or 23, 1982

all times while that of SN 015 shows the difference mentioned above. The data for the standard disk and the standard filter can be used to check the relative response of SN 003 and SN 015 which have been the test units at Otis. The response ratio of 003 to 015 is 1.74 which is close to the nominal value of 2.00. The gain of SN 003 would have to be multiplied by a factor of 1.15 to be equivalent to that of SN 015.

The calibrations of the voltage to frequency (V/F) converter can be determined from Table 4-4. They are 895 and 990 Hz/volt respectively for SN 003 and 004. The nominal calibration is 1000 Hz/volt.

4.2 CEILOMETERS

4.2.1 NWS Data Collection

In February 1982 considerable data had been collected at the NWS Sterling VA test site on two laser ceilometers: Impulsphysics LD-WHL and ASEA QL 1211. The LD-WHL unit had been modified to rectify the problems discovered in the Arcata tests. The wedged windows were replaced with parallel-surface windows and the standard operation was restored. An additional modified LD-WHL unit was moved to Sterling for side-by-side testing of two units. These units were later used for the attenuator tests described below. Finally the second LD-WHL was moved to Otis at the end of April to be interfaced to the Artais AWOS.

The Sterling ceilometer data acquisition system recorded cloud hit data from the three laser ceilometers on magnetic tape cassettes. Cloud hits from a reference rotating beam ceilometer were generated by two different electronic circuits and also stored on the cassettes. The data system generated real-time printouts of cloud hits from each ceilometer on a minute by minute basis.

A report evaluating the Sterling Ceilometer data was prepared in March 1982 and is attached to this report as Appendix B. The response of the laser ceilometers under various conditions (clear, rain, snow, fog) and for various cloud heights was observed. The evaluation used the Dulles airport surface observations (several miles away) to determine the visibility and obstruction to vision. The printouts rather than the data cassettes were used for the cloud hit data. The printouts contain only one line each minute and therefore cannot indicate how often hits are missed. The results of this NWS report will be discussed in Section 6.3.

4.2.2 Attenuation Test

One of the fundamental characteristics of a laser ceilometer is its capability of penetrating obscuration (fog, rain, snow) to detect a cloud. The NWS reporting algorithm requires a cloud-hit probability of at least 60 or 70 percent for visibilities of 1-1/2 or 2 miles. The practical upper range of a ceilometer is set by this requirement.

The effect of obscuration on a ceiling measurement is, to reduce the intensity of the signal returning from a cloud. This effect can be simulated by inserting attenuation into the ceilometer beam. A comparison of the cloud-hit probability with and without the attenuation under unobscured conditions can be used to determine the "excess" signal available to penetrate obscuration. The attenuation would be adjusted until the cloud-hit probability dropped to the minimum acceptable value. It is important to use real clouds for this measurement since hard targets are unlikely to properly simulate the statistical variations in cloud reflectivity. Appendix C describes a test of this technique.

The excess signal can be related to a minimum visibility requirement. For example, suppose a 5000-foot ceilometer is to operate in two-mile daytime visibility. If the visibility of two miles is uniform up to a cloud base at 5000 feet, the returning signal is reduced by a factor of 20. An "excess" signal of a factor of 20 would be needed to meet this requirement.

4.3 HUMAN OBSERVATIONS

Surface Weather Observations are made 24 hours per day at the Otis Control Tower one mile from the test site. Tower personnel made the observation forms available for copying at the end of each month. These observations were used to identify obstructions to vision and to correlate with the output from the Artais AWOS. The observations were not used to evaluate sensors. The variation in human observations are far too great to allow a meaningful evaluation of sensor accuracy, especially when the sensor and observer are far apart.

4.4 ARTAIS INTERFACE

The Artais Weathercheck® AWOS system was installed in mid May. The processor and recording equipment was installed in a trailer belonging to TSC which was placed as shown in Figure 4-1. The wind sensor was placed on a nearby 20-foot tower. The temperature and dew point sensors were mounted at the 8-foot level. The Impulsphysics LD-WHL ceilometer was located, as shown in Figure 4-1, next to the receiver from the rotating beam ceilometer (RBC). The Artais AWOS was interfaced to two visibility sensors (Figure 4-1): an RVV-700 and a FOG-15 (SN 003). The Artais reports were output to a voice unit which could be called via telephone.

4.4.1 Interface Definition

The Artais interface to the Impulsphysics LD-WHL ceilometer makes use of the sensor's RS232 110 Baud serial ASCII output. Reports are generated every 15 seconds. The initial three characters of a normal report are "?**"; they are followed by one or two cloud heights. If any failure is detected by the sensor self checks, one of the asterisks changes to a letter indicating the nature of the failure. Failure checks include laser power, receiver sensitivity and power supply voltage. In the case of a failure the cloud height fields of the report may contain data on the failure. This interface format allows simple failure detection. Interface failures are also easily detected by the absence of a valid report.

The RVV-700 interface consists of six parallel bits: 4 visibility bits (Table 4-1), 1 data valid bit, and a day/night bit. In addition, provision is made for the Artais processor to set all data bits to "1" or "0" to check for stuck bits. The day-night bit is transferred as the 110 VAC signal on the day/night switch. All others are made by means of optical isolation to avoid grounding problems. The RVV-700 computer outputs two other bits which would be useful in an operational environment: a failure bit and a computer-in-test-mode bit. The failure bit, although not necessary to ensure valid data, was interfaced midway through the test period. The RVV-700 computer checks for lamp or cable failures, as well as unrealistic signal or background levels. Although the RVV-700 computer generates a new visibility value every 49 seconds, the Artais processor samples only every minute. The RVV-700 readings are averaged for 10 minutes as called for by the NWS reporting algorithm.

The Artais interface to the FOG-15 makes use of the frequency modulated current (10mA) output to drive an optical isolator. A frequency-to-voltage (F/V) converter is used to generate a voltage that is sampled every 10 seconds. The zero signal frequency of the FOG-15 is set to 100 Hz. The full scale signal (10 VDC) generates 10,100 Hz and corresponds to 500 $10^{-4}m^{-1}$ (which is half the standard full scale response). The 100 Hz offset allows for failure detection. A frequency below 50 Hz is considered to be a failure. The FOG-15 sensor checks for lamp or chopper motor failure and shuts off the frequency output. Cable failures also generate a failure indication.

4.4.2 Data Acquisition

Both raw and processed data from the test sensors were recorded in a microprocessor-based data acquisition system built at TSC to record ceilometer data. It recorded the Weathercheck ASCII reports which were sent to the voice unit every minute. The laser ceilometer ASCII outputs occurred every 15 seconds. The RVV-700 reports occured every 48.75 seconds. Both RVR-500 and FOG-15 data were averaged and sampled for the same period. In addition, the transmissometer background check signal was recorded. In other words the same visibility data recorded on the Fluke DAS were also recorded along with the ceilometer and Artais data. In summary the data tapes contained:

a) Weathercheck reports
b) RVV-700 computer output (RVV) (also day/night)
c) RVV-700 raw data
d) RVR-500 raw data
e) Transmissometer background check indicator
f) FOG-15 raw data
g) LD-WHL cloud hit messages
h) Day and time

The ASCII messages from the ceilometer and Artais were listed on printers. In addition, stripcharts of the WTF rotating-beam ceilometer data were generated.

The interfaces of the sensors to the recording system were carefully designed to sense exactly the same data received by the Artais processor. The ceilometer RS232 signal was connected in parallel. The visibility sensor signals were hooked up to series optical isolators.

Completion of the Artais data recording installation was delayed until mid June because of compatability problems with the Artais message and because of needed debugging of the recording system, especially the display which showed the data accepted by the microprocessor. The amount of data recorded was limited. Some sensor interfaces were damaged by lightning surges on two occasions in late June. The tape recorder failed on July 13. However, sufficient data were recorded to evaluate the interfaces. The Artais processor correctly reports data "missing" in the event of sensor or interface failure.

5. DATA ANALYSIS

5.1 RELATIONSHIP BETWEEN VISIBILITY AND EXTINCTION COEFFICIENT

The NWS visibility reporting algorithm uses the same equations to relate visibility to extinction coefficient as are defined for Runway Visibility Value (RVV):

Day: $\sigma = 2.90/V$ (1)

Night: $\sigma = (\ln(.00336V))/V$ (2)

where σ is the extinction coefficient and V is the visibility. The day equation corresponds to a 5.5-percent contrast visibility threshold. The night equation corresponds to the visibility of an omnidirectional 25 candela lamp. These equations are plotted in Figure 5-1 where the value of extinction coefficient has been converted to the units used in this report: $10^{-4}\ m^{-1}$ or 1/10 km.

5.2 Sensor Errors

5.2.1 Systematic Errors

Because the sensors actually measure extinction coefficient, most errors assume a simpler form when related to extinction coefficient rather than to visibility. In particular, one can relate the measured extinction coefficient σ_1 for sensor 1 to the actual extinction coefficient σ by the equation

$$\sigma_1 = K_1\sigma + D_1 \qquad (3)$$

where K_1 not equal to unity is a slope or gain error and D_1 not equal to zero is an offset error.

5.2.1.1 Forward-Scatter Meter

A forward-scatter meter (FSM) generates an output signal proportional to the extinction coefficient. The constant of

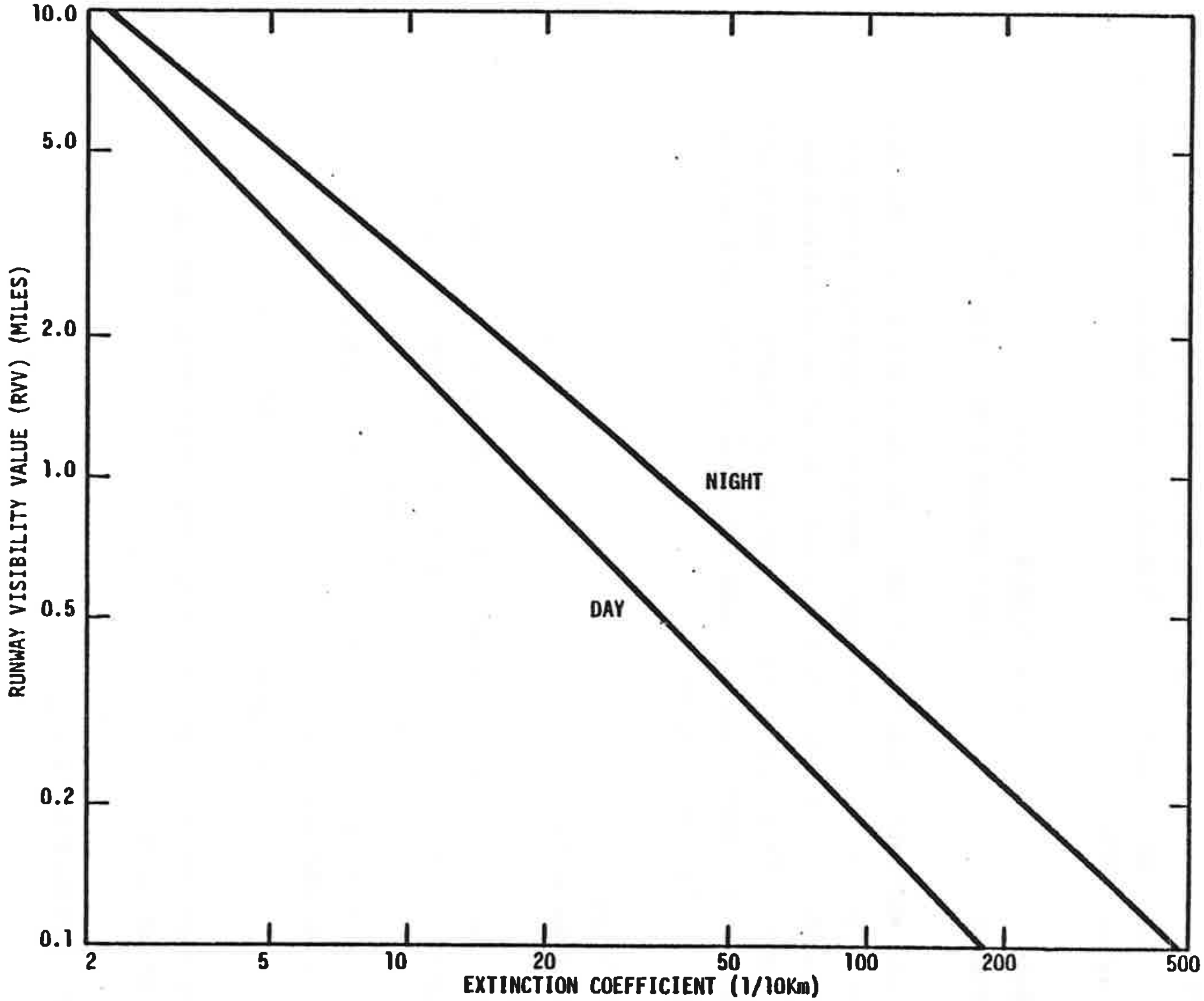

FIGURE 5-1. RVV VERSUS EXTINCTION COEFFICIENT (LOGARITHMIC SCALES).

proportionality depends upon the lamp intensity, the geometry of the optics, the receiver sensitivity, and, to some extent (e.g. in rain), the obstruction to vision.

The primary question concerning FSM's is how well the constant K_1 in Equation 3 can be kept at unity. The offset D_1 is normally very small for a forward-scatter meter which uses a chopped light source. Only if the background light fluctuations are large enough to cause clipping in the electronics will a significant value of D be generated. Such clipping generally occurs only under sunny conditions. It is usually of short duration (a few minutes) and can be minimized by proper sensor siting.

5.2.1.2 Transmissometer

The transmissometer is subject to errors in both slope (K) and offset (D). The slope errors, in contrast to the FSM, are not likely to be large. The first potential source of slope error is the use of light outside the visible range. The extensive use of infrared light in U.S. sensors, both FSM's and transmissometers, could conceivably introduce errors under haze conditions. A second potential source of slope error in transmissometers is due to forward-scattered light being collected by the receiver. This error leads to an overestimate of the visibility. Forward-scatter errors are most troublesome for very short baselines where the receiver field of view must be large to include the full transmitted beam. One can show that the forward-scatter error introduces a fixed percentage error in slope K if one considers only single scattering and a fixed droplet size distribution. (See Appendix E.)

For high visibilities the most important transmissometer error involves the light setting corresponding to 100-percent transmittance. Errors in 100-percent setting produce an offset D in measured extinction coefficient, which can be readily calculated. The basic equation for the transmissometer is:

$$T = \exp(-\sigma b) \quad (4)$$

where T is the transmittance, b is the baseline and σ is the extinction coefficient averaged along the baseline. This equation can be rearranged to give

$$\sigma = -(\ln T)/b. \quad (5)$$

If "f" is the measured transmittance when there is no loss in the atmosphere (T=1.00) (i.e.,f = the 100-percent calibration) then the measured transmittance is

$$T_m = Tf. \quad (6)$$

The measured extinction coefficient is obtained by combining Equations 2, 3, and 4:

$$\sigma_m = \sigma - (\ln f)/b. \quad (7)$$

The offset is thus identified as

$$D = -(\ln f)/b. \quad (8)$$

Contributing to the 100-percent error are (1) window contamination, (2) calibration error, (3) lamp drift, and (4) receiver drift. In state-of-the-art transmissometers the drifts are relatively unimportant in producing offsets. The calibration error can be important for long baselines. Window contamination and calibration error are thus the dominant sources of offset error.

The one remaining transmissometer error is background light, the effect of which is not simply an offset or a slope error. Background light produces an offset error for high transmittances but the error increases for smaller transmittances.

5.2.1.3 Least-Square Fit

The fact that most sensor systematic errors can be described by Equation 3 means that a linear-least-square fit to the measurements of two sensors can be used to identify relative systematic errors. In this case the extinction coefficient measurements of the two sensors, 1 and 2, are fitted to the equation:

$$\sigma_1 = K_{12}\sigma_2 + D_{12} \quad (9)$$

where K_{12} will be the ratio of K_1 and K_2 and D_{12} will be approximately $D_1 - D_2$ for K_1 and K_2 near unity. This method yields an additional bonus that the residual error in σ_1 can be used as a measurement of the sensor disagreement.

The least-square fit method will be illustrated by the fog event shown in Figure 5-2 which will be termed Event #1. This event was selected because the visibility is slowly varying so that sensor comparisons should have relatively little scatter. Actually, Figure 5-2 shows only part of the event which lasts from 2000 on 6/16 to 0700 on 6/17. The airport surface observations were used to verify the lack of precipitation during this event.

Figure 5-3 shows extinction coefficient scatter plots for Event #1 comparing the measurements of the two 1000-foot baseline transmissometers, RVV-700 and RVR-500. The dashed lines in the plots correspond to ± 15 percent disagreements. The solid line is the linear least-square fit to the measurements. There is a considerable offset "D" in this case and also the slope "K" is less than one. Table 5-1 contains the numerical information of the fit. The top line of the table represents the fit plotted in Figure 5-3 (K=0.896, D=6.11). It includes all the data points. The other lines in the table represent least-square fits to selected ranges of the data. The extinction-coefficient range is listed on the left and the corresponding daytime-visibility range on the right. These are the ranges for sensor 2 which is plotted on the X-axis of the scatter plot.

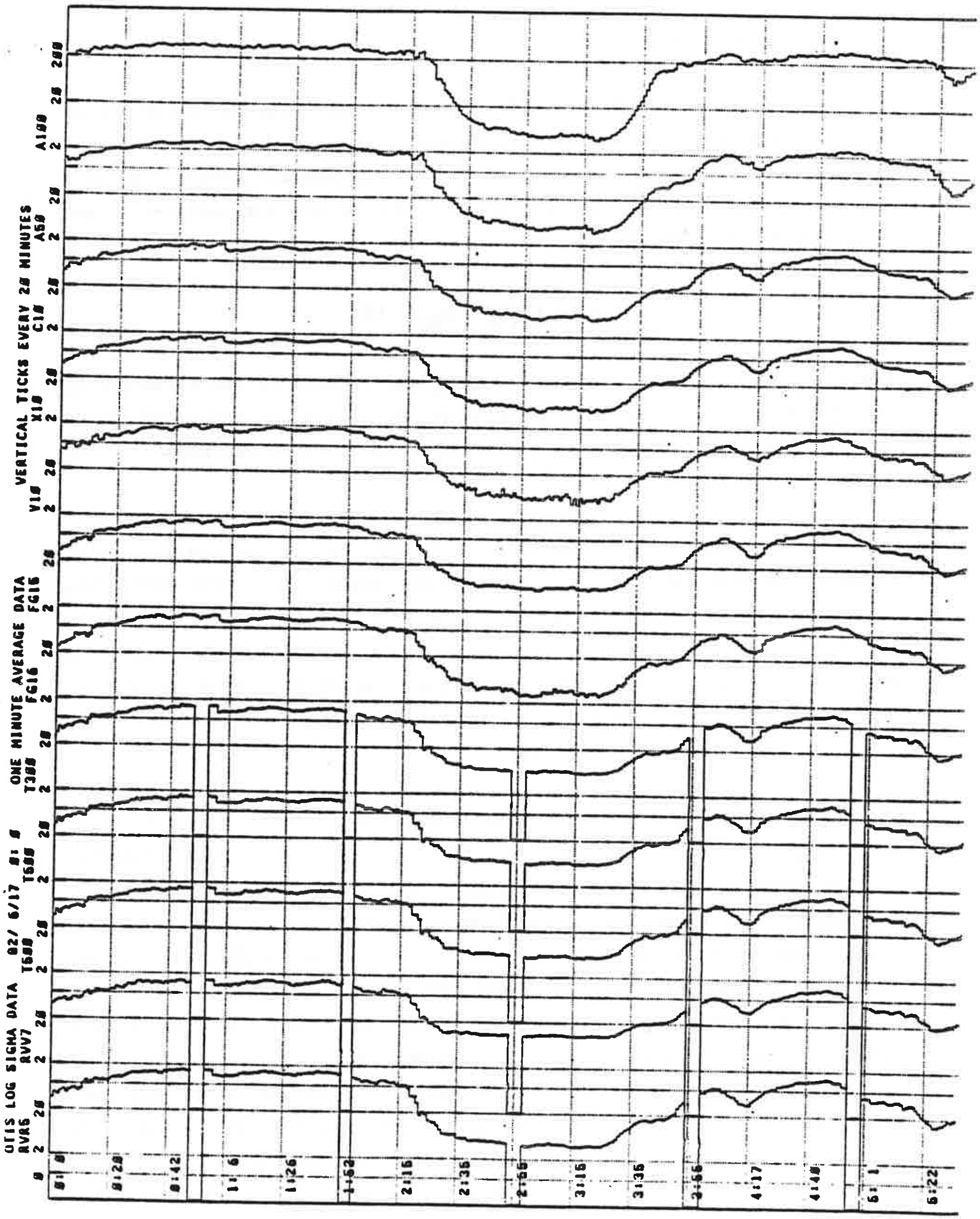

FIGURE 5-2. EXTINCTION COEFFICENT STRIPCHART FOR PART OF EVENT #1. The dropouts for the Transmissometers Occur During the Background check.

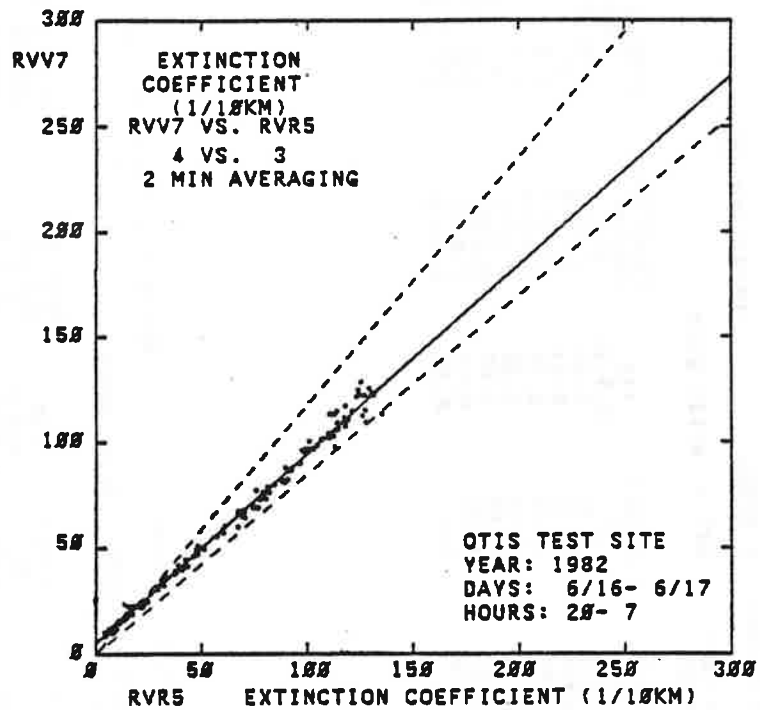

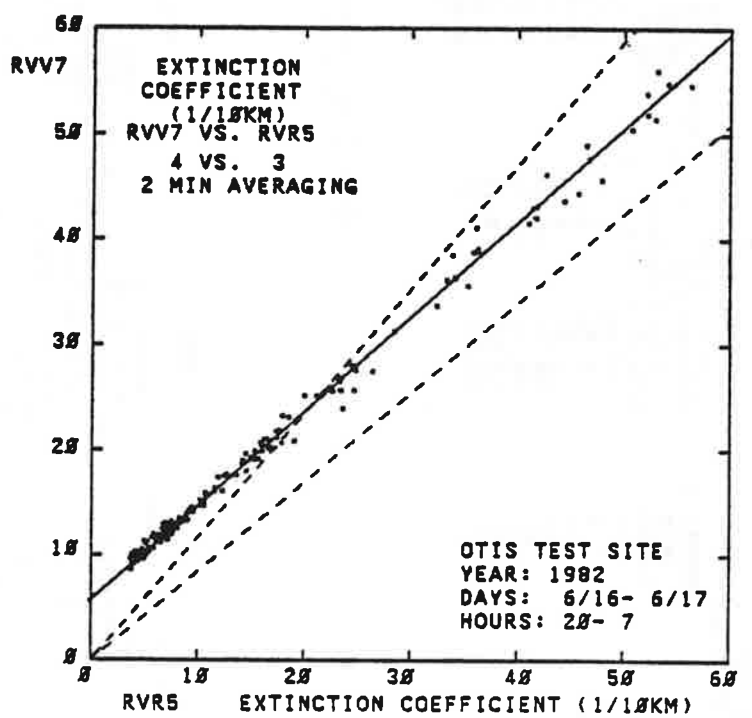

FIGURE 5-3. EXTINCTION COEFFICIENT SCATTER PLOTS FOR FOG EVENT #1. RVV-700 versus RVR 500, 1000-foot Baselines. Note the Different Scales on the Two Plots.

TABLE 5-1. LINEAR LEAST-SQUARE FITS TO EVENT #1:
RVV-700 versus 1000-FOOT RVR 500.

NO CORRECTIONS

OT82Ø6.16

5Ø2

1ST: SENSOR 4 RVV7
K1= 1.ØØØ

2ND: SENSOR 3
D1= Ø.ØØ

K2= 1.ØØØ RVR5

D2= Ø.ØØ

YEAR: 1982

AVERAGING INTERVAL= 2 MINS.

DAYS: 6/16- 6/17

HSTART=2Ø HSTOP= 7

DATA LIMITS	QUANTITY DATA POINTS	AVERAGE EXTINCTION COEFFICIENTS SENSOR 1	SENSOR 2	CORRELATION COEFFICIENT R	SLOPE K	OFFSET D	FIT R.S.D.	FRACTION SENSOR 1 R.S.D.	VISIBILITY LIMITS (MILES)
Ø.6Ø-1ØØØ.	296	4Ø.56	38.44	Ø.998	Ø.896	6.11	2.46	Ø.Ø6Ø8	Ø - 3Ø
Ø.6Ø - 38.	2Ø3	14.93	9.77	Ø.995	Ø.882	6.31	Ø.64	Ø.Ø429	Ø.5 - 3Ø
Ø.6Ø - 12.67	156	11.84	6.27	Ø.974	Ø.889	6.26	Ø.45	Ø.Ø378	1.5 - 3Ø
38.Ø-1ØØØ.	93	96.52	1Ø1.Ø3	Ø.991	Ø.9Ø7	4.86	4.3Ø	Ø.Ø446	Ø - Ø.5
12.67-38.Ø	47	25.18	21.39	Ø.986	Ø.877	6.43	1.Ø7	Ø.Ø424	Ø.5 - 1.5
7.6-12.67	37	14.59	9.43	Ø.956	Ø.927	5.85	Ø.44	Ø.Ø3Ø1	1.5 - 2.5
3.45-7.6	119	1Ø.98	5.29	Ø.92Ø	Ø.92Ø	6.11	Ø.46	Ø.Ø41Ø	2.5 - 5.5

OFFSET AND SLOPE CORRECTIONS

OT82Ø6.16

5Ø2

1ST: SENSOR 4 RVV7
K1= 1.1ØØ

2ND: SENSOR 3
D1= -6.7Ø

K2= 1.ØØØ RVR5

D2= Ø.ØØ

YEAR: 1982

AVERAGING INTERVAL= 2 MINS.

DAYS: 6/16- 6/17

HSTART=2Ø HSTOP= 7

DATA LIMITS	QUANTITY DATA POINTS	AVERAGE EXTINCTION COEFFICIENTS SENSOR 1	SENSOR 2	CORRELATION COEFFICIENT R	SLOPE K	OFFSET D	FIT R.S.D.	FRACTION SENSOR 1 R.S.D.	VISIBILITY LIMITS (MILES)
Ø.6Ø-1ØØØ.	296	37.91	38.44	Ø.998	Ø.986	Ø.Ø1	2.71	Ø.Ø716	Ø - 3Ø
Ø.6Ø - 38.	2Ø3	9.71	9.77	Ø.995	Ø.969	Ø.24	Ø.71	Ø.Ø729	Ø.5 - 3Ø
Ø.6Ø - 12.67	156	6.31	6.27	Ø.973	Ø.976	Ø.19	Ø.5Ø	Ø.Ø79Ø	1.5 - 3Ø
38.Ø-1ØØØ.	93	99.47	1Ø1.Ø3	Ø.991	Ø.998	-1.37	4.74	Ø.Ø476	Ø - Ø.5
12.67-38.Ø	47	2Ø.99	21.39	Ø.986	Ø.964	Ø.37	1.18	Ø.Ø561	Ø.5 - 1.5
7.6-12.67	37	9.35	9.43	Ø.956	1.Ø15	-Ø.22	Ø.48	Ø.Ø516	1.5 - 2.5
3.45-7.6	119	5.37	5.29	Ø.917	1.Ø11	Ø.Ø3	Ø.5Ø	Ø.Ø938	2.5 - 5.5

The value of D=6 in the least-square fit of Figure 5-3 corresponds to a value f=0.87 according to Equation 8. This loss of 13 percent in the 100-percent calibration is consistent with the measurement two days later of a realignment gain of 12 percent coupled with a recalibration gain of 6 percent.

Figure 5-4 (a, c) shows the effect on daytime visibility of the systematic errors shown in Figure 5-3. The large offset causes a big error for visibilities above one mile.

The software for generating scatter plots allows for the correction of systematic errors by means of the equation:

$$\sigma_{cor} = K\sigma_{meas} + D \quad (10)$$

The values K = 1.1 and D= -6.7 correct the RVV-700 data of Figure 5-3 to give the results of Figure 5-5 which show no systematic errors. Table 5-1 shows the least-square fits for these corrections. Figures 5-4b, d show the corresponding corrected visibility plots.

5.2.2. Random Errors

Random errors in visibility measurements can arise from a number of sources. The first is the intrinsic noise of the sensor. The second is the statistical fluctuations which occur when there are few particles within the sample volume sensed (relevant to rain and snow). The third is spatial variations in the extinction coefficient. All random errors can be reduced by averaging for a longer period of time. The second and third source of error can also be reduced by averaging over a larger volume of space.

The least-square fit method described in the last section can be used to measure the random variation between two sensors. The residual standard deviation (R.S.D) errors listed in Table 5-1 represent the

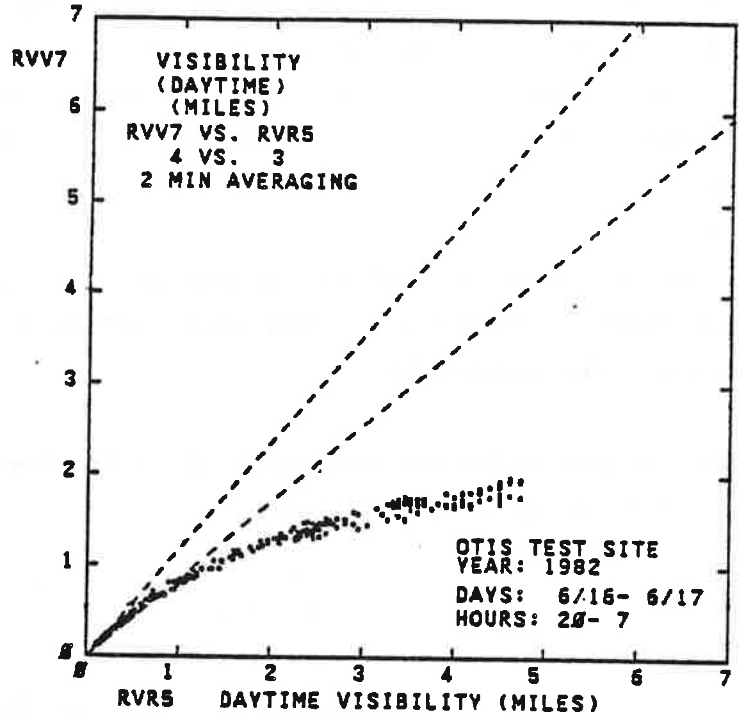

(a)

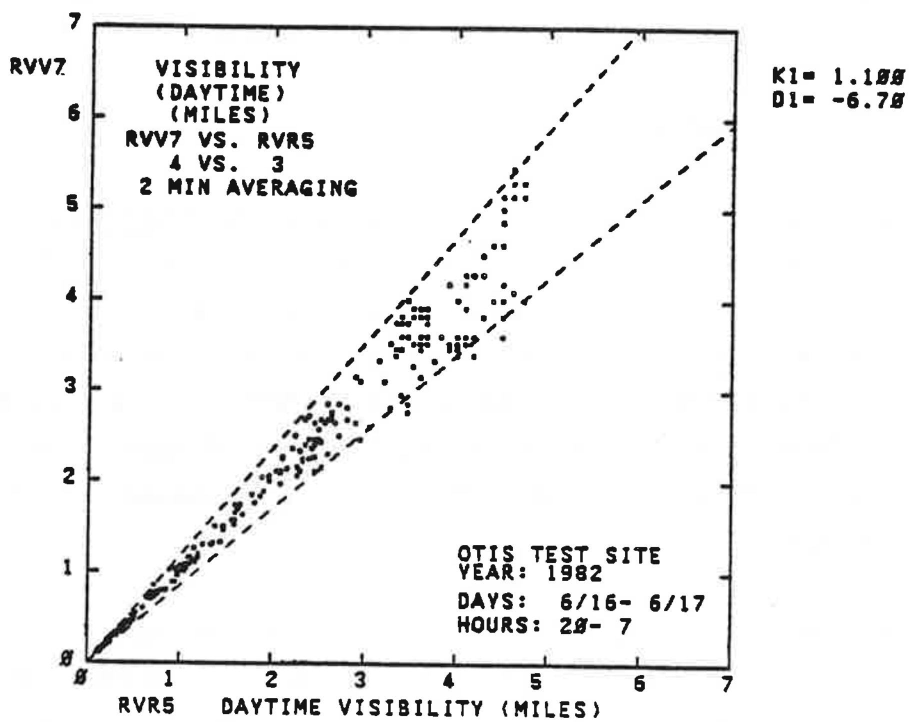

(b)

FIGURE 5-4. VISIBILITY SCATTER PLOTS FOR EVENT #1: RVV-700 versus 1000-FOOT RVR 500: (a), (c) UNCORRECTED: (b), (d) CORRECTED.

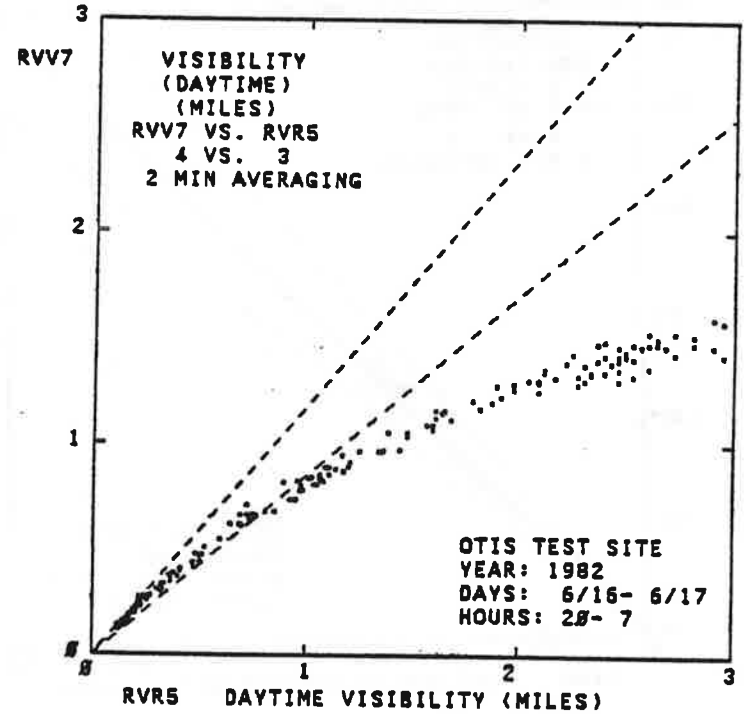

(c)

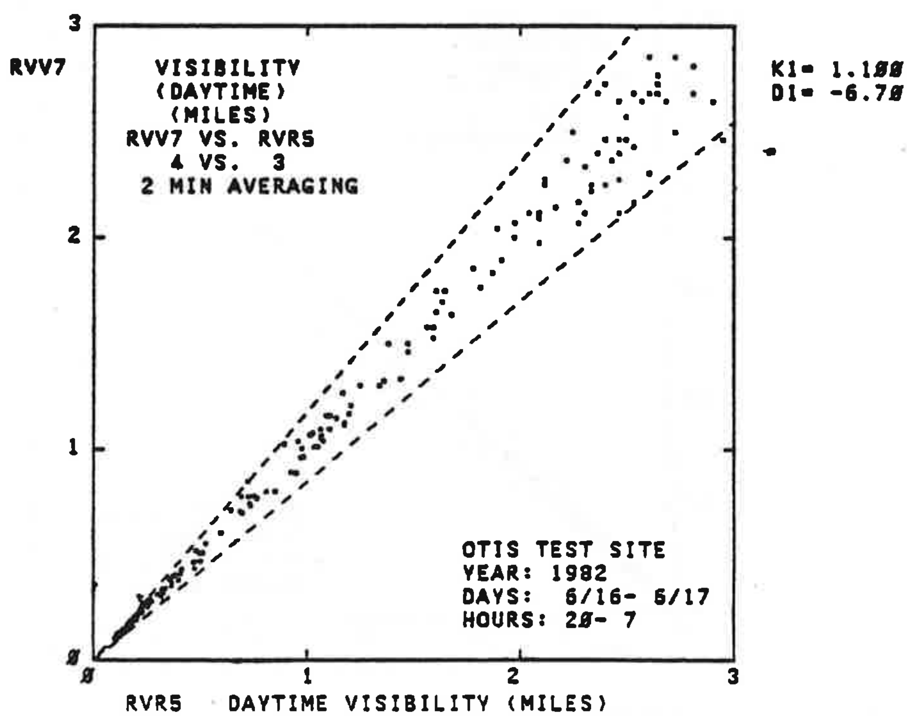

(d)

FIGURE 5-4. (concluded)

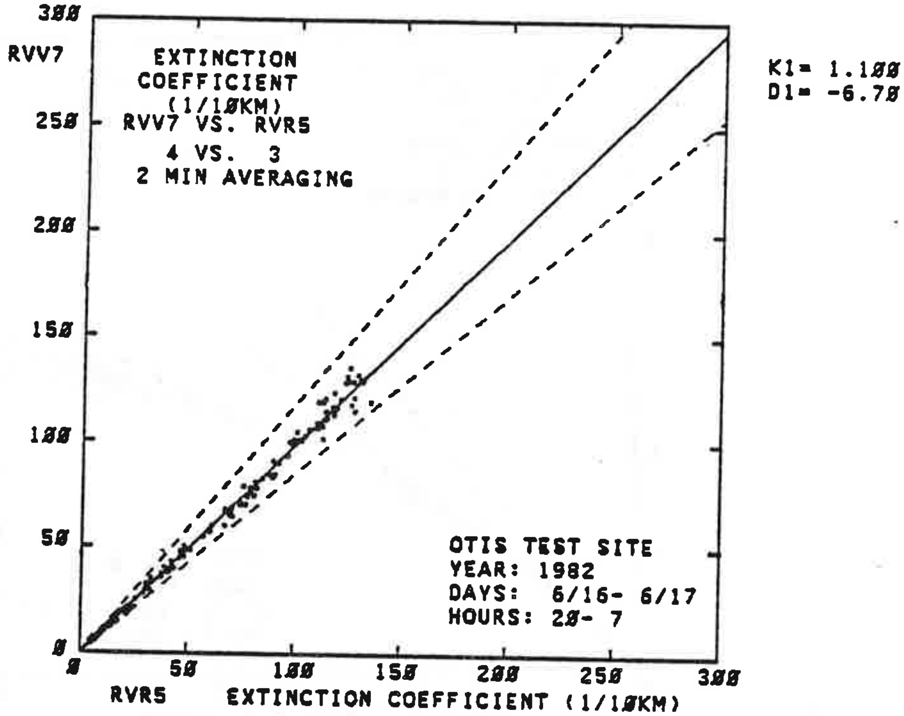

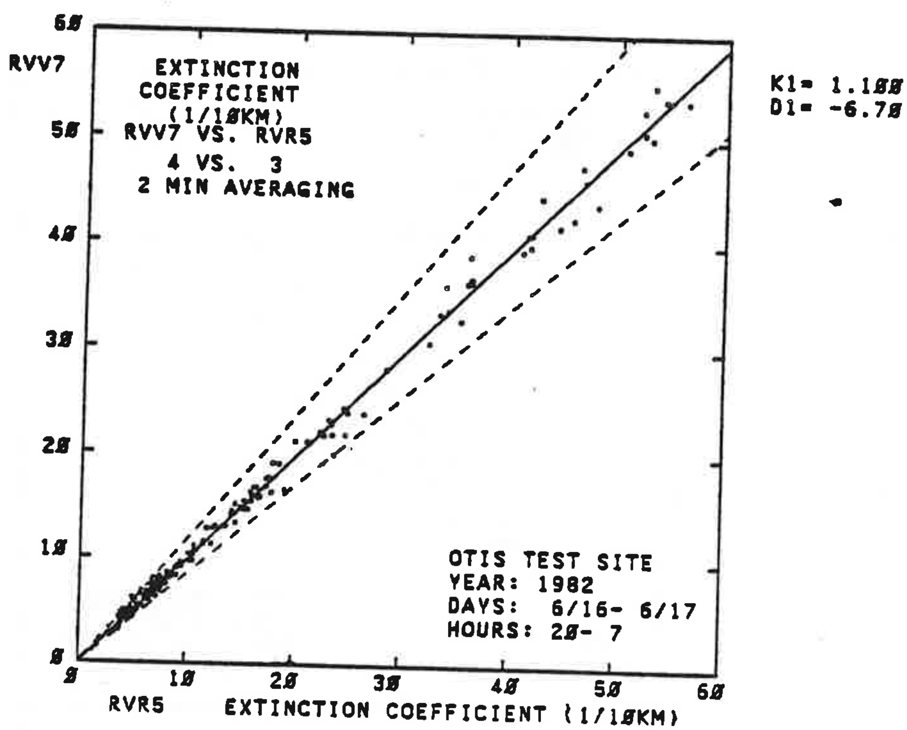

FIGURE 5-5. EXTINCTION COEFFICIENT SCATTER PLOTS FOR EVENT #1. RVV-700 versus 1000-Foot RVR 500; WITH RVV-700 CORRECTIONS.

variation in σ_1 which is not explained by Equation 3. Because the variation tends to be a fraction of the extinction coefficient, it is useful to divide the rms error of σ_1 by the mean value of σ_1. The resulting fraction sensor 1 R.S.D. errors are listed in the second to last column of Table 5-1. This normalization also allows the comparisons of rms errors for different sensors to be independent of slope (K) errors.

5.2.3 Additional Analysis Techniques

Fractional errors are more easily visualized on logarithmic scatter plots than on the linear plots of Figure 5-3,4,5. Figure 5-6 shows both extinction coefficient and visibility plots of the same data. Again the dashed lines represent disagreements of ± 15 percent. The slope error K causes the data lines to be displaced from the diagonal of the plots. The offset error D causes the data lines to curve on the log-log plots.

According to Equation 1, 3 and 8, the fractional error in visibility or extinction coefficient be represented as:

$$(V_m-V)/V_m = (\sigma-\sigma_m)/\sigma = (\ln f)V/2.9b \quad (11)$$

Since the 100-percent calibration errors (lnf) are similar for all transmissometers, the fractional errors depend upon the ratio of the visibility to the baseline (V/b). Errors in background correction also lead to fractional errors depending only on V/b. Figure 5-7 shows a plot of fractional error (Equation 11) versus V/b for the two 1000-foot transmissometers for Event #1. When the systematic errors are corrected (Figure 5-7b) the fractional error becomes almost independent of V/b.

The implementation of the pass/fail criteria for this report requires a comparison of the reporting values for the test sensor compared to a standard sensor which is taken to be the 1000-foot RVR-500 transmissometer (termed "RVR5"). Table 5-2 shows the form of such a

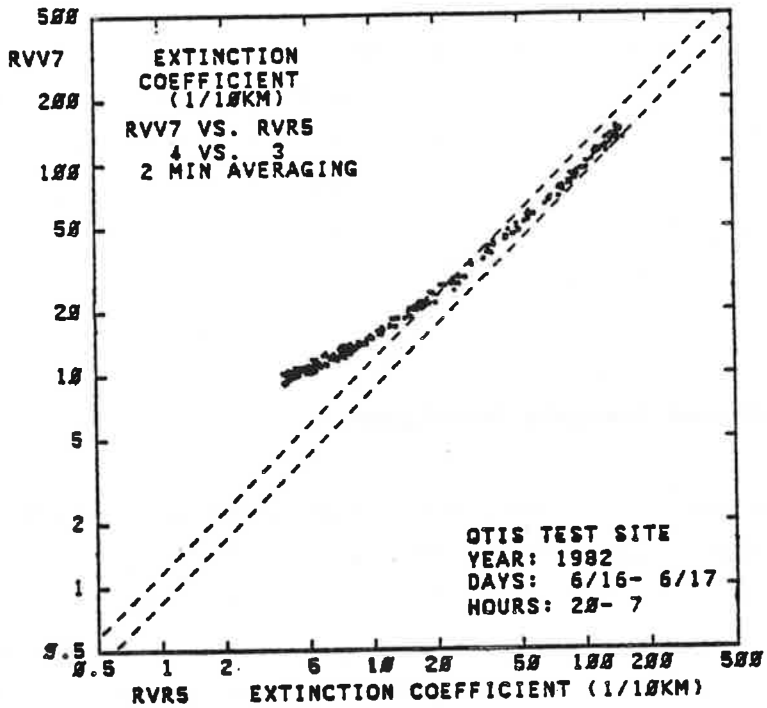

(a)

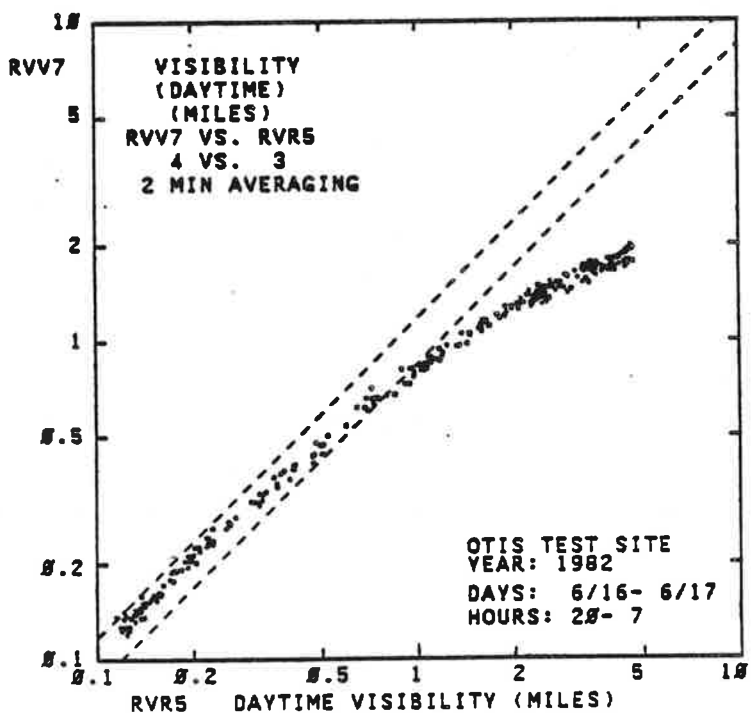

(b)

FIGURE 5-6. LOGARITHMIC SCATTER PLOTS FOR EVENT #1.
RVV-700 versus RVR 500: NO CORRECTIONS:
(a) EXTINCTION COEFFICIENT; (b) VISIBILITY.

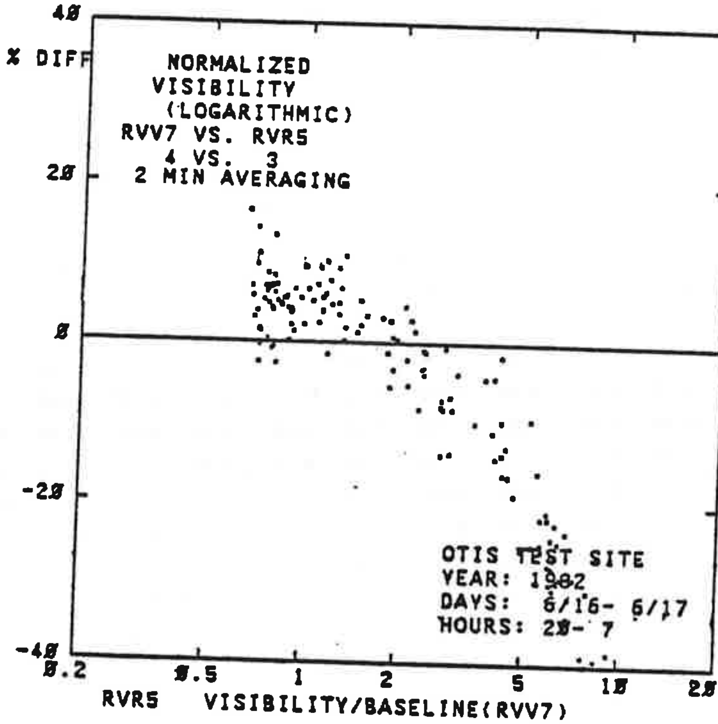

(a)

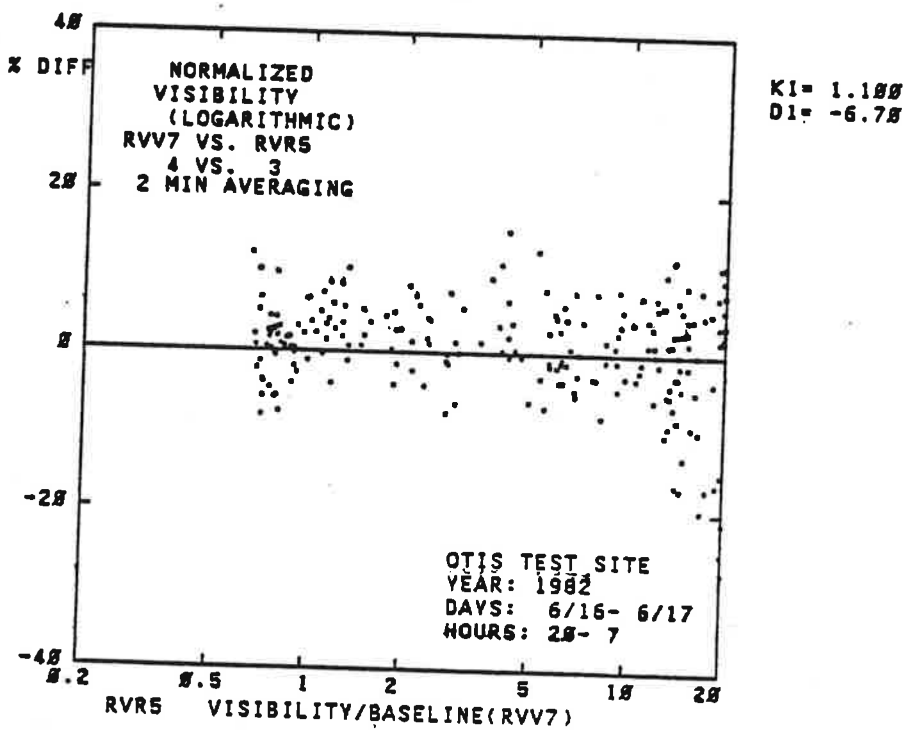

(b)

FIGURE 5-7. FRACTIONAL ERROR versus (VISIBILITY/BASELINE) FOR THE TWO 1000-FOOT TRANSMISSOMETERS FOR EVENT #1.

TABLE 5-2. REPORTING VALUE SCATTER TABLE FOR EVENT #1: RVV-700 VERSUS 1000-FOOT RVR 500: CORRECTED DATA

VISIBILITY COUNT FRACTION

FILE: OT8206.16 RVV7 VS. RVR5 SITE: OTIS YEAR: 1982 DAYS: 6/16- 6/17 HOURS: 20- 7

AVERAGING 2

K1= 1.100
D1= -6.7

		<1/4	1/4	1/2	3/4	1.00	1.25	1.50	2.00	2.50	3.00	4	5	>5
	TOTALS:	57	27	16	12	18	9	12	17	35	29	45	19	0
	>6:	0.00	0.00	0.00	0.00	0.00	0.00	0.00	0.00	0.00	0.00	0.00	0.00	[0.00]
	5:	0.00	0.00	0.00	0.00	0.00	0.00	0.00	0.00	0.00	0.00	0.07	[0.63]	0.00
	4:	0.00	0.00	0.00	0.00	0.00	0.00	0.00	0.00	0.00	0.41	[0.73]	0.37	0.00
RVV7	3.00:	0.00	0.00	0.00	0.00	0.00	0.00	0.00	0.00	0.09	[0.45]	0.20	0.00	0.00
	2.50:	0.00	0.00	0.00	0.00	0.00	0.00	0.00	0.24	[0.74]	0.14	0.00	0.00	0.00
DAY	2.00:	0.00	0.00	0.00	0.00	0.00	0.00	0.00	[0.76]	0.17	0.00	0.00	0.00	0.00
	1.50:	0.00	0.00	0.00	0.00	0.00	0.00	[0.92]	0.00	0.00	0.00	0.00	0.00	0.00
	1.25:	0.00	0.00	0.00	0.00	0.11	[0.89]	0.00	0.00	0.00	0.00	0.00	0.00	0.00
	1.00:	0.00	0.00	0.00	0.00	[0.89]	0.11	0.00	0.00	0.00	0.00	0.00	0.00	0.00
	3/4:	0.00	0.00	0.00	[1.00]	0.00	0.00	0.00	0.00	0.00	0.00	0.00	0.00	0.00
	1/2:	0.00	0.07	[1.00]	0.00	0.00	0.00	0.00	0.00	0.00	0.00	0.00	0.00	0.00
	1/4:	0.05	[0.89]	0.00	0.00	0.00	0.00	0.00	0.00	0.00	0.00	0.00	0.00	0.00
	<1/4:	[0.95]	0.04	0.00	0.00	0.00	0.00	0.00	0.00	0.00	0.00	0.00	0.00	0.00
		<1/4	1/4	1/2	3/4	1.00	1.25	1.50	2.00	2.50	3.00	4	5	>5

RVR5

		<1/4	1/4	1/2	3/4	1.00	1.25	1.50	2.00	2.50	3.00	4	5	>5
	TOTALS:	0	45	28	17	9	9	11	18	14	20	39	48	41
	>6:	0.07	0.00	0.00	0.00	0.00	0.00	0.00	0.00	0.00	0.00	0.00	0.04	[0.68]
	5:	0.00	0.00	0.00	0.00	0.00	0.00	0.00	0.00	0.00	0.00	0.03	[0.84]	0.32
	4:	0.00	0.00	0.00	0.00	0.00	0.00	0.00	0.00	0.00	0.15	[0.74]	0.11	0.00
RVV7	3.00:	0.00	0.00	0.00	0.00	0.00	0.00	0.00	0.00	0.14	[0.85]	0.23	0.00	0.00
	2.50:	0.00	0.00	0.00	0.00	0.00	0.00	0.00	0.00	[0.64]	0.00	0.00	0.00	0.00
NITE	2.00:	0.00	0.00	0.00	0.00	0.00	0.00	0.27	[1.00]	0.21	0.00	0.00	0.00	0.00
	1.50:	0.00	0.00	0.00	0.00	0.00	0.44	[0.73]	0.00	0.00	0.00	0.00	0.00	0.00
	1.25:	0.00	0.00	0.00	0.00	0.00	[0.56]	0.00	0.00	0.00	0.00	0.00	0.00	0.00
	1.00:	0.00	0.00	0.00	0.00	[1.00]	0.00	0.00	0.00	0.00	0.00	0.00	0.00	0.00
	3/4:	0.00	0.00	0.00	[1.00]	0.00	0.00	0.00	0.00	0.00	0.00	0.00	0.00	0.00
	1/2:	0.00	0.02	[1.00]	0.00	0.00	0.00	0.00	0.00	0.00	0.00	0.00	0.00	0.00
	1/4:	0.00	[0.98]	0.00	0.00	0.00	0.00	0.00	0.00	0.00	0.00	0.00	0.00	0.00
	<1/4:	[0.00]	0.00	0.00	0.00	0.00	0.00	0.00	0.00	0.00	0.00	0.00	0.00	0.00
		<1/4	1/4	1/2	3/4	1.00	1.25	1.50	2.00	2.50	3.00	4	5	>5

RVR5

comparison. Two scatter tables are generated from the measured extinction coefficients, the first using the daytime visibility equation (Equation 1) and the second using the nighttime equation (Equation 2). The top line of each scatter table shows the total number of measurements falling in each reporting increment (listed at the bottom of the column) for the standard sensor (RVR5 in this case). The numbers in the body of the table represent the fraction of the time the test sensor (RVV7) has the reporting values listed in the left column. The fraction of time that the reporting values are identical is enclosed in brackets to make the table easier to read. Even though the systematic errors have been corrected in Table 5-2, the random errors still produce some disagreements in reporting values. No error larger than one increment is observed in this case.

Figure 5-8 shows the extinction coefficient strip chart for Event #2 which consisted of rain which may have had some fog mixed in. Figure 5-9 shows the visibility scatter plots for this event for the two 1000-foot transmissometers. The remarkable feature of this event is the close agreement of the two sensors, In contrast to Event #1 (Figure 5-4), there is no significant slope error or offset and very little scatter.

5.3 RVV-700

As discussed above, the measurement accuracy of a transmissometer depends upon the ratio of the visibility to the baseline. Figures 5-10, shows how well the RVR-700 ("NTAS") agreed with the RVR-500 ("OTAS") during the Arcata tests. The percentage error is plotted against the visibility divided by the baseline of 720 feet. Figure 5-10 shows one month's data collected with background checks on the RVV-700. Almost no low visibilities occurred. Figure 5-11a shows the next month's data where the RVV-700 background checks were disabled. The data consistency is much improved in Figure 5-11b where only night data are plotted. One can draw the following conclusions from the plot Figure 5-11b:

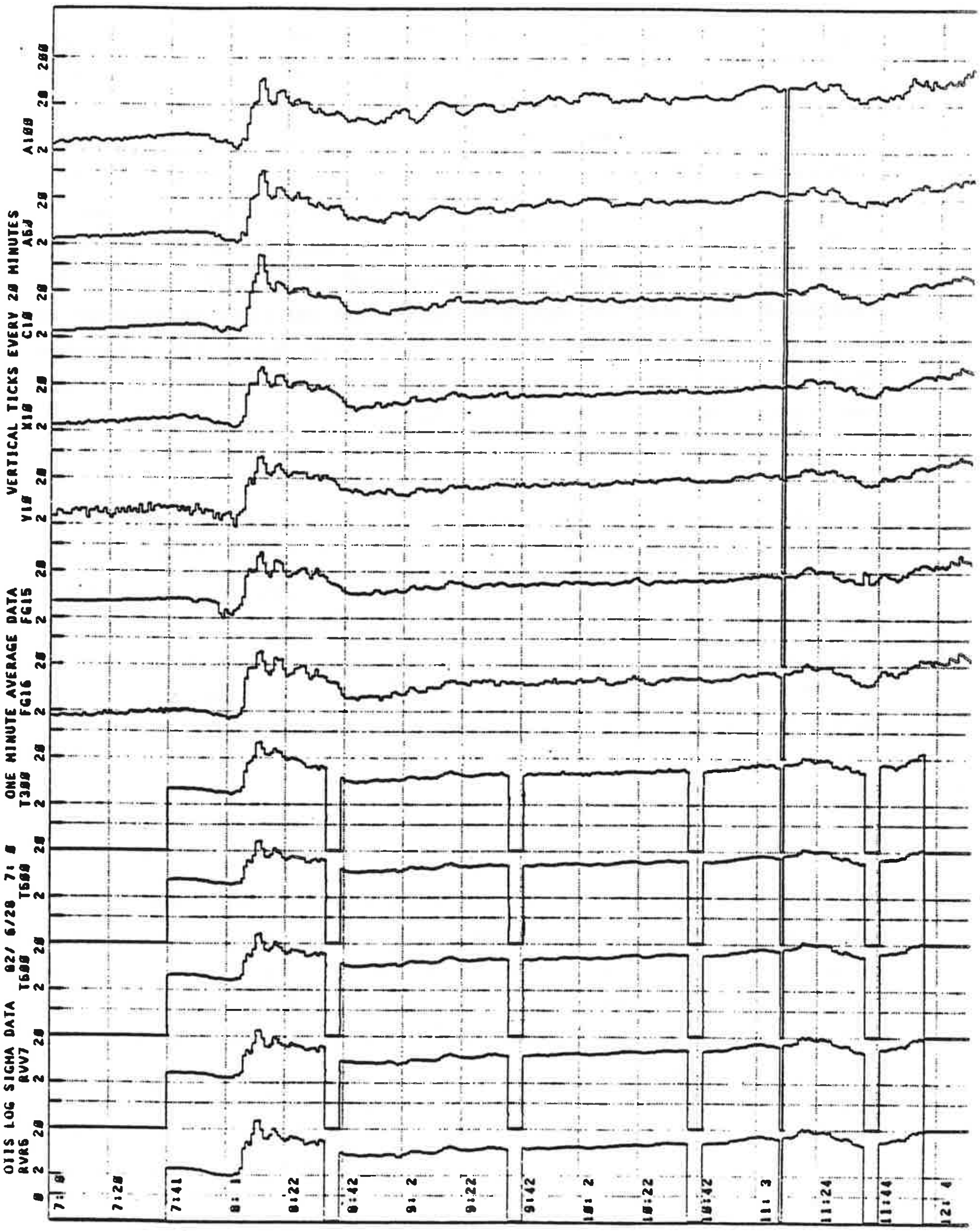

FIGURE 5-8. EXTINCTION COEFFICIENT STRIPCHART FOR EVENT #2 (0900-1200).

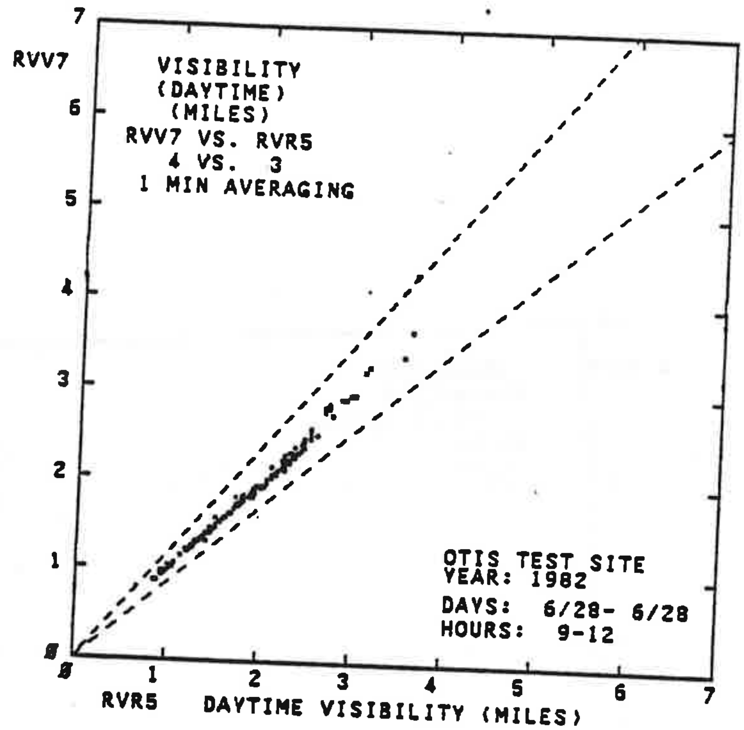

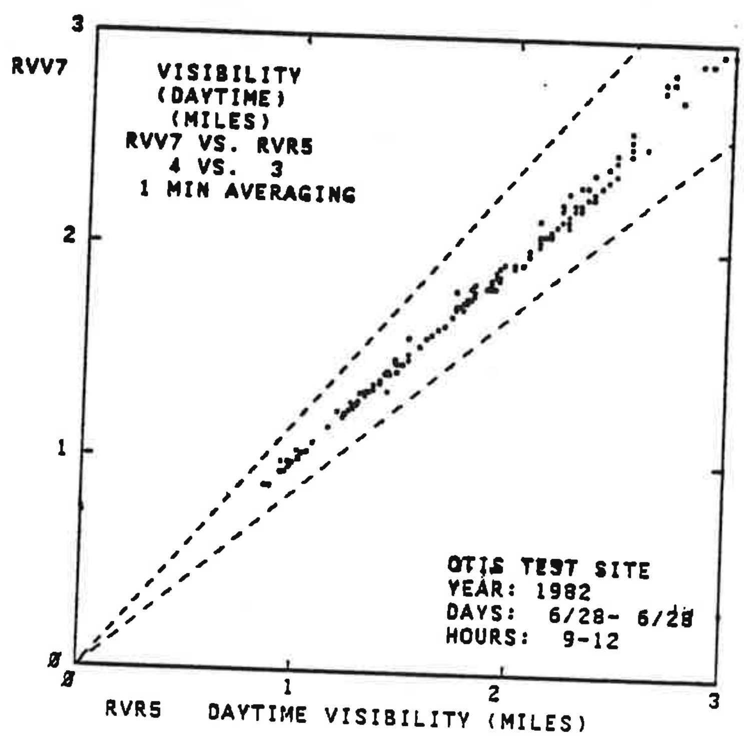

FIGURE 5-9. VISIBILITY SCATTER PLOTS FOR EVENT #2: RVV-700 versus 1000-FOOT RVR 500.

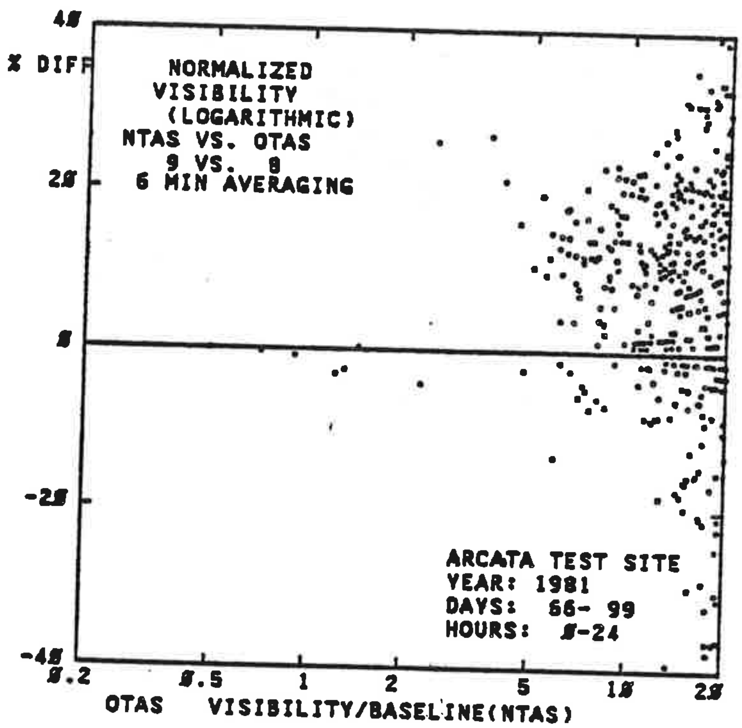

FIGURE 5-10. NORMALIZED VISIBILITY ACCURACY: RVV-700 with BACKGROUND CHECKS.

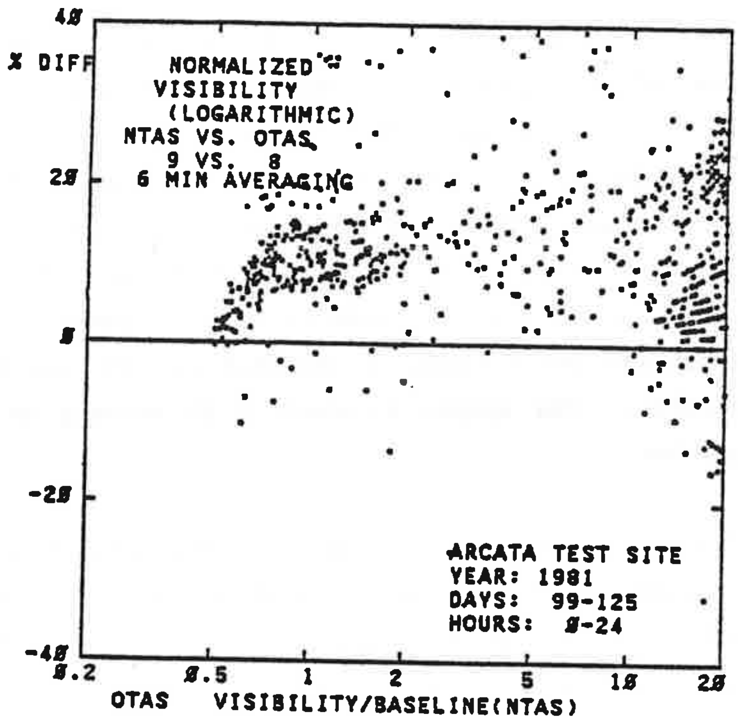

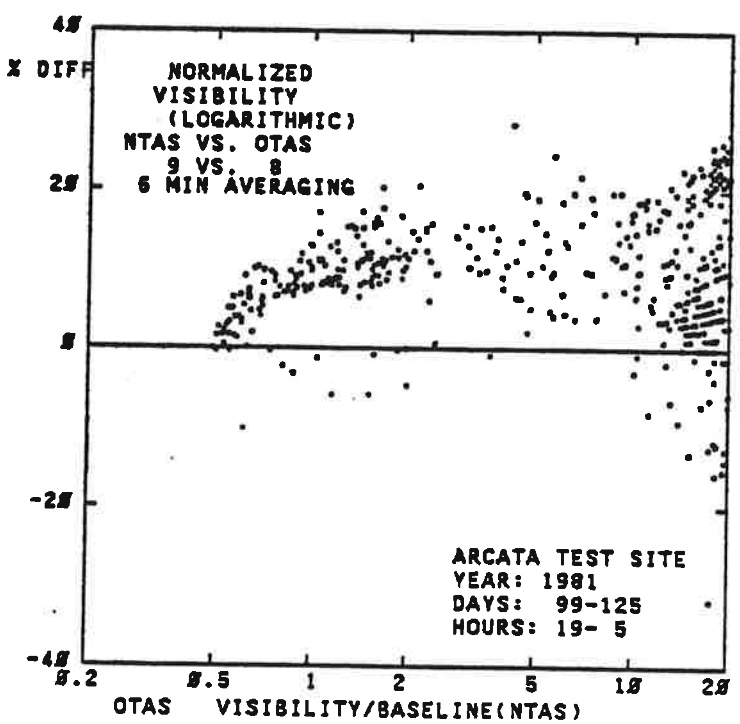

FIGURE 5-11. NORMALIZED VISIBILITY ACCURACY:
RVV-700 WITHOUT BACKGROUND CHECKS: (a) ALL DATA,
(b) NIGHT DATA.

1) The RVV-700 visibilities are 10 percent higher with a variation of ± 10 percent for normalized visibilities between 0.7 and 10 times the baseline.
2) The two units tend to agree better between 0.5 and 0.7 times the baseline where they are both receiving very little light from the projector. No data exist below 0.5 times the baseline where the transmittance is only 0.3 percent.
3) The percentage error tends to increase rapidly above 10 times the baseline. The spread is about ± 20 percent at 20 times the baseline.

Figure 5-12 shows normalized RVV-700 accuracy data from Otis for the two 10-day periods where data were available and the alignment was stable. The bad data points in Figure 5-12a are probably due to extremely inhomogeneous fog conditions. The July data in Figure 5-12b correlate better than the June data and also better than the Arcata data; they probably represent the optimum sensor performance since both the 100-percent calibration and the alignment were stable for this period.

The normalization of transmissometer data can also be done on the shorter baseline RVR-500 transmissometers at Otis. Figure 5-13 compares the 300-and 500-foot baselines with the 1000-foot baseline for the same period in Figure 5-12a. Note the sharp drop which occurs at the left where the 1000-foot baseline saturates, but the shorter baselines do not. Figure 5-14 comparing the 300-foot to the 500-foot baseline does not clip. The different RVR-500 baselines have smaller systematic differences than the 10-percent difference between the 1000-foot RVR-500 and RVV-700 in Figure 5-12.

5.3.1 Slope Discrepancy

The events illustrated in Section 5.3 were selected to illustrate the 10-percent slope discrepancy between the 1000-foot RVV-700 and RVR-500 transmissometers. The data of Event #1 are typical of most other

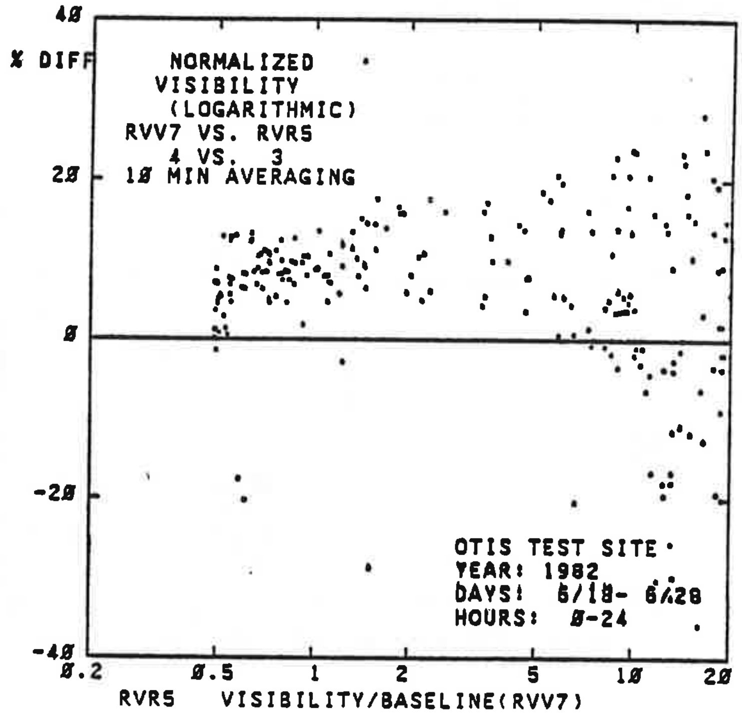

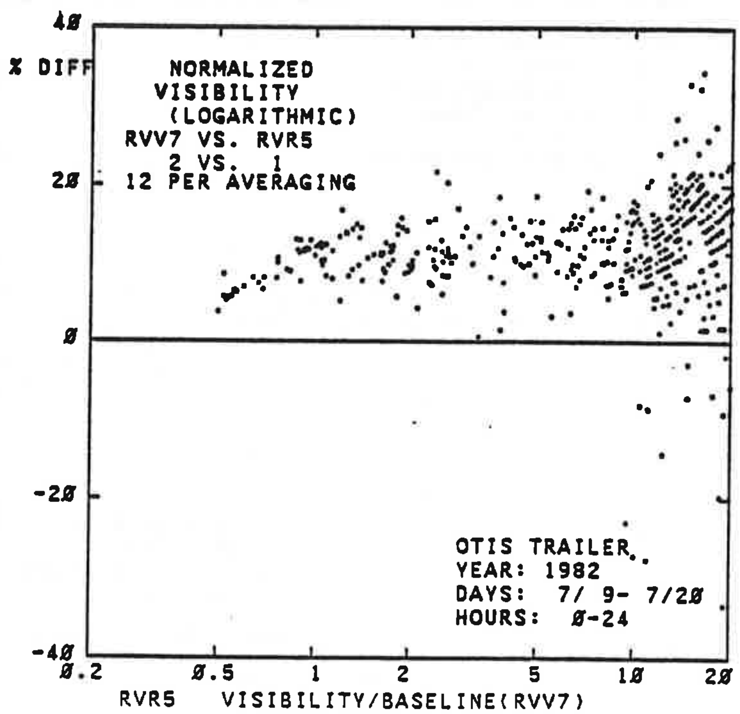

FIGURE 5-12. NORMALIZED VISIBILITY ACCURACY: RVV-700 versus RVR 500: 1000-FOOT BASELINES. (a) 6/18-6/28; (b) 7/9-7/20.

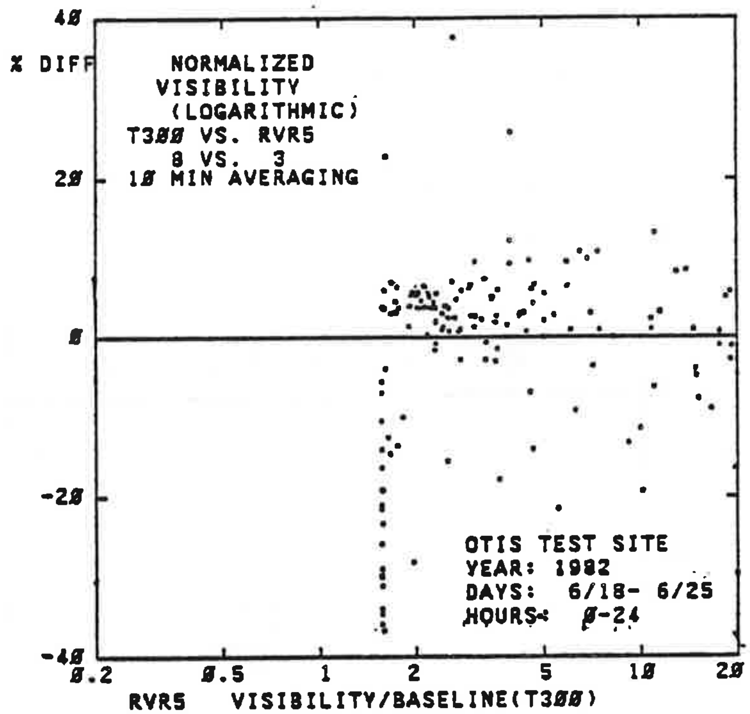

(a)

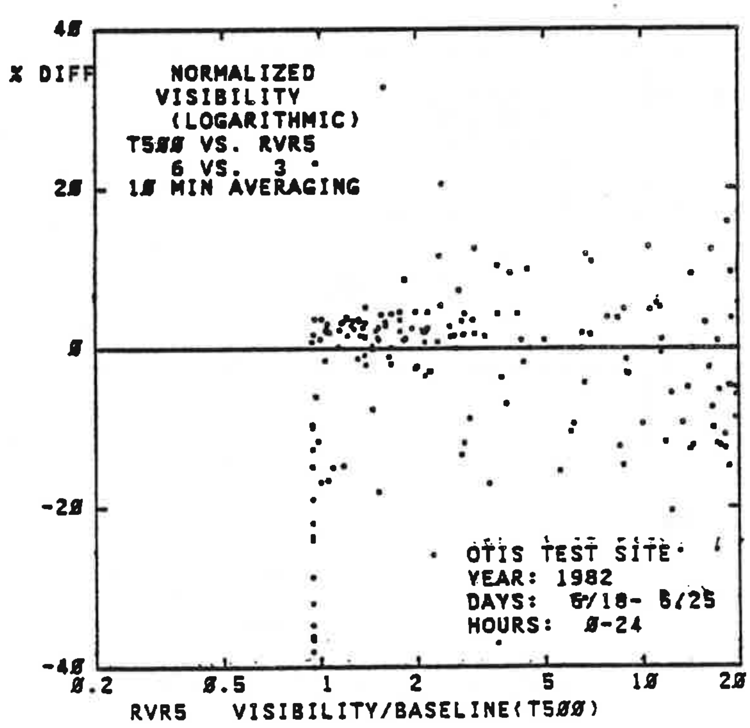

(b)

FIGURE 5-13. NORMALIZED VISIBILITY ACCURACY: (a) 300-FOOT RVR 500 and (b) 500-FOOT RVR 500 REFERENCED TO THE 1000-FOOT RVR 500.

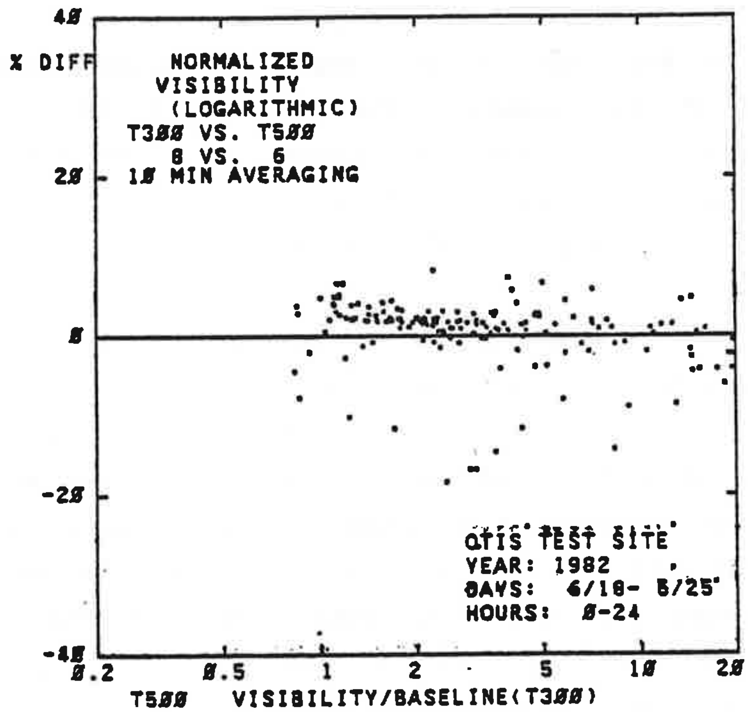

FIGURE 5-14. NORMALIZED VISIBILITY ACCURACY: 300-FOOT RVR 500 REFERENCED TO THE 500-FOOT RVR 500.

events in showing a 10-percent difference in slope and a fair amount of scatter. Event #2 was unique in showing exact agreement with little scatter between the two 1000-foot baseline transmissometers. The interpretation of these observations will be deferred to Section 6.1.

The data of Figure 5-12 are presented as reporting value scatter tables in Tables 5-3,4,5. Tables 5-3,5 include a 10-percent correction factor (K1 = 1.10). The data of Table 5-3 do not meet the pass/fail test (90 percent of the test sensor's reporting values within one reporting increment of the standard). The July data in Tables 5-4, 5 meet the pass/fail test both with and without the correction factor K1=1.10. A comparison of Tables 5-4 and 5-5 show that the 10-percent correction, however, does improve the agreement between the sensors.

The greater scatter in the June data (Figure 5-12a, Table 5-3) than the July data (Figure 5-13a, Tables 5-4,5 was first attributed to the receiver instability problem which was not cleared up until June 23. A closer examination showed that the instability problem made no major contribution to the observed differences. The majority of the disagreements in both June and July occurred under ground fog conditions where the fog was patchy according to the other visibility sensors. The RVV-700 actually read higher fog densities (points below the zero line in Figure 5-12) than the RVR-500 under these conditions, presumably because of its lower height coupled with a sharp decrease in fog density with height. Only one or two disagreements were associated with data recording glitches. A correlation of disagreement with background light variation was noted. Significant differences between the sensors (i.e., reporting values differing by more than one increment) were more likely to occur toward the end of the hour between background checks, particularly in the evening or morning when the background levels are changing. In this case the background errors add to the other errors present to make a significant disagreement more likely.

TABLE 5-3· SCATTER TABLE: 6/18-6/28: RVV-700 versus 1000-FOOT RVR 500

VISIBILITY COUNT FRACTION

FILE: OT0206.ALL RVV7 VS. RVR5 SITE: OTIS YEAR: 1982 DAYS: 6/10- 6/28 HOURS: 0-24

AVERAGING 10

K1= 1.100

	TOTALS:	102	31	14	11	14	10	26	22	22	25	39	45	1017
	>5:	0.00	0.00	0.00	0.00	0.00	0.00	0.00	0.00	0.00	0.00	0.03	0.33	[0.89]
	5:	0.00	0.00	0.00	0.00	0.00	0.00	0.00	0.00	0.00	0.00	0.23	[0.36]	0.03
	4:	0.00	0.00	0.00	0.00	0.00	0.00	0.00	0.00	0.00	0.12	[0.33]	0.20	0.01
RVV7	3.00:	0.00	0.00	0.00	0.00	0.00	0.00	0.00	0.05	0.23	[0.52]	0.31	0.11	0.00
	2.50:	0.00	0.00	0.00	0.00	0.00	0.00	0.00	0.09	[0.14]	0.20	0.10	0.00	0.00
DAY	2.00:	0.00	0.00	0.00	0.00	0.00	0.00	0.19	[0.23]	0.36	0.08	0.00	0.00	0.03
	1.50:	0.00	0.00	0.00	0.00	0.00	0.00	[0.50]	0.50	0.23	0.00	0.00	0.00	0.01
	1.25:	0.00	0.00	0.00	0.00	0.14	[0.50]	0.15	0.05	0.05	0.00	0.00	0.00	0.00
	1.00:	0.00	0.00	0.00	0.00	[0.71]	0.10	0.00	0.05	0.00	0.00	0.00	0.00	0.00
	3/4:	0.00	0.00	0.21	[0.64]	0.00	0.20	0.04	0.05	0.00	0.00	0.00	0.00	0.00
	1/2:	0.00	0.03	[0.43]	0.18	0.14	0.20	0.04	0.00	0.00	0.00	0.00	0.00	0.00
	1/4:	0.00	[0.71]	0.29	0.18	0.00	0.00	0.00	0.00	0.00	0.00	0.00	0.00	0.00
	<1/4:	[1.00]	0.26	0.07	0.00	0.00	0.00	0.00	0.00	0.00	0.00	0.00	0.00	0.00
		<1/4	1/4	1/2	3/4	1.00	1.25	1.50	2.00	2.50	3.00	4	5	>5

RVR5

	TOTALS:	0	07	38	12	4	8	14	19	22	27	30	30	1087
	>5:	0.00	0.00	0.00	0.00	0.00	0.00	0.00	0.00	0.00	0.00	0.00	0.20	[0.92]
	5:	0.00	0.00	0.00	0.00	0.00	0.00	0.00	0.00	0.00	0.04	0.13	[0.27]	0.02
	4:	0.00	0.00	0.00	0.00	0.00	0.00	0.00	0.00	0.00	0.07	[0.37]	0.50	0.01
RVV7	3.00:	0.00	0.00	0.00	0.00	0.00	0.00	0.00	0.00	0.14	[0.26]	0.33	0.03	0.03
	2.50:	0.00	0.00	0.00	0.00	0.00	0.00	0.00	0.11	[0.77]	0.48	0.17	0.00	0.01
NITE	2.00:	0.00	0.00	0.00	0.00	0.00	0.00	0.21	[0.53]	0.05	0.07	0.00	0.00	0.00
	1.50:	0.00	0.00	0.00	0.00	0.00	0.00	[0.43]	0.21	0.00	0.07	0.00	0.00	0.00
	1.25:	0.00	0.00	0.00	0.00	0.00	[0.62]	0.00	0.11	0.00	0.00	0.00	0.00	0.00
	1.00:	0.00	0.00	0.00	0.08	[0.25]	0.25	0.07	0.05	0.05	0.00	0.00	0.00	0.00
	3/4:	0.00	0.00	0.08	[0.75]	0.00	0.00	0.21	0.00	0.00	0.00	0.00	0.00	0.00
	1/2:	0.00	0.00	[0.76]	0.00	0.75	0.12	0.07	0.00	0.00	0.00	0.00	0.00	0.00
	1/4:	0.00	[0.71]	0.16	0.17	0.00	0.00	0.00	0.00	0.00	0.00	0.00	0.00	0.00
	<1/4:	[0.00]	0.29	0.00	0.00	0.00	0.00	0.00	0.00	0.00	0.00	0.00	0.00	0.00
		<1/4	1/4	1/2	3/4	1.00	1.25	1.50	2.00	2.50	3.00	4	5	>5

RVR5

TABLE 5-4. SCATTER TABLE: 7/9-720: RVV-700 versus 1000-FOOT RV 500: NO CORRECTION

VISIBILITY COUNT FRACTION:

FILE: OTIS82.ALL RVV7 VS. RVRS SITE: TRAILER YEAR: 1982 DAYS: 7/ 9- 7/2Ø HOURS: Ø-24

AVERAGING 12 PER

RVV7 DAY	RVRS:	<1/4	1/4	1/2	3/4	1.ØØ	1.25	1.5Ø	2.ØØ	2.5Ø	3.ØØ	4	5	>5
	TOTALS:	43	43	33	24	21	18	43	88	85	124	163	2ØØ	763
	>5:	Ø.ØØ	Ø.ØØ	Ø.ØØ	Ø.ØØ	Ø.ØØ	Ø.ØØ	Ø.ØØ	Ø.ØØ	Ø.ØØ	Ø.ØØ	Ø.Ø1	Ø.45	[Ø.96]
	5:	Ø.ØØ	Ø.ØØ	Ø.ØØ	Ø.ØØ	Ø.ØØ	Ø.ØØ	Ø.ØØ	Ø.ØØ	Ø.ØØ	Ø.Ø1	Ø.36	[Ø.43]	Ø.Ø4
	4:	Ø.ØØ	Ø.ØØ	Ø.ØØ	Ø.ØØ	Ø.ØØ	Ø.ØØ	Ø.ØØ	Ø.Ø2	Ø.Ø2	Ø.59	[Ø.58]	Ø.12	Ø.ØØ
RVV7	3.ØØ:	Ø.ØØ	Ø.ØØ	Ø.ØØ	Ø.ØØ	Ø.ØØ	Ø.ØØ	Ø.ØØ	Ø.Ø1	Ø.62	[Ø.35]	Ø.Ø4	Ø.ØØ	Ø.ØØ
	2.5Ø:	Ø.ØØ	Ø.ØØ	Ø.ØØ	Ø.ØØ	Ø.ØØ	Ø.ØØ	Ø.ØØ	Ø.61	[Ø.32]	Ø.Ø2	Ø.ØØ	Ø.ØØ	Ø.ØØ
DAY	2.ØØ:	Ø.ØØ	Ø.ØØ	Ø.ØØ	Ø.ØØ	Ø.ØØ	Ø.ØØ	Ø.47	[Ø.33]	Ø.ØØ	Ø.Ø1	Ø.ØØ	Ø.ØØ	Ø.ØØ
	1.5Ø:	Ø.ØØ	Ø.ØØ	Ø.ØØ	Ø.ØØ	Ø.ØØ	Ø.61	[Ø.49]	Ø.Ø2	Ø.Ø1	Ø.Ø2	Ø.ØØ	Ø.ØØ	Ø.ØØ
	1.25:	Ø.ØØ	Ø.ØØ	Ø.ØØ	Ø.ØØ	Ø.57	[Ø.39]	Ø.Ø2	Ø.ØØ	Ø.ØØ	Ø.Ø1	Ø.ØØ	Ø.ØØ	Ø.ØØ
	1.ØØ:	Ø.ØØ	Ø.ØØ	Ø.ØØ	Ø.42	[Ø.43]	Ø.ØØ	Ø.ØØ	Ø.ØØ	Ø.Ø1	Ø.ØØ	Ø.ØØ	Ø.ØØ	Ø.ØØ
	3/4:	Ø.ØØ	Ø.ØØ	Ø.Ø6	[Ø.58]	Ø.ØØ	Ø.ØØ	Ø.ØØ	Ø.ØØ	Ø.ØØ	Ø.ØØ	Ø.ØØ	Ø.ØØ	Ø.ØØ
	1/2:	Ø.ØØ	Ø.21	[Ø.94]	Ø.ØØ	Ø.ØØ	Ø.ØØ	Ø.ØØ	Ø.ØØ	Ø.Ø1	Ø.ØØ	Ø.ØØ	Ø.ØØ	Ø.ØØ
	1/4:	Ø.23	[Ø.77]	Ø.ØØ	Ø.ØØ	Ø.ØØ	Ø.ØØ	Ø.Ø2	Ø.ØØ	Ø.ØØ	Ø.ØØ	Ø.ØØ	Ø.ØØ	Ø.ØØ
	<1/4:	[Ø.77]	Ø.Ø2	Ø.ØØ	Ø.ØØ	Ø.ØØ	Ø.ØØ	Ø.ØØ	Ø.ØØ	Ø.ØØ	Ø.ØØ	Ø.ØØ	Ø.ØØ	Ø.ØØ

RVRS

RVV7 NITE	RVRS:	<1/4	1/4	1/2	3/4	1.ØØ	1.25	1.5Ø	2.ØØ	2.5Ø	3.ØØ	4	5	>5
	TOTALS:	Ø	27	39	33	19	13	2Ø	31	37	1Ø7	142	14Ø	1Ø4Ø
	>5:	Ø.ØØ	Ø.ØØ	Ø.ØØ	Ø.ØØ	Ø.ØØ	Ø.ØØ	Ø.ØØ	Ø.ØØ	Ø.ØØ	Ø.Ø2	Ø.Ø2	Ø.54	[Ø.98]
	5:	Ø.ØØ	Ø.ØØ	Ø.ØØ	Ø.ØØ	Ø.ØØ	Ø.ØØ	Ø.ØØ	Ø.ØØ	Ø.ØØ	Ø.ØØ	Ø.51	[Ø.42]	Ø.Ø2
	4:	Ø.ØØ	Ø.ØØ	Ø.ØØ	Ø.ØØ	Ø.ØØ	Ø.ØØ	Ø.ØØ	Ø.ØØ	Ø.ØØ	Ø.59	[Ø.42]	Ø.Ø2	Ø.ØØ
RVV7	3.ØØ:	Ø.ØØ	Ø.ØØ	Ø.ØØ	Ø.ØØ	Ø.ØØ	Ø.ØØ	Ø.ØØ	Ø.ØØ	Ø.59	[Ø.36]	Ø.Ø1	Ø.ØØ	Ø.ØØ
	2.5Ø:	Ø.ØØ	Ø.ØØ	Ø.ØØ	Ø.ØØ	Ø.ØØ	Ø.ØØ	Ø.ØØ	Ø.39	[Ø.38]	Ø.Ø3	Ø.Ø1	Ø.Ø1	Ø.ØØ
NITE	2.ØØ:	Ø.ØØ	Ø.ØØ	Ø.ØØ	Ø.ØØ	Ø.ØØ	Ø.ØØ	Ø.5Ø	[Ø.61]	Ø.ØØ	Ø.ØØ	Ø.Ø1	Ø.ØØ	Ø.ØØ
	1.5Ø:	Ø.ØØ	Ø.ØØ	Ø.ØØ	Ø.ØØ	Ø.ØØ	Ø.54	[Ø.5Ø]	Ø.ØØ	Ø.ØØ	Ø.ØØ	Ø.Ø1	Ø.ØØ	Ø.ØØ
	1.25:	Ø.ØØ	Ø.ØØ	Ø.ØØ	Ø.ØØ	Ø.26	[Ø.46]	Ø.ØØ	Ø.ØØ	Ø.ØØ	Ø.ØØ	Ø.ØØ	Ø.ØØ	Ø.ØØ
	1.ØØ:	Ø.ØØ	Ø.ØØ	Ø.ØØ	Ø.33	[Ø.74]	Ø.ØØ	Ø.ØØ	Ø.ØØ	Ø.ØØ	Ø.ØØ	Ø.Ø1	Ø.ØØ	Ø.ØØ
	3/4:	Ø.ØØ	Ø.ØØ	Ø.21	[Ø.67]	Ø.ØØ	Ø.ØØ	Ø.ØØ	Ø.ØØ	Ø.Ø3	Ø.ØØ	Ø.ØØ	Ø.ØØ	Ø.ØØ
	1/2:	Ø.ØØ	Ø.26	[Ø.77]	Ø.ØØ	Ø.ØØ	Ø.ØØ	Ø.ØØ	Ø.ØØ	Ø.ØØ	Ø.ØØ	Ø.ØØ	Ø.ØØ	Ø.ØØ
	1/4:	Ø.ØØ	[Ø.74]	Ø.ØØ	Ø.ØØ	Ø.ØØ	Ø.ØØ	Ø.ØØ	Ø.ØØ	Ø.ØØ	Ø.ØØ	Ø.ØØ	Ø.ØØ	Ø.ØØ
	<1/4:	[Ø.ØØ]	Ø.ØØ	Ø.Ø3	Ø.ØØ	Ø.ØØ	Ø.ØØ	Ø.ØØ	Ø.ØØ	Ø.ØØ	Ø.ØØ	Ø.ØØ	Ø.ØØ	Ø.ØØ

RVRS

TABLE 5-5. SCATTER TABLE: 7/ 9-7/20: RVV-700 versus 1000-FOOT RVR 500: WITH 10-PERCENT SLOPE CORRECTION.

VISIBILITY COUNT FRACTION:

FILE: OTIS82.ALL   RVV7 VS. RVR5   SITE: TRAILER: YEAR: 1982 DAYS: 7/ 9- 7/20   HOURS: 0-24

K1= 1.100   AVERAGING 12 PER

RVV7 DAY

		<1/4	1/4	1/2	3/4	1.00	1.25	1.50	2.00	2.50	3.00	4	5	>5
	TOTALS:	43	43	33	24	21	18	43	88	85	124	163	200	763
	>5:	0.00	0.00	0.00	0.00	0.00	0.00	0.00	0.00	0.00	0.00	0.00	0.22	[0.89]
	5:	0.00	0.00	0.00	0.00	0.00	0.00	0.00	0.00	0.00	0.00	0.11	[0.56]	0.09
	4:	0.00	0.00	0.00	0.00	0.00	0.00	0.00	0.02	0.00	0.24	[0.60]	0.22	0.01
RVV7	3.00:	0.00	0.00	0.00	0.00	0.00	0.00	0.00	0.00	0.32	[0.65]	0.29	0.00	0.00
	2.50:	0.00	0.00	0.00	0.00	0.00	0.00	0.00	0.23	[0.61]	0.06	0.00	0.00	0.00
DAY	2.00:	0.00	0.00	0.00	0.00	0.00	0.00	0.19	[0.70]	0.04	0.01	0.00	0.00	0.00
	1.50:	0.00	0.00	0.00	0.00	0.00	0.22	[0.74]	0.03	0.00	0.02	0.00	0.00	0.00
	1.25:	0.00	0.00	0.00	0.00	0.14	[0.67]	0.05	0.01	0.01	0.01	0.00	0.00	0.00
	1.00:	0.00	0.00	0.00	0.12	[0.86]	0.11	0.00	0.00	0.00	0.00	0.00	0.00	0.00
	3/4:	0.00	0.00	0.00	[0.83]	0.00	0.00	0.00	0.00	0.01	0.00	0.00	0.00	0.00
	1/2:	0.00	0.00	[1.00]	0.04	0.00	0.00	0.00	0.00	0.01	0.00	0.00	0.00	0.00
	1/4:	0.02	[0.98]	0.00	0.00	0.00	0.00	0.02	0.00	0.00	0.00	0.00	0.00	0.00
	<1/4:	[0.98]	0.02	0.00	0.00	0.00	0.00	0.00	0.00	0.00	0.00	0.00	0.00	0.00
		<1/4	1/4	1/2	3/4	1.00	1.25	1.50	2.00	2.50	3.00	4	5	>5

RVR5

		<1/4	1/4	1/2	3/4	1.00	1.25	1.50	2.00	2.50	3.00	4	5	>5
	TOTALS:	0	27	39	33	19	13	20	31	37	107	142	140	1040
	>5:	0.00	0.00	0.00	0.00	0.00	0.00	0.00	0.00	0.00	0.00	0.00	0.18	[0.95]
	5:	0.00	0.00	0.00	0.00	0.00	0.00	0.00	0.00	0.00	0.02	0.31	[0.71]	0.05
	4:	0.00	0.00	0.00	0.00	0.00	0.00	0.00	0.00	0.00	0.18	[0.61]	0.09	0.00
RVV7	3.00:	0.00	0.00	0.00	0.00	0.00	0.00	0.00	0.00	0.19	[0.76]	0.06	0.01	0.00
	2.50:	0.00	0.00	0.00	0.00	0.00	0.00	0.00	0.16	[0.76]	0.05	0.01	0.01	0.00
NITE	2.00:	0.00	0.00	0.00	0.00	0.00	0.00	0.00	[0.84]	0.03	0.01	0.01	0.00	0.00
	1.50:	0.00	0.00	0.00	0.00	0.00	0.31	[1.00]	0.00	0.00	0.00	0.01	0.00	0.00
	1.25:	0.00	0.00	0.00	0.00	0.05	[0.69]	0.00	0.00	0.00	0.00	0.00	0.00	0.00
	1.00:	0.00	0.00	0.00	0.09	[0.89]	0.00	0.00	0.00	0.00	0.00	0.01	0.00	0.00
	3/4:	0.00	0.00	0.03	[0.91]	0.05	0.00	0.00	0.00	0.03	0.00	0.00	0.00	0.00
	1/2:	0.00	0.11	[0.96]	0.00	0.00	0.00	0.00	0.00	0.00	0.00	0.00	0.00	0.00
	1/4:	0.00	[0.89]	0.00	0.00	0.00	0.00	0.00	0.00	0.00	0.00	0.00	0.00	0.00
	<1/4:	[0.00]	0.00	0.03	0.00	0.00	0.00	0.00	0.00	0.00	0.00	0.00	0.00	0.00
		<1/4	1/4	1/2	3/4	1.00	1.25	1.50	2.00	2.50	3.00	4	5	>5

RVR5

5.3.2 Background Levels

The RVV-700 background levels observed with the 1000-foot baseline at Otis are illustrated in Figure 5-15. The upper curve is for a typical sunny day while the lower curve shows how the background can be reduced on a cloudy day. The 1000-foot RVR-500 had background levels approximately half those of the RVV-700 because of higher lamp current (15 A vs 12 A). The maximum RVV-700 background levels were between 4 and 5 percent.

At Arcata the RVV-700 (720-foot baseline) had somewhat lower maximum background levels (3 to 3.5 percent) which were symmetrical between morning and evening rather than showing the evening peak of Figure 5-15. The 720-foot RVR-500 had a much lower background level (0.3 percent) because of a smaller field stop and a higher lamp current (perhaps the 20A for which the lamp is rated).

The background levels can change rapidly enough in one hour to affect the visibility measurement. Figure 5-15 shows changes of 2 percent in an hour, and even larger jumps are possible. One way of estimating the errors due to background changes is to compare the transmissometer measurements to a forward-scatter meter which is relatively insensitive to sunlight. Such a comparison was carried out for 10 sunny days. Figure 5-16 shows one example. The rest are in Appendix D. The scatter plot on the left covers the data before and during sunset. The right plot shows the data following in the night. NOTE: the times are GMT. This comparison usually shows a significant broadening of about 1 $10^{-4}m^{-1}$in the measured extinction coefficient. This broadening corresponds to a 100-percent calibration error of about 2 percent, which is reasonable.

5.3.3 100-Percent Calibration

The 100-percent calibration stability in the evaluation will be assessed from the calibration log. It is possible, however, to assess the 100-percent calibration level by comparison with the standard

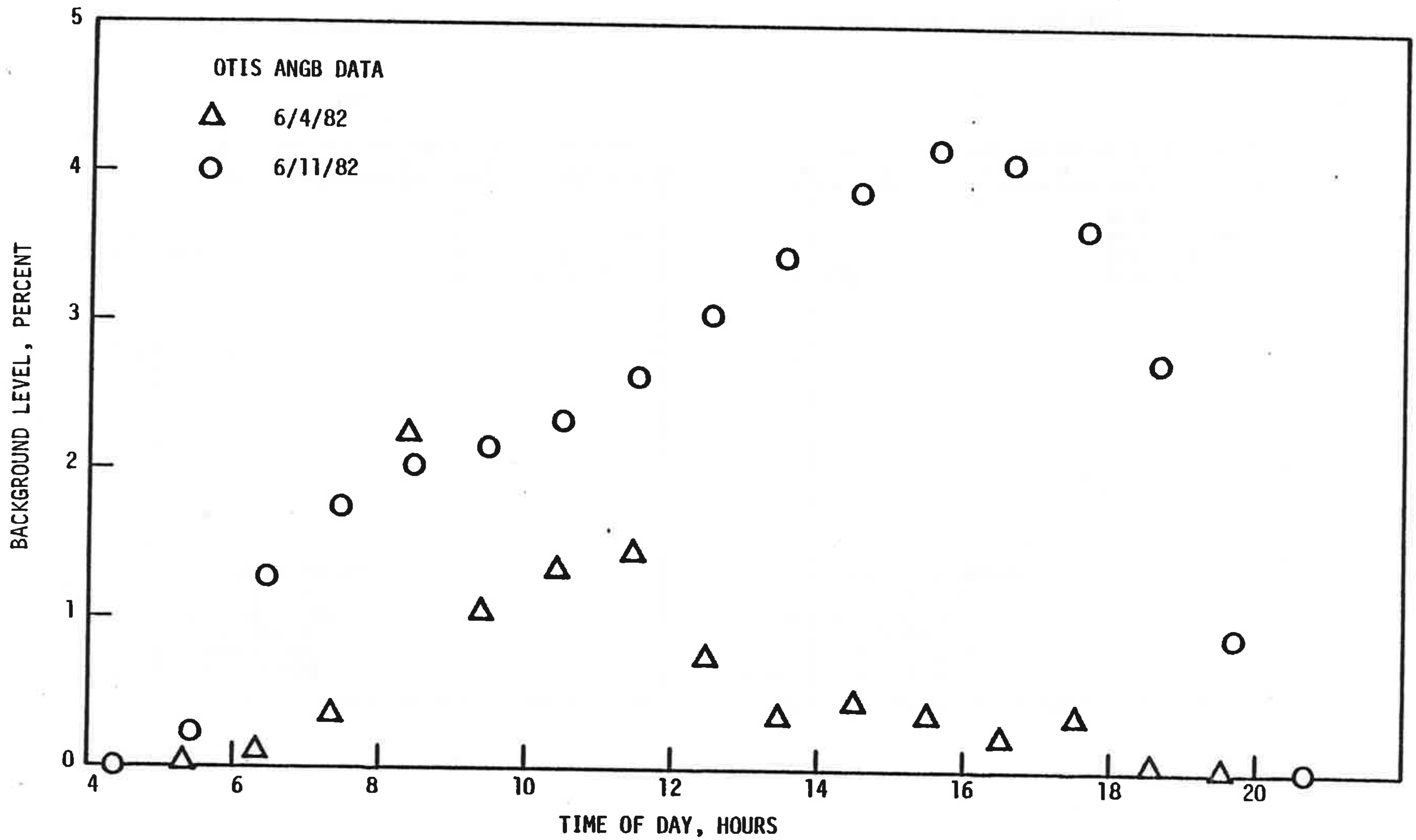

FIGURE 5-15. RVV-700 BACKGROUND LEVEL versus LOCAL TIME OF DAY (EDT, not GMT)

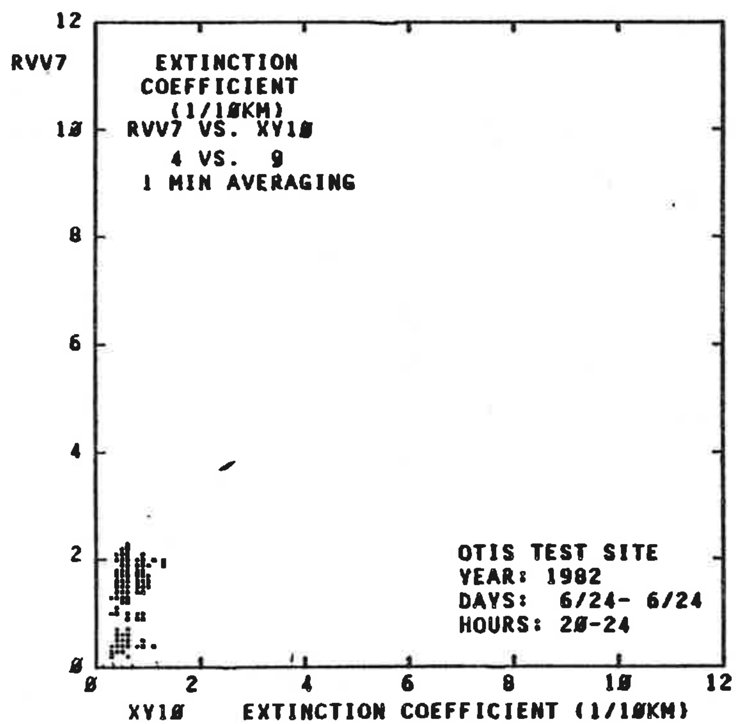

(a)

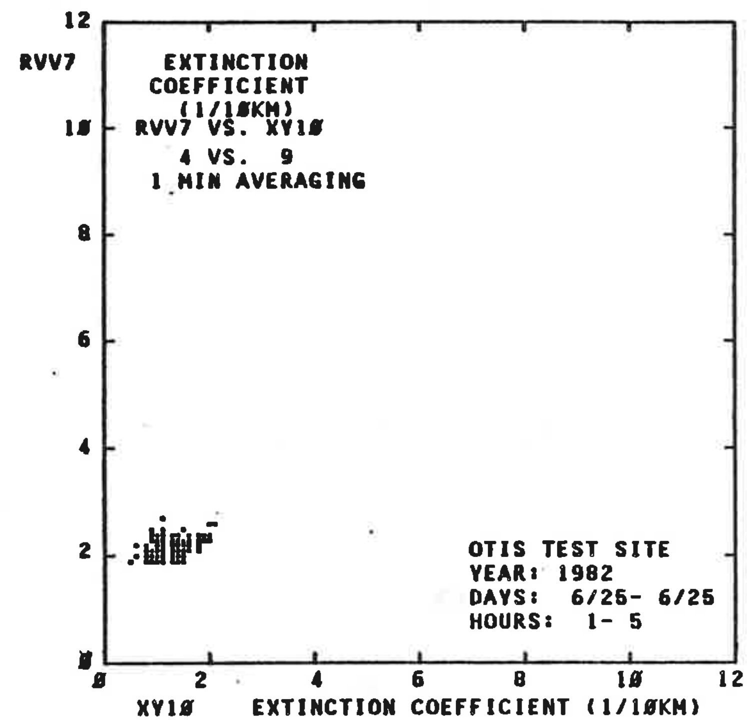

(b)

FIGURE 5-16. EXTINCTION COEFFICIENT SCATTER PLOTS: RVV-700 versus AVERAGE OF TWO EG&G 207 SENSORS (X10, Y10): (a) LATE AFTERNOON THROUGH SUNSET: (b) NIGHT.

transmissometer (as in Figure 5-3) or with forward-scatter meters as in Figure 5-16 and Appendix D.

5.3.4 Computer Breakpoints

Figures 5-17 and 18 compare the RVV-700 computer reading to the raw data value for day and night respectively. A given reporting value is output for a range of raw data values. The breakpoints should be those shown in Table 4-1. The scatter plots in Figure 5-17 show daytime visibility so that the daytime breakpoints can be verified by inspection. The night breakpoints in Figure 5-18 are also correct, but must be verified by comparison of extinction coefficients with Table 3-2. The data are stored as equivalent extinction coefficient and the software uses only the day calibration to generate visibility.

5.4. FOG-15

5.4.1 Non-Linear Calibration

For fog events the FOG-15 data consistently show greater slope with respect to the transmissometers at low ($\sigma < 30 \quad 10^{-4}m^{-1}$) extinction coefficient than at high extinction coefficients. Figure 5-19 shows the scatter plots of Event #1 comparing the FOG-15 (SN 015) data to the standard transmissometer. The offset (D1) of -3.6 corrects for the 36 mV sensor offset. Table 5-6 shows the least-square fits to the data. The calibration assumed that 1.00 volt corresponded to an extinction coefficient of 100 $10^{-4}m^{-1}$, which gave reasonable overall agreement:

$$\sigma = 100 \text{ V}$$

where σ is the extinction coefficient and V is the sensor voltage. The least-square fits (Tables 5-6) were used as a guide toward defining a nonlinear calibration curve. The fit for $0.6 < \sigma < 38$ gave a slope of 1.3 with a very small offset. The fit for $38 < \sigma < 1000.$ gave a slope of 0.9. These numbers were used to calculate the new calibration curve:

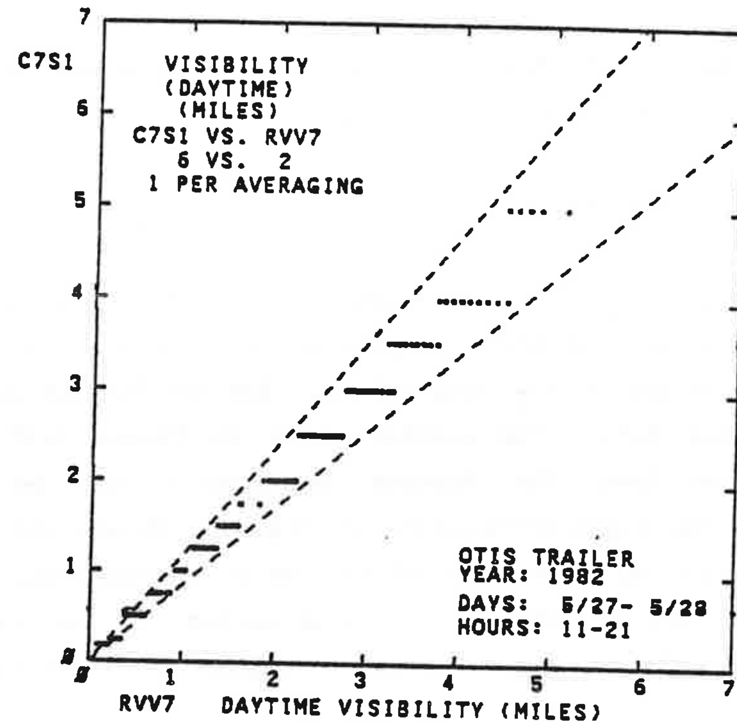

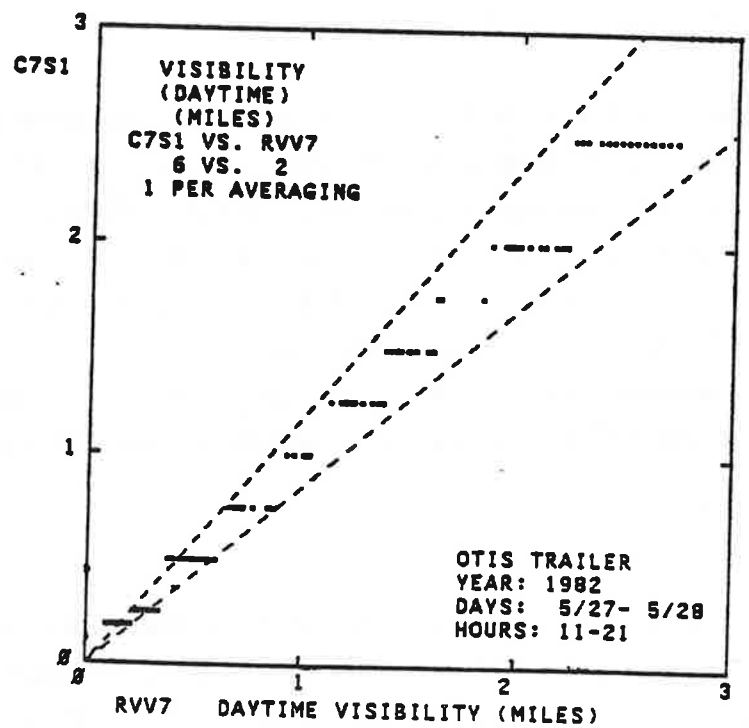

FIGURE 5-17. DAY VISIBILITY SCATTER PLOTS: RVV-700 COMPUTER (C7S1) versus RVV-700 RAW DATA: NO AVERAGING.

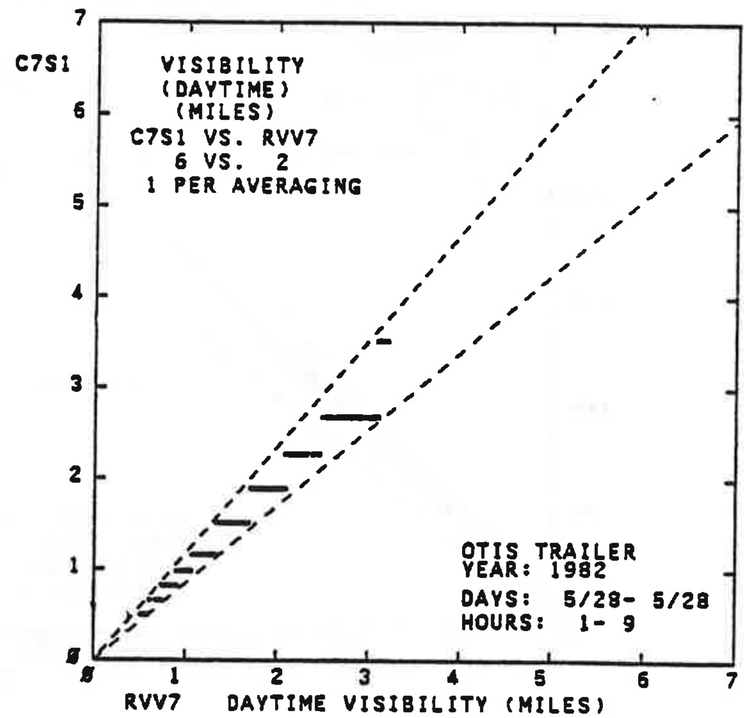

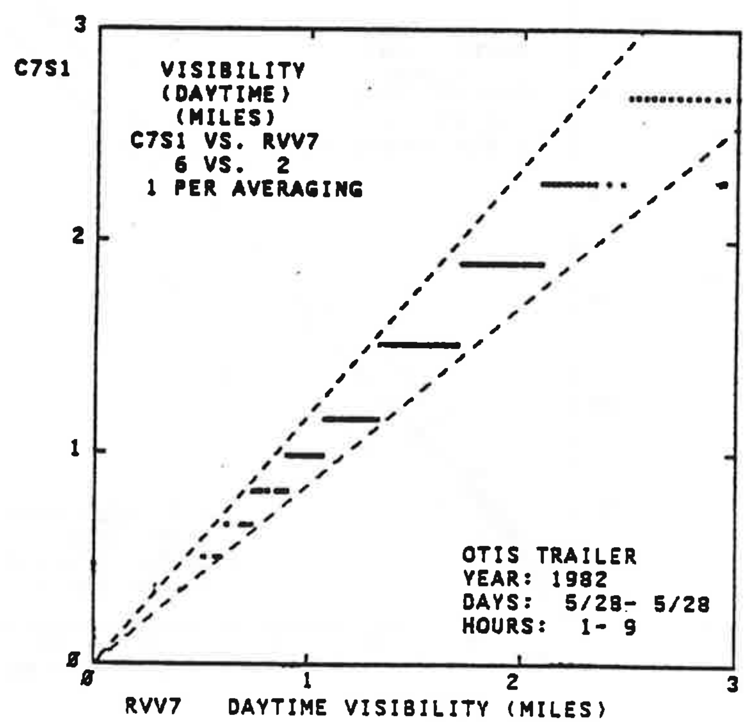

FIGURE 5-18. NIGHT VISIBILITY SCATTER PLOTS: RVV-700 COMPUTER (C7S1) versus RVV-700 RAW DATA: NO AVERAGING.

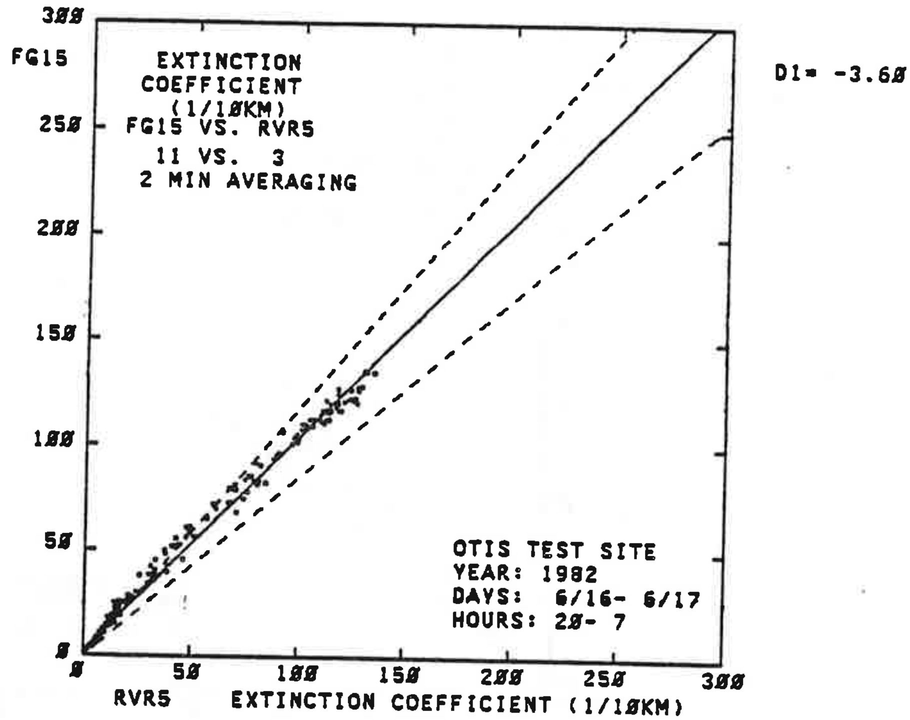

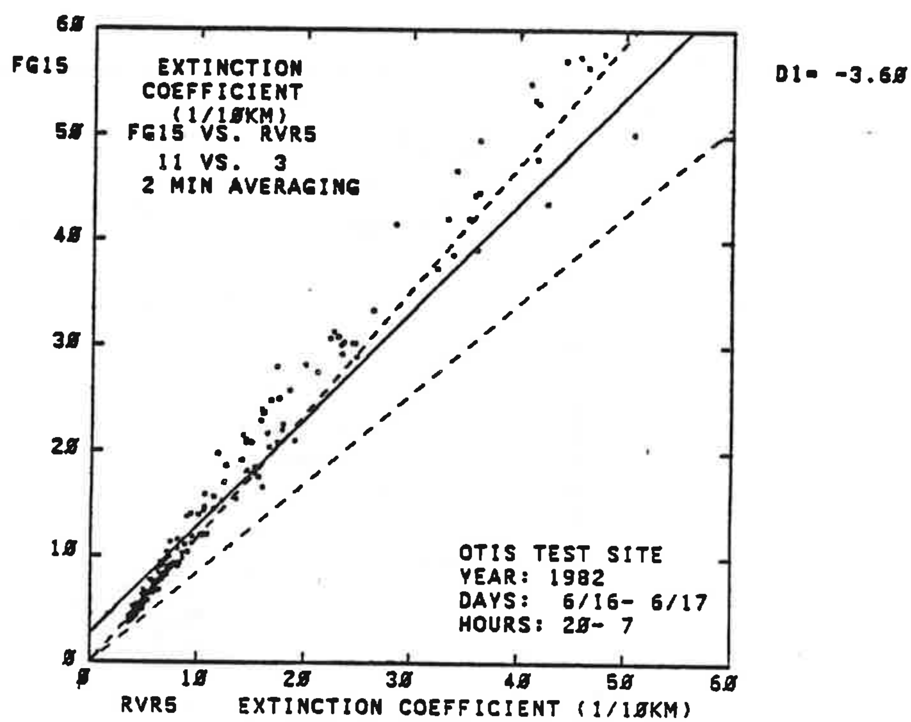

FIGURE 5-19. SCATTER PLOTS FOR EVENT #1: FOG 15 (SN 015) versus 1000-FOOT BASELINE RVR 500: ORIGINAL CALIBRATION: (a), (b), (c) EXTINCTION COEFFICIENT: (d) VISIBILITY.

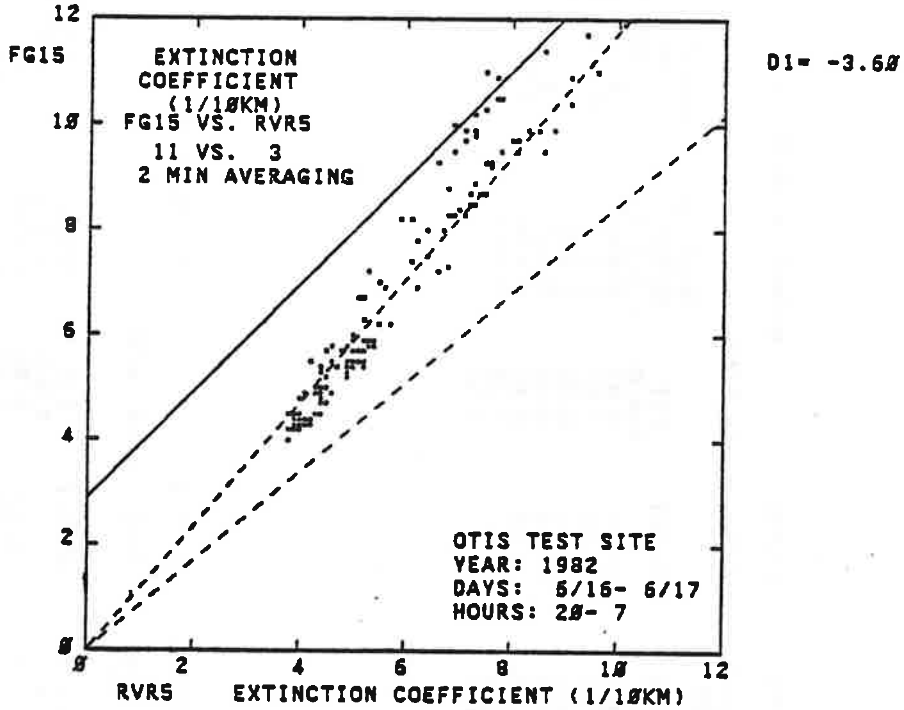

(c)

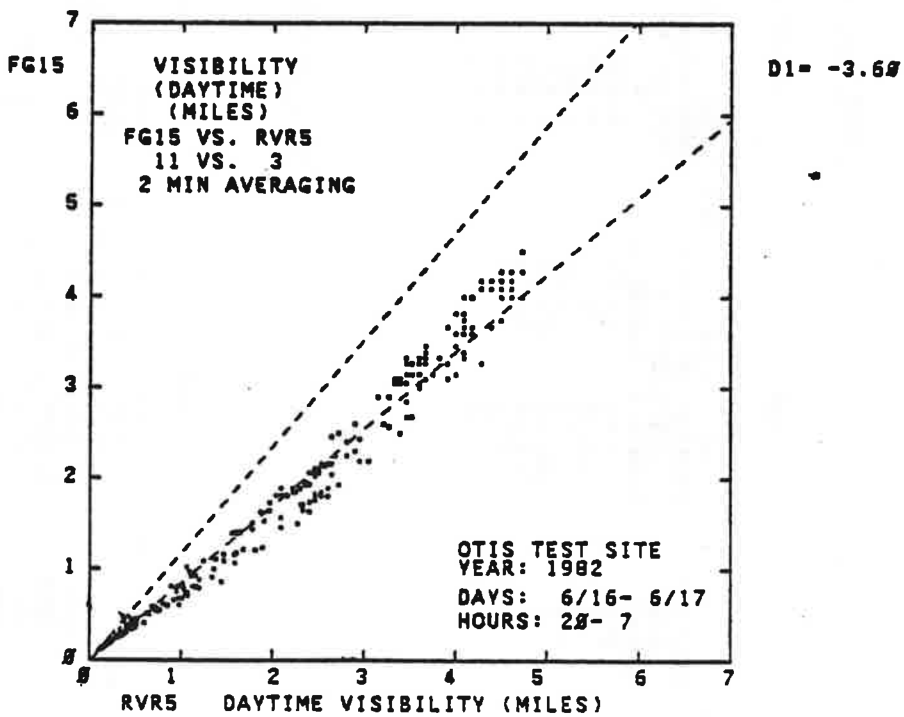

(d)

FIGURE 5-19. (concluded).

TABLE 5-6. LEAST-SQUARE FITS TO EVENT #1: FOG-15 (SN 015) versus 1000-FOOT RVR 500.

ORIGINAL CALIBRATION

OL82Ø6.16 5Ø2 AVERAGING INTERVAL= 2 MINS. HSTART=2Ø HSTOP= 7

1ST: SENSOR 11 FG15 2ND: SENSOR 3 RVR5 YEAR: 1982 DAYS: 6/16- 6/17

K1= 1.ØØØ D1= -3.6Ø K2= 1.ØØØ D2= Ø.ØØ

DATA LIMITS	QUANTITY DATA POINTS	AVERAGE EXTINCTION COEFFICIENTS SENSOR 1	SENSOR 2	CORRELATION COEFFICIENT R	SLOPE K	OFFSET D	FIT R.S.D.	FRACTION SENSOR 1 R.S.D.	VISIBILITY LIMITS (MILES)
Ø.6Ø-1ØØØ.	296	42.Ø3	38.44	Ø.996	1.Ø18	2.89	4.Ø7	Ø.Ø969	Ø - 3Ø
Ø.6Ø - 38.	2Ø3	12.3Ø	9.77	Ø.988	1.3Ø7	-Ø.46	1.51	Ø.1225	Ø.5 - 3Ø
Ø.6Ø - 12.67	156	7.63	6.27	Ø.967	1.447	-1.44	Ø.83	Ø.1Ø84	1.5 - 3Ø
38.Ø-1ØØØ.	93	1Ø6.93	1Ø1.Ø3	Ø.991	Ø.9Ø5	15.52	4.45	Ø.Ø417	Ø - Ø.5
12.67-38.Ø	47	27.8Ø	21.39	Ø.957	1.164	2.9Ø	2.62	Ø.Ø9Ø5	Ø.5 - 1.5
7.6-12.67	37	12.14	9.43	Ø.84Ø	1.46Ø	-1.63	1.46	Ø.12Ø1	1.5 - 2.5
3.45-7.6	119	6.23	5.29	Ø.959	1.5Ø1	-1.7Ø	Ø.51	Ø.Ø817	2.5 - 5.5

NEW CALIBRATION

OT82Ø6.16 5Ø2 AVERAGING INTERVAL= 2 MINS. HSTART=2Ø HSTOP= 7

1ST: SENSOR 11 FG15 2ND: SENSOR 3 RVR5 YEAR: 1982 DAYS: 6/16- 6/17

K1= 1.ØØØ D1= -2.8Ø K2= 1.ØØØ D2= Ø.ØØ

DATA LIMITS	QUANTITY DATA POINTS	AVERAGE EXTINCTION COEFFICIENTS SENSOR 1	SENSOR 2	CORRELATION COEFFICIENT R	SLOPE K	OFFSET D	FIT R.S.D.	FRACTION SENSOR 1 R.S.D.	VISIBILITY LIMITS (MILES)
Ø.6Ø-1ØØØ.	296	38.82	38.44	Ø.998	1.Ø21	-Ø.43	2.92	Ø.Ø751	Ø - 3Ø
Ø.6Ø - 38.	2Ø3	9.43	9.77	Ø.988	1.ØØ9	-Ø.43	1.16	Ø.1232	Ø.5 - 3Ø
Ø.6Ø - 12.67	156	5.83	6.27	Ø.967	1.112	-1.14	Ø.64	Ø.1Ø92	1.5 - 3Ø
38.Ø-1ØØØ.	93	1Ø2.98	1Ø1.Ø3	Ø.991	1.ØØ4	1.62	4.9Ø	Ø.Ø476	Ø - Ø.5
12.67-38.Ø	47	21.39	21.39	Ø.956	Ø.9Ø6	2.ØØ	1.97	Ø.Ø92Ø	Ø.5 - 1.5
7.6-12.67	37	9.31	9.43	Ø.84Ø	1.116	-1.22	1.12	Ø.1199	1.5 - 2.5
3.45-7.6	119	4.75	5.29	Ø.957	1.149	-1.32	Ø.4Ø	Ø.Ø839	2.5 - 5.5

$V < 0.50 \qquad \sigma = 100V/1.3$

$V > 0.50 \qquad \sigma = 50/1.3 + 100\ (V - 0.50)/0.9$

Figure 5-20 a, b shows the extinction coefficient scatter plots for Event #1 with this new calibration. The results are much improved. Figure 5-20 b,c shows the corresponding visibility scatterplots. Figure 5-21 shows the visibility scatter plots for the other FOG-15 sensor tested (SN 003), which is termed "FG16" in the plots. The calibration correction factor of K1= 1.15 is used to convert the calibration to an absolute standard (Section 4.1.2.2). An alternative non-linear calibration using equivalent voltage rather than extinction coefficient was tried for SN 003 which has twice the sensitivity of SN 015. Basing the nonlinear calibration on extinction coefficient gave better results.

5.4.2 Accuracy

Tables 5-7 and 5-8 present the reporting value scatter tables corresponding to Figures 5-20 and 5-21. For this smoothly varying fog event both FOG-15 sensors meet the pass/fail test of having at least 90-percent of the test sensor's values within one increment of the standard sensor's values. Figures 5-22 and 5-23 show the FOG-15 visibility scatter plots for Event #2 which was a rain event. Tables 5-9 and 5-10 show the corresponding scatter tables. For this event SN 015 passes but SN 003 just fails because of low readings in the 1.25 mile region.

A valid sensor evalution should include data from many events. Tables 5-11 through 5-15 show several weeks worth of data for the two FOG-15 units. In this case the sensors do not meet the pass/fail test. They came closer to passing the week of 6/11-18/82 when the calibration was defined using Event #1 than they do on the following week. Presumably some of the disagreement is due to events having rapidly changing visibility where the different averaging volumes of the FOG-15 and 1000-foot RVR-500 preclude good agreement. Averaging two forward-scatter meters together should improve the agreement. This hypothesis was tested by using the X10 and Y10 EG&G 207 sensors which are

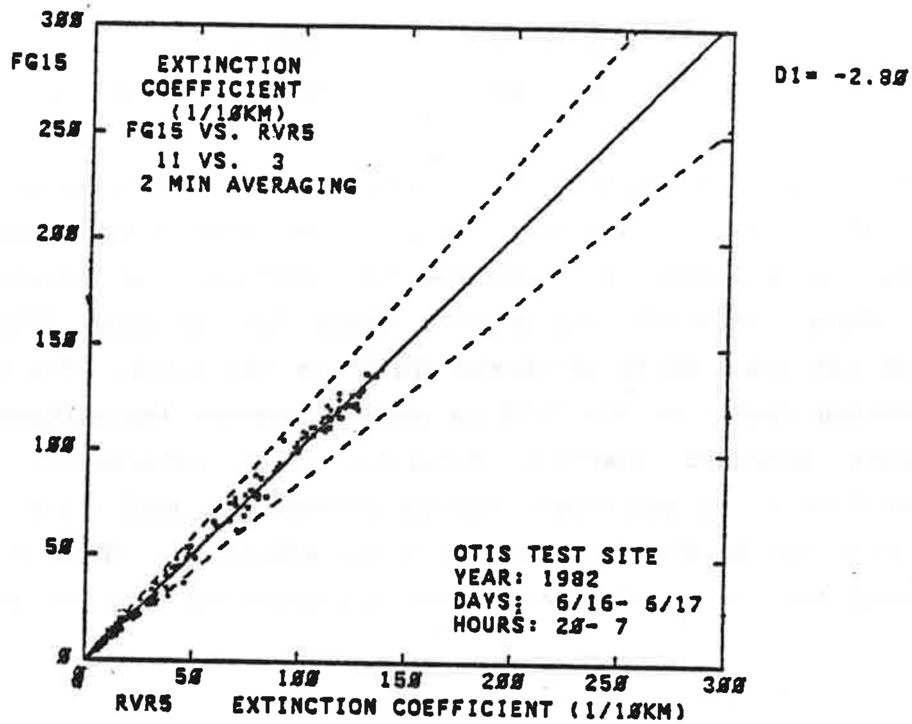

(a)

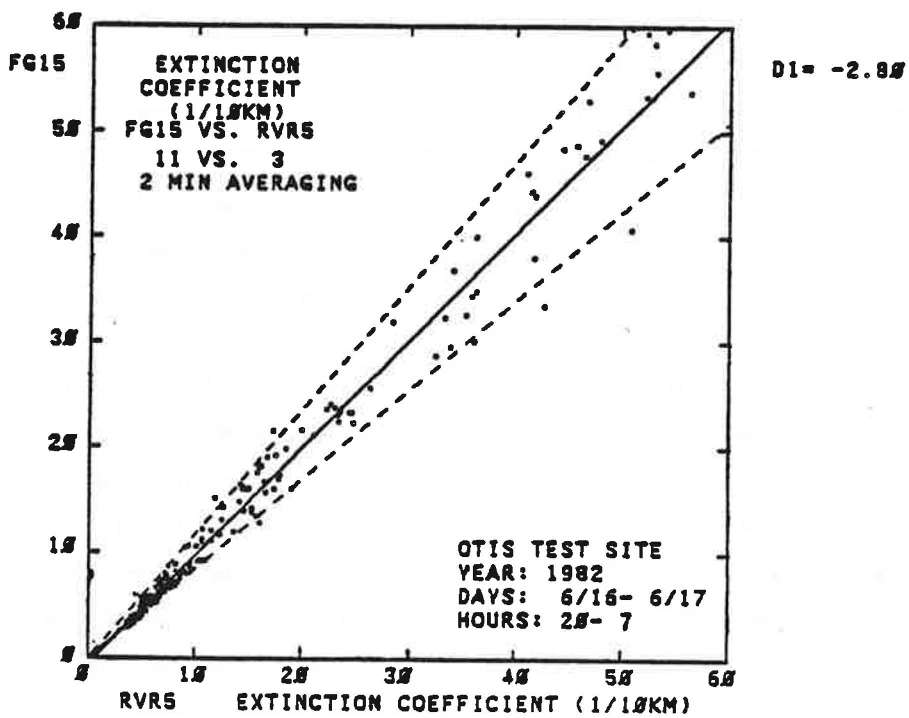

(b)

FIGURE 5-20. SCATTER PLOTS FOR EVENT #1: FOG-15 (SN 015) versus 1000-FOOT BASELINE RVR 500: NEW CALIBRATION: (a), (b) EXTINCTION COEFFICIENT: (c), (d) VISIBILITY.

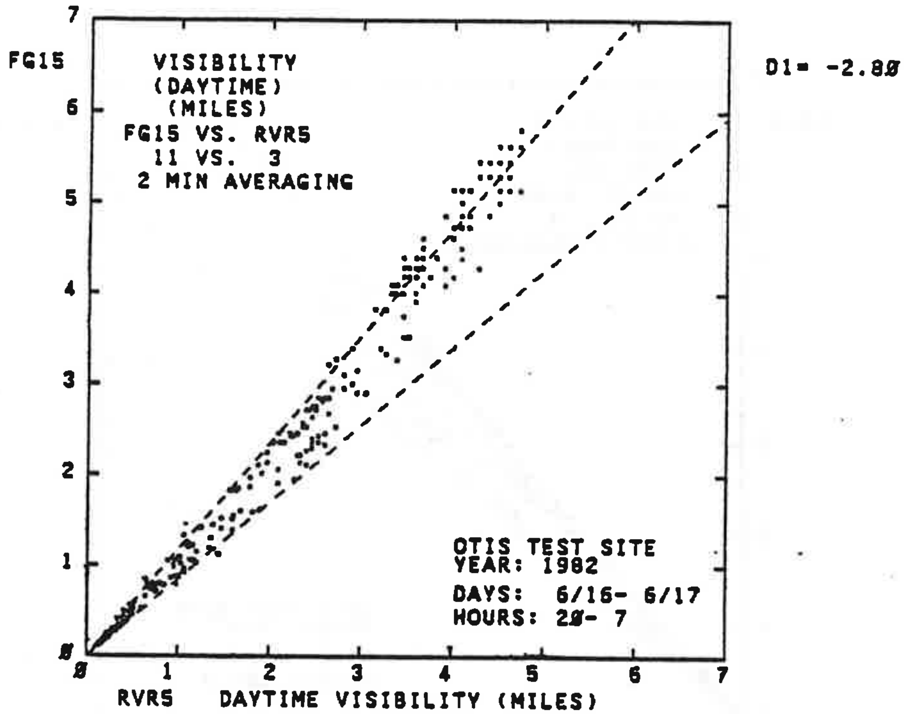

(c)

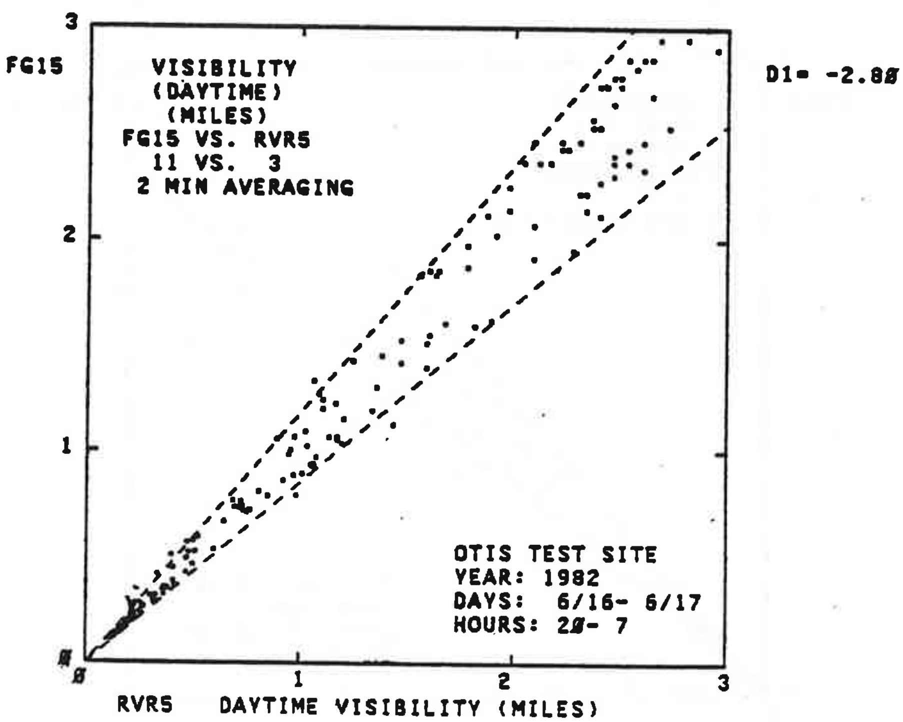

(d)

FIGURE 5-20. (concluded)

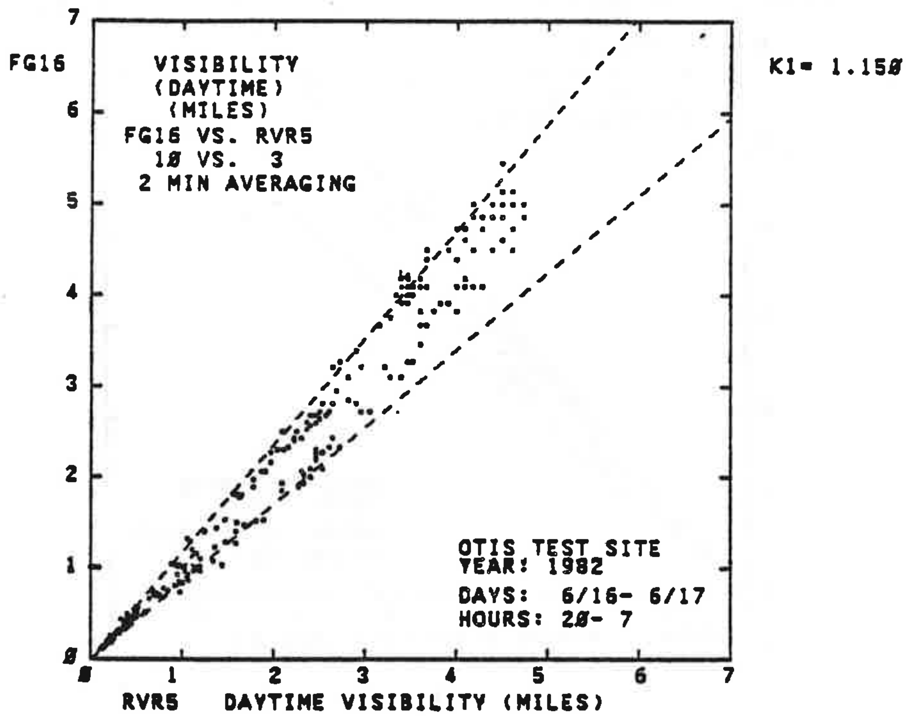

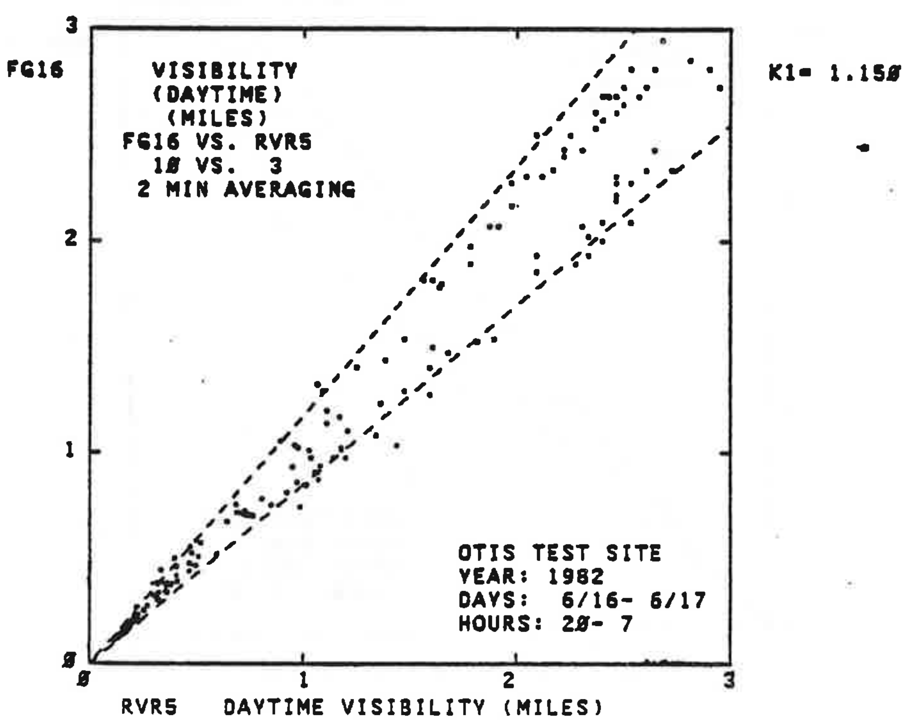

FIGURE 5-21. VISIBILITY SCATTER PLOTS FOR EVENT #1: FOG-15 (SN 003) versus 1000-FOOT BASELINE RVR 500.

TABLE 5-7, SCATTER TABLE: EVENT #1: FOG-15 (SN 015) versus 1000-FOOT RVR 500

VISIBILITY COUNT FRACTION

FILE: OT8206.16 FG15 VS. RVRS SITE: OTIS YEAR: 1982 DAYS: 6/16- 6/17 HOURS: 20- 7

AVERAGING 2

DI= -2.8

	TOTALS:	57	27	16	12	10	9	12	17	35	29	45	19	0
	>5:	0.00	0.00	0.00	0.00	0.00	0.00	0.00	0.00	0.00	0.00	0.00	0.42	[0.00]
	5:	0.00	0.00	0.00	0.00	0.00	0.00	0.00	0.00	0.00	0.00	0.47	[0.58]	0.00
	4:	0.00	0.00	0.00	0.00	0.00	0.00	0.00	0.00	0.00	0.66	[0.53]	0.00	0.00
FG15	3.00:	0.00	0.00	0.00	0.00	0.00	0.00	0.00	0.00	0.26	[0.34]	0.00	0.00	0.00
	2.50:	0.00	0.00	0.00	0.00	0.00	0.00	0.00	0.47	[0.57]	0.00	0.00	0.00	0.00
DAY	2.00:	0.00	0.00	0.00	0.00	0.00	0.00	0.33	[0.41]	0.17	0.00	0.00	0.00	0.00
	1.50:	0.00	0.00	0.00	0.00	0.00	0.11	[0.58]	0.12	0.00	0.00	0.00	0.00	0.00
	1.25:	0.00	0.00	0.00	0.00	0.22	[0.44]	0.00	0.00	0.00	0.00	0.00	0.00	0.00
	1.00:	0.00	0.00	0.00	0.00	[0.67]	0.44	0.00	0.00	0.00	0.00	0.00	0.00	0.00
	3/4:	0.00	0.00	0.00	[1.00]	0.11	0.00	0.00	0.00	0.00	0.00	0.00	0.00	0.00
	1/2:	0.00	0.04	[0.87]	0.00	0.00	0.00	0.00	0.00	0.00	0.00	0.00	0.00	0.00
	1/4:	0.02	[0.85]	0.12	0.00	0.00	0.00	0.00	0.00	0.00	0.00	0.00	0.00	0.00
	<1/4:	[0.98]	0.11	0.00	0.00	0.00	0.00	0.00	0.00	0.00	0.00	0.00	0.00	0.00
		<1/4	1/4	1/2	3/4	1.00	1.25	1.50	2.00	2.50	3.00	4	5	>5

RVRS

	TOTALS:	0	45	20	17	9	9	11	10	14	20	39	46	41
	>5:	0.00	0.00	0.00	0.00	0.00	0.00	0.00	0.00	0.00	0.00	0.00	0.00	[1.00]
	5:	0.00	0.00	0.00	0.00	0.00	0.00	0.00	0.00	0.00	0.00	0.10	[0.20]	0.00
	4:	0.00	0.00	0.00	0.00	0.00	0.00	0.00	0.00	0.00	0.40	[0.77]	0.00	0.00
FG15	3.00:	0.00	0.00	0.00	0.00	0.00	0.00	0.00	0.00	0.29	[0.50]	0.13	0.00	0.00
	2.50:	0.00	0.00	0.00	0.00	0.00	0.00	0.00	0.06	[0.50]	0.10	0.00	0.00	0.00
NITE	2.00:	0.00	0.00	0.00	0.00	0.00	0.00	0.27	[0.67]	0.21	0.00	0.00	0.00	0.00
	1.50:	0.00	0.00	0.00	0.00	0.00	0.33	[0.55]	0.28	0.00	0.00	0.00	0.00	0.00
	1.25:	0.00	0.00	0.00	0.00	0.11	[0.56]	0.18	0.00	0.00	0.00	0.00	0.00	0.00
	1.00:	0.00	0.00	0.00	0.12	[0.70]	0.11	0.00	0.00	0.00	0.00	0.00	0.00	0.00
	3/4:	0.00	0.00	0.00	[0.71]	0.11	0.00	0.00	0.00	0.00	0.00	0.00	0.00	0.00
	1/2:	0.00	0.00	[0.96]	0.18	0.00	0.00	0.00	0.00	0.00	0.00	0.00	0.00	0.00
	1/4:	0.00	[1.00]	0.04	0.00	0.00	0.00	0.00	0.00	0.00	0.00	0.00	0.00	0.00
	<1/4:	[0.00]	0.00	0.00	0.00	0.00	0.00	0.00	0.00	0.00	0.00	0.00	0.00	0.00
		<1/4	1/4	1/2	3/4	1.00	1.25	1.50	2.00	2.50	3.00	4	5	>5

RVRS

TABLE 5-8. SCATTER TABLE: EVENT #1: FOG-15 (SN 003) versus 1000-FOOT RVR 500

VISIBILITY COUNT FRACTION

FILE: OT0206.16 FG16 VS. RVRS SITE: OTIS YEAR: 1982 DAYS: 6/16- 6/17 HOURS: 20- 7

AVERAGING 2

K1= 1.150

	TOTALS:	57	27	16	12	18	9	12	17	35	29	45	19	0
	>6:	0.00	0.00	0.00	0.00	0.00	0.00	0.00	0.00	0.00	0.00	0.00	0.00	[0.00]
	5:	0.00	0.00	0.00	0.00	0.00	0.00	0.00	0.00	0.00	0.00	0.33	[1.00]	0.00
	4:	0.00	0.00	0.00	0.00	0.00	0.00	0.00	0.00	0.00	0.59	[0.62]	0.00	0.00
FG16	3.00:	0.00	0.00	0.00	0.00	0.00	0.00	0.00	0.00	0.14	[0.34]	0.04	0.00	0.00
	2.50:	0.00	0.00	0.00	0.00	0.00	0.00	0.00	0.47	[0.57]	0.07	0.00	0.00	0.00
DAY	2.00:	0.00	0.00	0.00	0.00	0.00	0.00	0.33	[0.41]	0.29	0.00	0.00	0.00	0.00
	1.50:	0.00	0.00	0.00	0.00	0.00	0.11	[0.42]	0.12	0.00	0.00	0.00	0.00	0.00
	1.25:	0.00	0.00	0.00	0.00	0.22	[0.22]	0.17	0.00	0.00	0.00	0.00	0.00	0.00
	1.00:	0.00	0.00	0.00	0.00	[0.50]	0.67	0.08	0.00	0.00	0.00	0.00	0.00	0.00
	3/4:	0.00	0.00	0.00	[1.00]	0.28	0.00	0.00	0.00	0.00	0.00	0.00	0.00	0.00
	1/2:	0.00	0.07	[0.94]	0.00	0.00	0.00	0.00	0.00	0.00	0.00	0.00	0.00	0.00
	1/4:	0.04	[0.81]	0.06	0.00	0.00	0.00	0.00	0.00	0.00	0.00	0.00	0.00	0.00
	<1/4:	[0.96]	0.11	0.00	0.00	0.00	0.00	0.00	0.00	0.00	0.00	0.00	0.00	0.00
		<1/4	1/4	1/2	3/4	1.00	1.25	1.50	2.00	2.50	3.00	4	5	>6

RVRS

	TOTALS:	0	46	28	17	9	9	11	18	14	20	39	45	41
	>5:	0.00	0.00	0.00	0.00	0.00	0.00	0.00	0.00	0.00	0.00	0.00	0.58	[0.98]
	5:	0.00	0.00	0.00	0.00	0.00	0.00	0.00	0.00	0.00	0.00	0.10	[0.38]	0.02
	4:	0.00	0.00	0.00	0.00	0.00	0.00	0.00	0.00	0.00	0.40	[0.64]	0.04	0.00
FG16	3.00:	0.00	0.00	0.00	0.00	0.00	0.00	0.00	0.00	0.29	[0.50]	0.26	0.00	0.00
	2.50:	0.00	0.00	0.00	0.00	0.00	0.00	0.00	0.06	[0.36]	0.10	0.00	0.00	0.00
NITE	2.00:	0.00	0.00	0.00	0.00	0.00	0.00	0.27	[0.50]	0.36	0.00	0.00	0.00	0.00
	1.50:	0.00	0.00	0.00	0.00	0.00	0.11	[0.55]	0.44	0.00	0.00	0.00	0.00	0.00
	1.25:	0.00	0.00	0.00	0.00	0.11	[0.78]	0.18	0.00	0.00	0.00	0.00	0.00	0.00
	1.00:	0.00	0.00	0.00	0.18	[0.89]	0.11	0.00	0.00	0.00	0.00	0.00	0.00	0.00
	3/4:	0.00	0.00	0.00	[0.82]	0.00	0.00	0.00	0.00	0.00	0.00	0.00	0.00	0.00
	1/2:	0.00	0.00	[0.96]	0.00	0.00	0.00	0.00	0.00	0.00	0.00	0.00	0.00	0.00
	1/4:	0.00	[1.00]	0.04	0.00	0.00	0.00	0.00	0.00	0.00	0.00	0.00	0.00	0.00
	<1/4:	[0.00]	0.00	0.00	0.00	0.00	0.00	0.00	0.00	0.00	0.00	0.00	0.00	0.00
		<1/4	1/4	1/2	3/4	1.00	1.25	1.50	2.00	2.50	3.00	4	5	>5

RVRS

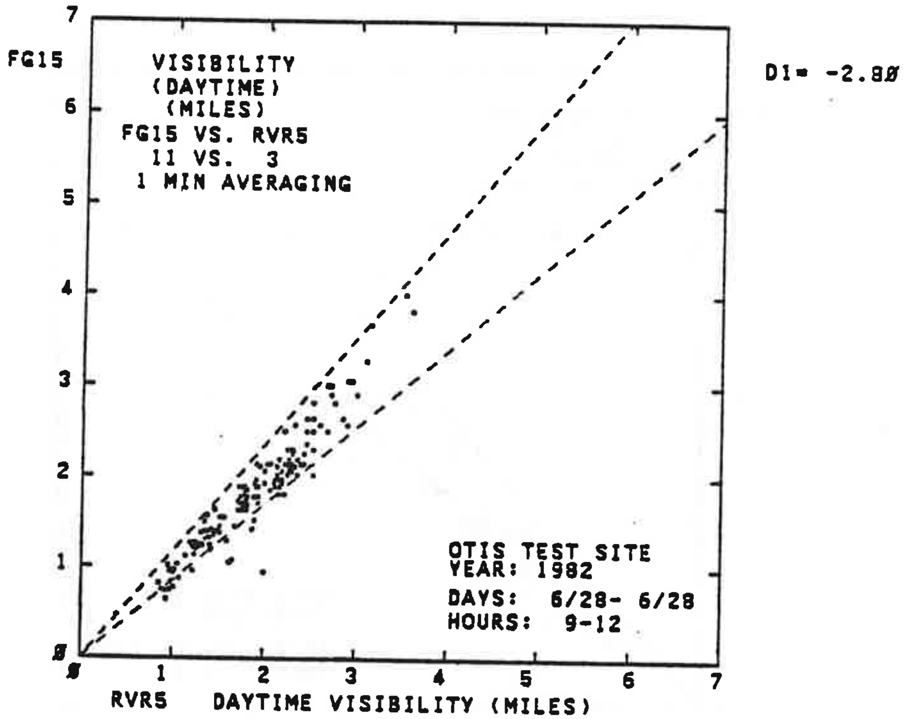

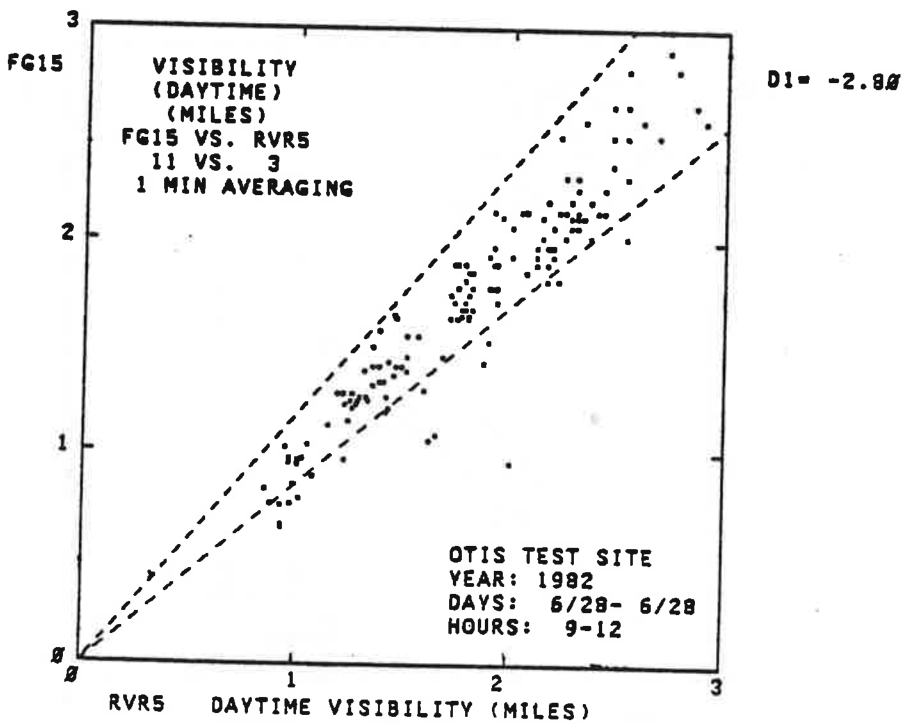

FIGURE 5-22. VISIBILITY SCATTER PLOTS FOR EVENT #2: FOG-15 (SN 015) versus 1000-FOOT BASELINE RVR 500.

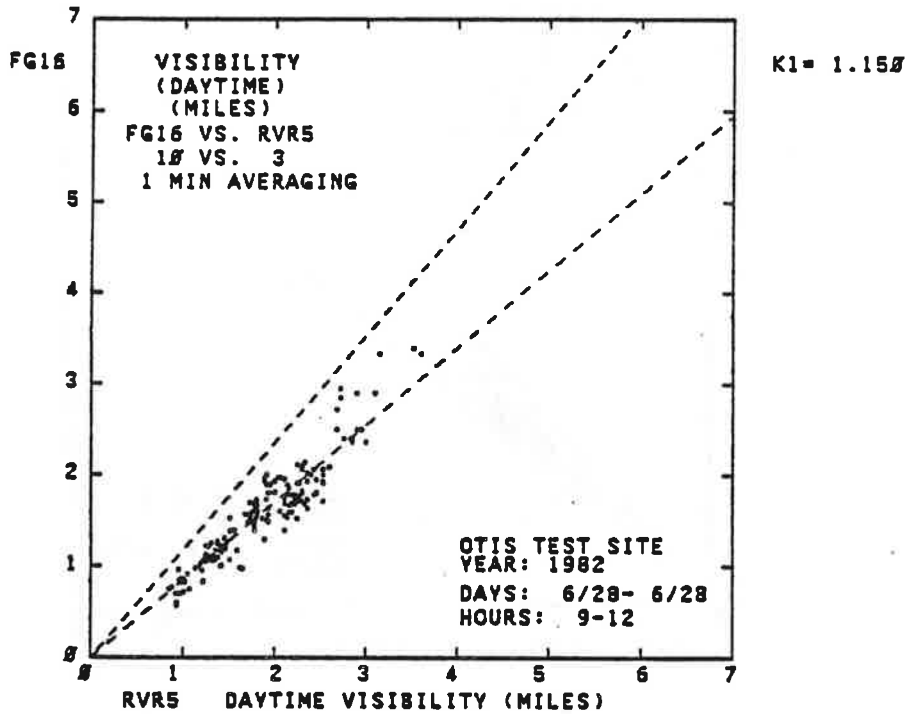

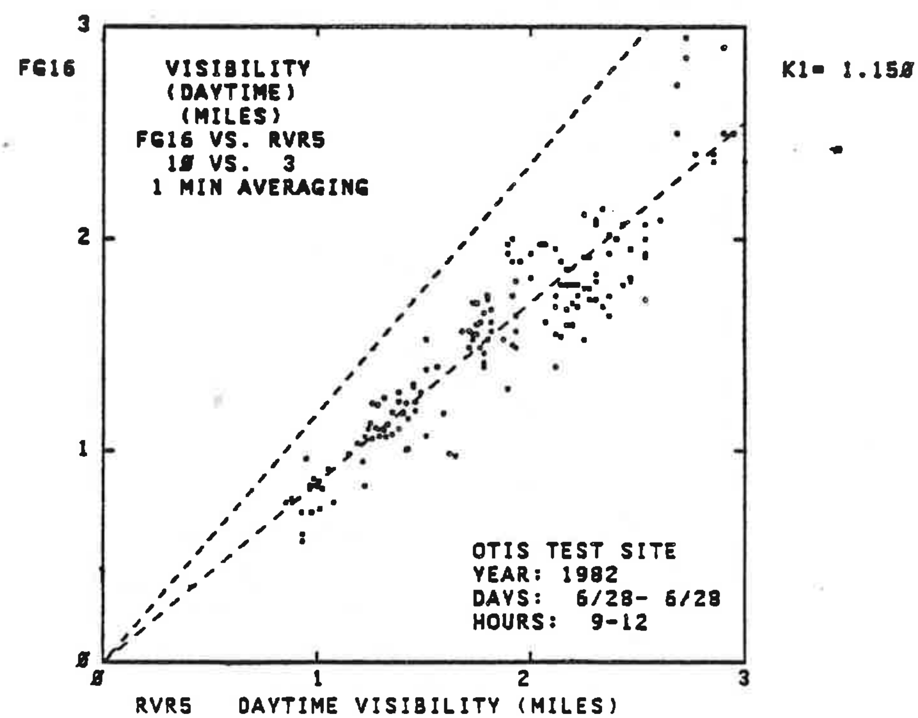

FIGURE 5-23. VISIBILITY SCATTER PLOTS FOR EVENT #2: FOG-15 (SN 003) versus 1000-FOOT BASELINE RVR 500.

TABLE 5-9. SCATTER TABLE: EVENT #2: FOG-15 (SN 015) versus 1000-FOOT RVR 500

VISIBILITY COUNT FRACTION

FILE: OT8286.28 FG15 VS. RVR5 SITE: OTIS YEAR: 1982 DAYS: 6/28- 6/28 HOURS: 9-12

AVERAGING 1

D1= -2.0

	TOTALS:	0	0	0	1	15	19	29	51	36	9	2	0	0
	>5:	0.00	0.00	0.00	0.00	0.00	0.00	0.00	0.00	0.00	0.00	0.00	0.00	[0.00]
	5:	0.00	0.00	0.00	0.00	0.00	0.00	0.00	0.00	0.00	0.00	0.00	[0.00]	0.00
	4:	0.00	0.00	0.00	0.00	0.00	0.00	0.00	0.00	0.00	0.11	[1.00]	0.00	0.00
FG15	3.00:	0.00	0.00	0.00	0.00	0.00	0.00	0.00	0.00	0.14	[0.56]	0.00	0.00	0.00
	2.50:	0.00	0.00	0.00	0.00	0.00	0.00	0.00	0.02	[0.36]	0.33	0.00	0.00	0.00
DAY	2.00:	0.00	0.00	0.00	0.00	0.00	0.00	0.14	[0.75]	0.50	0.00	0.00	0.00	0.00
	1.50:	0.00	0.00	0.00	0.00	0.00	0.21	[0.55]	0.22	0.00	0.00	0.00	0.00	0.00
	1.25:	0.00	0.00	0.00	0.00	0.00	[0.74]	0.24	0.00	0.00	0.00	0.00	0.00	0.00
	1.00:	0.00	0.00	0.00	0.00	[0.53]	0.06	0.07	0.02	0.00	0.00	0.00	0.00	0.00
	3/4:	0.00	0.00	0.00	[1.00]	0.47	0.00	0.00	0.00	0.00	0.00	0.00	0.00	0.00
	1/2:	0.00	0.00	[0.00]	0.00	0.00	0.00	0.00	0.00	0.00	0.00	0.00	0.00	0.00
	1/4:	0.00	[0.00]	0.00	0.00	0.00	0.00	0.00	0.00	0.00	0.00	0.00	0.00	0.00
	<1/4:	[0.00]	0.00	0.00	0.00	0.00	0.00	0.00	0.00	0.00	0.00	0.00	0.00	0.00
		<1/4	1/4	1/2	3/4	1.00	1.25	1.50	2.00	2.50	3.00	4	5	>5

RVR5

	TOTALS:	0	0	0	0	0	0	10	22	24	67	36	3	0
	>5:	0.00	0.00	0.00	0.00	0.00	0.00	0.00	0.00	0.00	0.00	0.00	0.33	[0.00]
	5:	0.00	0.00	0.00	0.00	0.00	0.00	0.00	0.00	0.00	0.00	0.03	[0.67]	0.00
	4:	0.00	0.00	0.00	0.00	0.00	0.00	0.00	0.00	0.00	0.03	[0.61]	0.00	0.00
FG15	3.00:	0.00	0.00	0.00	0.00	0.00	0.00	0.00	0.00	0.00	[0.81]	0.36	0.00	0.00
	2.50:	0.00	0.00	0.00	0.00	0.00	0.00	0.00	0.09	[0.62]	0.15	0.00	0.00	0.00
NITE	2.00:	0.00	0.00	0.00	0.00	0.00	0.00	0.10	[0.64]	0.37	0.00	0.00	0.00	0.00
	1.50:	0.00	0.00	0.00	0.00	0.00	0.00	[0.70]	0.27	0.00	0.01	0.00	0.00	0.00
	1.25:	0.00	0.00	0.00	0.00	0.00	[0.00]	0.20	0.00	0.00	0.00	0.00	0.00	0.00
	1.00:	0.00	0.00	0.00	0.00	[0.00]	0.00	0.00	0.00	0.00	0.00	0.00	0.00	0.00
	3/4:	0.00	0.00	0.00	[0.00]	0.00	0.00	0.00	0.00	0.00	0.00	0.00	0.00	0.00
	1/2:	0.00	0.00	[0.00]	0.00	0.00	0.00	0.00	0.00	0.00	0.00	0.00	0.00	0.00
	1/4:	0.00	[0.00]	0.00	0.00	0.00	0.00	0.00	0.00	0.00	0.00	0.00	0.00	0.00
	<1/4:	[0.00]	0.00	0.00	0.00	0.00	0.00	0.00	0.00	0.00	0.00	0.00	0.00	0.00
		<1/4	1/4	1/2	3/4	1.00	1.25	1.50	2.00	2.50	3.00	4	5	>5

RVR5

TABLE 5-10. SCATTER TABLE: EVENT #2: FOG-15 (SN 003) versus 1000-FOOT RVR 500

VISIBILITY COUNT FRACTION

FILE: OT0206.20 FG16 VS. RVR5 SITE: OTIS YEAR: 1982 DAYS: 6/28- 6/28 HOURS: 9-12

AVERAGING 1

K1= 1.150

	TOTALS:	0	0	0	1	15	19	29	51	36	9	2	0	0
	>5:	0.00	0.00	0.00	0.00	0.00	0.00	0.00	0.00	0.00	0.00	0.00	0.00	[0.00]
	5:	0.00	0.00	0.00	0.00	0.00	0.00	0.00	0.00	0.00	0.00	0.00	[0.00]	0.00
	4:	0.00	0.00	0.00	0.00	0.00	0.00	0.00	0.00	0.00	0.00	[0.00]	0.00	0.00
FG16	3.00:	0.00	0.00	0.00	0.00	0.00	0.00	0.00	0.00	0.06	[0.33]	1.00	0.00	0.00
	2.50:	0.00	0.00	0.00	0.00	0.00	0.00	0.00	0.00	[0.06]	0.67	0.00	0.00	0.00
DAY	2.00:	0.00	0.00	0.00	0.00	0.00	0.00	0.00	[0.37]	0.67	0.00	0.00	0.00	0.00
	1.50:	0.00	0.00	0.00	0.00	0.00	0.00	[0.41]	0.61	0.22	0.00	0.00	0.00	0.00
	1.25:	0.00	0.00	0.00	0.00	0.00	[0.32]	0.30	0.02	0.00	0.00	0.00	0.00	0.00
	1.00:	0.00	0.00	0.00	0.00	[0.13]	0.63	0.21	0.00	0.00	0.00	0.00	0.00	0.00
	3/4:	0.00	0.00	0.00	[1.00]	0.73	0.05	0.00	0.00	0.00	0.00	0.00	0.00	0.00
	1/2:	0.00	0.00	[0.00]	0.00	0.13	0.00	0.00	0.00	0.00	0.00	0.00	0.00	0.00
	1/4:	0.00	[0.00]	0.00	0.00	0.00	0.00	0.00	0.00	0.00	0.00	0.00	0.00	0.00
	<1/4:	[0.00]	0.00	0.00	0.00	0.00	0.00	0.00	0.00	0.00	0.00	0.00	0.00	0.00
		<1/4	1/4	1/2	3/4	1.00	1.25	1.50	2.00	2.50	3.00	4	5	>5

RVR5

	TOTALS:	0	0	0	0	0	0	10	22	24	67	36	3	0
	>5:	0.00	0.00	0.00	0.00	0.00	0.00	0.00	0.00	0.00	0.00	0.00	0.00	[0.00]
	5:	0.00	0.00	0.00	0.00	0.00	0.00	0.00	0.00	0.00	0.00	0.00	[1.00]	0.00
	4:	0.00	0.00	0.00	0.00	0.00	0.00	0.00	0.00	0.00	0.00	[0.33]	0.00	0.00
FG16	3.00:	0.00	0.00	0.00	0.00	0.00	0.00	0.00	0.00	0.00	[0.48]	0.61	0.00	0.00
	2.50:	0.00	0.00	0.00	0.00	0.00	0.00	0.00	0.00	[0.17]	0.51	0.06	0.00	0.00
NITE	2.00:	0.00	0.00	0.00	0.00	0.00	0.00	0.00	[0.59]	0.79	0.01	0.00	0.00	0.00
	1.50:	0.00	0.00	0.00	0.00	0.00	0.00	[0.60]	0.36	0.04	0.00	0.00	0.00	0.00
	1.25:	0.00	0.00	0.00	0.00	0.00	[0.00]	0.30	0.05	0.00	0.00	0.00	0.00	0.00
	1.00:	0.00	0.00	0.00	0.00	[0.00]	0.00	0.10	0.00	0.00	0.00	0.00	0.00	0.00
	3/4:	0.00	0.00	0.00	[0.00]	0.00	0.00	0.00	0.00	0.00	0.00	0.00	0.00	0.00
	1/2:	0.00	0.00	[0.00]	0.00	0.00	0.00	0.00	0.00	0.00	0.00	0.00	0.00	0.00
	1/4:	0.00	[0.00]	0.00	0.00	0.00	0.00	0.00	0.00	0.00	0.00	0.00	0.00	0.00
	<1/4:	[0.00]	0.00	0.00	0.00	0.00	0.00	0.00	0.00	0.00	0.00	0.00	0.00	0.00
		<1/4	1/4	1/2	3/4	1.00	1.25	1.50	2.00	2.50	3.00	4	5	>5

RVR5

TABLE 5-11. SCATTER TABLE: 6/11 - 6/18: FOG-15 (SN 015) versus 1000-FOOT RVR 500.

VISIBILITY COUNT FRACTION

FILE: OT8206.11 FG15 VS. RVR5 SITE: OTIS YEAR: 1982 DAYS: 6/11- 6/18 HOURS: 0-24

AVERAGING 10

D1= -2.0

	TOTALS:	12	9	10	9	12	8	13	19	26	31	41	41	754
	>5:	0.00	0.00	0.00	0.00	0.00	0.00	0.00	0.00	0.00	0.00	0.00	0.51	[1.00]
	5:	0.00	0.00	0.00	0.00	0.00	0.00	0.00	0.00	0.00	0.10	0.39	[0.39]	0.00
	4:	0.00	0.00	0.00	0.00	0.00	0.00	0.00	0.00	0.04	0.39	[0.51]	0.10	0.00
FG15	3.00:	0.00	0.00	0.00	0.00	0.00	0.00	0.00	0.21	0.23	[0.32]	0.10	0.00	0.00
	2.50:	0.00	0.00	0.00	0.00	0.00	0.00	0.00	0.11	[0.50]	0.16	0.00	0.00	0.00
DAY	2.00:	0.00	0.00	0.00	0.00	0.00	0.00	0.15	[0.32]	0.23	0.03	0.00	0.00	0.00
	1.50:	0.00	0.00	0.00	0.00	0.08	0.12	[0.46]	0.37	0.00	0.00	0.00	0.00	0.00
	1.25:	0.00	0.00	0.00	0.11	0.50	[0.50]	0.15	0.00	0.00	0.00	0.00	0.00	0.00
	1.00:	0.00	0.00	0.00	0.33	[0.33]	0.25	0.00	0.00	0.00	0.00	0.00	0.00	0.00
	3/4:	0.00	0.00	0.20	[0.44]	0.00	0.12	0.00	0.00	0.00	0.00	0.00	0.00	0.00
	1/2:	0.00	0.11	[0.60]	0.11	0.08	0.00	0.00	0.00	0.00	0.00	0.00	0.00	0.00
	1/4:	0.08	[0.78]	0.20	0.00	0.00	0.00	0.00	0.00	0.00	0.00	0.00	0.00	0.00
	<1/4:	[0.92]	0.11	0.00	0.00	0.00	0.00	0.00	0.00	0.00	0.00	0.00	0.00	0.00
		<1/4	1/4	1/2	3/4	1.00	1.25	1.50	2.00	2.50	3.00	4	5	>5

RVR5

	TOTALS:	0	10	8	5	8	5	9	14	12	24	38	36	816
	>5:	0.00	0.00	0.00	0.00	0.00	0.00	0.00	0.00	0.17	0.00	0.13	0.42	[0.99]
	5:	0.00	0.00	0.00	0.00	0.00	0.00	0.00	0.00	0.00	0.04	0.13	[0.50]	0.01
	4:	0.00	0.00	0.00	0.00	0.00	0.00	0.00	0.00	0.00	0.25	[0.55]	0.00	0.00
FG15	3.00:	0.00	0.00	0.00	0.00	0.00	0.00	0.00	0.00	0.00	[0.50]	0.10	0.00	0.00
	2.50:	0.00	0.00	0.00	0.00	0.00	0.00	0.00	0.43	[0.60]	0.21	0.00	0.00	0.00
NITE	2.00:	0.00	0.00	0.00	0.00	0.00	0.20	0.56	[0.50]	0.17	0.00	0.00	0.00	0.00
	1.50:	0.00	0.00	0.00	0.00	0.00	0.40	[0.22]	0.07	0.00	0.00	0.00	0.00	0.00
	1.25:	0.00	0.00	0.00	0.00	0.37	[0.20]	0.22	0.00	0.00	0.00	0.00	0.00	0.00
	1.00:	0.00	0.00	0.00	0.20	[0.50]	0.20	0.00	0.00	0.00	0.00	0.00	0.00	0.00
	3/4:	0.00	0.00	0.00	[0.80]	0.12	0.00	0.00	0.00	0.00	0.00	0.00	0.00	0.00
	1/2:	0.00	0.00	[1.00]	0.00	0.00	0.00	0.00	0.00	0.00	0.00	0.00	0.00	0.00
	1/4:	0.00	[1.00]	0.00	0.00	0.00	0.00	0.00	0.00	0.00	0.00	0.00	0.00	0.00
	<1/4:	[0.00]	0.00	0.00	0.00	0.00	0.00	0.00	0.00	0.00	0.00	0.00	0.00	0.00
		<1/4	1/4	1/2	3/4	1.00	1.25	1.50	2.00	2.50	3.00	4	5	>5

RVR5

TABLE 5-12. SCATTER TABLE: 6/18-6/25: FOG-15 (SN 015) versus 1000-FOOT RVR 500

VISIBILITY COUNT FRACTION

FILE: OT8206.10 FG15 VS. RVRS SITE: OTIS YEAR: 1982 DAYS: 6/18- 6/25 HOURS: 0-24

AVERAGING 10

DI= -2.8

		<1/4	1/4	1/2	3/4	1.00	1.25	1.50	2.00	2.50	3.00	4	5	>5
	TOTALS:	102	31	14	10	10	8	21	9	8	16	26	32	602
	>5:	0.00	0.00	0.00	0.00	0.00	0.00	0.00	0.00	0.00	0.00	0.42	0.97	[1.00]
	5:	0.00	0.00	0.00	0.00	0.00	0.00	0.00	0.00	0.12	0.19	0.42	[0.03]	0.00
	4:	0.00	0.00	0.00	0.00	0.00	0.00	0.00	0.00	0.25	0.62	[0.15]	0.00	0.00
FG15	3.00:	0.00	0.00	0.00	0.00	0.00	0.00	0.14	0.22	0.37	[0.19]	0.00	0.00	0.00
	2.50:	0.00	0.00	0.00	0.00	0.00	0.00	0.10	0.22	[0.12]	0.00	0.00	0.00	0.00
DAY	2.00:	0.00	0.00	0.00	0.10	0.00	0.00	0.14	[0.56]	0.12	0.00	0.00	0.00	0.00
	1.50:	0.00	0.00	0.00	0.10	0.40	0.50	[0.57]	0.00	0.00	0.00	0.00	0.00	0.00
	1.25:	0.00	0.00	0.00	0.00	0.20	[0.37]	0.00	0.00	0.00	0.00	0.00	0.00	0.00
	1.00:	0.00	0.03	0.00	0.30	[0.40]	0.12	0.05	0.00	0.00	0.00	0.00	0.00	0.00
	3/4:	0.00	0.00	0.57	[0.50]	0.00	0.00	0.00	0.00	0.00	0.00	0.00	0.00	0.00
	1/2:	0.00	0.26	[0.43]	0.00	0.00	0.00	0.00	0.00	0.00	0.00	0.00	0.00	0.00
	1/4:	0.06	[0.58]	0.00	0.00	0.00	0.00	0.00	0.00	0.00	0.00	0.00	0.00	0.00
	<1/4:	[0.94]	0.13	0.00	0.00	0.00	0.00	0.00	0.00	0.00	0.00	0.00	0.00	0.00
		<1/4	1/4	1/2	3/4	1.00	1.25	1.50	2.00	2.50	3.00	4	5	>5

RVRS

		<1/4	1/4	1/2	3/4	1.00	1.25	1.50	2.00	2.50	3.00	4	5	>5
	TOTALS:	0	87	38	12	4	8	11	15	18	12	14	18	732
	>5:	0.00	0.00	0.00	0.00	0.00	0.00	0.00	0.00	0.00	0.00	0.36	0.67	[1.00]
	5:	0.00	0.00	0.00	0.00	0.00	0.00	0.00	0.00	0.00	0.00	0.29	[0.28]	0.00
	4:	0.00	0.00	0.00	0.00	0.00	0.00	0.00	0.00	0.22	0.42	[0.29]	0.06	0.00
FG15	3.00:	0.00	0.00	0.00	0.00	0.00	0.00	0.09	0.13	0.17	[0.58]	0.07	0.00	0.00
	2.50:	0.00	0.00	0.00	0.00	0.00	0.00	0.09	0.40	[0.56]	0.00	0.00	0.00	0.00
NITE	2.00:	0.00	0.00	0.00	0.00	0.00	0.12	0.27	[0.33]	0.00	0.00	0.00	0.00	0.00
	1.50:	0.00	0.00	0.03	0.00	0.75	0.50	[0.55]	0.13	0.06	0.00	0.00	0.00	0.00
	1.25:	0.00	0.00	0.00	0.08	0.25	[0.37]	0.00	0.00	0.00	0.00	0.00	0.00	0.00
	1.00:	0.00	0.00	0.00	0.33	[0.00]	0.00	0.00	0.00	0.00	0.00	0.00	0.00	0.00
	3/4:	0.00	0.00	0.13	[0.58]	0.00	0.00	0.00	0.00	0.00	0.00	0.00	0.00	0.00
	1/2:	0.00	0.07	[0.76]	0.00	0.00	0.00	0.00	0.00	0.00	0.00	0.00	0.00	0.00
	1/4:	0.00	[0.61]	0.00	0.00	0.00	0.00	0.00	0.00	0.00	0.00	0.00	0.00	0.00
	<1/4:	[0.00]	0.32	0.00	0.00	0.00	0.00	0.00	0.00	0.00	0.00	0.00	0.00	0.00
		<1/4	1/4	1/2	3/4	1.00	1.25	1.50	2.00	2.50	3.00	4	5	>5

RVRS

TABLE 5-13. SCATTER TABLE: 6/11-6/18: FOG-15 (SN 003) versus 1000-FOOT RVR 500

VISIBILITY COUNT FRACTION

FILE: OT8206.11 FG16 VS. RVR5 SITE: OTIS YEAR: 1982 DAYS: 6/11- 6/18 HOURS: 0-24

AVERAGING 10

K1= 1.150

	TOTALS:	12	9	10	9	12	8	13	19	26	31	41	41	754
	>5:	0.00	0.00	0.00	0.00	0.00	0.00	0.00	0.00	0.00	0.03	0.02	0.24	[0.99]
	5:	0.00	0.00	0.00	0.00	0.00	0.00	0.00	0.00	0.00	0.13	0.22	[0.46]	0.01
	4:	0.00	0.00	0.00	0.00	0.00	0.00	0.00	0.00	0.04	0.23	[0.49]	0.29	0.00
FG16	3.00:	0.00	0.00	0.00	0.00	0.00	0.00	0.08	0.11	0.08	[0.32]	0.24	0.00	0.00
	2.50:	0.00	0.00	0.00	0.00	0.00	0.00	0.08	0.16	[0.54]	0.23	0.02	0.00	0.00
DAY	2.00:	0.00	0.00	0.00	0.00	0.00	0.00	0.23	[0.26]	0.27	0.06	0.00	0.00	0.00
	1.50:	0.00	0.00	0.00	0.00	0.08	0.12	[0.38]	0.37	0.08	0.00	0.00	0.00	0.00
	1.25:	0.00	0.00	0.00	0.00	0.42	[0.50]	0.15	0.00	0.00	0.00	0.00	0.00	0.00
	1.00:	0.00	0.00	0.00	0.33	[0.33]	0.25	0.08	0.00	0.00	0.00	0.00	0.00	0.00
	3/4:	0.00	0.00	0.20	[0.56]	0.08	0.00	0.00	0.05	0.00	0.00	0.00	0.00	0.00
	1/2:	0.00	0.11	[0.70]	0.11	0.00	0.12	0.00	0.00	0.00	0.00	0.00	0.00	0.00
	1/4:	0.08	[0.78]	0.10	0.00	0.08	0.00	0.00	0.00	0.00	0.00	0.00	0.00	0.00
	<1/4:	[0.92]	0.11	0.00	0.00	0.00	0.00	0.00	0.05	0.00	0.00	0.00	0.00	0.00
		<1/4	1/4	1/2	3/4	1.00	1.25	1.50	2.00	2.50	3.00	4	5	>5

RVR5

	TOTALS:	0	10	8	5	8	5	9	14	12	24	38	36	816
	>5:	0.00	0.00	0.00	0.00	0.00	0.00	0.00	0.00	0.00	0.00	0.11	0.25	[0.98]
	5:	0.00	0.00	0.00	0.00	0.00	0.00	0.00	0.00	0.00	0.00	0.11	[0.39]	0.01
	4:	0.00	0.00	0.00	0.00	0.00	0.00	0.00	0.00	0.17	0.26	[0.53]	0.36	0.00
FG16	3.00:	0.00	0.00	0.00	0.00	0.00	0.00	0.00	0.00	0.25	[0.29]	0.21	0.00	0.00
	2.50:	0.00	0.00	0.00	0.00	0.00	0.00	0.00	0.21	[0.33]	0.37	0.05	0.00	0.00
NITE	2.00:	0.00	0.00	0.00	0.00	0.00	0.00	0.22	[0.64]	0.25	0.00	0.00	0.00	0.00
	1.50:	0.00	0.00	0.00	0.00	0.12	0.60	[0.44]	0.07	0.00	0.04	0.00	0.00	0.00
	1.25:	0.00	0.00	0.00	0.00	0.37	[0.20]	0.22	0.07	0.00	0.00	0.00	0.00	0.00
	1.00:	0.00	0.00	0.00	0.00	[0.37]	0.20	0.00	0.00	0.00	0.00	0.00	0.00	0.00
	3/4:	0.00	0.00	0.00	[0.80]	0.00	0.00	0.11	0.00	0.00	0.00	0.00	0.00	0.00
	1/2:	0.00	0.00	[1.00]	0.20	0.12	0.00	0.00	0.00	0.00	0.00	0.00	0.00	0.00
	1/4:	0.00	[1.00]	0.00	0.00	0.00	0.00	0.00	0.00	0.00	0.04	0.00	0.00	0.00
	<1/4:	[0.00]	0.00	0.00	0.00	0.00	0.00	0.00	0.00	0.00	0.00	0.00	0.00	0.00
		<1/4	1/4	1/2	3/4	1.00	1.25	1.50	2.00	2.50	3.00	4	5	>5

RVR5

TABLE 5-14, SCATTER TABLE: 6/18-25 FOG-15 (SN 003) versus 1000-FOOT RVR 500

VISIBILITY COUNT FRACTION

·LE: OT8206.18 FG16 VS. RVR5 SITE: OTIS YEAR: 1982 DAYS: 6/18- 6/25 HOURS:* 0-24

AVERAGING 10

* 1.150

	TOTALS:	102	31	14	10	10	8	21	9	8	16	26	32	682
	>6:	0.00	0.00	0.00	0.00	0.00	0.00	0.00	0.00	0.00	0.06	0.31	0.91	[1.00]
	6:	0.00	0.00	0.00	0.00	0.00	0.00	0.00	0.00	0.25	0.19	0.35	[0.09]	0.00
	4:	0.00	0.00	0.00	0.00	0.00	0.00	0.00	0.00	0.12	0.44	[0.27]	0.00	0.00
FG16	3.00:	0.00	0.00	0.00	0.00	0.00	0.00	0.10	0.22	0.25	[0.19]	0.00	0.00	0.00
	2.50:	0.00	0.00	0.00	0.00	0.00	0.00	0.10	0.22	[0.12]	0.12	0.00	0.00	0.00
DAY	2.00:	0.00	0.00	0.00	0.10	0.00	0.00	0.14	[0.22]	0.25	0.00	0.00	0.00	0.00
	1.50:	0.00	0.00	0.00	0.00	0.30	0.25	[0.57]	0.33	0.00	0.00	0.00	0.00	0.00
	1.25:	0.00	0.00	0.00	0.10	0.20	[0.37]	0.05	0.00	0.00	0.00	0.00	0.00	0.00
	1.00:	0.00	0.00	0.00	0.20	[0.40]	0.12	0.00	0.00	0.00	0.00	0.00	0.00	0.00
	3/4:	0.00	0.03	0.36	[0.40]	0.00	0.25	0.05	0.00	0.00	0.00	0.00	0.00	0.00
	1/2:	0.00	0.23	[0.57]	0.20	0.10	0.00	0.00	0.00	0.00	0.00	0.00	0.00	0.00
	1/4:	0.07	[0.52]	0.07	0.00	0.00	0.00	0.00	0.00	0.00	0.00	0.00	0.00	0.00
	<1/4:	[0.93]	0.23	0.00	0.00	0.00	0.00	0.00	0.00	0.00	0.00	0.00	0.00	0.00
		<1/4	1/4	1/2	3/4	1.00	1.25	1.50	2.00	2.50	3.00	4	5	>6

RVR5

	TOTALS:	0	87	30	12	4	8	11	15	10	12	14	10	732
	>5:	0.00	0.00	0.00	0.00	0.00	0.00	0.00	0.00	0.00	0.00	0.36	0.50	[0.99]
	5:	0.00	0.00	0.00	0.00	0.00	0.00	0.00	0.00	0.00	0.00	0.21	[0.44]	0.00
	4:	0.00	0.00	0.00	0.00	0.00	0.00	0.00	0.00	0.17	0.42	[0.29]	0.06	0.00
FG16	3.00:	0.00	0.00	0.00	0.00	0.00	0.00	0.09	0.07	0.11	[0.33]	0.14	0.00	0.00
	2.50:	0.00	0.00	0.00	0.00	0.00	0.00	0.00	0.27	[0.67]	0.25	0.00	0.00	0.00
NITE	2.00:	0.00	0.00	0.00	0.00	0.00	0.12	0.27	[0.33]	0.00	0.00	0.00	0.00	0.00
	1.50:	0.00	0.00	0.00	0.00	0.00	0.62	[0.45]	0.20	0.06	0.00	0.00	0.00	0.00
	1.25:	0.00	0.00	0.03	0.00	0.25	[0.12]	0.18	0.07	0.00	0.00	0.00	0.00	0.00
	1.00:	0.00	0.00	0.00	0.42	[0.50]	0.00	0.00	0.07	0.00	0.00	0.00	0.00	0.00
	3/4:	0.00	0.00	0.10	[0.42]	0.00	0.12	0.00	0.00	0.00	0.00	0.00	0.00	0.00
	1/2:	0.00	0.06	[0.61]	0.00	0.25	0.00	0.00	0.00	0.00	0.00	0.00	0.00	0.00
	1/4:	0.00	[0.59]	0.10	0.00	0.00	0.00	0.00	0.00	0.00	0.00	0.00	0.00	0.00
	<1/4:	[0.00]	0.36	0.00	0.00	0.00	0.00	0.00	0.00	0.00	0.00	0.00	0.00	0.00
		<1/4	1/4	1/2	3/4	1.00	1.25	1.50	2.00	2.50	3.00	4	5	>5

RVR5

TABLE 5-15. SCATTER TABLE: 7/ 9 - 7/16: FOG-15 (SN 003) versus 1000-FOOT RVR 500

VISIBILITY COUNT FRACTION

FILE: OTIS82.190 FG15 VS. RVRS SITE: TRAILER YEAR: 1982 DAYS: 7/ 9- 7/16 HOURS: 0-24

AVERAGING 12 PER

K1= 1.150

	TOTALS:	29	22	19	16	10	12	24	32	24	28	47	85	664
	>5:	0.00	0.05	0.00	0.06	0.00	0.00	0.00	0.03	0.00	0.11	0.72	1.00	[1.00]
	5:	0.00	0.00	0.00	0.00	0.00	0.00	0.00	0.00	0.00	0.32	0.26	[0.00]	0.00
	4:	0.00	0.00	0.00	0.00	0.00	0.00	0.00	0.03	0.04	0.39	[0.02]	0.00	0.00
FG15	3.00:	0.00	0.00	0.00	0.00	0.00	0.00	0.00	0.03	0.62	[0.11]	0.00	0.00	0.00
	2.50:	0.00	0.00	0.00	0.00	0.00	0.00	0.04	0.28	[0.17]	0.00	0.00	0.00	0.00
DAY	2.00:	0.00	0.00	0.00	0.00	0.00	0.00	0.17	[0.56]	0.00	0.04	0.00	0.00	0.00
	1.50:	0.00	0.00	0.00	0.00	0.10	0.50	[0.71]	0.06	0.12	0.04	0.00	0.00	0.00
	1.25:	0.00	0.00	0.00	0.06	0.40	[0.50]	0.00	0.00	0.00	0.00	0.00	0.00	0.00
	1.00:	0.00	0.05	0.00	0.25	[0.50]	0.00	0.00	0.00	0.00	0.00	0.00	0.00	0.00
	3/4:	0.00	0.00	0.21	[0.62]	0.00	0.00	0.00	0.00	0.04	0.00	0.00	0.00	0.00
	1/2:	0.00	0.14	[0.74]	0.00	0.00	0.00	0.00	0.00	0.00	0.00	0.00	0.00	0.00
	1/4:	0.07	[0.77]	0.05	0.00	0.00	0.00	0.00	0.00	0.00	0.00	0.00	0.00	0.00
	<1/4:	[0.93]	0.00	0.00	0.00	0.00	0.00	0.00	0.00	0.00	0.00	0.00	0.00	0.00
		<1/4	1/4	1/2	3/4	1.00	1.25	1.50	2.00	2.50	3.00	4	5	>5

RVRS

	TOTALS:	0	22	22	15	9	9	11	17	26	35	36	37	773
	>5:	0.00	0.00	0.00	0.07	0.00	0.11	0.00	0.00	0.00	0.03	0.19	0.95	[1.00]
	5:	0.00	0.00	0.00	0.00	0.00	0.00	0.00	0.00	0.00	0.03	0.22	[0.05]	0.00
	4:	0.00	0.00	0.00	0.00	0.00	0.00	0.00	0.00	0.04	0.31	[0.42]	0.00	0.00
FG15	3.00:	0.00	0.00	0.00	0.00	0.00	0.00	0.00	0.00	0.19	[0.57]	0.03	0.00	0.00
	2.50:	0.00	0.00	0.00	0.00	0.00	0.00	0.00	0.29	[0.73]	0.03	0.11	0.00	0.00
NITE	2.00:	0.00	0.00	0.00	0.00	0.00	0.00	0.27	[0.59]	0.04	0.03	0.00	0.00	0.00
	1.50:	0.00	0.00	0.05	0.00	0.11	0.11	[0.73]	0.12	0.00	0.00	0.00	0.00	0.00
	1.25:	0.00	0.00	0.00	0.00	0.11	[0.78]	0.00	0.00	0.00	0.00	0.03	0.00	0.00
	1.00:	0.00	0.00	0.00	0.53	[0.78]	0.00	0.00	0.00	0.00	0.00	0.00	0.00	0.00
	3/4:	0.00	0.00	0.23	[0.40]	0.00	0.00	0.00	0.00	0.00	0.00	0.00	0.00	0.00
	1/2:	0.00	0.09	[0.73]	0.00	0.00	0.00	0.00	0.00	0.00	0.00	0.00	0.00	0.00
	1/4:	0.00	[0.91]	0.00	0.00	0.00	0.00	0.00	0.00	0.00	0.00	0.00	0.00	0.00
	<1/4:	[0.00]	0.00	0.00	0.00	0.00	0.00	0.00	0.00	0.00	0.00	0.00	0.00	0.00
		<1/4	1/4	1/2	3/4	1.00	1.25	1.50	2.00	2.50	3.00	4	5	>5

RVRS

symmetrically placed (Figure 4-2) along the 1000-foot baseline. Surprisingly, averaging the two sensors together produced more consistent improvement in the slowly varying events than in the rapidly varying ones. Apparently the spatial variation was so great for the rapidly varying events that more than two sensors would be required to equal the averaging of the transmissometer, even for ten-minute averaging times. Figure 5-24 shows how much the visibility can differ between the FOG-15 and the 1000-foot RVR-500 for the most rapidly varying events observed, which were due to ground fog.

5.4.3 Calibration Stability

A number of fog events were examined both at the beginning and end of the test period to determine the stability of the FOG-15 calibration. In general the fog response over a four-month period remained consistent to within about ten percent. On some occasions the nonlinearity of the response was somewhat less than that used to calibrate Event #1 on June 16-17. On one occasion (June 19-20 hours: 19-4) the low extinction response reverted to its usual value, a factor of 1.3 lower than assumed in the nonlinear response. This time period covers afternoon to the middle of the night. Most of the other fog events examined cover from the middle of the night until mid-morning. This difference in response for different time periods is probably the effect of sunlight (see Section 6.2).

5.4.4 Response To Rain and Snow

An extensive study of the FOG-15 and EG&G 207 response to rain and snow was prepared for a preliminary report on this project. Only data from earlier FOG-15 versions were included. Figure 5-25 shows the slope of the response relative to the 500-foot transmissometer for a number of events. The forward-scatter meters were calibrated to give agreement with the transmissometers in fog and the calibration appeared to remain stable over the time period examined. The events were selected to avoid contamination of the rain and snow with fog as much as possible and to

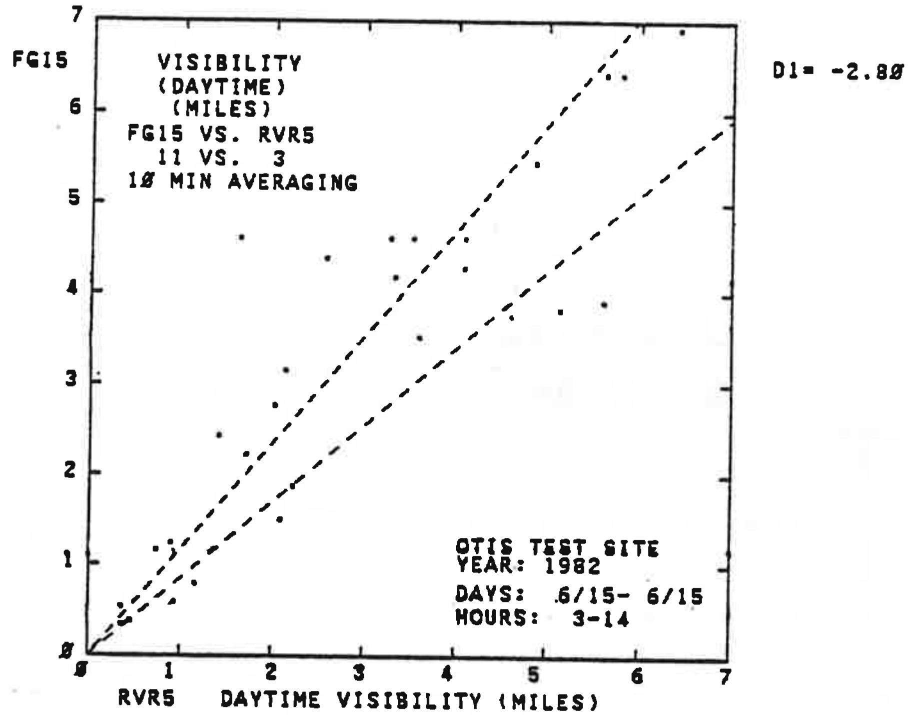

(a)

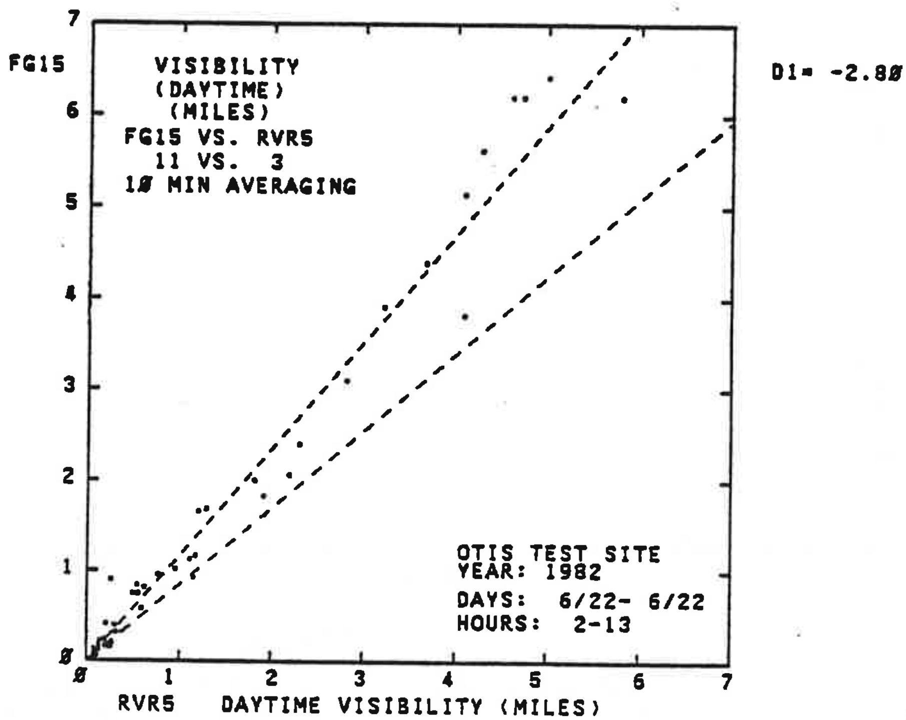

(b)

FIGURE 5-24. VISIBILITY SCATTER PLOTS FOR RAPIDLY VARYING EVENTS FOG-15 versus 1000-FOOT RVR 500.

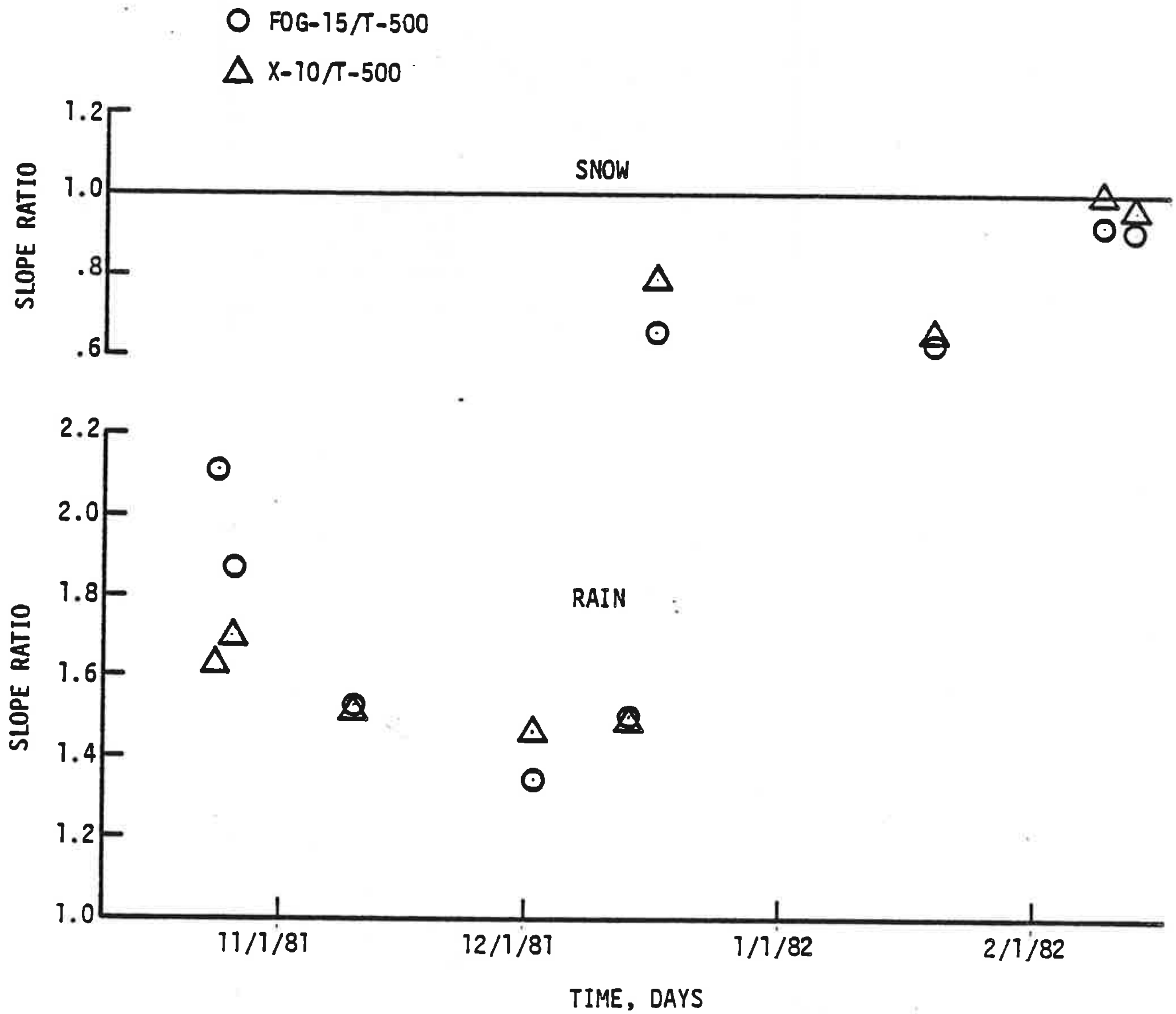

FIGURE 5-25. RAIN AND SNOW RESPONSE OF FORWARD-SCATTER METERS RELATIVE TO THE 500-FOOT BASELINE TRANSMISSOMETER: FSM'S WERE CALIBRATED FOR FOG.

have good correlation between the two sensors. The rain response is consistently higher by a factor greater than 1.5. The snow response was generally somewhat lower than or the same as the fog response.

Few candidate fogless rain events were identified in the spring tests. Figure 5-26 shows one event where rain and fog occurred. The slope for one period was a factor of 1.5 higher than the other period, perhaps reflecting the difference between rain and fog.

5.4.5 Calibration of Earlier Instruments

Figure 5-27 shows extinction-coefficient scatter plots comparing an earlier version of the FOG-15 to the 500-foot RVR 500 using the new nonlinear calibration for the FOG-15. Instead of straightening out the response as in Figures 5-20 and 5-21, the new calibration generates a break in the response curve. The break in the response if any should be below 10 $10^{-4}m^{-1}$ rather than at 38.5 $10^{-4}m^{-1}$ as in the current calibration.
In this respect the response of the earlier instrument is more like the EG&G 207 which tends to show a low extinction nonlinearity.

5.5 ARTAIS INTERFACES

The reports from the Artais AWOS generally agreed with the Otis tower surface observations (SA's). Table 5-16 compares the temperature, dew point, and winds for one day in June. The Artais altimeter setting was never properly set up and is not included in Table 5-16. Table 5-17 compares the visibility and cloud reports from the AWOS to all the surface observations for the same period of time as Table 5-16. This period (including Event #1) was selected for analysis because both ceilometer data and the Artais reports were recorded on magnetic tape.

Large differences in reported visibility are noted in Table 5-16. At high visibility the low AWOS reports are caused by the 100-percent error of the RVV-700 which was about 13 percent at this time. The human

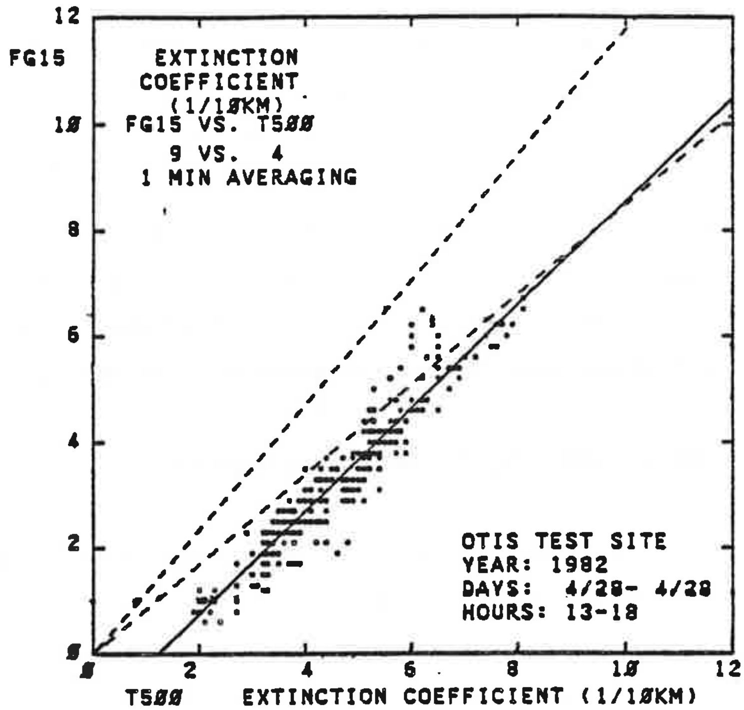

(a)

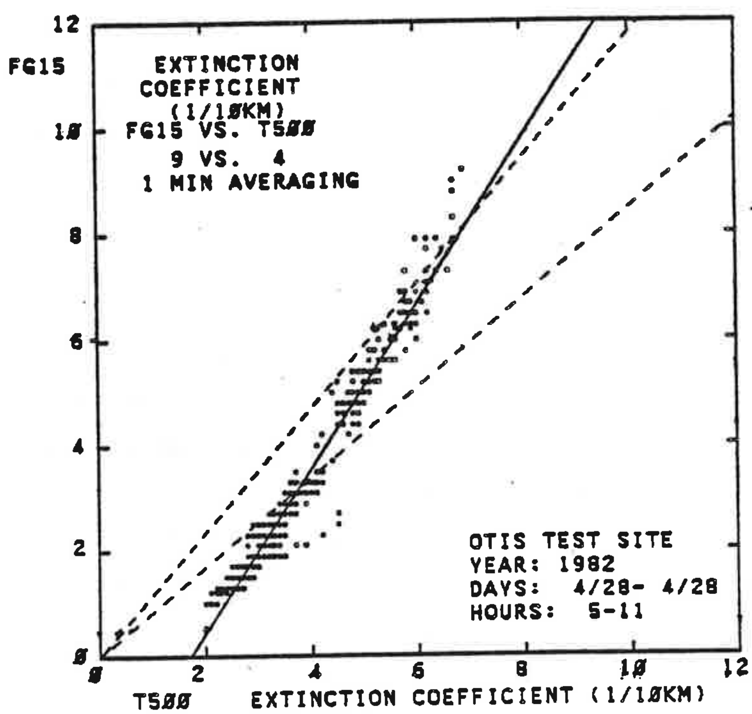

(b)

FIGURE 5-26. SCATTER PLOTS COMPARING THE FOG-15 RESPONSE TO THE TRANSMISSOMETER RESPONSE FOR A FOG/RAIN EVENT: HOURS (a) 1300-1800, (b) 0500-1100.

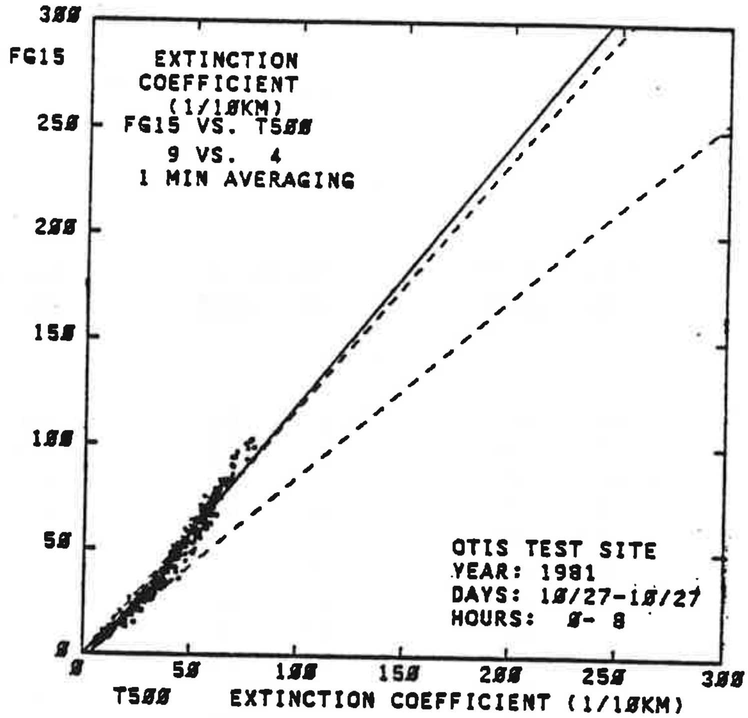

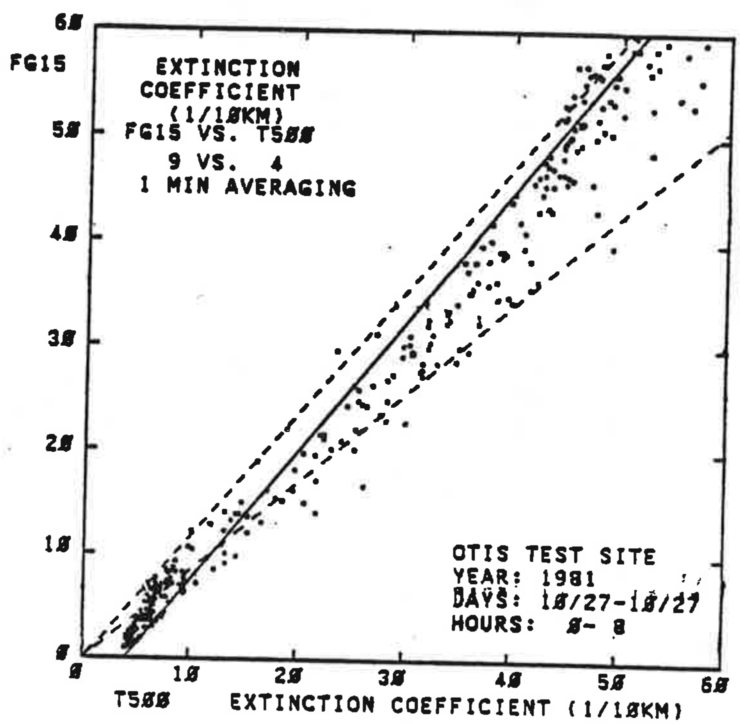

FIGURE 5-27. FOG RESPONSE OF EARLIER MODEL FOG-15 COMPARED WITH THE 500-FOOT RVR 500.

TABLE 5-16. COMPARISON OF AWOS OUTPUT TO SURFACE OBSERVATIONS: TEMP, DEW, WIND

June 16 & 17, 1982

Time	Temperature		Dew Point		Direction		Speed	
	SA	AWOS	SA	AWOS	SA	AWOS	SA	AWOS
11:55	64	64	57	55	230	240	16	25
12:55	65	65	57	55	270	230	17	21
13:55	67	67	58	57	250	250	18	21
14:55	68	69	59	57	240	240	18	26
15:55	68	68	60	57	230	240	18	26
17:55	66	65	59	56	240	240	18	25
18:55	64	64	59	56	250	240	18	29
19:55	65	64	59	56	240	230	14	19
20:55	65	62	59	55	240	240	14	19
21:55	61	61	58	55	240	250	10	19
22:55	61	61	58	55	250	240	12	13
23:55	60	60	58	55	250	240	10	12
00:55	60	60	59	56	240	230	14	10
01:55	60	60	59	56	240	230	15	20
02:55	61	61	59	57	260	260	06	6
03:55	61	60	58	56	250	240	08	12
04:55	60	59	59	55	240	230	08	8
05:55	59	59	57	55	230	240	08	9
06:55	60	60	57	55	250	250	04	9
07:55	60	60	58	56	200	170	10	5
08:55	60	60	58	56	000	180	00	3
09:55	61	61	59	57	180	190	02	7
10:55	62	62	60	58	190	210	04	9
11:55	61	62	60	58	200	210	07	10
12:55	62	63	60	58	220	230	06	9
13:55	67	68	62	61	230	240	08	11
14:55	70	70	63	61	210	230	08	10

TABLE 5-17. COMPARISONS OF AWOS VISIBILITY AND CLOUD REPORTS TO HUMAN REPORTS

Time	Obstruct. SA	Visib. SA	Visib. AWOS	Surface Clouds	AWOS Clouds
11:55		7	2.5	25 SCT 100 SCT E 200 OVC	CLR BLO 50
12:55		7	3	15 SCT 25 SCT 100 SCT 200 OVC	CLR BLO 50
13:55		7	3	15 SCT 25 SCT E 100 BKN 200 OVC	12 SCT
14:55	H	5	2	15 SCT 25 SCT 100 SCT 200 OVC	FEW CLDS 14
15:45	H	5	2	M15 BKN 100 BKN 200 OVC	11 SCT
15:55	H	5	2	M15 BKN 100 BKN 200 OVC	11 SCT
16:25	H	5	2	M11 BKN 15 OVC	M9 BKN CIG 8 V11
16:40	H	4	2	-X M10 BKN 15 OVC	M7 BKN 10 OVC CIG 7 V9
16:55	H	4	2	-X 8 SCT M10 BKN 15 OVC	M7 OVC CIG 7 V9
17:55	H	4	2	-X 9 SCT M10 BKN 15 OVC	M6 OVC CIG 6 V8
18:55	H	4	2	M10 BKN 15 OVC	M5 OVC CIG 5 V7
19:13	H	4	2	M7 OVC	M5 OVC CIG 4 V7
19:55	H	3	2	M7 OVC	M4 OVC CIG 4 V6
20:55	H	3	1.75	M7 OVC	M4 OVC CIG 2 V6
21:05	H	2	1.75	M5 OVC	M3 OVC CIG 2 V5
21:55	H	2	1.75	M5 OVC	M2 OVC CIG 2 V4
22:11	F	1.5	1.5	M4 OVC	M2 OVC CIG 2 V4
22:32	F	1.25	1.75	M3 OVC	M2 OVC
22:55	F	1.25	1.25	M3 OVC	-X M2 OVC
23:35	F	.75	1	W2 X	-X M1 OVC CIG 1 V2
23:47	F	.50	.75	W1 X	-X M1 OVC CIG 1 V2
23:55	F	.50	.75	W1 X	-X M1 OVC CIG 1 V2
00:13	F	.25	.25	W1 X	-X M1 OVC
00:55	F	.125	.25	W1 X	-X M1 OVC
01:55	F	.25	.25	W1 X	-X M1 OVC
02:07	R-F	.25	.50	W1 X	-X M1 OVC
02:33	R-F	1	2	M2 OVC	M1 OVC CIG 1 V3
02:43	R-F	3	2.5	M4 OVC	

TABLE 5-17. (concluded)

02:55	R-F	4	3	M4 OVC	1 SCT 4 SCT
03:55	F	1	1.25	W4 X	M1 OVC
04:29	F	.75	.75	W3 X	-X M1 OVC
04:39	F	.50	.50	W2 X	-X M1 OVC
04:55	F	.50	.50	W2 X	-X M1 OVC
05:55	F	.50	2	W2 X	M1 OVC CIG 1 V2
06:55	F	.50	3	W2 X	2 SCT 48 SCT
07:07	F	2	3	2 SCT E 35 OVC	45 SCT
07:15	F	3	3	E 40 OVC	M 45 BKN BKN V SCT
07:27	TRW-F	3	3	E 40 OVC	2 SCT 44 SCT
07:55	TRW-F	3	2.5	10 SCT E 40 OVC	2 SCT 5 SCT
08:43	R-F	2	2.5	10 SCT E 40 OVC	CLR BLO 50
08:55	R-F	2	2	10 SCT E 40 OVC	40 SCT
09:51	F	.75	1	W3 X	-X M1 BKN 13 OVC CIG 1 V2
09:55	F	.75	1	W3 X	-X M1 OVC CIG 1 V2
10:14	F	.50	.75	W2 X	-X M1 OVC CIG 1 V2
10:20	F	.25	.50	W1 X	-X M1 OVC
10:42	F	.75	.50	W2 X	-X M1 OVC CIG 1 V2
10:47	F	.75		W3 X	
10:55	F	.75	1.50	W3 X	M1 OVC CIG 1 V2
11:10	F	.5		W2 X	M1 OVC CIG 1 V2
11:16			1.25		M1 OVC CIG 1 V2
11:26			1.25		-X M1 OVC CIG 1 V2
11:31			1.25		-X M1 OVC CIG 1 V2
11:43	R-F	.75	1	W3 X	-X M1 OVC
11:55	F	.75	1.25	W3 X	-X M1 OVC CIG 1 V2
12:20	F	.50	1.25	W2 X	-X M1 OVC CIG 1 V2
12:30			1.25		-X M1 OVC
12:45			.75		-X M1 OVC CIG 1 V2
12:55	F	.50	1	W2 X	-X M1 OVC CIG 1 V2
13:37	F	1	1.50	W2 X	-X M1 OVC CIG 1 V3
13:40	F	1.50	2	-X E 100 BKN 200 OVC	M1 OVC CIG 1 V4

observations are lower in dense fog probably because the tower height (96 feet) has a higher fog density than the ground.

The AWOS cloud reports in Table 5-18 generally agree with the human observations. The following differences are noted:

1) The AWOS reports are simpler, listing fewer layers.
2) The AWOS ceilings tend to be lower.
3) The AWOS ceilometer measures cloud layers where the human reports "obscured."
4) The AWOS reports variable ceiling too often.
5) Sometimes the detailed reports differ significantly in cloud cover.

These effects are due to various sources including the separation between the tower and the test site (effect 5), the properties of the ceilometer (effects 2,3), and errors in the reporting algorithm (effects 2,4). The ceilometer tends to report nonexistent low clouds when the visibility is low, thus leading to effects 2 and 3.

5.5.1 Ceilometer

The NWS cloud layer reporting algorithm was programmed in FORTRAN for use in comparing the Artais reports to the reports generated by computation from the ceilometer hit data. The description of the NWS cloud layer algorithm contains some ambiguities. When ambiguities arose, the selection of parameters was made to give results similar to those of Artais. Table 5-18 compares the computed reports (CMP1-3) with the Artais report (WEAT) for selected periods of time. Three computed values are generated. CMP1 uses all the LD-WHL data (every 15 seconds). CMP2 and CMP3 use every other data report as is used by Artais. One would expect either CMP2 or CMP3 to agree with Artais since one of them should be using the same data. There is usually little difference among the three computed reports. The NWS cloud layer algorithm analyzes the last 30 minutes worth of data. The reports in Table 5-18 are listed every 5 minutes.

TABLE 5-18. COMPARISON OF AWOS CLOUD REPORTS TO COMPUTED REPORTS.

6/16/82	10:26:00	CMP1:	CLR BLO 50
		CMP2:	CLR BLO 50
		CMP3:	CLR BLO 50
		WEAT:	CLR BLO 50
6/16/82	10:31:00	CMP1:	FEW CLDS 42
		CMP2:	CLR BLO 50
		CMP3:	CLR BLO 50
		WEAT:	41 SCT
6/16/82	10:36:00	CMP1:	42 SCT
		CMP2:	42 SCT
		CMP3:	42 SCT
		WEAT:	41 SCT
6/16/82	12:51:00	CMP1:	CLR BLO 50
		CMP2:	CLR BLO 50
		CMP3:	CLR BLO 50
		WEAT:	CLR BLO 50
6/16/82	12:56:00	CMP1:	FEW CLDS 13
		CMP2:	CLR BLO 50
		CMP3:	CLR BLO 50
		WEAT:	FEW CLDS 12
6/16/82	13: 1:00	CMP1:	FEW CLDS 13
		CMP2:	CLR BLO 50
		CMP3:	13 SCT
		WEAT:	FEW CLDS 12
6/16/82	13: 6:00	CMP1:	12 SCT
		CMP2:	12 SCT
		CMP3:	12 SCT
		WEAT:	12 SCT
6/16/82	13:11:00	CMP1:	12 SCT
		CMP2:	12 SCT
		CMP3:	12 SCT
		WEAT:	11 SCT
6/16/82	13:56:00	CMP1:	13 SCT
		CMP2:	13 SCT
		CMP3:	13 SCT
		WEAT:	12 SCT
6/16/82	14: 1:00	CMP1:	13 SCT
		CMP2:	13 SCT
		CMP3:	13 SCT
		WEAT:	12 SCT
6/16/82	14: 6:00	CMP1:	14 SCT
		CMP2:	14 SCT
		CMP3:	14 SCT
		WEAT:	13 SCT
6/16/82	16:13:00	CMP1:	11 BKN
		CMP2:	10 BKN
		CMP3:	11 BKN
		WEAT:	M9 BKN 12 BKN CIG 9 V 11
6/16/82	16:18:00	CMP1:	10 BKN
		CMP2:	10 BKN
		CMP3:	10 BKN
		WEAT:	M9 BKN 12 BKN CIG 9 V 11
6/16/82	16:23:00	CMP1:	10 BKN BKN VRBL OVC
		CMP2:	10 BKN BKN VRBL OVC
		CMP3:	10 OVC OVC VRBL BKN
		WEAT:	M9 BKN CIG 9 V 11
6/16/82	16:28:00	CMP1:	10 OVC
		CMP2:	10 OVC OVC VRBL BKN
		CMP3:	9 OVC
		WEAT:	M8 BKN 11 OVC CIG 7 V 10
6/16/82	16:33:00	CMP1:	9 OVC
		CMP2:	9 OVC
		CMP3:	9 OVC
		WEAT:	M8 OVC CIG 7 V 10
6/16/82	16:38:00	CMP1:	9 OVC
		CMP2:	9 OVC
		CMP3:	9 OVC
		WEAT:	M8 OVC CIG 7 V 10
6/16/82	16:43:00	CMP1:	8 OVC HIR CLDS VSB
		CMP2:	8 OVC
		CMP3:	8 OVC HIR CLDS VSB
		WEAT:	M7 OVC CIG 7 V 9
6/16/82	19:43:00	CMP1:	5 OVC
		CMP2:	5 OVC
		CMP3:	5 OVC
		WEAT:	M4 OVC CIG 4 V 6
6/16/82	19:48:00	CMP1:	5 OVC
		CMP2:	5 OVC
		CMP3:	5 OVC
		WEAT:	M4 OVC CIG 4 V 6
6/16/82	19:53:00	CMP1:	5 OVC
		CMP2:	5 OVC
		CMP3:	5 OVC
		WEAT:	M4 OVC CIG 4 V 6
6/16/82	19:58:00	CMP1:	5 OVC
		CMP2:	5 OVC
		CMP3:	5 OVC
		WEAT:	M4 OVC CIG 4 V 6

TABLE 5-18. (continued)

6/16/82 21: 3:00 CMP1: 4 OVC
CMP2: 4 OVC
CMP3: 4 OVC
WEAT: M3 OVC CIG 2 V 5
6/16/82 21: 8:00 CMP1: 4 OVC
CMP2: 4 OVC
CMP3: 4 OVC
WEAT: M3 OVC CIG 2 V 5
6/16/82 21:13:00 CMP1: 4 OVC
CMP2: 4 OVC
CMP3: 4 OVC
WEAT: M2 BKN 5 OVC CIG 2 V 4
6/16/82 21:18:00 CMP1: 3 OVC
CMP2: 3 OVC
CMP3: 3 OVC
WEAT: M2 OVC CIG 2 V 4

6/16/82 21:53:00 CMP1: 3 OVC
CMP2: 3 OVC
CMP3: 3 OVC
WEAT: M2 OVC CIG 2 V 4
6/16/82 21:58:00 CMP1: 3 OVC
CMP2: 3 OVC
CMP3: 3 OVC
WEAT: M2 OVC CIG 2 V 4
6/16/82 22: 3:00 CMP1: 2 OVC HIR CLDS VSB
CMP2: 2 OVC HIR CLDS VSB
CMP3: 2 OVC HIR CLDS VSB
WEAT: M2 OVC CIG 2 V 4

6/16/82 23:39:00 CMP1: -X 2 OVC
CMP2: -X 2 OVC
CMP3: -X 2 OVC
WEAT: -X M1 OVC CIG 1 V 2
6/16/82 23:44:00 CMP1: -X 2 OVC
CMP2: -X 2 OVC
CMP3: -X 2 OVC
WEAT: -X M1 OVC CIG 1 V 2
6/16/82 23:49:00 CMP1: -X 2 OVC
CMP2: -X 2 OVC
CMP3: -X 2 OVC
WEAT: -X M1 OVC CIG 1 V 2

6/17/82 1:14:00 CMP1: -X 1 OVC
CMP2: -X 1 OVC
CMP3: -X 1 OVC
WEAT: -X M1 OVC
6/17/82 1:19:00 CMP1: -X 1 OVC
CMP2: -X 1 OVC
CMP3: -X 1 OVC
WEAT: -X M1 OVC

6/17/82 2:24:00 CMP1: -X 1 OVC
CMP2: -X 1 OVC
CMP3: -X 1 OVC
WEAT: -X M1 OVC CIG 1 V 2
6/17/82 2:29:00 CMP1: 1 OVC
CMP2: 1 OVC
CMP3: 1 OVC
WEAT: M1 OVC CIG 1 V 3
6/17/82 2:34:00 CMP1: 2 OVC HIR CLDS VSB
CMP2: 2 OVC HIR CLDS VSB
CMP3: 2 OVC HIR CLDS VSB
WEAT: M1 OVC CIG 1 V 3
6/17/82 2:39:00 CMP1: 2 BKN 5 BKN
CMP2: 2 BKN 5 BKN
CMP3: 2 BKN 5 BKN
WEAT: M1 BKN 4 BKN CIG 1 V 3
6/17/82 2:44:00 CMP1: 2 BKN 5 BKN
CMP2: 2 BKN 5 BKN
CMP3: 2 BKN 5 BKN
WEAT:
6/17/82 2:49:00 CMP1: 2 SCT 5 SCT
CMP2: 2 SCT 5 SCT
CMP3: 2 SCT 5 SCT
WEAT: 1 SCT 4 SCT
6/17/82 2:54:00 CMP1: 3 SCT
CMP2: 3 SCT
CMP3: 2 SCT 5 SCT
WEAT: 1 SCT 4 SCT
6/17/82 2:59:00 CMP1: 3 SCT
CMP2: 3 SCT
CMP3: 3 SCT
WEAT: 3 SCT

6/17/82 3:39:00 CMP1: 2 SCT 7 SCT
CMP2: 2 SCT 5 SCT
CMP3: 2 SCT 5 SCT
WEAT: 1 SCT 4 SCT
6/17/82 3:44:00 CMP1: 2 BKN 4 BKN 7 BKN BKN VRBL SCT
CMP2: 2 BKN 5 BKN BKN VRBL SCT
CMP3: 2 BKN 5 BKN
WEAT: M1 BKN 4 BKN CIG 1 V 3
6/17/82 3:49:00 CMP1: 2 BKN 4 BKN 7 BKN
CMP2: 2 BKN 5 BKN
CMP3: 1 BKN 4 BKN
WEAT: M1 BKN 4 BKN CIG 1 V 3
6/17/82 3:54:00 CMP1: 1 OVC OVC VRBL BKN
CMP2: 1 OVC HIR CLDS VSB
CMP3: 1 OVC OVC VRBL BKN
WEAT: M1 BKN 4 OVC CIG 1 V 3
6/17/82 3:59:00 CMP1: -X 1 OVC
CMP2: -X 1 OVC
CMP3: -X 1 OVC
WEAT: -X M1 OVC CIG 1 V 3

TABLE 5-18, (continued)

```
6/17/82   6:24:00 CMP1:      2 BKN  BKN VRBL OVC
                  CMP2:      2 BKN  BKN VRBL OVC
                  CMP3:      2 BKN  BKN VRBL OVC
                  WEAT: M1 BKN CIG 1 V 3
6/17/82   6:29:00 CMP1:      2 BKN
                  CMP2:      2 BKN
                  CMP3:      2 BKN
                  WEAT: M1 BKN CIG 1 V 3
6/17/82   6:34:00 CMP1:      2 BKN  BKN VRBL SCT
                  CMP2:      2 SCT
                  CMP3:      2 BKN
                  WEAT: 1 SCT
6/17/82   6:39:00 CMP1:      2 SCT
                  CMP2:      2 SCT
                  CMP3:      2 SCT
                  WEAT: 2 SCT
6/17/82   6:44:00 CMP1:      2 SCT
                  CMP2:      2 SCT
                  CMP3:      2 SCT
                  WEAT: 2 SCT
6/17/82   6:49:00 CMP1:      2 SCT 49 SCT
                  CMP2:      2 SCT 49 SCT
                  CMP3:      2 SCT 49 SCT
                  WEAT: 2 SCT
6/17/82   6:54:00 CMP1:     49 SCT
                  CMP2:     49 SCT
                  CMP3:      2 SCT 49 SCT
                  WEAT: 2 SCT 48 SCT
6/17/82   6:59:00 CMP1:     48 SCT
                  CMP2:     48 SCT
                  CMP3:     48 SCT
                  WEAT: 47 SCT
6/17/82   7: 4:00 CMP1:     47 SCT
                  CMP2:     47 SCT
                  CMP3:     47 SCT
                  WEAT: 45 SCT

6/17/82   7:14:00 CMP1:     47 BKN
                  CMP2:     47 BKN  BKN VRBL SCT
                  CMP3:     47 BKN
                  WEAT: M45 BKN BKN V SCT
6/17/82   7:19:00 CMP1:     47 BKN  BKN VRBL SCT
                  CMP2:     47 SCT
                  CMP3:     47 BKN
                  WEAT: M45 BKN BKN V SCT
6/17/82   7:24:00 CMP1:     46 SCT
                  CMP2:     46 SCT
                  CMP3:      2 SCT 46 BKN  BKN VRBL SCT
                  WEAT: 2 SCT 44 SCT
6/17/82   7:29:00 CMP1:      2 SCT 46 SCT
                  CMP2:      2 SCT 46 SCT
                  CMP3:      2 SCT 46 BKN  BKN VRBL SCT
                  WEAT: 2 SCT 44 SCT
6/17/82   7:34:00 CMP1:      2 SCT 46 BKN  BKN VRBL SCT
                  CMP2:      2 SCT 46 SCT
                  CMP3:      2 SCT 46 BKN  BKN VRBL SCT
                  WEAT: 2 SCT 5 SCT M44 BKN BKN V SCT
6/17/82   7:39:00 CMP1:      2 SCT 45 SCT
                  CMP2:      2 SCT 45 SCT
                  CMP3:      2 SCT 46 SCT
                  WEAT: 2 SCT 5 SCT 44 SCT
6/17/82   7:44:00 CMP1:      2 SCT 46 SCT
                  CMP2:      2 SCT
                  CMP3:      2 SCT 46 SCT
                  WEAT: 2 SCT 5 SCT
6/17/82   7:49:00 CMP1:      2 SCT
                  CMP2:      2 SCT
                  CMP3:      2 SCT
                  WEAT: 2 SCT 5 SCT
6/17/82   7:56:00 CMP1:      2 SCT
                  CMP2:      2 SCT
                  CMP3:      2 SCT
                  WEAT: 2 SCT 5 SCT
6/17/82   8: 1:00 CMP1:      2 BKN  BKN VRBL SCT
                  CMP2:      2 BKN
                  CMP3:      2 BKN  BKN VRBL SCT
                  WEAT: 1 SCT M5 BKN CIG 5 V 7
6/17/82   8: 6:00 CMP1:      2 SCT
                  CMP2:      2 BKN  BKN VRBL SCT
                  CMP3:      2 SCT
                  WEAT: 1 SCT
6/17/82   8:11:00 CMP1:      2 SCT
                  CMP2:      2 BKN  BKN VRBL SCT
                  CMP3:      2 SCT
                  WEAT: M1 BKN CIG 1 V 3
6/17/82   8:16:00 CMP1:      2 SCT
                  CMP2:      2 BKN  BKN VRBL SCT
                  CMP3:      2 SCT
                  WEAT: M1 BKN CIG 1 V 3
6/17/82   8:21:00 CMP1:      2 SCT
                  CMP2:      2 BKN  BKN VRBL SCT
                  CMP3:      2 SCT
                  WEAT: 1 SCT

6/17/82   8:56:00 CMP1:     41 SCT
                  CMP2:     41 SCT
                  CMP3:     41 SCT
                  WEAT: 40 SCT
6/17/82   9: 1:00 CMP1:     41 SCT
                  CMP2:     41 SCT
                  CMP3:     41 SCT
                  WEAT: 19 SCT 40 SCT
6/17/82   9: 6:00 CMP1:     19 SCT 41 SCT
                  CMP2:     19 SCT 41 SCT
                  CMP3:     19 SCT 41 SCT
                  WEAT: 17 SCT 40 SCT
```

TABLE 5-18. (concluded)

```
6/17/82   9:11:00 CMP1:      18 SCT 41 BKN
                  CMP2:      18 SCT 41 BKN
                  CMP3:      18 SCT 41 BKN  BKN VRBL SCT
                  WEAT: 16 SCT 20 SCT M40 BKN
6/17/82   9:16:00 CMP1:      17 SCT 41 BKN
                  CMP2:      17 SCT 41 BKN
                  CMP3:      17 BKN 41 BKN        BKN VRBL SCT
                  WEAT: 15 SCT 19 SCT M40 BKN
6/17/82   9:21:00 CMP1:       2 SCT 19 BKN 16 SCT
                  CMP2:      16 SCT 19 BKN 41 BKN
                  CMP3:       2 SCT 16 BKN 20 BKN  BKN VRBL SCT
                  WEAT: 14 SCT M19 BKN 41 BKN CIG 19 V 22
6/17/82   9:26:00 CMP1:       2 SCT 16 BKN 19 OVC  OVC VRBL BKN
                  CMP2:       2 SCT 16 BKN 41 OVC  BKN VRBL OVC
                  CMP3:       2 SCT 16 BKN 20 OVC
                  WEAT: M14 BKN 19 BKN CIG 13 V 18
6/17/82   9:31:00 CMP1:       2 SCT 16 BKN 19 OVC  BKN VRBL OVC
                  CMP2:       2 SCT 16 BKN 19 OVC  BKN VRBL OVC
                  CMP3:       2 SCT 16 OVC         HIR CLDS VSB
                  WEAT: 1 SCT M14 OVC CIG 13 V 18
6/17/82   9:36:00 CMP1: -X   2 BKN 15 OVC  BKN VRBL SCT
                  CMP2: -X   2 SCT 15 OVC
                  CMP3: -X   2 BKN 15 OVC  BKN VRBL SCT
                  WEAT: -X 1 SCT M14 OVC CIG 13 V 17
6/17/82   9:41:00 CMP1: -X   2 BKN 15 OVC
                  CMP2: -X   2 BKN 15 OVC
                  CMP3: -X   2 BKN 15 OVC
                  WEAT: -X M1 BKN 13 OVC CIG 1 V 2
6/17/82   9:46:00 CMP1: -X   2 BKN 15 OVC  BKN VRBL OVC
                  CMP2: -X   2 BKN 15 OVC
                  CMP3: -X   2 BKN 15 OVC  BKN VRBL OVC
                  WEAT: -X M1 BKN 13 OVC CIG 1 V 2
6/17/82   9:51:00 CMP1: -X   2 OVC
                  CMP2: -X   2 OVC
                  CMP3: -X   2 OVC
                  WEAT: -X M1 BKN 13 OVC CIG 1 V 2

6/17/82  10:36:00 CMP1: -X   1 OVC
                  CMP2: -X   1 OVC
                  CMP3: -X   1 OVC
                  WEAT: -X M1 OVC
6/17/82  10:41:00 CMP1: -X   1 OVC
                  CMP2: -X   1 OVC
                  CMP3: -X   1 OVC
                  WEAT: -X M1 OVC CIG 1 V 2

6/17/82  10:56:00 CMP1:       1 OVC
                  CMP2:       1 OVC
                  CMP3:       1 OVC
                  WEAT: M1 OVC CIG 1 V 2
6/17/82  11: 1:00 CMP1:       2 OVC
                  CMP2:       2 OVC
                  CMP3:       2 OVC
                  WEAT: M1 OVC CIG 1 V 2

6/17/82  12:52:00 CMP1: -X   1 OVC
                  CMP2: -X   1 OVC
                  CMP3: -X   1 OVC
                  WEAT: -X M1 OVC CIG 1 V 2
6/17/82  12:57:00 CMP1: -X   1 OVC
                  CMP2: -X   1 OVC
                  CMP3: -X   1 OVC
                  WEAT: -X M1 OVC
6/17/82  13: 2:00 CMP1: -X   1 OVC
                  CMP2: -X   1 OVC
                  CMP3: -X   1 OVC
                  WEAT: -X M1 OVC
6/17/82  13: 7:00 CMP1: -X   1 OVC
                  CMP2: -X   1 OVC
                  CMP3: -X   1 OVC
                  WEAT: -X M1 OVC
6/17/82  13:12:00 CMP1: -X   1 OVC
                  CMP2: -X   1 OVC
                  CMP3: -X   1 OVC
                  WEAT: -X M1 OVC
6/17/82  13:17:00 CMP1: -X   1 OVC
                  CMP2: -X   1 OVC
                  CMP3: -X   1 OVC
                  WEAT: -X M1 OVC
6/17/82  13:22:00 CMP1: -X   1 OVC
                  CMP2: -X   1 OVC
                  CMP3: -X   1 OVC
                  WEAT: -X M1 OVC
6/17/82  13:27:00 CMP1: -X   1 OVC
                  CMP2: -X   1 OVC
                  CMP3: -X   1 OVC
                  WEAT: -X M1 OVC
6/17/82  13:32:00 CMP1: -X   1 OVC
                  CMP2: -X   1 OVC
                  CMP3: -X   1 OVC
                  WEAT: -X M1 OVC CIG 1 V 2
```

The frequent Artais reports of variable ceiling are due to a programming error which was identified last winter but not corrected in the software used in the tests. The Artais reports are biased toward lower ceilings because of round-down errors, as was noted in NWS software tests at the factory. Apart from these observations, the Artais reports generally agree with the computed values. An examination of the details of the computer processing showed that the differences arise when the measurements are near a breakpoint in the report.

5.5.2 Visibility Sensors

The RVV-700 computer is, strictly speaking, incompatible with the NWS visibility reporting algorithm. The algorithm calls for a 10-minute average of measured values while the computer puts out the reporting value for a 45-second average. The resolution of the RVV-700 values is thus rather coarse. Earlier NWS reporting algorithms called for averages of extinction coefficient. The current algorithm calls for a one-minute average of extinction coefficient, conversion to visibility, and then a 10-minute average of visibility. The coarseness of the RVV-700 values and the choice of extinction coefficient or visibility to average has little effect on the resulting visibility report, as will be illustrated using an event with rapid changes in visibility (shown in Figures 5-28, 29, 30). Figure 5-28 compares the visibility based on an extinction coefficient average of RVV-700 computer data to that based on RVV-700 raw data. Instead of the steps shown in Figures 5-16, 17, these plots show reasonable agreement. The coarseness of the resolution is lost when the data are averaged. Figure 5-29 shows the results of converting the RVV-700 computer average to reporting values. The final reporting values show clean breaks with respect to the raw data. Thus, the RVV 700 interface introduces no significant errors into the visibility reports. Figure 5-30 compares the results of averaging visibility to that of averaging extinction coefficient for the same event of Figures 5-28, 29. The method of averaging makes little difference.

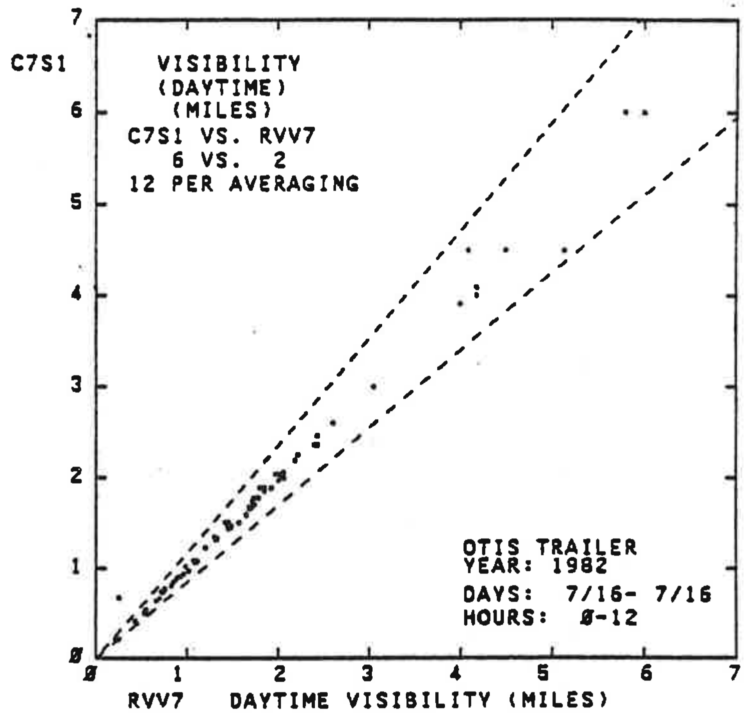

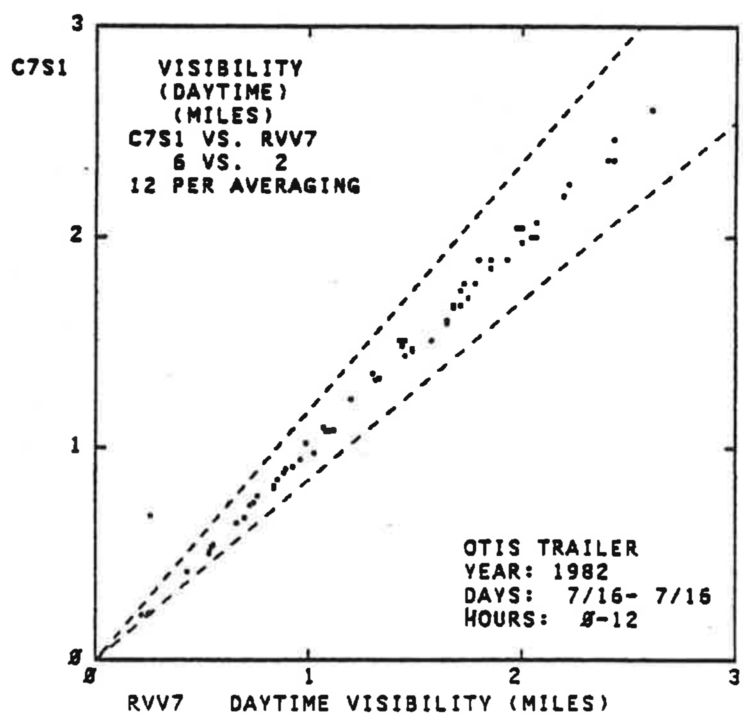

FIGURE 5-28. COMPARISON OF RVV-700 COMPUTER OUTPUT TO RVV-700 RAW DATA, AVERAGED FOR 10 MINUTES.

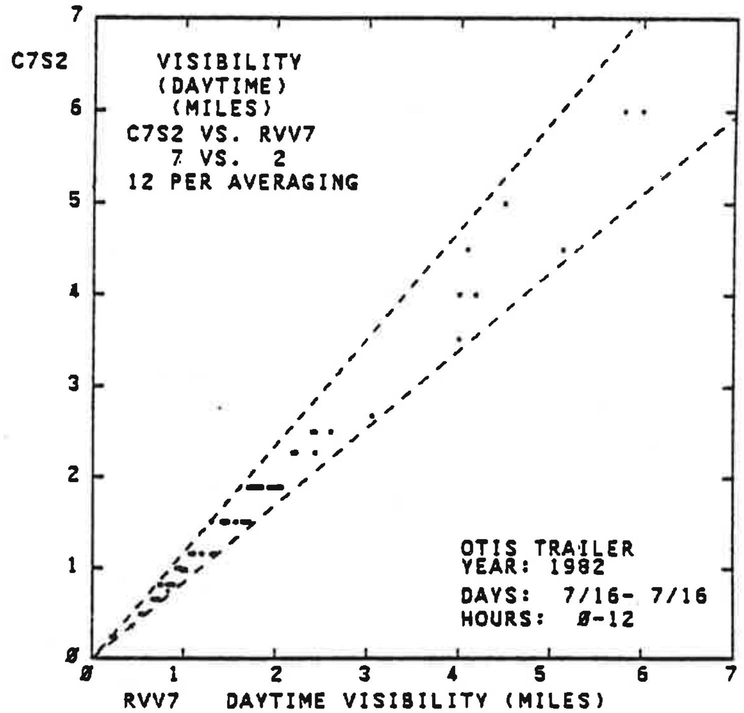

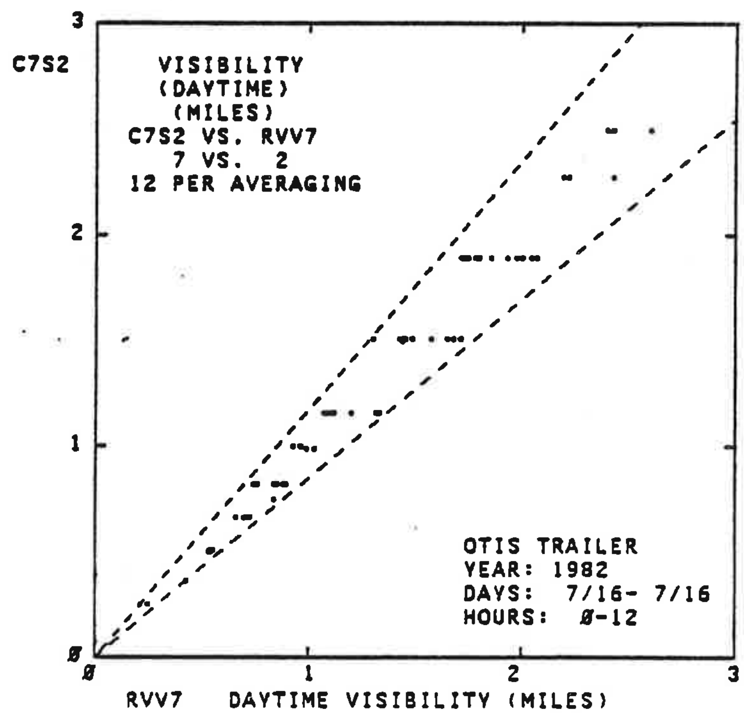

FIGURE 5-29. COMPARISON OF REPORTING VALUES ACCORDING TO THE ARTAIS ALGORITHM TO THE RAW DATA.

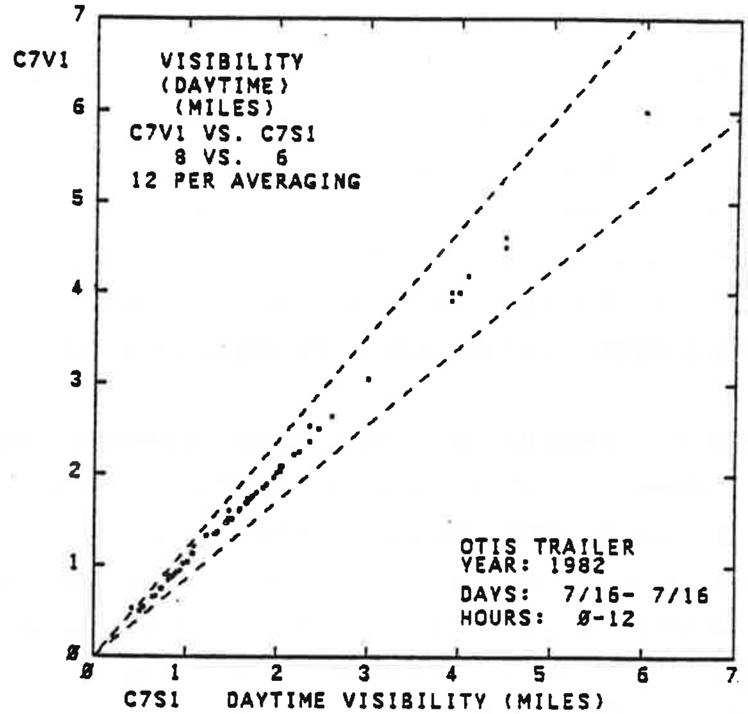

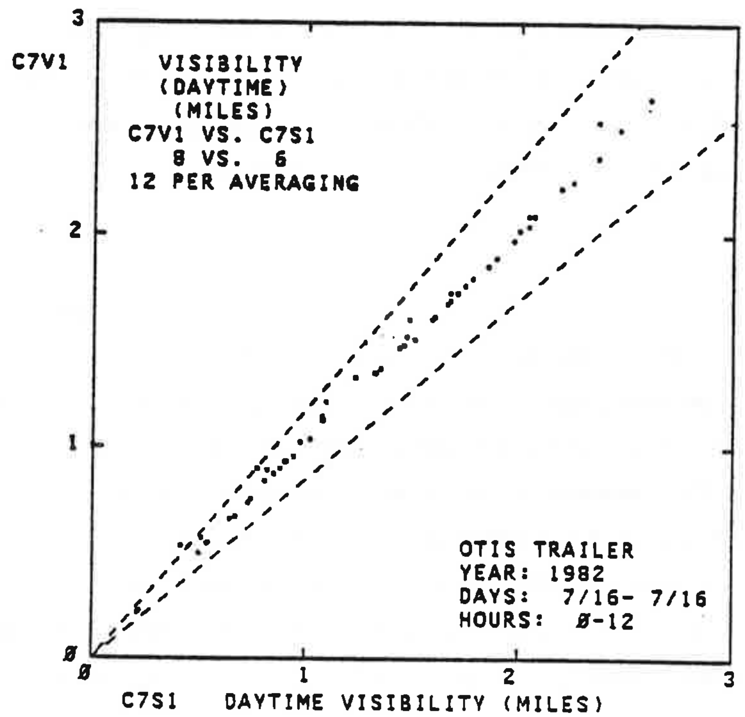

FIGURE 5-30. COMPARISON OF VISIBILITY AVERAGING TO EXTINCTION COEFFICIENT AVERAGING FOR RVV-700 COMPUTER DATA.

The test for the accuracy of the Artais interface (and reporting algorithm) for the RVV-700 and FOG-15 is shown in Tables 5-19 through 5-22 which compare the Artais reports to reports based on a 10-minute average of the raw sensor visibility value. Two periods of time are covered. The values in these tables differ from the earlier scatter tables in that the ten-minute averages are compared every minute. The data points are therefore not independent as they are in the previous scatter tables where non-overlapping averages were used.

The RVV-700 reports gave reasonable agreement during both time periods. However, there was a consistent tendency to report visibilities higher than those expected from the raw data. This overestimate of visibility may be related to an observed asymmetry in the time required for the Artais report to follow changes in the RVV-700 report. The Artais report followed increases in visibility in 2 or 3 minutes while 6 or 7 minutes were required to follow decreases in visibility. This asymmetry is the reverse of Artais' stated intention of following visibility decreases more rapidly than increases. This difference in response would lead to a bias toward higher visibility as is observed in Tables 5-19 and 5-21. This effect is most likely due to software rather than the interface. The correct readings of the RVV-700 computer bits was verified by displaying them on the Artais processor display.

The FOG-15 reports showed less satisfactory agreement than those of the RVV-700. The most notable defect is the absense of daytime reports below 1/4 mile and nighttime reports below 1/2 mile. This absense could be due to a saturation in the frequency to voltage converter of the interface. The second disagreement between the Artais reports and the raw sensor reports is different for the two time periods. During the June period (Table 5-20) the Artais report tended to read high for visibilities above 1 mile. On the other hand, the July period (Table 5-22) shows the Artais report reading low. Between the periods the

TABLE 5-19. COMPARISON OF ARTAIS VISIBILITY REPORTS TO RAW DATA REPORTS: RVV-700, 6/18-6/23

18JUN82 OTIS CHIDAS VISIBILITY DISTRIBUTIONS 10 MINUTE AVERAGES VERSUS ARTAIS P. 1

RVV-700 VISIBILITY 0.00

ARTAIS:	0.00	0.25	0.50	0.75	1.00	1.25	1.50	1.75	2.00	2.50	3.00	3.50	4.00	5.00	6.00	ALL
NUMBER	429	113	2	0	0	0	0	0	0	0	0	0	0	0	0	544
PERCENT	79	21	0	0	0	0	0	0	0	0	0	0	0	0	0	100

RVV-700 VISIBILITY 0.25

ARTAIS:	0.00	0.25	0.50	0.75	1.00	1.25	1.50	1.75	2.00	2.50	3.00	3.50	4.00	5.00	6.00	ALL
NUMBER	0	358	101	1	0	0	0	0	0	0	0	0	0	0	0	460
PERCENT	0	78	22	0	0	0	0	0	0	0	0	0	0	0	0	100

RVV-700 VISIBILITY 0.50

ARTAIS:	0.00	0.25	0.50	0.75	1.00	1.25	1.50	1.75	2.00	2.50	3.00	3.50	4.00	5.00	6.00	ALL
NUMBER	0	2	274	42	3	1	0	0	0	0	0	0	0	0	0	322
PERCENT	0	1	85	13	1	0	0	0	0	0	0	0	0	0	0	100

RVV-700 VISIBILITY 0.75

ARTAIS:	0.00	0.25	0.50	0.75	1.00	1.25	1.50	1.75	2.00	2.50	3.00	3.50	4.00	5.00	6.00	ALL
NUMBER	0	0	2	91	33	2	0	1	0	0	0	0	0	0	0	129
PERCENT	0	0	2	71	26	2	0	1	0	0	0	0	0	0	0	100

RVV-700 VISIBILITY 1.00

ARTAIS:	0.00	0.25	0.50	0.75	1.00	1.25	1.50	1.75	2.00	2.50	3.00	3.50	4.00	5.00	6.00	ALL
NUMBER	0	0	0	3	50	17	2	0	1	0	1	0	0	0	0	74
PERCENT	0	0	0	4	68	23	3	0	1	0	1	0	0	0	0	100

RVV-700 VISIBILITY 1.25

ARTAIS:	0.00	0.25	0.50	0.75	1.00	1.25	1.50	1.75	2.00	2.50	3.00	3.50	4.00	5.00	6.00	ALL
NUMBER	0	0	0	1	4	50	12	0	2	0	0	1	0	0	0	70
PERCENT	0	0	0	1	6	71	17	0	3	0	0	1	0	0	0	100

RVV-700 VISIBILITY 1.50

ARTAIS:	0.00	0.25	0.50	0.75	1.00	1.25	1.50	1.75	2.00	2.50	3.00	3.50	4.00	5.00	6.00	ALL
NUMBER	0	0	0	0	2	1	37	17	4	2	0	0	0	0	1	64
PERCENT	0	0	0	0	3	2	58	27	6	3	0	0	0	0	2	100

RVV-700 VISIBILITY 1.75

ARTAIS:	0.00	0.25	0.50	0.75	1.00	1.25	1.50	1.75	2.00	2.50	3.00	3.50	4.00	5.00	6.00	ALL
NUMBER	0	0	0	0	0	0	2	64	25	0	1	2	2	0	0	96
PERCENT	0	0	0	0	0	0	2	67	26	0	1	2	2	0	0	100

TABLE 5-19. (concluded)

18JUN82 OTIS CHIDAS VISIBILITY DISTRIBUTIONS 10 MINUTE AVERAGES VERSUS ARTAIS P. 2

RVV-700 VISIBILITY 2.00

ARTAIS:	0.00	0.25	0.50	0.75	1.00	1.25	1.50	1.75	2.00	2.50	3.00	3.50	4.00	5.00	6.00	ALL
NUMBER	0	0	0	0	0	0	0	0	66	15	0	3	0	3	1	88
PERCENT	0	0	0	0	0	0	0	0	75	17	0	3	0	3	1	100

RVV-700 VISIBILITY 2.50

ARTAIS:	0.00	0.25	0.50	0.75	1.00	1.25	1.50	1.75	2.00	2.50	3.00	3.50	4.00	5.00	6.00	ALL
NUMBER	0	0	0	0	0	0	0	0	2	80	21	0	2	0	2	107
PERCENT	0	0	0	0	0	0	0	0	2	75	20	0	2	0	2	100

RVV-700 VISIBILITY 3.00

ARTAIS:	0.00	0.25	0.50	0.75	1.00	1.25	1.50	1.75	2.00	2.50	3.00	3.50	4.00	5.00	6.00	ALL
NUMBER	0	0	0	0	0	0	0	0	0	6	70	31	5	1	1	114
PERCENT	0	0	0	0	0	0	0	0	0	5	61	27	4	1	1	100

RVV-700 VISIBILITY 3.50

ARTAIS:	0.00	0.25	0.50	0.75	1.00	1.25	1.50	1.75	2.00	2.50	3.00	3.50	4.00	5.00	6.00	ALL
NUMBER	0	0	0	0	0	0	0	0	0	0	2	37	35	3	3	80
PERCENT	0	0	0	0	0	0	0	0	0	0	3	46	44	4	4	100

RVV-700 VISIBILITY 4.00

ARTAIS:	0.00	0.25	0.50	0.75	1.00	1.25	1.50	1.75	2.00	2.50	3.00	3.50	4.00	5.00	6.00	ALL
NUMBER	0	0	0	0	0	0	0	0	0	0	1	5	90	15	23	134
PERCENT	0	0	0	0	0	0	0	0	0	0	1	4	67	11	17	100

RVV-700 VISIBILITY 5.00

ARTAIS:	0.00	0.25	0.50	0.75	1.00	1.25	1.50	1.75	2.00	2.50	3.00	3.50	4.00	5.00	6.00	ALL
NUMBER	0	0	0	0	0	0	0	0	0	0	0	1	6	88	81	176
PERCENT	0	0	0	0	0	0	0	0	0	0	0	1	3	50	46	100

RVV-700 VISIBILITY 6.00

ARTAIS:	0.00	0.25	0.50	0.75	1.00	1.25	1.50	1.75	2.00	2.50	3.00	3.50	4.00	5.00	6.00	ALL
NUMBER	0	0	0	0	0	0	0	0	0	0	0	0	1	1	318	320
PERCENT	0	0	0	0	0	0	0	0	0	0	0	0	0	0	99	100

RVV-700 VISIBILITY ALL

ARTAIS:	0.00	0.25	0.50	0.75	1.00	1.25	1.50	1.75	2.00	2.50	3.00	3.50	4.00	5.00	6.00	ALL
NUMBER	429	473	379	138	92	71	53	82	100	103	96	80	141	111	430	2778
PERCENT	15	17	14	5	3	3	2	3	4	4	3	3	5	4	15	100

TABLE 5-20. COMPARISON OF ARTAIS VISIBILITY REPORTS TO RAW DATA REPORTS: FOG-15, 6/18-6/23

18JUN82 OTIS CHIDAS VISIBILITY DISTRIBUTIONS 10 MINUTE AVERAGES VERSUS ARTAIS P. 3

FOG-15 VISIBILITY 0.00

ARTAIS:	0.00	0.25	0.50	0.75	1.00	1.25	1.50	1.75	2.00	2.50	3.00	3.50	4.00	5.00	6.00	ALL
NUMBER	0	204	129	0	0	0	0	0	0	0	0	0	0	0	0	333
PERCENT	0	61	39	0	0	0	0	0	0	0	0	0	0	0	0	100

FOG-15 VISIBILITY 0.25

ARTAIS:	0.00	0.25	0.50	0.75	1.00	1.25	1.50	1.75	2.00	2.50	3.00	3.50	4.00	5.00	6.00	ALL
NUMBER	0	109	419	0	0	0	0	0	0	0	0	0	0	0	0	528
PERCENT	0	21	79	0	0	0	0	0	0	0	0	0	0	0	0	100

FOG-15 VISIBILITY 0.50

ARTAIS:	0.00	0.25	0.50	0.75	1.00	1.25	1.50	1.75	2.00	2.50	3.00	3.50	4.00	5.00	6.00	ALL
NUMBER	0	20	368	14	1	0	0	0	0	0	0	0	0	0	0	403
PERCENT	0	5	91	3	0	0	0	0	0	0	0	0	0	0	0	100

FOG-15 VISIBILITY 0.75

ARTAIS:	0.00	0.25	0.50	0.75	1.00	1.25	1.50	1.75	2.00	2.50	3.00	3.50	4.00	5.00	6.00	ALL
NUMBER	0	0	24	93	7	1	0	0	0	0	0	0	0	0	0	125
PERCENT	0	0	19	74	6	1	0	0	0	0	0	0	0	0	0	100

FOG-15 VISIBILITY 1.00

ARTAIS:	0.00	0.25	0.50	0.75	1.00	1.25	1.50	1.75	2.00	2.50	3.00	3.50	4.00	5.00	6.00	ALL
NUMBER	0	0	0	6	85	16	0	0	0	0	0	0	0	0	0	107
PERCENT	0	0	0	6	79	15	0	0	0	0	0	0	0	0	0	100

FOG-15 VISIBILITY 1.25

ARTAIS:	0.00	0.25	0.50	0.75	1.00	1.25	1.50	1.75	2.00	2.50	3.00	3.50	4.00	5.00	6.00	ALL
NUMBER	0	0	0	0	7	66	46	0	0	0	0	0	0	0	0	119
PERCENT	0	0	0	0	6	55	39	0	0	0	0	0	0	0	0	100

FOG-15 VISIBILITY 1.50

ARTAIS:	0.00	0.25	0.50	0.75	1.00	1.25	1.50	1.75	2.00	2.50	3.00	3.50	4.00	5.00	6.00	ALL
NUMBER	0	0	0	0	0	4	69	36	12	0	0	0	0	0	0	121
PERCENT	0	0	0	0	0	3	57	30	10	0	0	0	0	0	0	100

FOG-15 VISIBILITY 1.75

ARTAIS:	0.00	0.25	0.50	0.75	1.00	1.25	1.50	1.75	2.00	2.50	3.00	3.50	4.00	5.00	6.00	ALL
NUMBER	0	0	0	0	0	0	0	20	49	4	2	0	2	1	0	78
PERCENT	0	0	0	0	0	0	0	26	63	5	3	0	3	1	0	100

TABLE 5-20. (concluded)

FOG-15 VISIBILITY 2.00

ARTAIS:	0.00	0.25	0.50	0.75	1.00	1.25	1.50	1.75	2.00	2.50	3.00	3.50	4.00	5.00	6.00	ALL
NUMBER	0	0	0	0	0	0	0	2	32	53	16	0	1	1	0	105
PERCENT	0	0	0	0	0	0	0	2	30	50	15	0	1	1	0	100

FOG-15 VISIBILITY 2.50

ARTAIS:	0.00	0.25	0.50	0.75	1.00	1.25	1.50	1.75	2.00	2.50	3.00	3.50	4.00	5.00	6.00	ALL
NUMBER	0	0	0	0	0	0	0	0	0	47	62	39	9	0	3	160
PERCENT	0	0	0	0	0	0	0	0	0	29	39	24	6	0	2	100

FOG-15 VISIBILITY 3.00

ARTAIS:	0.00	0.25	0.50	0.75	1.00	1.25	1.50	1.75	2.00	2.50	3.00	3.50	4.00	5.00	6.00	ALL
NUMBER	0	0	0	0	0	0	0	0	0	0	6	20	92	20	0	138
PERCENT	0	0	0	0	0	0	0	0	0	0	4	14	67	14	0	100

FOG-15 VISIBILITY 3.50

ARTAIS:	0.00	0.25	0.50	0.75	1.00	1.25	1.50	1.75	2.00	2.50	3.00	3.50	4.00	5.00	6.00	ALL
NUMBER	0	0	0	0	0	0	0	0	0	0	0	1	20	44	59	124
PERCENT	0	0	0	0	0	0	0	0	0	0	0	1	16	35	48	100

FOG-15 VISIBILITY 4.00

ARTAIS:	0.00	0.25	0.50	0.75	1.00	1.25	1.50	1.75	2.00	2.50	3.00	3.50	4.00	5.00	6.00	ALL
NUMBER	0	0	0	0	0	0	0	0	0	0	0	0	0	38	118	156
PERCENT	0	0	0	0	0	0	0	0	0	0	0	0	0	24	76	100

FOG-15 VISIBILITY 5.00

ARTAIS:	0.00	0.25	0.50	0.75	1.00	1.25	1.50	1.75	2.00	2.50	3.00	3.50	4.00	5.00	6.00	ALL
NUMBER	0	0	0	0	0	0	0	0	0	0	0	0	0	0	144	144
PERCENT	0	0	0	0	0	0	0	0	0	0	0	0	0	0	100	100

FOG-15 VISIBILITY 6.00

ARTAIS:	0.00	0.25	0.50	0.75	1.00	1.25	1.50	1.75	2.00	2.50	3.00	3.50	4.00	5.00	6.00	ALL
NUMBER	0	0	0	0	0	0	0	0	0	0	0	0	0	0	127	127
PERCENT	0	0	0	0	0	0	0	0	0	0	0	0	0	0	100	100

FOG-15 VISIBILITY ALL

ARTAIS:	0.00	0.25	0.50	0.75	1.00	1.25	1.50	1.75	2.00	2.50	3.00	3.50	4.00	5.00	6.00	ALL
NUMBER	0	333	940	113	100	87	115	58	93	104	86	60	124	104	451	2768
PERCENT	0	12	34	4	4	3	4	2	3	4	3	2	4	4	16	100

TABLE 5-21. COMPARISON OF ARTAIS VISIBILITY REPORTS TO RAW DATA REPORTS: RVV-700, 7/7 - 7/12.

7JUL82 OTIS CHIDAS VISIBILITY DISTRIBUTIONS 10 MINUTE AVERAGES VERSUS ARTAIS P. 1

RVV-700 VISIBILITY 0.00

ARTAIS:	0.00	0.25	0.50	0.75	1.00	1.25	1.50	1.75	2.00	2.50	3.00	3.50	4.00	5.00	6.00	ALL
NUMBER	47	15	0	0	0	0	0	0	0	0	0	0	0	0	0	62
PERCENT	76	24	0	0	0	0	0	0	0	0	0	0	0	0	0	100

RVV-700 VISIBILITY 0.25

ARTAIS:	0.00	0.25	0.50	0.75	1.00	1.25	1.50	1.75	2.00	2.50	3.00	3.50	4.00	5.00	6.00	ALL
NUMBER	0	118	28	0	0	0	0	0	0	0	0	0	0	0	0	146
PERCENT	0	81	19	0	0	0	0	0	0	0	0	0	0	0	0	100

RVV-700 VISIBILITY 0.50

ARTAIS:	0.00	0.25	0.50	0.75	1.00	1.25	1.50	1.75	2.00	2.50	3.00	3.50	4.00	5.00	6.00	ALL
NUMBER	0	0	126	40	0	0	0	0	0	0	0	0	0	0	0	166
PERCENT	0	0	76	24	0	0	0	0	0	0	0	0	0	0	0	100

RVV-700 VISIBILITY 0.75

ARTAIS:	0.00	0.25	0.50	0.75	1.00	1.25	1.50	1.75	2.00	2.50	3.00	3.50	4.00	5.00	6.00	ALL
NUMBER	0	0	4	73	34	3	0	0	0	0	0	0	0	0	0	114
PERCENT	0	0	4	64	30	3	0	0	0	0	0	0	0	0	0	100

RVV-700 VISIBILITY 1.00

ARTAIS:	0.00	0.25	0.50	0.75	1.00	1.25	1.50	1.75	2.00	2.50	3.00	3.50	4.00	5.00	6.00	ALL
NUMBER	0	0	0	1	86	15	3	1	1	0	0	0	0	0	0	107
PERCENT	0	0	0	1	80	14	3	1	1	0	0	0	0	0	0	100

RVV-700 VISIBILITY 1.25

ARTAIS:	0.00	0.25	0.50	0.75	1.00	1.25	1.50	1.75	2.00	2.50	3.00	3.50	4.00	5.00	6.00	ALL
NUMBER	0	0	0	0	4	51	21	1	3	1	0	0	0	0	0	81
PERCENT	0	0	0	0	5	63	26	1	4	1	0	0	0	0	0	100

RVV-700 VISIBILITY 1.50

ARTAIS:	0.00	0.25	0.50	0.75	1.00	1.25	1.50	1.75	2.00	2.50	3.00	3.50	4.00	5.00	6.00	ALL
NUMBER	0	0	0	0	0	5	40	28	2	0	0	0	0	0	0	75
PERCENT	0	0	0	0	0	7	53	37	3	0	0	0	0	0	0	100

RVV-700 VISIBILITY 1.75

ARTAIS:	0.00	0.25	0.50	0.75	1.00	1.25	1.50	1.75	2.00	2.50	3.00	3.50	4.00	5.00	6.00	ALL
NUMBER	0	0	0	0	0	0	1	53	25	1	0	0	0	0	0	80
PERCENT	0	0	0	0	0	0	1	66	31	1	0	0	0	0	0	100

TABLE 5-21. (concluded)

7JUL82 OTIS CHIDAS VISIBILITY DISTRIBUTIONS 10 MINUTE AVERAGES VERSUS ARTAIS P. 2

RVV-700 VISIBILITY 2.00

ARTAIS:	0.00	0.25	0.50	0.75	1.00	1.25	1.50	1.75	2.00	2.50	3.00	3.50	4.00	5.00	6.00	ALL
NUMBER	0	0	0	0	0	0	1	2	56	42	0	0	0	0	0	101
PERCENT	0	0	0	0	0	0	1	2	55	42	0	0	0	0	0	100

RVV-700 VISIBILITY 2.50

ARTAIS:	0.00	0.25	0.50	0.75	1.00	1.25	1.50	1.75	2.00	2.50	3.00	3.50	4.00	5.00	6.00	ALL
NUMBER	0	0	0	0	0	0	0	0	10	178	69	2	0	0	0	259
PERCENT	0	0	0	0	0	0	0	0	4	69	27	1	0	0	0	100

RVV-700 VISIBILITY 3.00

ARTAIS:	0.00	0.25	0.50	0.75	1.00	1.25	1.50	1.75	2.00	2.50	3.00	3.50	4.00	5.00	6.00	ALL
NUMBER	0	0	0	0	0	0	0	0	0	9	165	44	5	0	0	223
PERCENT	0	0	0	0	0	0	0	0	0	4	74	20	2	0	0	100

RVV-700 VISIBILITY 3.50

ARTAIS:	0.00	0.25	0.50	0.75	1.00	1.25	1.50	1.75	2.00	2.50	3.00	3.50	4.00	5.00	6.00	ALL
NUMBER	0	0	0	0	0	0	0	0	0	0	5	120	28	1	0	154
PERCENT	0	0	0	0	0	0	0	0	0	0	3	78	18	1	0	100

RVV-700 VISIBILITY 4.00

ARTAIS:	0.00	0.25	0.50	0.75	1.00	1.25	1.50	1.75	2.00	2.50	3.00	3.50	4.00	5.00	6.00	ALL
NUMBER	0	0	0	0	0	0	0	0	0	0	0	9	238	17	2	266
PERCENT	0	0	0	0	0	0	0	0	0	0	0	3	89	6	1	100

RVV-700 VISIBILITY 5.00

ARTAIS:	0.00	0.25	0.50	0.75	1.00	1.25	1.50	1.75	2.00	2.50	3.00	3.50	4.00	5.00	6.00	ALL
NUMBER	0	0	0	0	0	0	0	0	0	0	0	0	9	183	63	255
PERCENT	0	0	0	0	0	0	0	0	0	0	0	0	4	72	25	100

RVV-700 VISIBILITY 6.00

ARTAIS:	0.00	0.25	0.50	0.75	1.00	1.25	1.50	1.75	2.00	2.50	3.00	3.50	4.00	5.00	6.00	ALL
NUMBER	0	0	0	0	0	0	0	0	0	0	0	0	0	1	475	476
PERCENT	0	0	0	0	0	0	0	0	0	0	0	0	0	0	100	100

RVV-700 VISIBILITY ALL

ARTAIS:	0.00	0.25	0.50	0.75	1.00	1.25	1.50	1.75	2.00	2.50	3.00	3.50	4.00	5.00	6.00	ALL
NUMBER	47	133	158	114	124	74	66	85	97	231	239	175	280	202	540	2565
PERCENT	2	5	6	4	5	3	3	3	4	9	9	7	11	8	21	100

TABLE 5-22. COMPARISON OF ARTAIS VISIBILITY REPORTS TO RAW DATA REPORTS FOG-15, 7/7 - 7/12.

FOG-15 VISIBILITY 0.00

ARTAIS:	0.00	0.25	0.50	0.75	1.00	1.25	1.50	1.75	2.00	2.50	3.00	3.50	4.00	5.00	6.00	ALL
NUMBER	0	47	0	0	0	0	0	0	0	0	0	0	0	0	0	47
PERCENT	0	100	0	0	0	0	0	0	0	0	0	0	0	0	0	100

FOG-15 VISIBILITY 0.25

ARTAIS:	0.00	0.25	0.50	0.75	1.00	1.25	1.50	1.75	2.00	2.50	3.00	3.50	4.00	5.00	6.00	ALL
NUMBER	0	24	80	0	0	0	0	0	0	0	0	0	0	0	0	104
PERCENT	0	23	77	0	0	0	0	0	0	0	0	0	0	0	0	100

FOG-15 VISIBILITY 0.50

ARTAIS:	0.00	0.25	0.50	0.75	1.00	1.25	1.50	1.75	2.00	2.50	3.00	3.50	4.00	5.00	6.00	ALL
NUMBER	0	3	158	0	0	0	0	0	0	0	0	0	0	0	0	161
PERCENT	0	2	98	0	0	0	0	0	0	0	0	0	0	0	0	100

FOG-15 VISIBILITY 0.75

ARTAIS:	0.00	0.25	0.50	0.75	1.00	1.25	1.50	1.75	2.00	2.50	3.00	3.50	4.00	5.00	6.00	ALL
NUMBER	0	1	45	94	2	0	0	0	0	0	0	0	0	0	0	142
PERCENT	0	1	32	66	1	0	0	0	0	0	0	0	0	0	0	100

FOG-15 VISIBILITY 1.00

ARTAIS:	0.00	0.25	0.50	0.75	1.00	1.25	1.50	1.75	2.00	2.50	3.00	3.50	4.00	5.00	6.00	ALL
NUMBER	0	0	0	34	81	2	0	0	0	0	0	0	0	0	0	117
PERCENT	0	0	0	29	69	2	0	0	0	0	0	0	0	0	0	100

FOG-15 VISIBILITY 1.25

ARTAIS:	0.00	0.25	0.50	0.75	1.00	1.25	1.50	1.75	2.00	2.50	3.00	3.50	4.00	5.00	6.00	ALL
NUMBER	0	0	0	0	30	57	1	0	0	0	0	0	0	0	0	88
PERCENT	0	0	0	0	34	65	1	0	0	0	0	0	0	0	0	100

FOG-15 VISIBILITY 1.50

ARTAIS:	0.00	0.25	0.50	0.75	1.00	1.25	1.50	1.75	2.00	2.50	3.00	3.50	4.00	5.00	6.00	ALL
NUMBER	0	0	0	0	0	23	65	3	0	0	0	0	0	0	0	91
PERCENT	0	0	0	0	0	25	71	3	0	0	0	0	0	0	0	100

FOG-15 VISIBILITY 1.75

ARTAIS:	0.00	0.25	0.50	0.75	1.00	1.25	1.50	1.75	2.00	2.50	3.00	3.50	4.00	5.00	6.00	ALL
NUMBER	0	0	0	0	0	0	34	33	3	1	0	0	0	0	0	71
PERCENT	0	0	0	0	0	0	48	46	4	1	0	0	0	0	0	100

TABLE 5-22. (concluded)

FOG-15 VISIBILITY 2.00

ARTAIS:	0.00	0.25	0.50	0.75	1.00	1.25	1.50	1.75	2.00	2.50	3.00	3.50	4.00	5.00	6.00	ALL
NUMBER	0	0	0	0	0	0	0	35	60	2	1	0	0	0	0	98
PERCENT	0	0	0	0	0	0	0	36	61	2	1	0	0	0	0	100

FOG-15 VISIBILITY 2.50

ARTAIS:	0.00	0.25	0.50	0.75	1.00	1.25	1.50	1.75	2.00	2.50	3.00	3.50	4.00	5.00	6.00	ALL
NUMBER	0	0	0	0	0	0	0	0	112	129	0	1	0	0	0	242
PERCENT	0	0	0	0	0	0	0	0	46	53	0	0	0	0	0	100

FOG-15 VISIBILITY 3.00

ARTAIS:	0.00	0.25	0.50	0.75	1.00	1.25	1.50	1.75	2.00	2.50	3.00	3.50	4.00	5.00	6.00	ALL
NUMBER	0	0	0	0	0	0	0	0	0	108	65	0	0	0	0	173
PERCENT	0	0	0	0	0	0	0	0	0	62	38	0	0	0	0	100

FOG-15 VISIBILITY 3.50

ARTAIS:	0.00	0.25	0.50	0.75	1.00	1.25	1.50	1.75	2.00	2.50	3.00	3.50	4.00	5.00	6.00	ALL
NUMBER	0	0	0	0	0	0	0	0	0	0	85	32	0	0	0	117
PERCENT	0	0	0	0	0	0	0	0	0	0	73	27	0	0	0	100

FOG-15 VISIBILITY 4.00

ARTAIS:	0.00	0.25	0.50	0.75	1.00	1.25	1.50	1.75	2.00	2.50	3.00	3.50	4.00	5.00	6.00	ALL
NUMBER	0	0	0	0	0	0	0	0	0	0	3	61	69	1	0	134
PERCENT	0	0	0	0	0	0	0	0	0	0	2	46	51	1	0	100

FOG-15 VISIBILITY 5.00

ARTAIS:	0.00	0.25	0.50	0.75	1.00	1.25	1.50	1.75	2.00	2.50	3.00	3.50	4.00	5.00	6.00	ALL
NUMBER	0	0	0	0	0	0	0	0	0	0	0	0	147	45	7	199
PERCENT	0	0	0	0	0	0	0	0	0	0	0	0	74	23	4	100

FOG-15 VISIBILITY 6.00

ARTAIS:	0.00	0.25	0.50	0.75	1.00	1.25	1.50	1.75	2.00	2.50	3.00	3.50	4.00	5.00	6.00	ALL
NUMBER	0	0	0	0	0	0	0	0	0	0	0	0	3	114	640	757
PERCENT	0	0	0	0	0	0	0	0	0	0	0	0	0	15	85	100

FOG-15 VISIBILITY ALL

ARTAIS:	0.00	0.25	0.50	0.75	1.00	1.25	1.50	1.75	2.00	2.50	3.00	3.50	4.00	5.00	6.00	ALL
NUMBER	0	75	283	128	113	82	100	71	175	240	154	94	219	160	647	2541
PERCENT	0	3	11	5	4	3	4	3	7	9	6	4	9	6	25	100

optical isolater in the FOG-15 interface was damaged by a lightning surge and was replaced. The data thus indicate that the FOG-15 interface hardware was defective and also may have suffered a calibration change when the lightning damage was sustained.

6. EVALUATION

The evaluations in this report are based on data collected during a limited period of time in the late spring and early summer. No data on cold temperatures or freezing precipitation were collected for the final modifications of the sensors.

6.1 TASKER RVV-700 TRANSMISSOMETER

The RVV-700 transmissometer suffered from a number of maintenance/calibration problems, especially during the first month of testing. The initiation of the testing was delayed by some quality control and design problems which were rectified. During the first month the foundations settled and drastically misaligned the receiver several times. The 100-percent calibration drifted in the first two weeks by an unacceptable amount. At the beginning of the second month's testing the receiver electronics became unstable because of moisture leaking through an inadequate seal. After the first five weeks of testing, the RVV-700's problems mostly disappeared and the sensor gave good performance. Virtually no realignment was needed at the end of the second month of operation. The 100-percent calibration changed only about one percent in six weeks. The second month's operation, apart from the seal leakage problem, was consistent with a 30-day maintenance period. One should note, however, that the worst conditions of window contamination at the test site (southwest storms) did not occur during the two- month test period.

The RVV-700 met the pass/fail accuracy test adopted for the tests during July when stable operation was observed. It came close to meeting the pass/fail test in June when the operation was less stable. The failure to meet the pass/fail test in June was due to ground fog events where the fog density was significantly different at the locations of the RVV-700 and the standard RVR-500.

The only troublesome observation concerning the RVV-700 was the fact that it consistently (apart from a single rain event and short ground fog episodes) gave visibilities ten percent higher than the parallel RVR-500. This difference, however, did not affect the results of the pass/fail test. About 1 percent of the difference is due to a slight difference in baseline length. Since the optical characteristics of the two units are virtually identical, there are only two possible sources for the error:

1) Spatial differences between the two baselines, or
2) Some electronic problem generating an increased output pulse rate which still doesn't change the background level which is subtracted every hour or the 100-percent calibration which remains consistent.

A similar ten-percent difference between the RVV-700 and RVR-500 was noted in the Arcata tests. It was ascribed to the difference in heights of the two sensors. The RVV-700 was mounted 5 feet above the ground; the RVR-500 baseline was directly above the RVV-700 baseline at a height of 16 feet. The Otis test was set up with much less difference in vertical spacing (8 versus 12 feet), but with a 100-foot lateral spacing between the baselines. In both tests the separation between the baselines was too great to rule out spatial variations as an explanation for the discrepancy. The simplest method of eliminating spatial variation would be to use the FAA's laser calibrator attached directly to the RVV-700 tower as a standard of comparison. The laser calibrator would however, require significant optical and mechanical changes to operate on a 1000-foot baseline.

A number of approaches were taken to assess the effect of fog variation with height on the RVV-700/RVR-500 discrepancy. The observation of higher fog density by the RVV-700 in ground fog is evidence for such an effect. The observation of excellent agreement for Event #2 in rain is also consistent with the normal 10-percent disagreement being due to an increase in fog density with height. An attempt was made to use the other sensors at the Otis site (including two Videographs located at 6-and 20-foot heights) to assess the vertical variation in the fog density. The 10-percent difference between the RVV-700 and RVR-500 appeared to persist whether or not there was a significant height gradient. Both 1000-foot baseline transmissometers were compared with the 300-foot RVR-500 which crossed both baselines. The 300-foot baseline tended to read between the two 1000-foot baselines with 5 percent variation from event-to-event.

Until the source of the unexplained 9-percent discrepancy is identified, it would be advisable to apply a 9-percent correction (increase) to the extinction coefficient measured by the RVV-700 (equivalent to reducing the baseline used in the extinction coefficient calculation by 9 percent). If the source of the discrepancy turns out to be electronic, this correction is necessary. If the source is a general increase in fog density with height, as is expected for the advection fogs which were most common at Otis, then the correction represents an overestimate of fog density at the RVV-700 height. It is, in fact, equivalent to measuring at a higher level. Of course, the correction goes the wrong way in ground fog where the fog density decreases with height. In either case, the correction does not affect the pass/fail test.

6.2 WRIGHT & WRIGHT FOG-15

The lack of an absolute calibration method for the FOG-15 was rectified at the end of the test period. An after-the-fact calibration of the two units tested produced reasonably consistent results. The sensor gain remained reasonably stable over the course of the tests. The newer of the two units tested (SN 015) was quieter than the older one (SN 003), probably because of a higher quality photodiode. One component failure (the zero setting potentiometer in SN 015) was observed. The voltage-to-frequency converter in SN 003 showed some tendency to drift out of calibration.

Two significant problems were observed in the latest version of the FOG-15:

1) the calibration is nonlinear and
2) the calibration changes at high temperature.

According to the manufacturer both of these effects are due to a new "soft" clipping circuit which was added to the final FOG-15 version FOG-15 which was tested. The soft clipping reduces the signal gain for large signals and when large amounts of noise (i.e., sunlight) are present. This circuit thus accounts for the observed nonlinear response and reduced gain during the daytime. The manufacturer has returned to a "hard" clipping circuit which should restore the dynamic range and calibration consistency of the instrument. Unfortunately, the data from the current tests cannot be used to verify the characteristics of a modified instrument. The following results apply only to the "soft" clipped version.

A calibration curve with two slopes differing by a ratio of 1.44 was found to be needed to make the FOG-15 agree with a transmissometer in the fog. The break point occurs at 38.5 $10^{-4}m^{-1}$. Applying the same calibration to fog measurements of earlier "hard" clipped versions of the FOG-15 gave unsatisfactory results. The earlier FOG-15 units agree with the EG&G 207 in showing a possible break around 5 $10^{-4}m^{-1}$. The nonlinear calibration for fog was generally consistent over the four-month test period. For one daytime event the calibration was observed to revert to the previous linear calibration.

The earlier "hard" clipped versions of the FOG-15 showed a higher response to pure rain than to fog, as was also observed for the EG&G 207. The enhancement factor appeared to be between 1.5 and 2.0. Not enough rain data was accumulated with the "soft" clipped FOG-15 to establish its response to pure rain. One event indicated that the rain response may be similar to earlier versions.

6.3 IMPULSPHYSICS LD-WHL LASER CEILOMETER

The tests described in Appendix B showed that the LD-WHL was more sensitive to clouds than the ASEA QL 1211 and was at least as sensitive as the rotating beam ceilometer. The attenuation tests reported in Appendix C showed that, under clear conditions the LD-WHL can measure clouds to its maximum height of 5000 feet even when its received beam is attenuated by 35 percent. Under conditions of fog, rain, and snow the LD-WHL tends to report a nonexistent cloud layer at 200 to 300 feet. This false layer disappeared when the receiver beam was attenuated by 55 percent. The LD-WHL loses receiver sensitivity when illuminated by sunlight at a high elevation angle.

6.4 ARTAIS INTERFACES

The RVV-700 interface performed satisfactorily. All information was properly passed to the AWOS processor. The potential incompatability with the NWS reporting algorithm proved to be unimportant for actual data. The software showed minor inconsistencies with the NWS reporting algorithms. However, NWS factory testing verified the current Artais software.

The FOG-15 interface showed signs of saturating for large signal levels, and evidence for a shift in gain. Additional factory testing of this interface is required.

The LD-WHL interface performed satisfactorily. The cloud layer algorithm in the Artais processor showed signs of an error in reporting "variable" ceiling which had been identified earlier to the manufacturer. The NWS conducted factory tests on the corrected algorithm have verified that the current cloud layer software performs correctly.

The test plan was designed to perform a laboratory test of the Artais cloud layer software. Recorded data from earlier tests (including snow) was to be inserted into the Artais processor. However, this phase of the test was omitted since the field test served to check the processing algorithm on real-time data, so that playing back old data was not necessary.

The interface tests examined the failure detection capability of the Artais processor. All the sensors were properly reported as missing when they or their interfaces had failed.

6.5 Testing Methods

The pass/fail accuracy criteria adopted for the tests looks for outliers in the data. These outliers may be due to sensor problems, but could also be caused by unusual events, data recording/processing errors, or human activities such as calibrations and checks. It can be difficult to filter out all the non-sensor outliers in order to arrive at a true picture of sensor performance. It would be desirable to adopt a sensor accuracy test that depended on 90 percent of the measurements rather than the 10-percent extreme values.

The ceilometer attenuation tests described in Appendix C showed that the ceilometer sensitivity can be assessed in the relatively short period of nine days. The results of the test were somewhat surprising; the cloud hit probability dropped from near 100 percent to zero as the transmission of the attenuator dropped from 65 percent to 45 percent. This drop corresponds to an excess signal-to-threshold ratio of about 2.0 which is surprisingly low considering the good performance of the ceilometer even with significantly reduced visibilities. Informal discussions with the manufacturer indicated that a value of 5 should be expected. The explanation for this lower value may lie in the test. The multiplicity of attenuation filters may have increased the divergence of the receiver beam and thereby reduced the overlap between the transmitter and receiver beams.

Additional testing is needed before an attenuation test can be used to quickly assess ceilometer performance for acceptance or quality assurance testing. Some changes in methodology could be useful. Attenuating the transmitter beam rather than the receiver would give a fairer test of the effects of background light on the receiver, as well as avoiding a receiver failure report when the self-check signal is attenuated too much. A direct measurement of filter attenuation would be helpful. Likewise, some assurance that the filter does not affect the beam shape is needed.

APPENDIX A

VISIBILITY SENSOR ACCURACY REQUIREMENTS

VISIBILITY SENSOR ACCURACY REQUIREMENTS

Dr. David C. Burnham

1. INTRODUCTION

The current criteria for certifying AWOS visibility sensors (see Section 2.1) appear to be too stringent to be satisfied by any existing sensor. The purpose of this report is to verify this fact, to examine the actual sensor performance achieved, and to define realistic performance standards.

This report is intended to be a working document which will be used to present test results to the organizations responsible for setting standards. Information on sensor performance will be added as it becomes available. In particular, new ways of looking at sensor data will be developed to aid the process of setting standards. Revisions will be made in response to comments from those involved in the certification process.

2. PERFORMANCE STANDARDS

2.1 1980 CERTIFICATION STANDARDS

Standards for certifying AWOS visibility sensors were specified by the FAA Office of Aviation Standards on 2/13/80. An acceptable sensor should

(a) Be reliable, accurate, and low cost

(b) Be capable of extrapolating changes in visibility over the following range of values and accuracies (statute miles):

ACTUAL VISIBILITY	1/4-3	more than 3 to approx 7
SENSING/MEASURING	$\pm$1/8	$\pm$1/2

(c) Be capable of reporting visibility in 1/4 mile increments for measured visibilities of 1/4 to 3 miles and 1 mile increments for measured visibilities of more than 3 to approximately 7 miles.

(d) Be capable of meeting (b) and (c) in all commonly occurring visibility environments (i.e., rain, fog, snow, etc).

These standards are based on the way visibility is used in aviation. The following is a simplified description of the reasons for the standards. A visibility of three miles or more is needed to allow visual flight rules (VFR). For visibilities below three miles, instrument flight rules (IFR) are used. Minimum visibility values in quarter-mile increments are required for instrumented runways to allow an approach. Reported visibilities above three miles are less precise because they are needed only for forecasting, not for operations. The accuracy requirements were set to insure that the reported values are meaningful, i.e., that the accuracy is half the reporting interval.

The requirements as stated above are incomplete without a number of assumptions:

a) The first assumption is that visibility is derived from the measured extinction coefficient using the same equations as Runway Visibility Value (RVV). These equations assume a 5.5 percent contrast threshold in the daytime and a 25-candela omnidirectional lamp for viewing at night.

b) The second is that the extinction coefficient is averaged for a time of 10 minutes before being converted to visibility.

c) The third assumption is that the accuracy specifications represent one standard deviation.

2.2 DEMONSTRATION AWOS PROCUREMENT STANDARDS

Because the requirements established in 1980 appear to be too stringent, the FAA's Airway Facilities Service proposed in 1981 a relaxed set of requirements (entitled "AWOS Sensor Achievable Accuracies") to be used in procuring demonstration AWOS systems. The following reduced number of visibility increments (miles) are to be reported: <1/4, 1/4, 1/2, 3/4, 1 1/4, 1 1/2, 2, 2 1/2, 3, 3 1/2, 4, 5, >5. A laser transmissometer is specified as the visibility standard. Values reported by a candidate sensor must be within one increment of those reported by the standard 90 percent of the time for independent data samples. For example, if the standard reports 3 miles, the candidate report must be between 2-1/2 and 3-1/2 miles for at least 90 percent of the measurements. In precipitation (rain, snow, etc.) this requirement is relaxed to permit the candidate sensor to read two increments lower than the standard. This standard differs from the 1980 certification standard in that it deals with reported values which have a coarse resolution rather than measured values which have higher resolution. Section 5 shows how the two can be related.

3. AUTOMATED VISIBILITY OBSERVATIONS

A basic requirement on automated visibility observations is that they be at least as good as the human observations they are intended to replace. In principle, they need to be no better since human observations are now used to control and limit aircraft operations. However, because humans and sensors provide different types of measurements, it is not fair to use a single standard of comparison. A visibility sensor is superior to a human observer in terms of the consistency and timeliness of the measurements. It may be inferior in terms of how well the measurements represents the conditions to be encountered by the pilot. Human judgement can interpret unusual conditions and filter out misleading sensor readouts. The variability of human observations leads to large disagreements between human and sensor measurements (± 50% at best). This level of disagreement does not imply that sensor errors of ± 50 percent are acceptable. A much higher accuracy is expected from sensors in order to compensate for their possible deficiencies in representativeness and judgement.

The visibility accuracy standards of Section 2 are oriented toward the numbers used to report visibility without much consideration of what the numbers mean. The actual visibility is not as well defined as these numbers imply. The visibility is often not the same at the pilot's location as at the sensor's location. In addition, what the pilot can see varies from pilot-to-pilot. Finally, it is unlikely that a pilot can tell the difference in his view of the ground when the visibility is changed by a small amount such as 15 percent. These sources of variation are factored into the visibility standards used to control aircraft operations. Consequently, sensor errors which are smaller than these other sources of variation will have little impact on operations. One should note that these "natural" sources of variation generally introduce a percentage uncertainty in the visibility. Consequently, the most natural form of a visibility accuracy standard is in terms of percentage error.

4. VISIBILITY MEASUREMENTS

Visibility sensors actually measure the atmospheric extinction coefficient rather than the visibility. Standardized equations (RVV) are then used to translate the extinction coefficient into an estimate of visibility. The RVV equations were developed by comparing instrumental measurements to human observations. Figure 1 shows a plot of the equations. For the same extinction coefficient, the visibility is higher at night. Figure 2 shows how much greater the night visibility can be; it is a plot of the ratio of the night visibility to the day visibility for the same extinction coefficient, i.e., the same fog density.

4.1 TRANSMISSOMETER BASELINE

The selection of a transmissometer baseline is a compromise between accuracy at the high and low ends of the visibility range to be covered. Two baselines, 750 and 1000 feet, have been considered for AWOS use. Figure 3 shows the dependence of the transmission on visibility for these two choices. At the high visibility end, small changes in transmission correspond to large changes in visibility. For the same transmission accuracy, increasing the baseline from 750 to 1000 feet reduces the error by 25 percent. At the low visibility end the results are more dramatic. At 1/4-mile visibility, the 750-foot baseline yields a transmission of 18.2 percent and 1.8 percent for day and night respectively. The values drop to 10.3 percent and 0.47 percent for the 1000-foot baseline. The daytime values pose no particular measurement problems, but the night values could pose a problem, depending upon where the break point is set for reporting less than 1/4-mile visibility. Current transmissometer practice allows discrimination of 0.25 percent transmission (10 counts/minute) at night. This

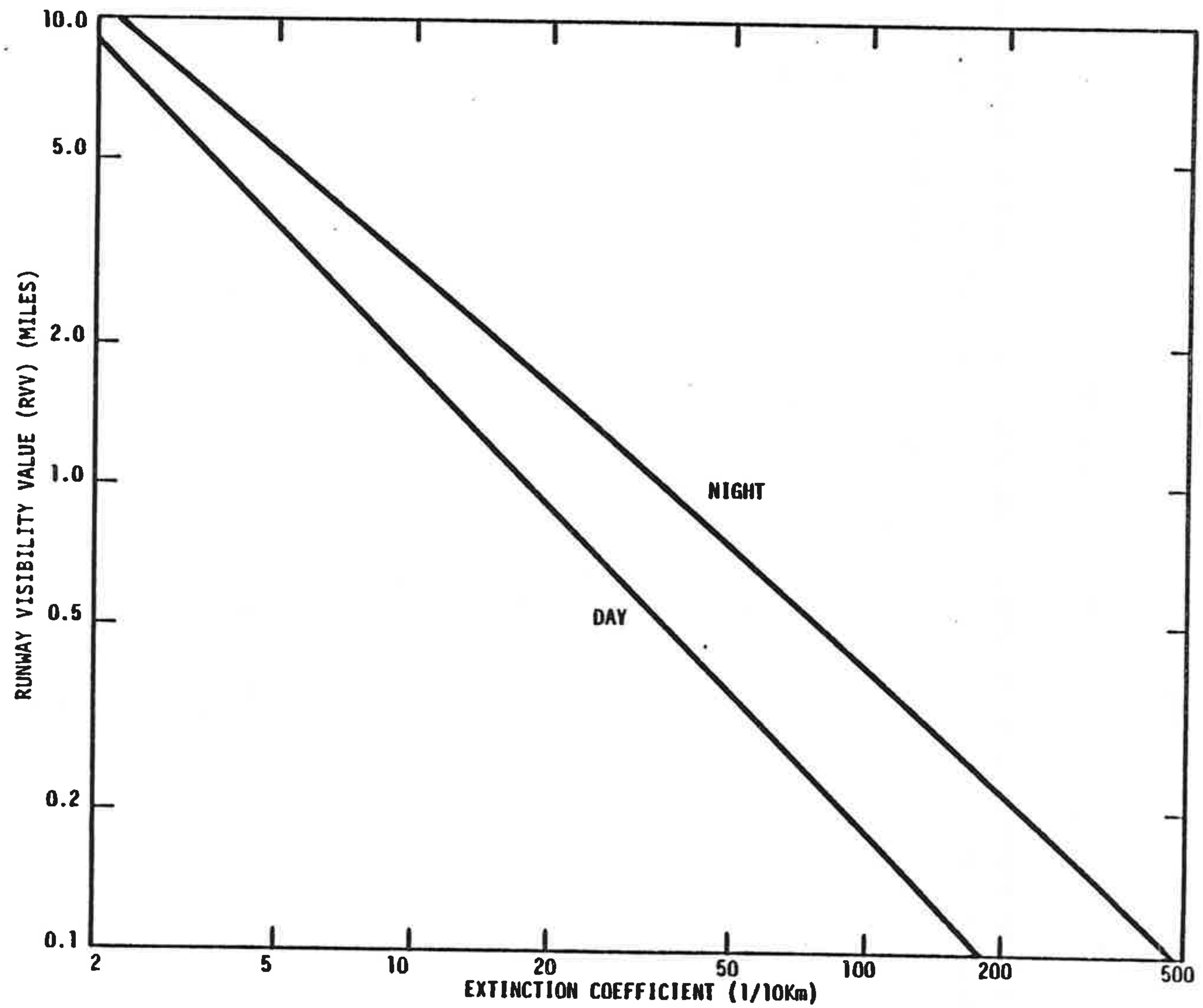

FIGURE 1. RVV VERSUS EXTINCTION COEFFICIENT (LOGARITHMIC SCALES).

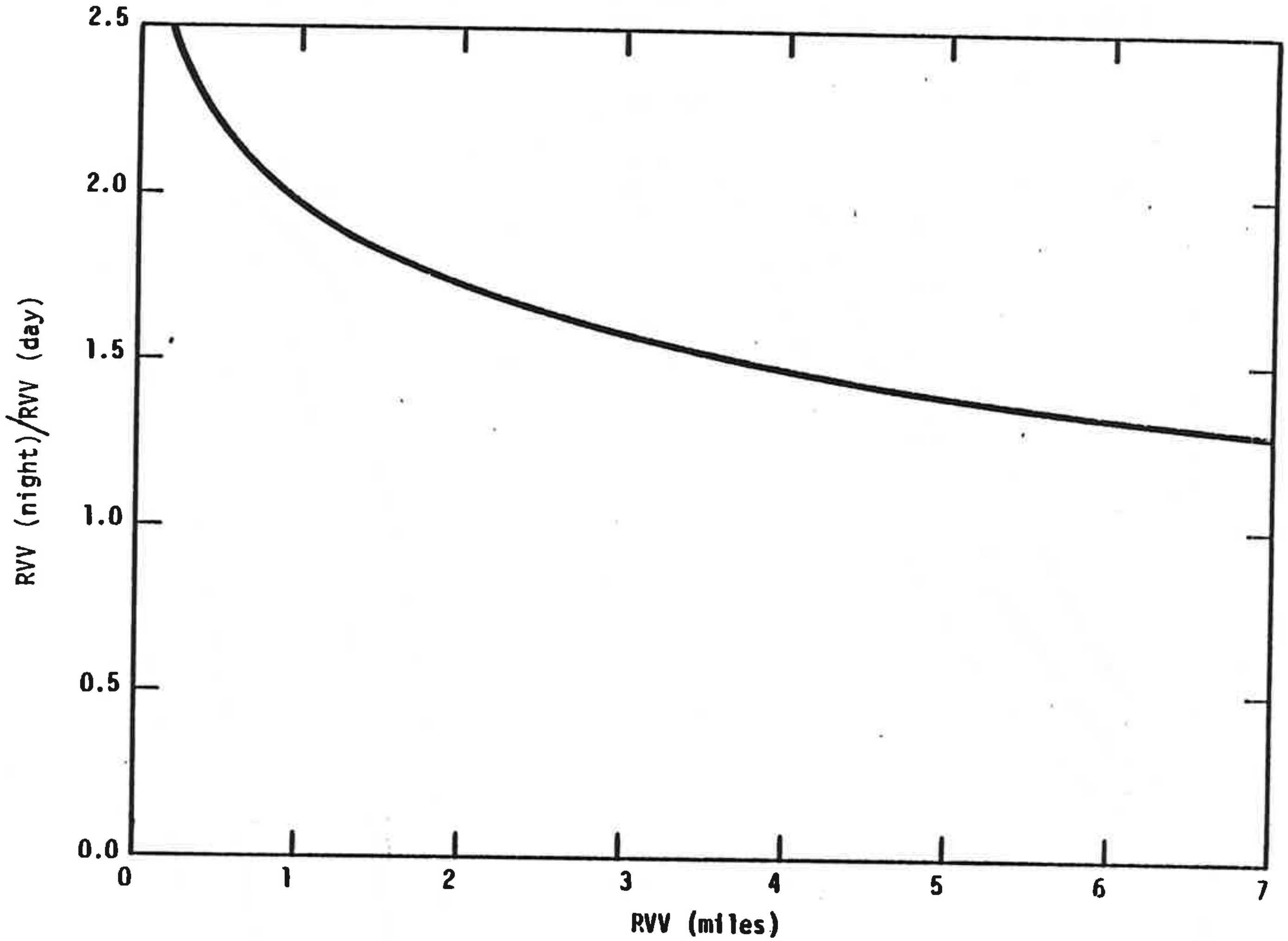

FIGURE 2. COMPARISON OF NIGHT AND DAY RVV VALUES FOR THE SAME EXTINCTION COEFFICIENT.

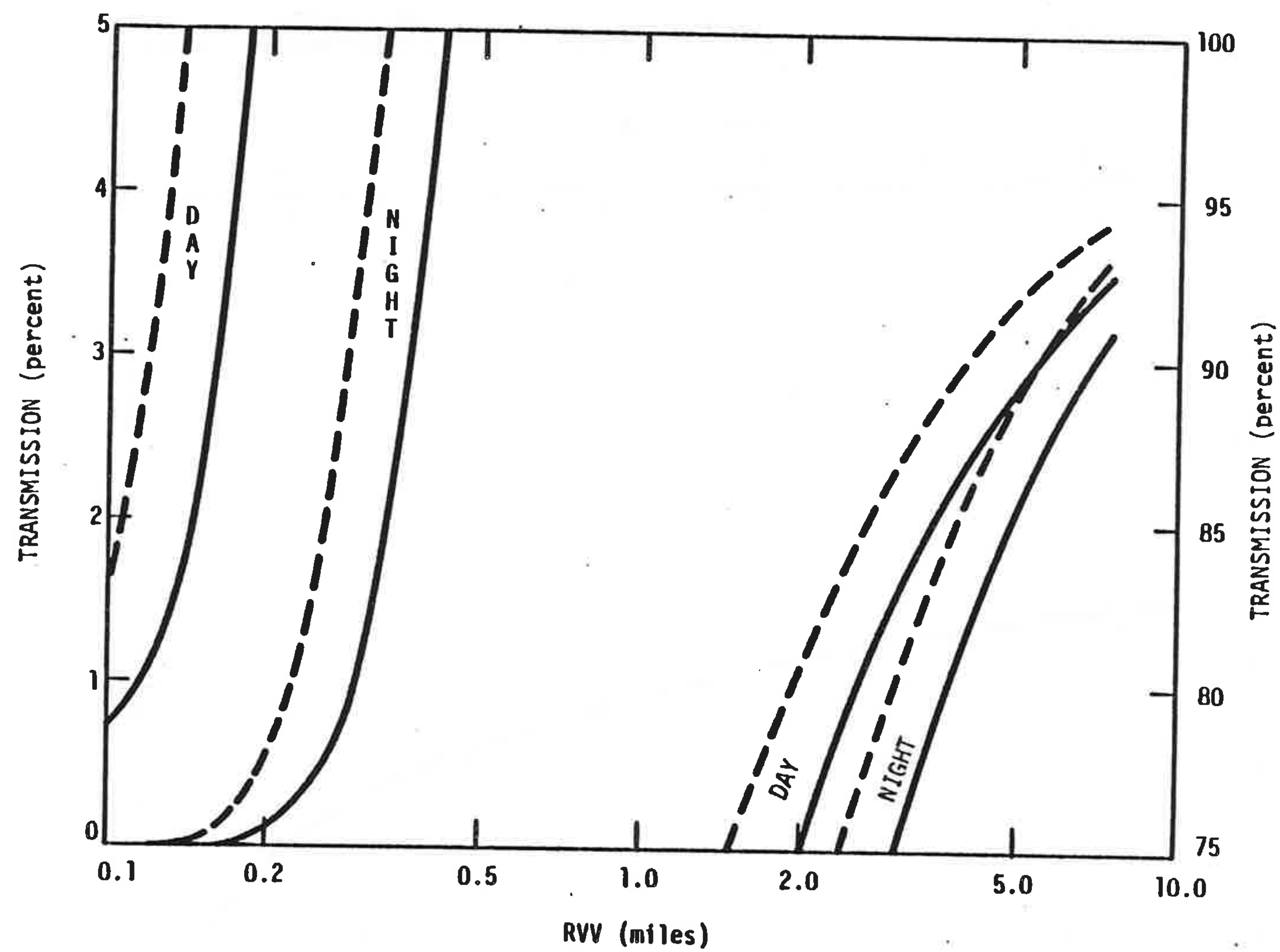

FIGURE 3. TRANSMISSION VERSUS RVV. The baselines are 1000 feet (solid lines) and 750 feet (dashed lines). The left vertical scale pertains to RVV < 0.5 and the right vertical scale to RVV > 1.0.

level would allow a 3/16-mile break point for the 750-foot baseline, but only a value slightly below 1/4 miles for a 100-foot baseline.

5. RELATIONSHIP BETWEEN SENSOR ACCURACY AND REPORTING CONSISTENCY

The two types of acceptance criteria in Section 2 can be related to each other by an analytical calculation. Two assumptions are required: First, an analytical form for the sensor error must be defined. Two different forms will be examined in the following subsections. Second, the distribution of actual visibilities must be defined. For a given reporting value (e.g., 3/4 mile) the actual visibility can assume a range of values (0.625 to 0.875 miles). For the calculation this range is divided into twenty increments (0.0125 mile wide). The actual visibility distribution is taken as one point in the middle of each increment, i.e., twenty values in all. The analytical model for the sensor error is then used to calculate the probability of the sensor reporting value being different from the actual reporting value. Of course, for small errors, the probability of a different reported value is higher when the actual visibility is near the edge of the range for a given reporting value than when it is in the middle. The probability is averaged over the twenty evenly spaced actual visibility values to represent all possible situations having the same actual reported visibility.

5.1 FRACTIONAL ERROR

One simple error form which appears to describe sensor disagreements under many conditions is a random fractional error (in the extinction coefficient). If the errors are assumed to have a normal distribution, they can be characterized by a single parameter, the fractional standard deviation. The probabilities of sensor value being beyond a limit are evaluated using the mathematical function called the error function.

Table 1 shows the results of the error probability calculation for a fractional standard deviation of 0.14. For each actual visibility the probabilities are calculated for the sensor report being more than one value low

TABLE 1. REPORTING ERRORS FOR SENSOR FRACTIONAL ERROR (STD. DEV.) = 0.140

	RVV(MI)	MIN SIGMA	REPORTING PROBABILITIES >1 LOW	1 LOW	SAME	1 HIGH	>1 HIGH	>1 DIFFERENT
DAY	<1/4	90.10	0.0000	0.0000	0.0000	0.0000	0.0000	0.000
DAY	1/4	48.05	0.0000	0.0636	0.8169	0.1192	0.0003	0.000
DAY	1/2	28.83	0.0000	0.0836	0.7771	0.1356	0.0037	0.004
DAY	3/4	20.59	0.0000	0.1393	0.6690	0.1767	0.0149	0.015
DAY	1.00	16.02	0.0002	0.1915	0.5721	0.2022	0.0340	0.034
DAY	1.25	13.11	0.0037	0.2325	0.4918	0.2469	0.0251	0.029
DAY	1.50	10.30	0.0100	0.1897	0.5575	0.2233	0.0194	0.029
DAY	2.00	8.01	0.0037	0.1879	0.5721	0.2022	0.0340	0.038
DAY	2.50	6.55	0.0037	0.2325	0.4918	0.2139	0.0581	0.062
DAY	3.00	5.54	0.0149	0.2571	0.4276	0.2162	0.0842	0.099
DAY	3.50	4.81	0.0340	0.2664	0.3764	0.2623	0.0609	0.095
DAY	4	4.00	0.0411	0.2140	0.4578	0.2442	0.0428	0.084
DAY	5	3.28	0.0180	0.2182	0.4918	0.2720	0.0000	0.018
DAY	>5	0.18	0.0000	0.0000	0.0000	0.0000	0.0000	0.000
NITE	<1/4	226.96	0.0000	0.0000	0.0000	0.0000	0.0000	0.000
NITE	1/4	110.63	0.0000	0.0552	0.8394	0.1053	0.0001	0.000
NITE	1/2	61.30	0.0000	0.0718	0.8065	0.1202	0.0016	0.002
NITE	3/4	41.40	0.0000	0.1184	0.7137	0.1603	0.0075	0.008
NITE	1.00	30.81	0.0000	0.1635	0.6274	0.1897	0.0194	0.019
NITE	1.25	24.30	0.0009	0.2037	0.5517	0.2312	0.0126	0.014
NITE	1.50	18.24	0.0036	0.1652	0.6178	0.2043	0.0090	0.013
NITE	2.00	13.49	0.0009	0.1594	0.6341	0.1878	0.0178	0.019
NITE	2.50	10.58	0.0007	0.1998	0.5595	0.2065	0.0335	0.034
NITE	3.00	8.64	0.0046	0.2305	0.4964	0.2162	0.0522	0.057
NITE	3.50	7.25	0.0136	0.2506	0.4440	0.2588	0.0331	0.047
NITE	4	5.79	0.0185	0.1970	0.5324	0.2314	0.0206	0.039
NITE	5	4.51	0.0057	0.1896	0.5697	0.2350	0.0000	0.006
NITE	>5	0.07	0.0000	0.0000	0.0000	0.0000	0.0000	0.000

(e.g., 1/4 mile reported for 1/2 mile actual), for one value low (1/4 mile reported for 1/2 mile actual), for the same reported and actual value (1/2 mile for 1/2 mile actual), for one value high (3/4 mile for 1/2 mile actual), and for more than one value high (1 mile or more for 1/2 mile actual). In addition, the total probability of being more than one value different is listed in the last column. The acceptance criteria of Section 2.2 requires that this last value be less than 0.10. A fractional deviation near 0.14 gives this limiting value for the specified AWOS reporting values. In the last column the highest value by far occurs for 3.00 mile visibility during the daytime. The errors are smaller at night because the reported value depends less strongly upon the extinction coefficient than during the daytime. NOTE: The error analysis is not done for 1/4 mile and 5 miles since the proper distribution of visibility cannot be reasonably defined. These values are included to show the break points.

Figure 4 shows how this error parameter (the probability for actual and reporting values differing by more than one value) depends upon the fractional error (standard deviation). The effect of deleting the 3.5-mile reporting value is also illustrated in Figure 4 (dashed line) and in Table 2. Deleting the 3.5-mile reporting value makes the reporting errors significantly smaller and also more uniform over the different reporting values.

5.2 100-PERCENT-TRANSMISSION ERROR

The primary cause of transmissometer error is window contamination, which causes a systematic error in the visibility measurement. This error will be modeled by assuming that the window contamination builds up uniformly to a loss of E percent (100-E maximum transmission), after which the 100-percent calibration is restored by window cleaning and/or recalibration. The 100-percent calibration error is thus distributed uniformly over the range 0 to E.

Table 3 shows the results of the error analysis for a 1000-foot baseline and E = 3.5 percent which represents the 10-percent limit on more than one value difference. In this case the maximum error occurs for 4-mile day visibility, which is higher than for fractional errors. This shift results from the enhanced

TABLE 2. REPORTING ERRORS FOR SENSOR FRACTIONAL ERROR (STD. DEV.) = 0.190

	RVV(MI)	MIN SIGMA	REPORTING PROBABILITIES >1 LOW	1 LOW	SAME	1 HIGH	>1 HIGH	>1 DIFFERENT
DAY	<1/4	90.10	0.0000	0.0000	0.0000	0.0000	0.0000	0.000
DAY	1/4	48.05	0.0000	0.0864	0.7522	0.1571	0.0043	0.004
DAY	1/2	28.83	0.0000	0.1135	0.7001	0.1673	0.0191	0.019
DAY	3/4	20.59	0.0000	0.1864	0.5677	0.1977	0.0482	0.048
DAY	1.00	16.02	0.0030	0.2429	0.4640	0.2068	0.0833	0.086
DAY	1.25	13.11	0.0191	0.2710	0.3875	0.2516	0.0708	0.090
DAY	1.50	10.30	0.0337	0.2206	0.4496	0.2366	0.0595	0.093
DAY	2.00	8.01	0.0176	0.2283	0.4640	0.2068	0.0833	0.101
DAY	2.50	6.55	0.0191	0.2710	0.3875	0.2516	0.0708	0.090
DAY	3.00	5.15	0.0337	0.2206	0.4496	0.2366	0.0595	0.093
DAY	4	4.00	0.0176	0.2283	0.4640	0.2068	0.0833	0.101
DAY	5	3.28	0.0191	0.2710	0.3875	0.3224	0.0000	0.019
DAY	>5	0.18	0.0000	0.0000	0.0000	0.0000	0.0000	0.000
NITE	<1/4	226.96	0.0000	0.0000	0.0000	0.0000	0.0000	0.000
NITE	1/4	110.63	0.0000	0.0749	0.7816	0.1415	0.0021	0.002
NITE	1/2	61.30	0.0000	0.0971	0.7379	0.1541	0.0109	0.011
NITE	3/4	41.40	0.0000	0.1594	0.6201	0.1896	0.0309	0.031
NITE	1.00	30.81	0.0007	0.2141	0.5213	0.2063	0.0577	0.058
NITE	1.25	24.30	0.0074	0.2516	0.4438	0.2512	0.0460	0.053
NITE	1.50	18.24	0.0164	0.2043	0.5110	0.2316	0.0366	0.053
NITE	2.00	13.49	0.0067	0.2043	0.5285	0.2059	0.0547	0.061
NITE	2.50	10.58	0.0065	0.2484	0.4514	0.2507	0.0430	0.050
NITE	3.00	7.89	0.0147	0.2015	0.5195	0.2303	0.0339	0.049
NITE	4	5.79	0.0057	0.2003	0.5379	0.2052	0.0510	0.057
NITE	5	4.51	0.0054	0.2440	0.4615	0.2891	0.0000	0.005
NITE	>5	0.07	0.0000	0.0000	0.0000	0.0000	0.0000	0.000

TABLE 3. REPORTING ERRORS FOR TRANSMISSOMETER WITH BASELINE = 1000. (FEET) WITH 100% TRANSMISSION ERROR OF 3.5%

	RVV(MI)	MAX TRANS	REPORTING PROBABILITIES					
			>1 LOW	1 LOW	SAME	1 HIGH	>1 HIGH	>1 DIFFERENT
DAY	<1/4	0.06414	0.0000	0.0000	0.0000	0.0000	0.0000	0.000
DAY	1/4	0.23111	0.0000	0.0000	1.0000	0.0000	0.0000	0.000
DAY	1/2	0.41523	0.0000	0.0161	0.9839	0.0000	0.0000	0.000
DAY	3/4	0.53377	0.0000	0.0515	0.9485	0.0000	0.0000	0.000
DAY	1.00	0.61368	0.0000	0.1023	0.8977	0.0000	0.0000	0.000
DAY	1.25	0.67065	0.0000	0.1715	0.8285	0.0000	0.0000	0.000
DAY	1.50	0.73059	0.0000	0.1727	0.8273	0.0000	0.0000	0.000
DAY	2.00	0.78338	0.0000	0.2137	0.7863	0.0000	0.0000	0.000
DAY	2.50	0.81893	0.0000	0.3617	0.6383	0.0000	0.0000	0.000
DAY	3.00	0.84449	0.0000	0.5414	0.4586	0.0000	0.0000	0.000
DAY	3.50	0.86374	0.0130	0.6523	0.3347	0.0000	0.0000	0.013
DAY	4	0.88508	0.0861	0.5470	0.3669	0.0000	0.0000	0.086
DAY	5	0.90495	0.0683	0.5960	0.3357	0.0000	0.0000	0.068
DAY	>5	0.99452	0.0000	0.0000	0.0000	0.0000	0.0000	0.000
NITE	<1/4	0.00099	0.0000	0.0000	0.0000	0.0000	0.0000	0.000
NITE	1/4	0.03432	0.0000	0.0000	1.0000	0.0000	0.0000	0.000
NITE	1/2	0.15437	0.0000	0.0000	1.0000	0.0000	0.0000	0.000
NITE	3/4	0.28315	0.0000	0.0196	0.9804	0.0000	0.0000	0.000
NITE	1.00	0.39099	0.0000	0.0416	0.9584	0.0000	0.0000	0.000
NITE	1.25	0.47679	0.0000	0.0736	0.9264	0.0000	0.0000	0.000
NITE	1.50	0.57358	0.0000	0.0760	0.9240	0.0000	0.0000	0.000
NITE	2.00	0.66286	0.0000	0.0970	0.9030	0.0000	0.0000	0.000
NITE	2.50	0.72426	0.0000	0.1697	0.8303	0.0000	0.0000	0.000
NITE	3.00	0.76856	0.0000	0.2665	0.7335	0.0000	0.0000	0.000
NITE	3.50	0.80179	0.0000	0.3895	0.6105	0.0000	0.0000	0.000
NITE	4	0.83827	0.0000	0.3610	0.6390	0.0000	0.0000	0.000
NITE	5	0.87159	0.0000	0.4150	0.5850	0.0000	0.0000	0.000
NITE	>5	0.99794	0.0000	0.0000	0.0000	0.0000	0.0000	0.000

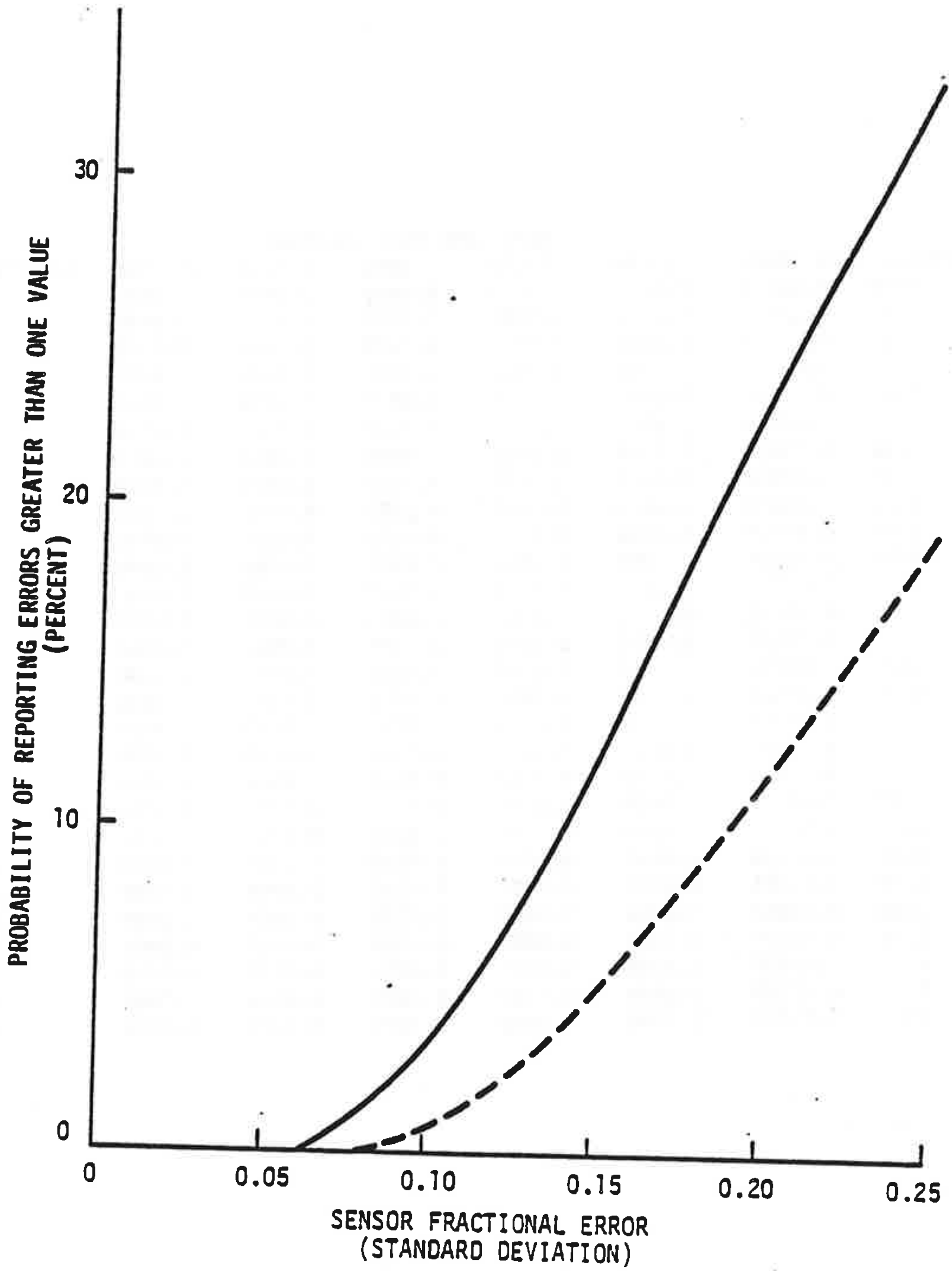

FIGURE 4. Effect of Sensor Fractional Error on the Probability of Reporting a Visibility More Than One Reporting Value in Error. The Dashed Line Shows the Effect of Eliminating the 3 1/2 Mile Reporting Value.

error sensitivity of a transmissometer at high visibilities. Figure 5 plots the probability for reporting a value more than one value away (below in this case) from the actual value as a function of the maximum error (E) in 100-percent transmission. Plots are shown for baselines of 1000 and 750 feet (solid lines). The effect of deleting the 3-1/2 mile reporting value is also shown (as dashed lines). Table 4 shows the error distribution for this case. The largest error now occurs for 5 miles. As before, eliminating the 3-1/2-mile value significantly reduces the sensitivity to errors. The error distribution, on the other hand remains skewed to high visibility.

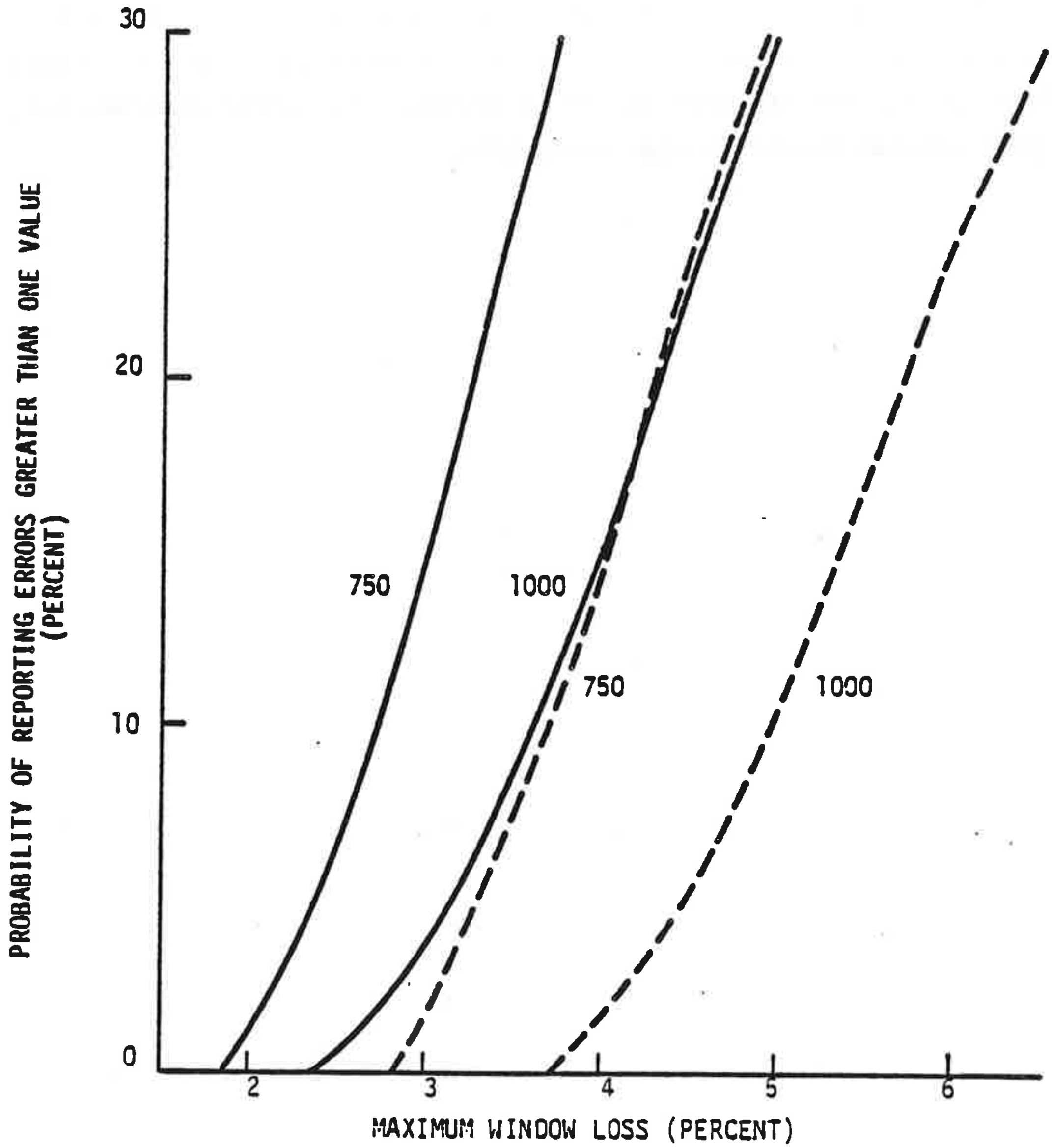

FIGURE 5. Effect of Transmissometer Window Loss on the Probability of Reporting Visibility With an Error of More Than One Reporting Value. The Dashed Lines Show the Effect of Eliminating the 3 1/2 Mile Reporting Value. Transmissometer Baselines of 750 and 1000 Feet are Illustrated.

TABLE 4. REPORTING ERRORS FOR TRANSMISSOMETER WITH BASELINE = 1000 (FEET) WITH 100% TRANSMISSION ERROR OF 5.0%

	RVV(MI)	MAX TRANS	REPORTING PROBABILITIES >1 LOW	1 LOW	SAME	1 HIGH	>1 HIGH	>1 DIFFERENT
DAY	<1/4	0.06414	0.0000	0.0000	0.0000	0.0000	0.0000	0.000
DAY	1/4	0.23111	0.0000	0.0000	1.0000	0.0000	0.0000	0.000
DAY	1/2	0.41523	0.0000	0.0263	0.9737	0.0000	0.0000	0.000
DAY	3/4	0.53377	0.0000	0.0751	0.9249	0.0000	0.0000	0.000
DAY	1.00	0.61368	0.0000	0.1497	0.8503	0.0000	0.0000	0.000
DAY	1.25	0.67065	0.0000	0.2516	0.7484	0.0000	0.0000	0.000
DAY	1.50	0.73059	0.0000	0.2553	0.7447	0.0000	0.0000	0.000
DAY	2.00	0.78338	0.0000	0.3184	0.6816	0.0000	0.0000	0.000
DAY	2.50	0.81893	0.0000	0.5336	0.4664	0.0000	0.0000	0.000
DAY	3.00	0.85475	0.0083	0.5360	0.4556	0.0000	0.0000	0.008
DAY	4	0.88508	0.0159	0.6107	0.3734	0.0000	0.0000	0.016
DAY	5	0.90495	0.1043	0.6607	0.2350	0.0000	0.0000	0.104
DAY	>5	0.99452	0.0000	0.0000	0.0000	0.0000	0.0000	0.000
NITE	<1/4	0.00099	0.0000	0.0000	0.0000	0.0000	0.0000	0.000
NITE	1/4	0.03432	0.0000	0.0000	1.0000	0.0000	0.0000	0.000
NITE	1/2	0.15437	0.0000	0.0000	1.0000	0.0000	0.0000	0.000
NITE	3/4	0.28315	0.0000	0.0287	0.9713	0.0000	0.0000	0.000
NITE	1.00	0.39099	0.0000	0.0595	0.9405	0.0000	0.0000	0.000
NITE	1.25	0.47679	0.0000	0.1060	0.8940	0.0000	0.0000	0.000
NITE	1.50	0.57358	0.0000	0.1098	0.8902	0.0000	0.0000	0.000
NITE	2.00	0.66286	0.0000	0.1418	0.8582	0.0000	0.0000	0.000
NITE	2.50	0.72426	0.0000	0.2493	0.7507	0.0000	0.0000	0.000
NITE	3.00	0.78629	0.0000	0.2634	0.7366	0.0000	0.0000	0.000
NITE	4	0.83827	0.0000	0.3469	0.6531	0.0000	0.0000	0.000
NITE	5	0.87159	0.0000	0.5871	0.4129	0.0000	0.0000	0.000
NITE	>5	0.99794	0.0000	0.0000	0.0000	0.0000	0.0000	0.000

APPENDIX B

NWS EVALUATION OF ARCHIVED LASER CEILOMETER DATA

U.S. DEPARTMENT OF COMMERCE
National Oceanic and Atmospheric Administration
NATIONAL WEATHER SERVICE
Test & Evaluation Division
RD 1, Box 105
Sterling, Virginia 22170

March 18, 1982 OA/W544:SMI

TO: OA/432 - Richard Reynolds

ARD-410 Ray Colao
Federal Aviation Administration

FROM: OA/W544 - James T. Bradley *James T Bradley*

SUBJECT: Evaluation of ASEA and FF Impulsphysik Laser Cloud Height Indicators (CHIs)

We have evaluated the performance of the ASEA QL 1211 and FF Impulsphysik LD-WHL laser CHIs in rain, fog, snow, and haze. Comparisons were made between cloud height data collected through the T&ED automated CHI facility, which includes an RBC, observations made by T&ED personnel, and official NWS observations taken at Dulles Airport. The attached report details the evaluation process and the results obtained. While performing the evaluation, we noted other performance characteristics which were important and have also included them in our report.

In determining the response of the CHIs to the various weather occurrences, which includes the response to changes in intensity, type, etc., careful examination of essentially each CHI observation in association with the prevailing weather conditions was required. As a result, our results/conclusions are not based upon "number crunching" of voluminous data but are more qualitative in nature. The major conclusions are:

a. The performance of the Impulsphysik CHI was found to be superior to that of the ASEA.

b. The Impulsphysik CHI was found to demonstrate performance reasonably close to that of an RBC, though it tended to be somewhat conservative (lower cloud heights) in rain, fog, and snow.

c. The Impulsphysik CHI exhibited characteristics which tend to make its cloud height output amenable for use with current observational algorithms or for additional algorithm development and refinement. These included good cloud consistency (frequency of cloud hits) and predictability for different weather types, ability to detect clouds up to its stated maximum range of 5000 feet during various weather occurrences, and failure to exhibit excessive false, or "noisy" cloud hits which were reported at times by the ASEA and RBC.

Its been well documented that laser CHIs will all report about the same cloud heights in "good" weather. Our evaluation focused on the CHI response during poor weather conditions. Based upon all the information accumulated, we would recommend the Impulsphysik LD-WHL CHI for use in automated observing systems. The CHI has not been tested under environmental extremes and we haven't addressed other aspects such as maintenance philosophy, etc.

If you would like any further discussions or have any questions, myself and Steve Imbembo, the task leader, will be available.

<u>Attachment</u> (1)
Evaluation of ASEA and Impulsphysik CHIs

cc:
OA/W54 - RStrickler

Performance of the ASEA QL1211 and FF Impulsphysik LD-WHL Laser Cloud Height Indicators (CHIs) in Rain, Snow, Fog and Haze

A number of rain, fog, snow, and haze events were examined in detail. Available as data sources were the printout of cloud heights from the Test and Evaluation Division (T&ED) automated CHI facility, observations made by T&ED personnel, and official NWS observations taken at Dulles Airport (hourly and special reports). Cloud heights from the printouts were output once a minute or more frequently depending upon the mode of operation selected for the data acquisition facility. Once a minute data comprised the great majority of data collected. Though indicated on the printout as pairs of simultaneous observations, due to the different sampling rates of the sensors involved (which also included an RBC) some cloud heights reported may have differed in time as much as 45 seconds or so. However, during any particular weather episode, such differences are not considered significant over the entire period evaluated. Essentially, then, the cloud heights acquired can be termed "simultaneous." The ASEA has been in the T&ED CHI facility since late May 1981, and the Impulsphysik since late September 1981.

Data from the T&ED RBC are fed through the AUTOB and WIIS (AV-AWOS) processing schemes. The Impulsphysik CHI has two-layer reporting capability, while the ASEA reports only one cloud height. In as many instances as possible, the weather events selected occurred during "working hours" so that T&ED personnel could make pertinent observations as the events occurred. Each weather episode and corresponding CHI and RBC response were evaluated on a case by case basis. Enough cases were sampled to ensure that the nature of CHI response could be determined with a good degree of confidence.

To determine the response of the CHIs to various weather occurrences (including response to changes in intensity, type, etc.) required careful examination of each CHI observation in conjunction with the nature of prevailing meteorological conditions. As such, the observations/conclusions made concerning sensor performance are of a qualitative nature and express the observed tendencies of the CHIs. Certain performance characteristics became apparent, though not exhibited in every case.

The following summarizes the T&ED experience with the ASEA and Impulsphysik CHIs:

1. Performance in Rain

Thirty-two rain episodes were analyzed. Almost all of these occurred with fog. Subsequent discussion will be broken down into categories based upon rain intensity. The Impulsphysik CHI will be referred to as the FF CHI for purposes of brevity.

Light Rain

a. Generally, the ASEA and FF cloud heights agree with the human and RBC with visibilities around 2 miles or more. With visibilities less than 2 miles, both CHIs will at times be "drowned-out" to a large extent. About 40 percent of the light rain episodes (from a total of 16) exhibited this tendency to some degree.

b. The above mentioned "drowning-out" is manifested by heights in the 200-250 foot range for the FF and 100-200 feet for the ASEA. At 1 mile or below, heights for both the ASEA and FF were occasionally below 100 and 200, respectively, indicative of similar occurrences in fog (see later discussion on fog). These heights were usually about 50-300 feet lower than those reported by the Dulles observer and the T&ED RBC. Below 1 mile the difference between the CHIs and RBC was closer to the minimum value. Some cases were associated with "obscurations" reported by the human, at which time vertical visibilities were compared with CHI heights. Quite frequently when the FF is at 200-250 feet, a higher layer will be reported which is in agreement with the human and RBC.

c. The ASEA shows a tendency to report "zero" (indicative of no signal being received by the photodiode) for periods of time ranging from about 10 minutes to over 2 hours. During these periods, the FF is usually consistently outputting cloud heights, as is the RBC. Nearly 45 percent of the light rain cases examined exhibited this situation. Visibilities during these times were varied, ranging from 1 mile to 6 miles. The FF performed similarly on three occasions but for periods of 20 minutes or less. When the FF fails to detect a return, no indication is output except the absence of a report. In general, then, more cloud "hits" are reported by the FF CHI vs. the ASEA. The T&ED RBC consistently outputs data.

d. During drizzle, the performance of the ASEA and FF approaches that in fog (see later discussion). This is not unexpected since the two phenomena are similar.

Moderate and Heavy Rain

Relatively few cases of moderate and heavy rain were examined due to their infrequent occurrence and short duration. Effect of the rain on the CHIs was mixed during moderate intensities and showed a pronounced influence in heavy rain.

a. Thirteen periods of moderate rain were examined with the ASEA in operation. Visibilities observed ranged from less than 1 mile to around 3 miles. Roughly half of the cases showed good agreement with the human and RBC. In three instances the ASEA dropped to zero, in two cases the number of cloud hits was reduced by about 50 percent, and during two periods heights were well below the human and RBC. In many respects performance of the ASEA paralelled the RBC, which also responded at times with zero or obviously "noisy," sporadic heights. Only five FF cases were evaluated. Three of these showed no rain effect, whereas during the other two heights dropped to 150-600 feet, which ranged from 350-2000 feet below the human and RBC. More moderate rain data would be desirable to get a better "handle" on CHI performance.

b. Very few instances of heavy rain were observed. Visibilities were generally 1 mile or less. In all cases, the CHIs either went to zero or reported extremely low cloud heights. The ASEA (four cases) either went to zero or reported heights below 100 feet (32, 49, 65, 98 were prevalent). The FF (only one case) reported heights between 150 and 185 feet. In two instances of comparison with the ASEA, the T&ED RBC reported clouds in the 250-700 foot range (in good agreement with the human), but otherwise reported zeroes, which also included the single instance of FF comparison. The human reported cloud layers several hundred feet above the ASEA and FF.

Other Comments

The extent to which accompanying fog contributes to CHI performance is open to conjecture. For example, fog may play a role in producing the low cloud height reported in light rain with visibilities less than 1 mile. Since the heights reported are similar to those in pure fog, it appears that the fog is the dominant factor affecting the CHI output. Similar speculation can be applied to moderate and heavy rain.

Precipitation on the sensor cover glass seems to play an important role in cloud detection, at least as far as the FF CHI is concerned. During a period of rain and fog, the heights reported by the FF inexplicably dropped to zero from 2900 feet (visibility was about 3 miles). The cover glass was examined and it was noted that approximately 50 percent of the glass was covered by large water drops. Following cleaning, the heights briefly increased to 500-700 feet, still well below the RBC which continued at 2900 feet. However, readings again returned to zero, which prompted another examination of the cover glass. Again the glass had the same coverage as before. By this time, some moderate rain was falling. The cover glass was cleared once more and observations were in the 250-600 foot range with the RBC still reporting 2900 feet or so. Heights did not return to zero this time. Examination of the cover glass indicated that droplets were forming more rapidly and rolling off the glass rapidly, unlike the situation in light rail where the rain drops remained on the glass for much longer periods.

As soon as the rain lessened to light intensity, the heights increased to 2800-2900 feet, in agreement with the RBC. Rain then became moderate, and heights dropped to 250-750 once more, followed by zero readings (rain had became light again). The cover glass was cleared and once again heights improved to 2850. The same sequence of events occurred again with similar return of valid data once the cover glass was cleared.

Unfortunately, the ASEA was inoperable during the experimentation with the cover glass. Nevertheless, clearing the cover glass of the FF CHI improved its detection capability. Whether the distribution of droplets on the glass and how long they remain is a major factor affecting detection performance would require further investigation. There may be several factors involved here, including possibly subtle changes in rain intensity, but the presence of water on the cover glass seems to have significance.

2. Performance in Fog

Thirteen fog episodes were analyzed. Somewhat better cloud detection ability was noted for both the ASEA and FF than in rain, down to about 1 mile visibility.

a. Down to about 1 mile visibility, the AREA and FF are in good agreement with the RBC and human, including comparison of the figures for vertical visibilities when "obscurations" are reported by the human. In rain some degradation in cloud detection was noticed below 2 miles.

b. Below 1 mile, the ASEA will report heights below 100 feet. Typical values are 16, 32, 65, and 98 feet. The FF will usually output heights below 200 feet. The lowest height noted during the evaluation was 105, with 150 the typical value. Typically the FF either agrees with both the human and RBC or runs below them by anywhere from 50-200 feet. The most prevalent situation would show the FF lower by 50-100 feet. Obviously these differences would be larger for the ASEA since it usually reported lower heights than the FF below 1 mile.

c. As in rain, the ASEA has a pronounce tendency to report zero as the cloud height for significant periods of time. In 9 out of the 12 fog periods examined this was the case, whereas the FF and RBC normally would miss few cloud heights. Only one such major episode was noted for the FF. Visibilities during the ASEA "zero periods" were about equally divided between cases above and below 1 mile (the highest was 3 miles).

d. Three instances are worthy of special mention. In each case the FF was able to detect clouds in fog at heights ranging from 4000-5000 feet. The ASEA could not detect a cloud return each time. Visibilities during these events ranged from about 1-1/2 miles (one case) to 3 miles (two cases). Five thousand feet is the maximum cloud height which can be reported by both the ASEA and FF. What is notable is that the FF could detect clouds close to its maximum range in other than a clear atmosphere. The ASEA often failed to detect clouds above 3500 feet or so even with optimum atmospheric conditions. Later on in this report these occurrences will be discussed in more detail.

e. One case of thick "ground fog" occurred which was observed by T&ED personnel in "real" time. The fog depth was estimated between 15 and 20 feet, and visibility at 3/4 mile. Neither the ASEA, FF, or T&ED RBC could penetrate the fog to report a broken to overcast layer at 3300 feet (as reported by the Dulles Airport observer). The terrain at T&ED is susceptible to ground fog occurrence which apparently was not the case at the airport on this day. The ASEA was reporting 32 feet and the FF 150 feet, both typical values in fog. RBC values were sporadic, ranging from zero to around 400 feet. Once the ground fog cleared, all systems reported the overcase layer.

f. The frequency of report of dual FF cloud heights, where in rain the upper level was in agreement with the human and RBC, is less in fog, at least for the episodes evaluated.

3. Performance in Snow

CHI performance in snow proved to be the most erratic and difficult to characterize. In general, their ability to detect clouds was poorer in snow than in either rain or fog when compared with the human observer and RBC. More variability in output was noted. Fourteen episodes were analyzed. About half the cases were observed with fog present.

a. Above 2 miles visibility when reporting heights, as a general rule, ASEA and FF are in agreement with the human and RBC. However, during portions of four of the episodes, the ASEA, FF, and RBC heights were lower than the human report, and in the neighborhood of 200-600 feet lower. In cases where "obscuration" was reported by the human, vertical visibility heights were used for comparison.

b. Below or at 2 miles visibility, the FF will report from 150-250 feet quite consistently. There are two cases, though, where such heights was reported when the visibility was close to 3 miles. The ASEA is much less predictable. Heights were very variable and sporadic, ranging from up to several hundred feet above or below the human and/or RBC. In few instances was there good agreement. Infrequently (three instances were noted) though, the ASEA would report higher than the FF and in agreement with the human. When comparing the FF with the human and RBC, it was apparent that the FF often was reading lower than the human (up to 1500 feet in one case but generally less than 700 feet) and about on a par with the RBC. The FF also frequently reported two layers with its lower level in the 150-250 foot range. The upper layer often was consistent with the human observation. An upper level was reported in at least 50 percent of the appropriate observations. At times there was some consistency lacking in the reporting of these upper levels, as for example, one observation would have an upper level, the next two may not, the next six may, and so forth.

c. Once again the ASEA reported significant intervals of "zero" cloud heights, as much as three hours at a time. The FF, while considerably more consistent, had a greater frequency of such occurrences than in rail and fog.

Out of the 14 episodes evaluated, 10 showed the ASEA with intervals of zeroes. Four episodes had the FF indicating a failure to report, for similar time frames as the ASEA. The RBC also dropped to zero about as frequently as the FF. No particular correlation with visibility was apparent.

d. Both the ASEA and FF were able to detect clouds in the 3500-5000 foot range. The FF detected clouds at these heights more consistently and more often (twice as often in the samples examined). In all cases, the visibility was 5 miles or greater.

Other Comments

All of the previous discussion was based on data obtained in light snow. Very few periods of moderate and heavy snow were experienced. Consequently, only three intervals each of moderate and heavy snow were evaluated. Visibilities in all cases were 1/2 mile or less, and the human observer reported "total obscuration" in all observations.

The FF was very consistent in its output, with heights at either 150 or 200 feet for both moderate and heavy snow. Heights were mostly similar to those of the RBC. As in light snow, the ASEA was less predictable. Heights reported were either zero (the most prevalent height), below 200 feet, and over 1000 feet. In one instance of moderate snow, the RBC reported zeroes while the FF reported its customary heights. The ASEA also was reporting zeroes during this time.

4. Performance in Haze

In haze the ASEA and FF suffered no degradation of cloud detection capability. In each case, both CHIs were in excellent agreement with the human and RBC. A total of seven episodes were examined, with visibilities in the 3-6 mile range. The cases selected were "pure" haze occurrences, in conjunction with no other phenomena.

5. Other Performance Characteristics

While analyzing the CHI cloud data to determine performance in rain, fog, snow, and haze, some other characteristics of the sensors became evident. Though not specifically seeking to report on these additional characteristics, they were very obvious and prevalent throughout the period of data collection and are of major significance. A summary of each item now follows.

ASEA Reliability

Frequently the ASEA would stop reporting any indication whatsoever. It's fairly certain that a malfunction in the lasing process is at fault. Periods of inactivity ranged from a few minutes up to several hours. No relation to weather type, temperature, day/night, etc., was apparent. There is no question that considerable amounts of data were lost. Whether the difficulty is a problem of only the particular CHI at T&ED is uncertain. At this time, T&ED has no knowledge of other similar model units encountering this failure.

"Noisy" ASEA Reports

On days when the sky is clear or clouds are well above the maximum sensor range and visibility is high (15 miles or more), the ASEA has been observed at times to report cloud heights for several hours at a time. These occurrences were noticed both night and day, which eliminates the theory that sunlight could be affecting the sensor's receiver. Electronic "noise" may be responsible. What is more significant about these "noisy" cloud hits is the effect such data would have on the current NWS could height algorithms. From the cases examined, as many as 30 cloud heights per half-hour were output. Since the algorithms operate using a half-hour as the sampling period, the potential for output of false cloud information is present. Any number of cloud hits of five or more will cause the algorithm to output cloud information. In all four of the cases examined, this rate was well exceeded.

Limitation on ASEA Maximum Range

The ASEA and FF both list 5000 feet as their maximum range of detection. However, the ASEA cannot reach 5000 feet or is seriously impaired under certain atmospheric conditions, or if it does, observations are very sporatic. Some of those conditions have already been discussed in earlier sections of this report. Even when the atmosphere is free of obstructions to vision such as fog, there are conditions which preclude the ASEA from detecting within the full range of its stated capability.

Actually, the height above which the ASEA has problems in a "clear" atmosphere is around 3500 feet. In one case this height was as low as 2850 feet. During these periods the FF will report continuous cloud heights up to and including 5000 feet, and the ASEA will either report zero as the cloud height (indicative of no return) or report the correct height very sporadically. Twenty-nine instances were examined to see if there were any patterns associated with the poorer performance of the ASEA.

Strong evidence supports the following conclusions:

a. The ASEA will generally have trouble detecting clouds about 3500 feet or so during the daylight hours, except on "dark" overcast days. It appears that daylight/sunlight is affecting the ASEA's sensitivity to clouds during the daytime.

b. At night, the ASEA will normally "see" clouds to 5000 feet even with broken or scattered cloud conditions.

c. The FF is generally not affected by daylight/sunlight. One noteworthy and fairly typical example should be mentioned here. The sky conditions were scattered to broken with some bright sunlight and haze. The T&ED RBC, the human, and the FF were indicating clouds between 2850-4200 feet. The ASEA, except for an isolated hit, separated by over 30 minutes at times, was not reporting these clouds. In fact, the

FF was indicating more heights than the RBC, which reported a great deal of "noisy" heights of below 100 feet.

6. Summary

Based upon an essentially qualitative evaluation of the ASEA QL 1211 and FF Impulsphysik LD-WHL laser CHIs in rain, fog, snow, and haze, the Impulsphysik unit was found to be the superior of the two. Other aspects of performance were also identified. The FF CHI was found to demonstrate performance fairly close to that of an RBC, and exhibited characteristics which tend to make its cloud height output amenable to use with current observational algorithms or to any additional algorithm development or refinement. The basic findings are:

a. In rain, fog, and snow, the FF CHI demonstrated better overall comparability with the human and RBC than the ASEA. Both the ASEA and FF tended to be somewhat more conservative (lower cloud heights) than the human and RBC in certain situations. In haze, both the ASEA and FF showed excellent agreement with the RBC and human.

b. Perhaps the greatest strength of the FF CHI is its consistency (frequency of cloud hits) and predictability when reporting heights in the meteorological conditions examined. In comparison with the RBC, the FF showed only slightly less consistency. The ASEA demonstrated a frequent tendency to output "zero" as the cloud height. Its cloud heights were often quite variable and sporadic. Good data consistency and predictability make the FF much more adaptable to use with observational algorithms than the ASEA. Certainly any refinements to existing algorithms could be accomplished more readily.

c. The FF CHI was able to detect clouds up to its stated maximum range of 5000 feet during the various weather occurrences. The ASEA frequently was unable to detect clouds above 3500 feet or so. This was particularly evident during the daylight hours when the atmosphere was free of precipitation and/or fog, which suggests that background light seriously degrades the ASEA's performance. The FF appeared not to be seriously affected by background light.

d. False, "or noisy" cloud hits were observed from the ASEA at times during cloudless conditions. The frequency of such hits was of a sufficient magnitude to cause false cloud information to be output if used with the current NWS cloud algorithms. No such occurrences were observed with the FF CHI. The T&ED RBC was observed to report "noisy" cloud data (under 100 feet) with scattered to broken clouds around 3000 feet and above under bright, hazy conditions. The FF CHI reported a considerably higher frequency of accurate cloud hits, with no apparent effects from the bright sky condition.

APPENDIX C

NWS EVALUATION OF CURRENT

CEILOMETER DATA

U.S. DEPARTMENT OF COMMERCE
National Oceanic and Atmospheric Administration
NATIONAL WEATHER SERVICE
Test & Evaluation Division
RD 1, Box 105
Sterling, Virginia 22170

March 19, 1982 OA/W544:JTB

TO: ARD-410 - Ray Colao
Federal Aviation Administration

OA/W432 - Richard Reynolds

FROM: OA/W544 - James T. Bradley

SUBJECT: Comparison of Two Impulsphysik Cloud Height Indicators (CHIs)

ACTION: For Your Information

Richard Lewis has completed the comparisons of the two German CHIs. Our conclusions are they are essentially the same. This means that the unit used at Arcata was not functioning properly. Coupled with the data that Steve Imbembo developed on our first German CHI, we think the German systems are pretty good and could be used in an automated observation. However, we have to put down some conditions:

1) They have not been tested in our environmental chambers, and as you remember, last summer the FF CHI exhibited some strange behavior near noon under strong sun.

2) The ASEA shows good cloud height agreement to 3000-3500 feet when reporting clouds, but does not see many clouds above that height. This is in agreement with our earlier report of April 1978.

3) Because of the unique behavior of the FF CHI in rain, fog, and snow conditions, our cloud algorithm should be tailored to the particular CHI in use.

4) The validity of using a single cloud height sensor at any station must be independently determined by a site survey. This is in consonance with our AV-AWOS recommendations contained in FAA Report RD-79-63.

5) Finally, some maintenance schedule must be determined.

cc: OA/W54 - RCStrickler

U.S. DEPARTMENT OF COMMERCE
National Oceanic and Atmospheric Administration
NATIONAL WEATHER SERVICE
Test & Evaluation Division
RD 1, Box 105
Sterling, Virginia 22170

July 21, 1982 OA/W544:RL

TO: OA/W544 - James T. Bradley

FROM: OA/W544 - Richard Lewis *Richard Lewis*

SUBJECT: Ceilometer Attenuation Test

ACTION: For your Information

This memorandum summarizes the results to date of our test to determine the detection capability of the Impulsphysik laser ceilometer LD-WHL when the beam is attenuated. The objective was to simulate a visibility obstruction to see if the laser ceilometer could penetrate it and still detect clouds. An additional objective was to setup an acceptance standard for ceilometers. Dr. Dave Burnham of the Transportation Systems Center (TSC) and Ray Colao of the Federal Aviation Administration (FAA) were both consulted in developing the test procedure.

The LD-WHL system is designed to detect clouds to 5000 feet. It is range normalized to improve the signal-to-noise (S/N) ratio by firing more laser pulses as the range increases. Twenty-one pulses are fired in the lowest 50-foot bin at 150 feet. This is increased linearly to about 1000 pulses at 5000 feet. This normalization provides the best S/N from a uniform cloud base at 2500 feet.

The first tests of the system showed that it would range to 5000 feet even in bright sunlight. It's detection capability was superior to the Rotating Beam Ceilometer (RBC). Our next step was to attenuate the returned beam by installing neutral density filter discs directly above the photodiode's optical filter which transmits at 908 nm (half width 14 nm). The objective was to see at what attenuation the ceilometer would begin to miss clouds.

We were aided by the ceilometer's self-check capability. A precisely controlled light emitting diode (.84 - .92 μm bandwidth) is periodically fired onto the photodiode. The amplified signal will be a constant if the amplifier is performing properly. The measured sensitivity is reported by the system every hour as a percentage (nominally 67%). When a neutral density filter is installed, the reported value drops to a lower percentage, which should be directly proportional to the transmission value of the filter.

We used gelatin filters (No. 96) from Kodak. Their specifications indicate that the filters are only about 50 percent of the stated neutral density value at the 908 wavelength of the laser (See Figure 1). Table 1 shows the neutral density values, which should be obtained by overlaying a series of neutral density filters (N.D.F. 2) above the optical filter. The expected neutral density is half this value. The expected transmission is shown. This should be the same as the measured transmission shown in the last column. The first two filters give the transmission that would be expected from one filter (about 80 percent). Subsequent filters then attenuate approximately as expected. The reason for this is not clear though it may be related to the affect of background light on the receiver threshold or internal reflections between discs. In any case, subsequent analysis assumes that the measured transmission (last column) is a simulation of the atmospheric attenuation that would be experienced by a transmitted and returned pulse.

Actual cloud measurements with the filters installed were performed in good visibility conditions. Two collocated Impulsphysik laser ceilometers had previously beeen shown to perform consistently. The filters were then installed on one of them and their respective percentages of cloud hits were calculated. Table 2 shows the results of these tests.

The data shows that with 65 percent of the original signal intensity the laser still ranges effectively to 4100 feet with some reduction in rate of returns at 4800 feet. With 58 percent of signal intensity, clouds are still detected at 3700 feet with 100 percent effectiveness with 25 miles visibility. Even with 45 percent of signal, clouds at 4000 feet can be detected with a lower rate of return. However, clouds at 4700 feet are missed entirely with 45 percent attenuation.

While these results are not complete, they do demonstrate the effects of beam attenuation. Additional data taken during rain and low visibility showed another interesting affect, as demonstrated in the section of printout in Figure 2. This shows that the returns from rain at 250 feet, as reported by one ceilometer (GER2 L&U), are not detected by the ceilometer (GER L&U) with the beam attenuated by 55 percent (equivalent to 37.2 percent sensitivity). The visibility at this time was 1 1/2 miles in light rain and fog. The observer at Dulles was reporting a broken cloud layer at 600 feet. The effect of the filter is to actually enhance the ceilometers capability to detect the layer at 400 to 700 feet.

One conclusion from these results is that with the excess power available, the ceilometer should range to well above 5000 feet under good visibility conditions. The signal can be attenuated by about two-thirds and still range to 5000 feet with near 100 percent effectiveness. When the simulated attenuation is removed, the power will be increased by a factor of 1.5; the range would then increase to $\sqrt{1.5} \times 5000$ or 6700 feet.

The more difficult problem is determining the maximum range when the beam is attenuated by obstructions to vision. Calculations based on measured

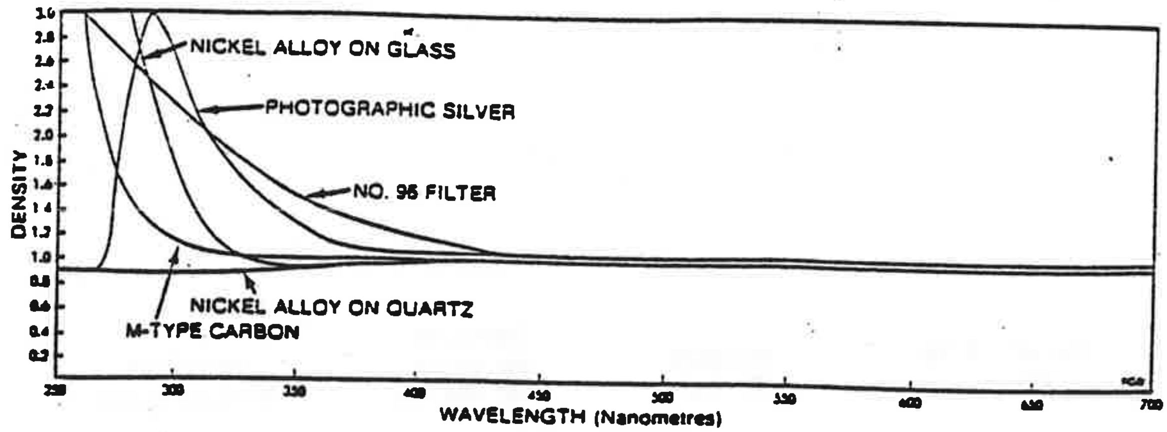

FIGURE : Typical* Transmittance of KODAK Light Attenuator Materials.

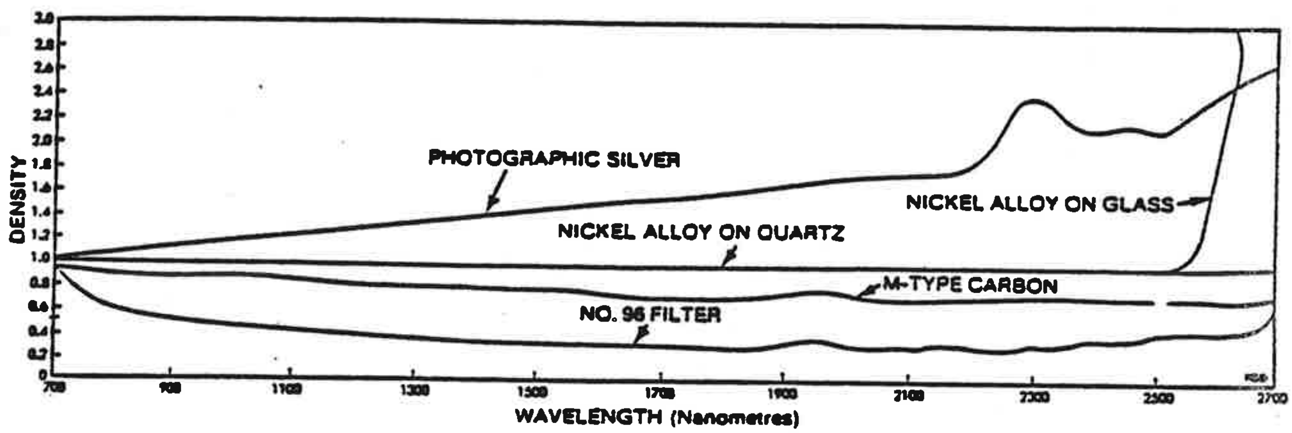

FIGURE 1: Typical* Transmittance of KODAK Light Attenuator Materials.

*These curves indicate typical densities found over an expanded spectrum. They are not routinely measured values by Kodak. Should these be of particular concern, the user should measure these densities on the specific sample involved. Also, those interested in work in the ultraviolet region should note that acetate materials tend to fluoresce there.

TABLE 1. FILTER ATTENUATION

(expected and measured values)

No of .2 ND Filters	Nominal ND Value	Expected ND Value at 908 nm	Expected Transmission	Measured Transmission
1	.2	.1	79.4	91
2	.4	.2	63.1	82
3	.6	.3	50.1	64
4	.8	.4	39.8	53
5	1.0	.5	31.6	40

TABLE 2. PERCENTAGE CLOUD RETURNS FROM IMPULSPHYSIK CEILOMETERS

(with and w/o attenuators)

Date/Time	No. of .2 ND Filters	Measured Attenuation	Cloud Height	% Cloud Returns Ceilometers With Filters	% Cloud Returns Ceilometers W/O Filters	VSB
4/20 1400	1	91	2000	100	100	12
4/20 1430	1	94	4000	100	100	15
4/20 1500	1	94	3000	100	100	15
4/20 1600	2	82	4300	100	100	15
4/20 1652	2	82	2600	100	100	12
4/20 1720	2	82	5000	100	100	15
4/20 1830	3	66	4900	53	68	15
4/20 1855	3	66	3500	92	100	15
4/20 1900	3	64	4100	100	100	15
4/20 2023	3	65	3100	100	100	15
4/20 2200	3	65	1800	100	100	15
4/21 0730	3	64	4800	80	100	15
4/28 0020	4	57	1900	100	100	7
4/28 0230	4	60	4100	30	45	10
4/28 0530	4	58	3700	100	100	25
4/28 0700	5	45	3800	64	100	25
4/28 0730	5	45	3900	11	100	25
4/28 0815	5	45	4700	0.	74	25
4/28 0830	5	45	4300	13	58	25

DATE TIME	AUTOB	WIIS1	WIIS2	GER	LCU	GER2	LCU	FRENCH	r95	r21
04:26:07:58:04	873	797	892			**200	0	361	4	5
04:26:07:59:04	896	901	0	200		**200	0	410	4	5
04:26:08:01:04	836	846	0	200		**200	550	0	4	5
04:26:08:02:04	2617	846	2504			**200	0	459	4	5
04:26:08:03:04	0	0	0	550		**200	0	410	4	5
04:26:08:05:04	2357	947	2391	650		**250	550	0	4	5
04:26:08:06:04	0	0	0			**200	550	410	4	5
04:26:08:07:04	2112	401	2151	750		**200	0	410	4	5
04:26:08:08:04	695	363	698	800		**200	0	558	3	5
04:26:08:09:04	500	498	0	650		**250	550	459	4	5
LASER: 68.8 %		SENSITIVITY:	37.2 % - reported by GER							
04:26:08:11:04	535	522	0	350	600	**250	550	607	4	5
04:26:08:12:04	443	449	0	400		**250	0	509	4	5
04:26:08:14:04	476	486	0	600		**300	550	410	4	5
04:26:08:15:04	821	806	0	400		**250	0	361	4	5
04:26:08:17:04	540	554	0	600		**250	550	459	4	5
04:26:08:18:04	0	0	0	500		**250	600	702	4	5
04:26:08:19:04	603	616	0	550		**250	850	459	4	5
04:26:08:20:04	515	516	0	500		**250	0	459	4	5
04:26:08:21:04	720	728	0	500		**250	0	607	4	5
04:26:08:22:04	828	834	0	550		**250	500	656	4	5
04:26:08:23:04	592	598	0	650		**250	1000	410	4	5
04:26:08:24:04	0	0	0	450		**250	0	459	3	5
04:26:08:25:04	576	554	0	400		**250	0	459	3	5
04:26:08:26:04	395	397	0	450		**250	0	361	3	5
04:26:08:27:04	0	0	0	300		**250	0	607	3	5
04:26:08:28:04	443	433	0	450		**250	600	364	3	5
04:26:08:29:04	766	775	0	750		**250	0	459	3	5
04:26:08:30:04	490	498	0	600	750	**250	500	410	3	5
04:26:08:31:04	525	512	0	450		**250	0	312	3	5
04:26:08:32:04	443	453	0	450		**200	0	410	3	5
04:26:08:33:04	608	323	618	500		**250	550	308	3	5
04:26:08:34:04	535	538	0	500		**250	0	410	3	5
04:26:08:35:04	671	345	662	400		**250	400	656	3	5
04:26:08:36:04	683	265	433	600		**300	600	262	3	5
04:26:08:38:04	614	385	598	650		**200	0	410	4	5
04:26:08:39:04	386	388	0	550		**200	0	308	3	5
04:26:08:41:04	275	283	0	350		**200	0	213	4	5
04:26:08:42:04	457	373	467	400		**200	0	0	4	5
04:26:08:43:04	714	710	0	500		**200	0	410	4	5
04:26:08:44:04	759	775	0	450		**200	0	656	4	5
FAULT: SELF CHECK										
FAULT: FINISHED AFTER	0 MIN.									
04:26:08:47:04	636	652	0	450		**200	0	410	4	5
04:26:08:48:04	800	806	0	450		**200	800	410	4	5
04:26:08:49:04	850	870	0	650	850	**200	0	410	4	5
04:26:08:50:04	648	636	0	650		**200	0	463	4	5
04:26:08:51:04	581	0	0	600		**250	0	410	4	5
04:26:08:52:04	997	981	0	550		**200	950	853	4	5
04:26:08:53:04	759	0	0	500		**250	0	410	4	5
04:26:08:54:04	945	581	957	500		**200	0	413	4	5
04:26:08:55:04	625	630	0	500		**200	0	410	4	5
04:26:08:56:04	793	789	0	750		**200	0	410	4	5
04:26:08:57:04	881	413	861	600		**200	0	410	3	5

FIGURE 2. CLOUD HEIGHTS IN FEET

extinction coefficient must assume constant conditions from the surface to the cloud base. Also, the effects of rain and snow on the laser beam may be difficult to quantify. Additional testing will be required to distinguish the cloud base from precipitation effects and to more adequately define the range capability when the visibility is obstructed.

cc:
OA/W432 - R. Reynolds
FAA - R. Colao
TSC - D. Burnham ✓
FF - R. Brown

APPENDIX D

EFFECT OF BACKGROUND LIGHT ON RVV-700 ACCURACY

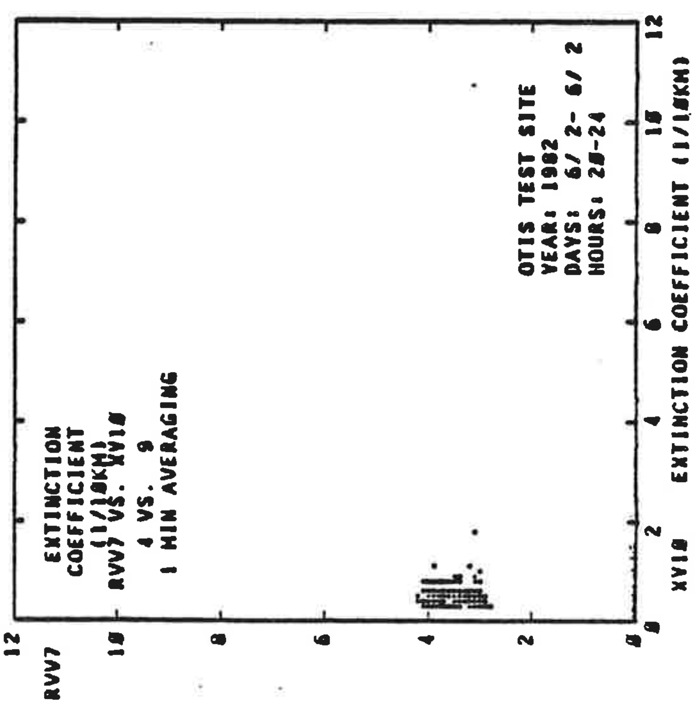
EXTINCTION
COEFFICIENT
(1/10KM)
RVV7 VS. XV10
4 VS. 9
1 MIN AVERAGING
OTIS TEST SITE
YEAR: 1982
DAYS: 6/ 2- 6/ 2
HOURS: 20-24
RVV7
XV10 EXTINCTION COEFFICIENT (1/10KM)
0
2
4
6
8
10
12

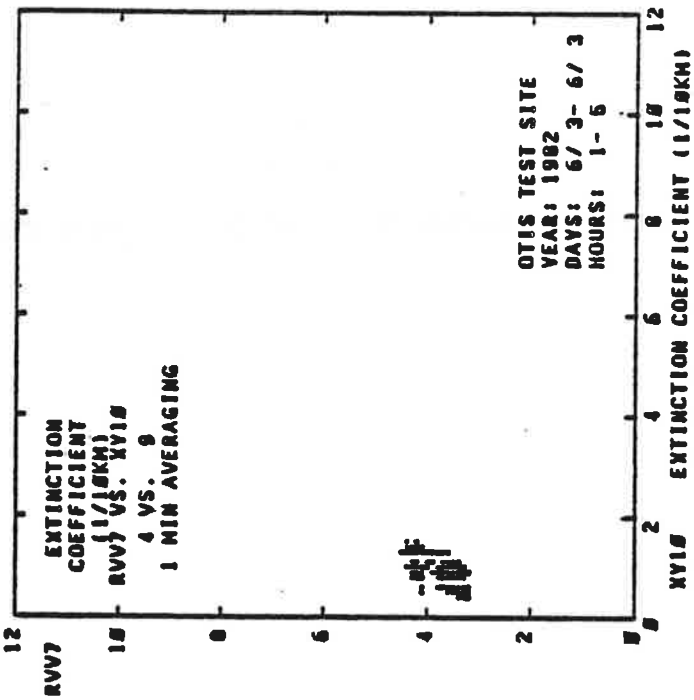
EXTINCTION
COEFFICIENT
(1/10KM)
RVV7 VS. XV10
4 VS. 9
1 MIN AVERAGING
OTIS TEST SITE
YEAR: 1982
DAYS: 6/ 3- 6/ 3
HOURS: 1- 5
RVV7
XV10 EXTINCTION COEFFICIENT (1/10KM)
0
2
4
6
8
10
12

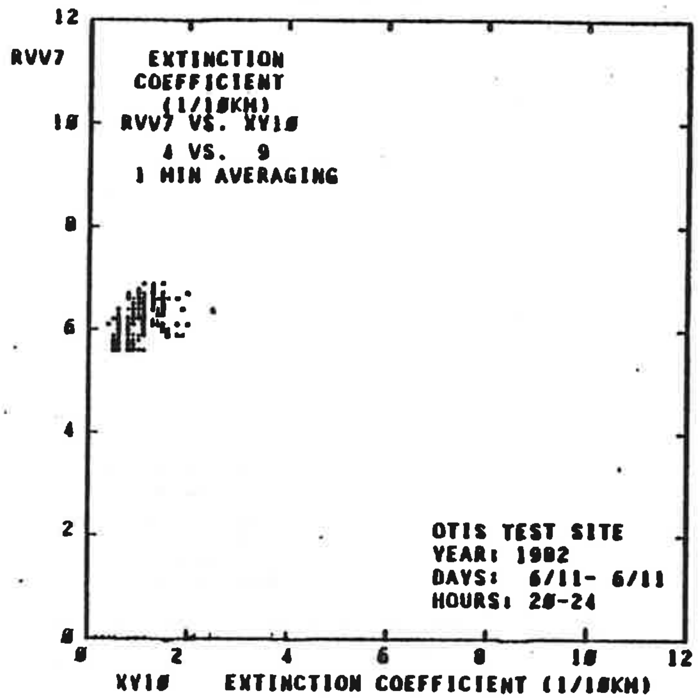
RVV7
EXTINCTION COEFFICIENT (1/10KM)
RVV7 VS. XV10
4 VS. 9
1 MIN AVERAGING
OTIS TEST SITE
YEAR: 1982
DAYS: 6/11- 6/11
HOURS: 20-24
XV10 EXTINCTION COEFFICIENT (1/10KM)
0
2
4
6
8
10
12

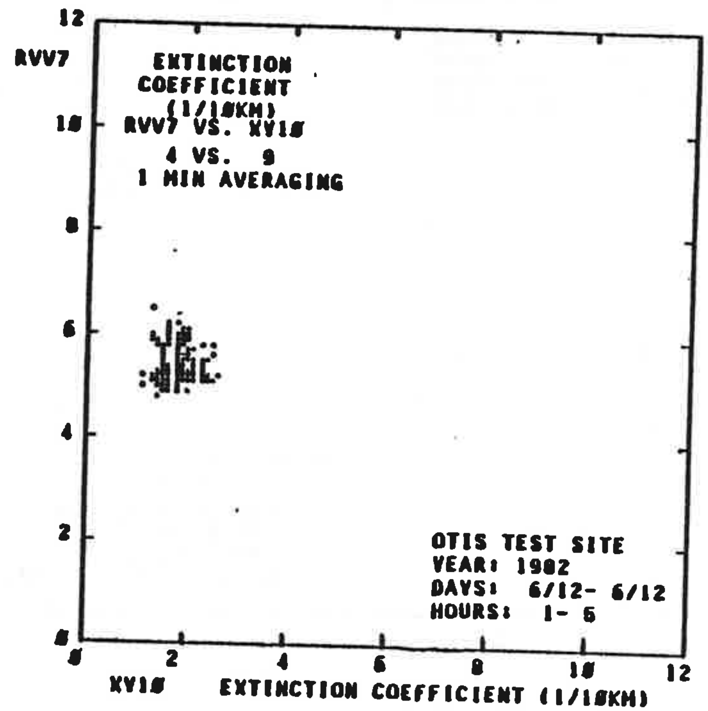
RVV7
EXTINCTION COEFFICIENT (1/10KM)
RVV7 VS. XV10
4 VS. 9
1 MIN AVERAGING
OTIS TEST SITE
YEAR: 1982
DAYS: 6/12- 6/12
HOURS: 1- 5
XV10 EXTINCTION COEFFICIENT (1/10KM)
0
2
4
6
8
10
12

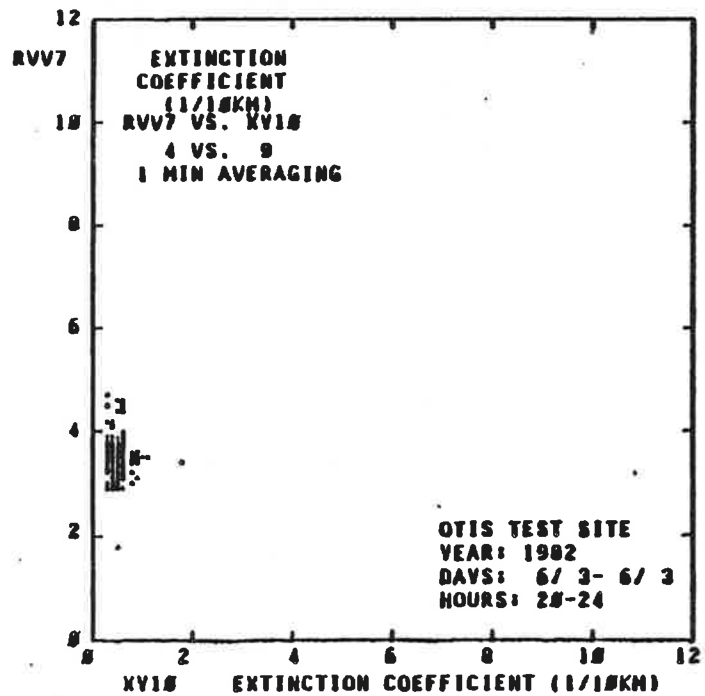
EXTINCTION
COEFFICIENT
(1/10KM)
RVV7 VS. XV10
4 VS. 9
1 MIN AVERAGING
RVV7
XV10
EXTINCTION COEFFICIENT (1/10KM)
OTIS TEST SITE
YEAR: 1982
DAYS: 6/ 3- 6/ 3
HOURS: 20-24

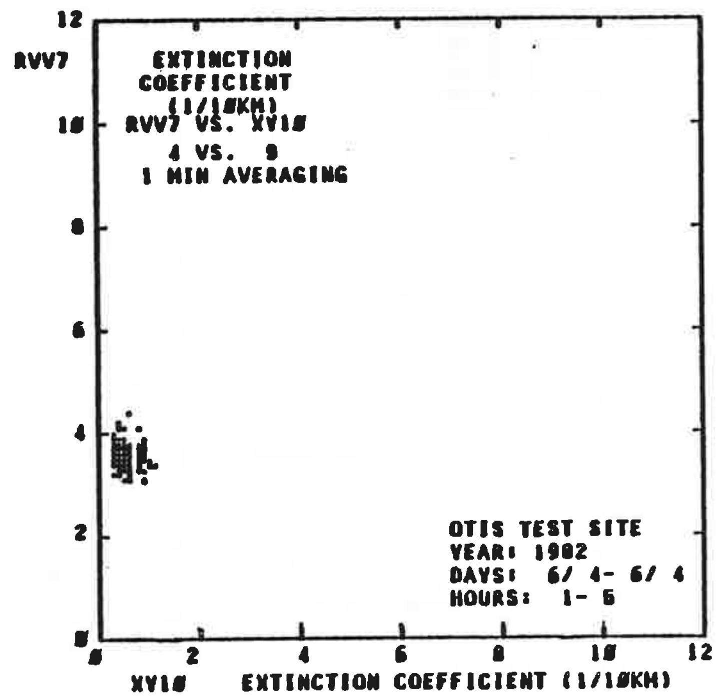
EXTINCTION
COEFFICIENT
(1/10KM)
RVV7 VS. XV10
4 VS. 9
1 MIN AVERAGING
RVV7
XV10
EXTINCTION COEFFICIENT (1/10KM)
OTIS TEST SITE
YEAR: 1982
DAYS: 6/ 4- 6/ 4
HOURS: 1- 5

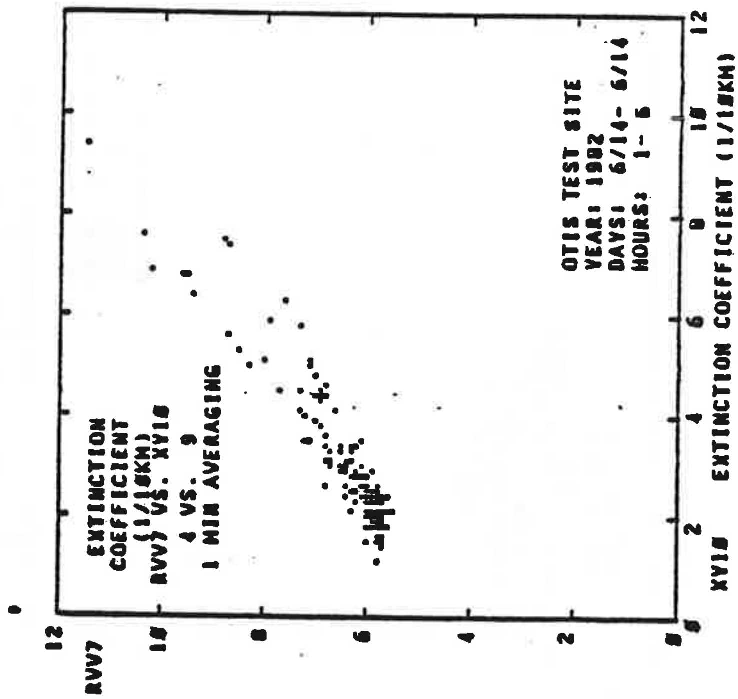
EXTINCTION
COEFFICIENT
(1/10KM)
RVV7 VS. XV10
4 VS. 9
1 MIN AVERAGING
OTIS TEST SITE
YEAR: 1982
DAYS: 6/14- 6/14
HOURS: 1- 6
RVV7
XV10 EXTINCTION COEFFICIENT (1/10KM)
0
2
4
6
8
10
12

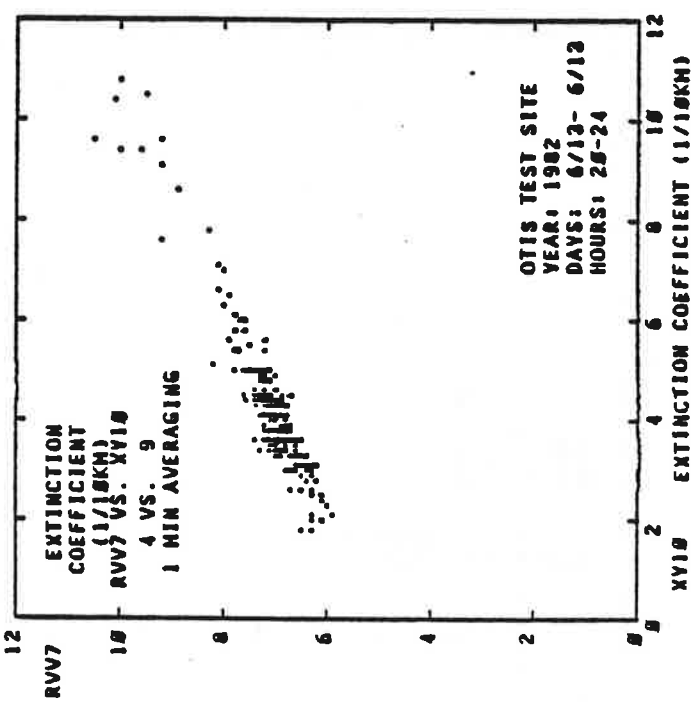
EXTINCTION
COEFFICIENT
(1/10KM)
RVV7 VS. XV10
4 VS. 9
1 MIN AVERAGING
OTIS TEST SITE
YEAR: 1982
DAYS: 6/13- 6/13
HOURS: 20-24
RVV7
XV10 EXTINCTION COEFFICIENT (1/10KM)
0
2
4
6
8
10
12

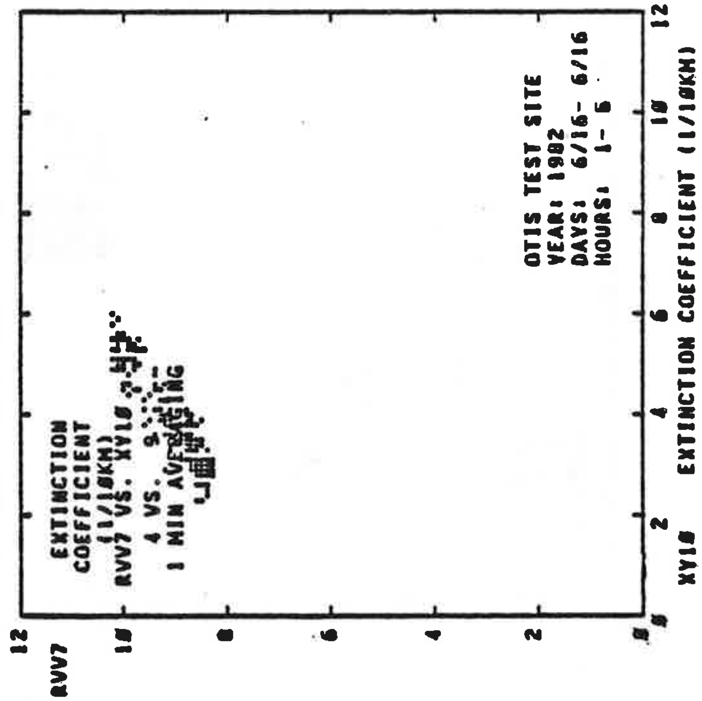
EXTINCTION
COEFFICIENT
(1/10KM)
RVV7 VS. XV10
4 VS. 9
1 MIN AVERAGING
OTIS TEST SITE
YEAR: 1982
DAYS: 6/16- 6/16
HOURS: 1- 5
RVV7
XV10 EXTINCTION COEFFICIENT (1/10KM)

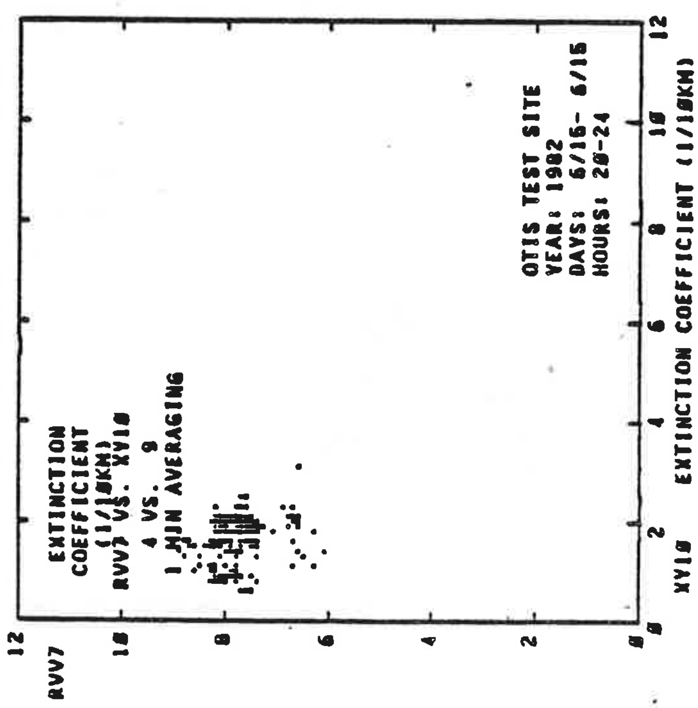
EXTINCTION
COEFFICIENT
(1/10KM)
RVV7 VS. XV10
4 VS. 9
1 MIN AVERAGING
OTIS TEST SITE
YEAR: 1982
DAYS: 6/15- 6/15
HOURS: 20-24
RVV7
XV10 EXTINCTION COEFFICIENT (1/10KM)

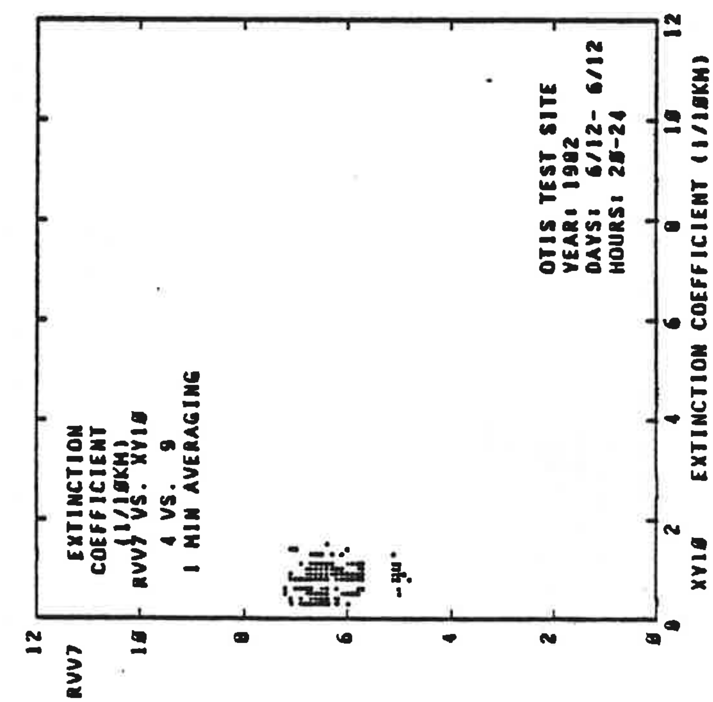
EXTINCTION
COEFFICIENT
(1/10KM)
RVV7 VS. XY10
4 VS. 9
1 MIN AVERAGING
OTIS TEST SITE
YEAR: 1982
DAYS: 6/12- 6/12
HOURS: 20-24
RVV7
XY10
EXTINCTION COEFFICIENT (1/10KM)
0
2
4
6
8
10
12

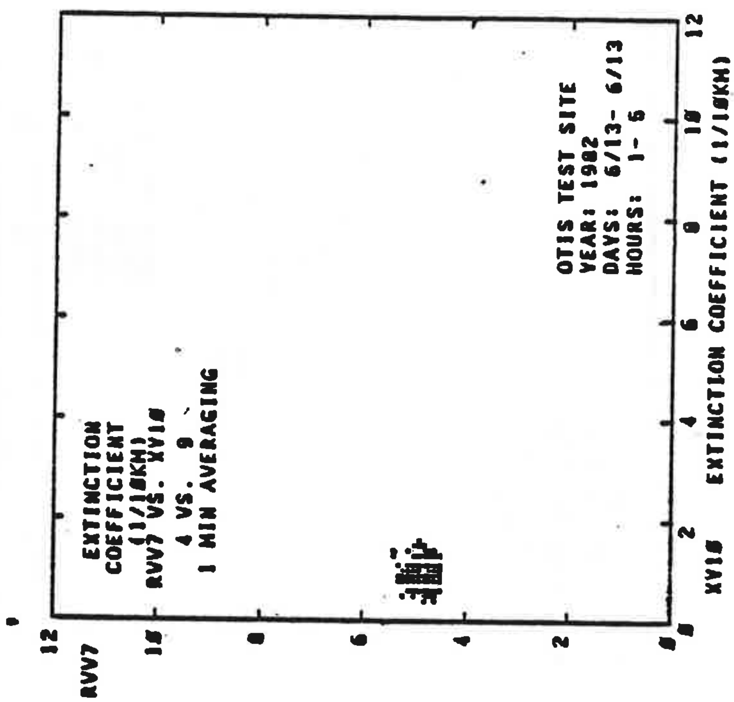
EXTINCTION
COEFFICIENT
(1/10KM)
RVV7 VS. XY10
4 VS. 9
1 MIN AVERAGING
OTIS TEST SITE
YEAR: 1982
DAYS: 6/13- 6/13
HOURS: 1- 5
RVV7
XY10
EXTINCTION COEFFICIENT (1/10KM)
0
2
4
6
8
10
12

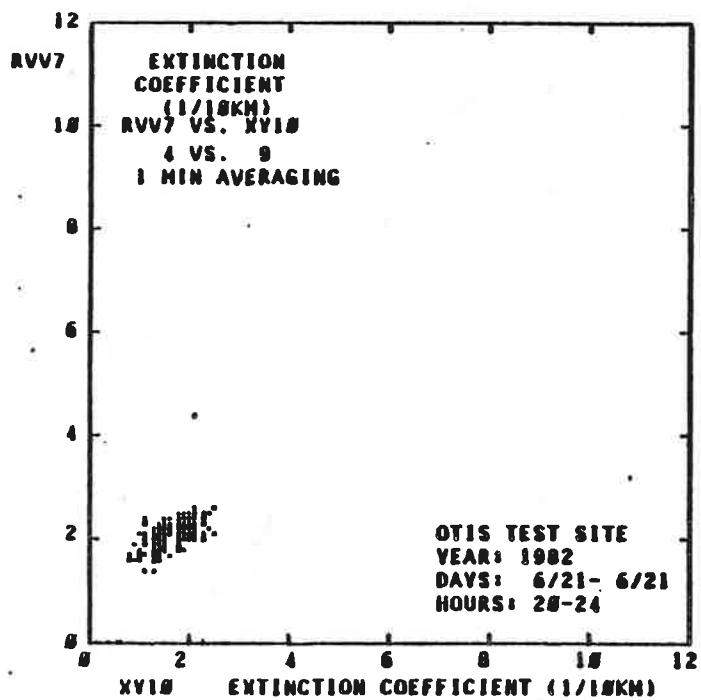

RVV7
EXTINCTION COEFFICIENT (1/10KM)
RVV7 VS. XV10
4 VS. 9
1 MIN AVERAGING
OTIS TEST SITE
YEAR: 1982
DAYS: 6/21- 6/21
HOURS: 20-24
XV10 EXTINCTION COEFFICIENT (1/10KM)
0
2
4
6
8
10
12

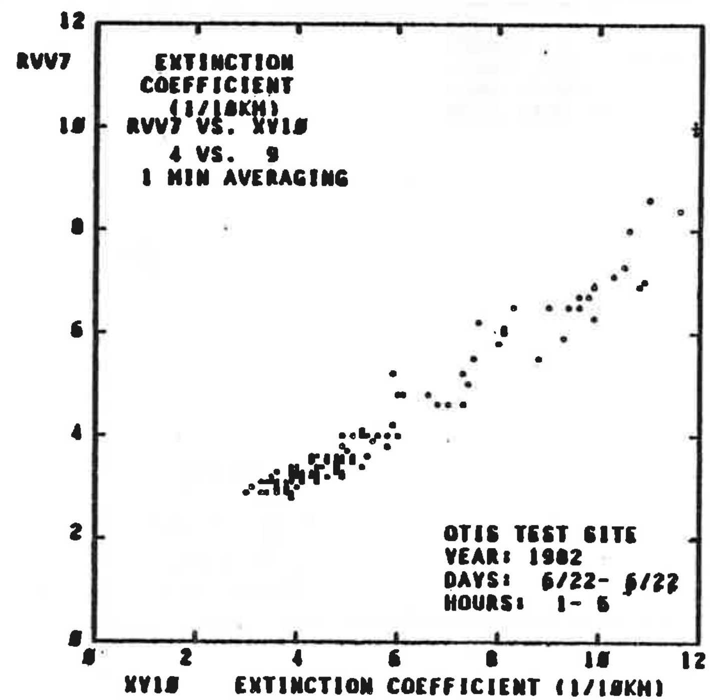

RVV7
EXTINCTION COEFFICIENT (1/10KM)
RVV7 VS. XV10
4 VS. 9
1 MIN AVERAGING
OTIS TEST SITE
YEAR: 1982
DAYS: 6/22- 6/22
HOURS: 1- 6
XV10 EXTINCTION COEFFICIENT (1/10KM)
0
2
4
6
8
10
12

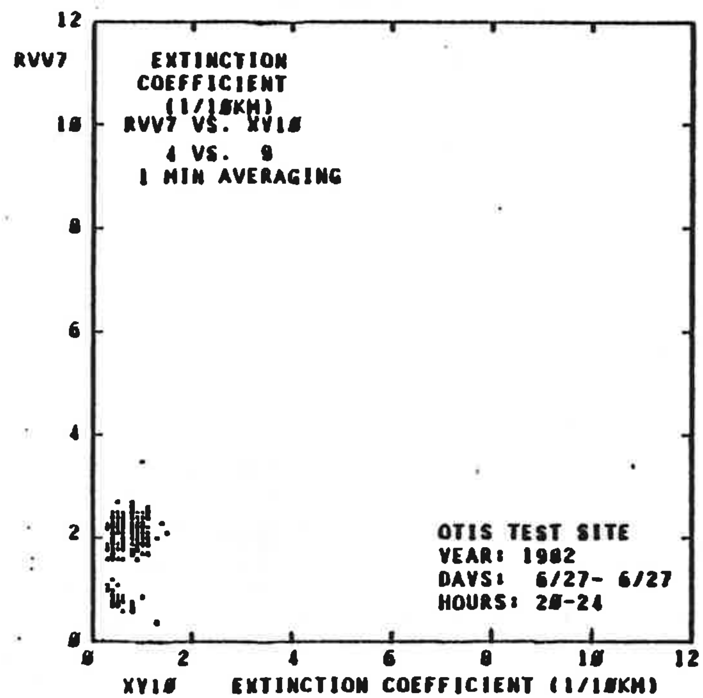

RVV7
EXTINCTION COEFFICIENT (1/10KM)
RVV7 VS. XV10
4 VS. 9
1 MIN AVERAGING
OTIS TEST SITE
YEAR: 1982
DAYS: 6/27- 6/27
HOURS: 20-24
XV10 EXTINCTION COEFFICIENT (1/10KM)
0 2 4 6 8 10 12

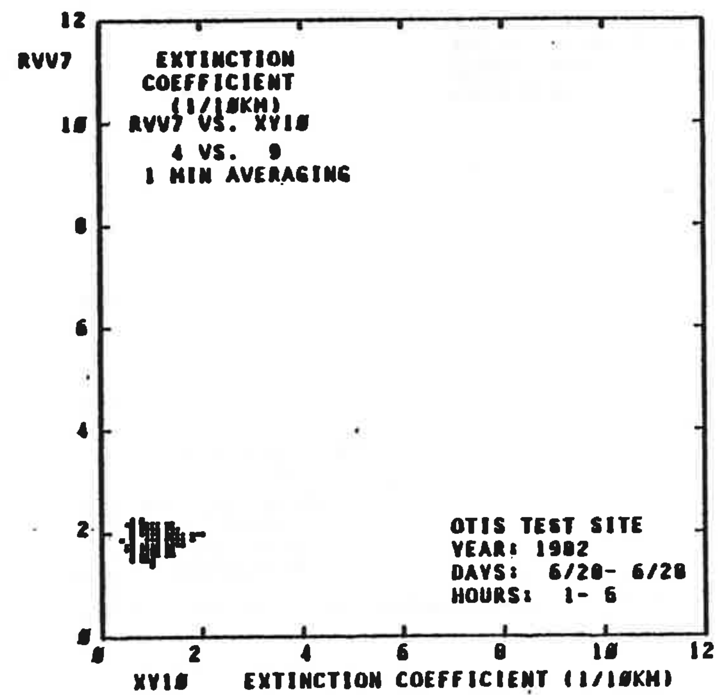

RVV7
EXTINCTION COEFFICIENT (1/10KM)
RVV7 VS. XV10
4 VS. 9
1 MIN AVERAGING
OTIS TEST SITE
YEAR: 1982
DAYS: 6/28- 6/28
HOURS: 1- 6
XV10 EXTINCTION COEFFICIENT (1/10KM)
0 2 4 6 8 10 12

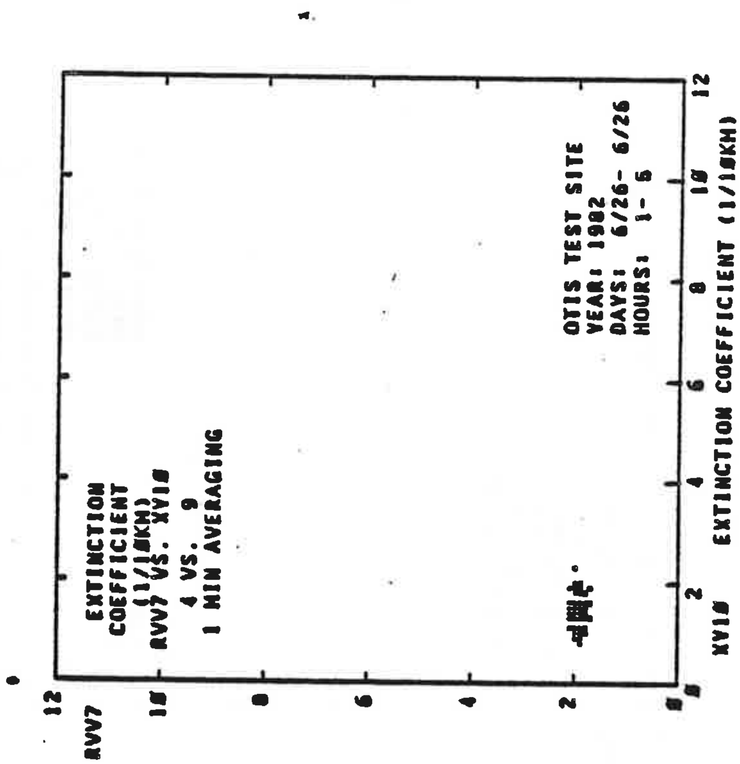
RVV7
EXTINCTION
COEFFICIENT
(1/10KM)
RVV7 VS. XV10
4 VS. 9
1 MIN AVERAGING
OTIS TEST SITE
YEAR: 1982
DAYS: 6/26- 6/26
HOURS: 1- 6
XV10 EXTINCTION COEFFICIENT (1/10KM)
0
2
4
6
8
10
12

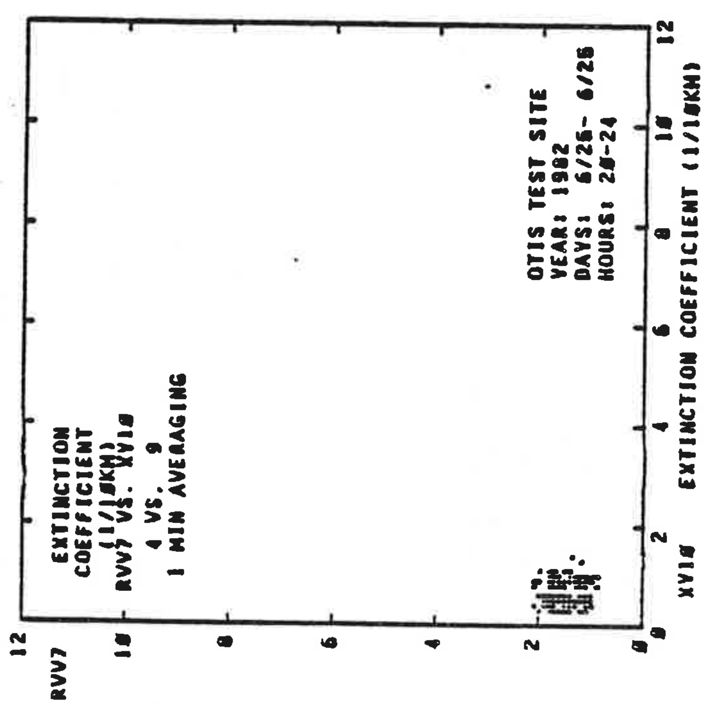
RVV7
EXTINCTION
COEFFICIENT
(1/10KM)
RVV7 VS. XV10
4 VS. 9
1 MIN AVERAGING
OTIS TEST SITE
YEAR: 1982
DAYS: 6/25- 6/25
HOURS: 20-24
XV10 EXTINCTION COEFFICIENT (1/10KM)
0
2
4
6
8
10
12

APPENDIX E

EFFECT OF FORWARD-SCATTERED LIGHT ON TRANSMISSOMETER MEASUREMENTS

David C. Burnham

1. INTRODUCTION

Middleton (Ref. 1) calculates the error introduced by single scattering into the measurements of a transmissometer. The geometry of his calculation is shown in Figure E-1. On page 178 he evaluates the direct light received from the projector:

$$E_a = (I_o/b^2)e^{-\sigma b} \qquad (1)$$

and the scattered light accepted by the receiver

$$E_2 = E_a \sigma b K \qquad (2)$$

$$K = 2\pi \int_o^{\Psi} \int_o^{1/(1 + \psi \cot \Theta)} \frac{\psi \beta(\phi) \, d x \, d \psi}{(1-x)^2 + \psi^2 x^2} \qquad (3)$$

Equations 2 and 3 have been rearranged by the substitutions $\beta' = \beta\sigma$ and $x = r/b$ to isolate the geometric integral given by K which depends only upon the receiver maximum half cone angle Ψ, the projector maximum half cone angle Θ, and the dependence of the scattering function $\beta(\phi)$ upon the scattering angle ϕ which is given by

$$\sin\phi = \psi/[(1-x)^2 + \psi^2 x^2]^{1/2}$$

It should be noted that as long as Ψ, Θ and $\beta(\phi)$ are fixed, the effect of the forward-scatter error is fixed by the constant K. The scattering coefficient $\beta(\phi)$ depends upon the droplet-size distribution but not the number of droplets. Larger drops produce scattering that is more strongly peaked in the forward direction. The integral of $\beta(\phi)$ is fixed by the relationship

$$2\pi \int_o^{\pi} \beta(\phi) \sin\phi \, d\phi = 1$$

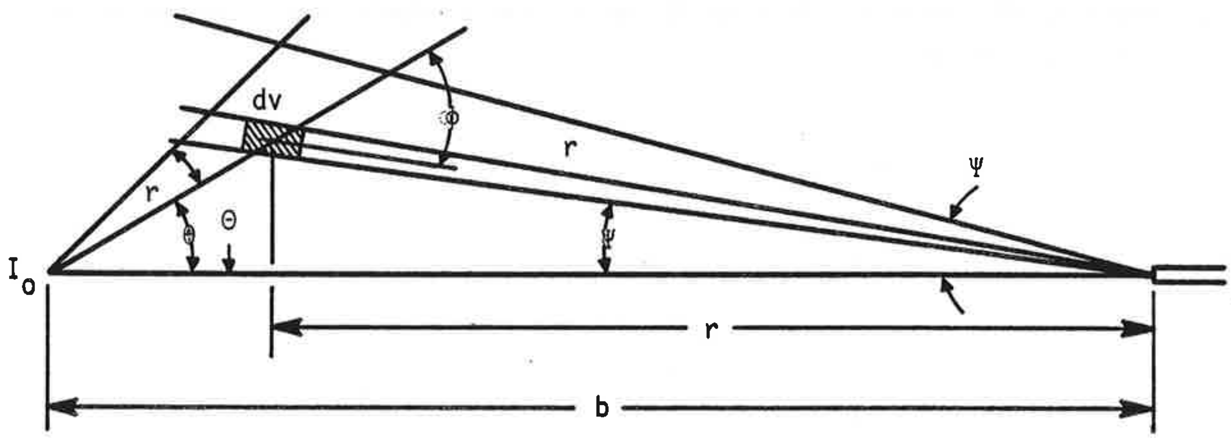

FIGURE E-1. GEOMETRY FOR THE CALCULATION OF THE TRANSMISSOMETER SCATTERING CORRECTION.

The effect of the forward-scatter error E_2 on the measured extinction coefficient can be determined by examining Equations 1 and 2. The correct transmittance is given by

$$T = E_a/(I_o/b^2) = e^{-\sigma b} \quad (6)$$

The measured transmittance is given by the expression

$$T_m = T(1 + K\sigma b) = e^{-\sigma_m b} \quad (7)$$

Equations 6 and 7 can be combined to yield the error in the measured transmittance:

$$\sigma_m - \sigma = -[\ell n(1 + K\sigma b)]/b \cong -K\sigma(1 - \frac{1}{2} K\sigma b) \quad (8)$$

where the last approximation assumes that the accepted light $(K\sigma b)$ is less than the direct light. The resulting fractional error in extinction coefficient becomes

$$\Delta\sigma/\sigma = (\sigma - \sigma_m)/\sigma \cong K(1 - \frac{1}{2} K\sigma b) \quad (9)$$

which is approximately the constant K until $\Delta\sigma b$ approaches one or T approaches $e^{-(1/K)}$.

2. TRANSMISSOMETER ESTIMATE

The integral in Equation 3 can be carried out under the assumption that Ψ and Θ are such small angles that $\beta(\phi)$ can be considered constant and equal to $\beta(o)$. The maximum accepted scattering angle is $\Theta + \Psi$. Under these assumptions $(1 - x)^2$ is much larger than $\psi^2 x^2$ and $\cot\Theta \cong 1/\Theta$. The resulting value for K is:

$$K = 2\pi\,\beta(o)\Theta\Psi \quad . \quad (10)$$

The forward-scatter error is proportional to the product of the projector half angle Θ and the receiver half angle Ψ. The estimate of Equation 10 is an upper limit since $\beta(\phi)$ generally decreases with ϕ and will reduce the integral below Equation 10 when a significant decrease occurs within the angle $\Psi + \Theta$. Since Ψ is generally much smaller than Θ for practical transmissometers, it is the projector that determines the applicability of Equation 10.

The simple approximation described here can be used to analyze the forward-scatter measurements reported by Douglas and Booker (Ref. 2, pp. 5-19 to 5-36). They used a 500-foot baseline tranmissometer. The results are analyzed in Table E-1. The projector lamp had a half angular spread of about $2^o \times 4^o$ which corresponds to a value of θ of approximately 0.05 radians. The receiver half angle ψ is 6.2 milliradians. The results for transmittances below 0.1 show a value for $\beta(o)$ which varies slowly with extinction coefficient. The Douglas and Booker values for other values of in Table E-2 are in rough agreement with the proportionality predicted by Equation 10. Thus Equation 10 appears to be a convenient estimate of forward-scatter errors even though its assumptions may not be completely valid and its range of validity is exceeded in Table E-1 ($\Delta\sigma$ b > 1).

3. LASER RVR CALIBRATOR

The FAA laser RVR calibrator is a tranmsissometer with a very narrow projector beam and a wider receiver beam. The calculation of the forward-scatter error is therefore somewhat simpler than that for the conventional transmissometer discussed in sections 1 and 2.

Figure E-2 shows the geometry of the RVR calibrator. At the normal operating distances (b) the laser beam diameter is much smaller than the diameter D of the receiver collecting optics. As in Section 1, the calculation will estimate the single-scattering contribution to the light accepted by the receiver.

Depending upon the position z of the scatterer in the laser beam, two

TABLE E-1. ANALYSIS OF FORWARD-SCATTER MEASUREMENTS

TRANSMITTANCE	σb	$\Delta\sigma/\sigma$	$\Delta\sigma b$	$\beta(o) \cong \Delta\sigma/\sigma\Theta\ \Psi\ 2\pi$
0.5	0.69	.054	0.04	28
0.1	2.30	.090	0.21	46
0.01	4.61	.107	0.55	55
0.001	6.91	.120	0.83	62
0.0001	9.21	.144	1.33	74

Ψ = 6.2 milliradians

TABLE E-2. ANALYSIS OF FORWARD-SCATTER MEASUREMENTS TO DETERMINE $\beta(o)$

	$\beta(o)$	$\beta(o)$	$\beta(o)$	$\beta(o)$
Ψ (milliradians)	1.2	1.8	2.5	3.7
T = 0.5	32	28	26	29
T = 0.1	53	44	41	52
T = 0.01	66	58	57	60
T = 0.001	85	74	70	71
T = 0.0001	117	101	92	90

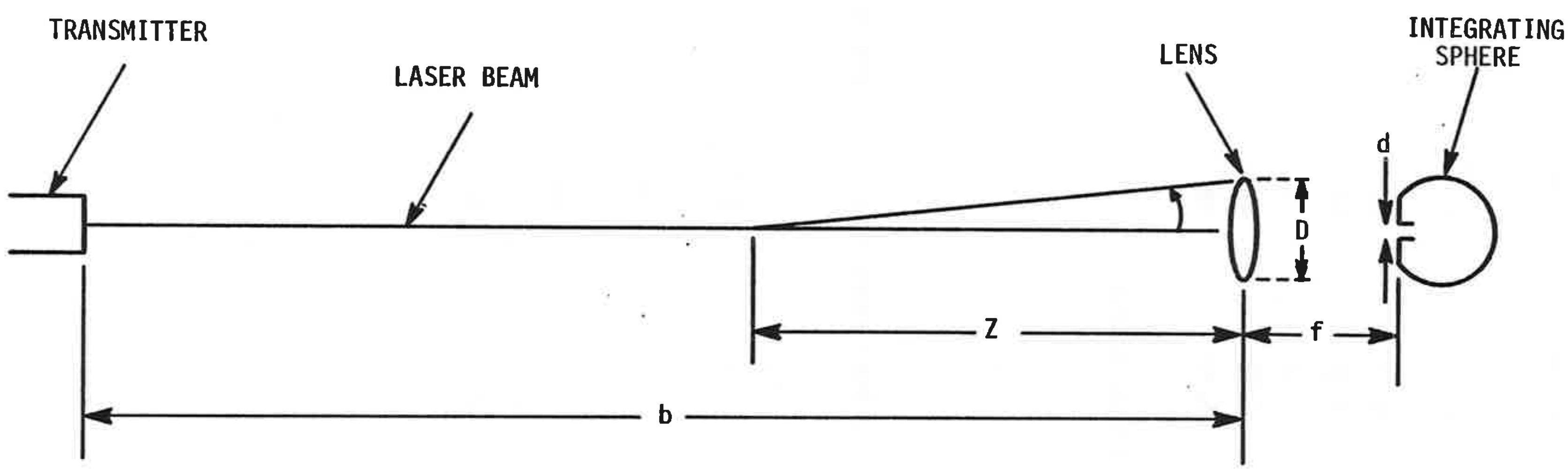

DEFINITIONS: b = BASELINE
Z = DISTANCE FROM RECEIVER
ϕ = SCATTERING ANGLE
D = RECEIVER LENS DIAMETER
f = RECEIVER LENS FOCAL BENGTH
d = INTEGRATING SPHERE APERTURE DIAMETER
α = d/2f = HALF ANGLE RESPONSE OF RECEIVER

FIGURE 2. RVR CALIBRATOR GEOMETRY

different limits are placed on the amount of scattered light collected by the receiver. For scattering near the receiver the solid angle accepted is limited by the receiver angular response (solid angle $\Delta\Omega = \pi\alpha^2$). Far from the receiver the solid angle is limited by the lens size ($\Delta\Omega = \pi D^2/4z^2$). The transition between the two limits takes place at the distance ($z = D/2\alpha$) where the two solid angles are equal. As in Section 2 the assumption is made that the volume scattering coefficient $\beta'(\phi)$ is constant $\beta(o)$ over the scattering angles of interest (i.e. up to α). The amount of scattered light collected from an increment dz is then given by

$$dF_s = F(z)e^{-\sigma z} \Delta\Omega\beta'(o)dz \tag{11}$$

where F(z) is the beam flux at point z and $e^{-\sigma z}$ represents the attenuation of the scattered light. The flux F(z) is also attenuated and is given by:

$$F(z) = F_o e^{-\sigma(b-z)} \tag{12}$$

The expression for the total amount of scattered light collected is obtained by integrating Equation 11:

$$F_s/F_o \doteq \beta'(o)e^{-\sigma b}\left[\int_o^{D/2\alpha} \pi\alpha^2 dz + \int_{D/2\alpha}^{b} (\pi D^2/4z^2)dz\right] \tag{13}$$

$$= Kb\sigma \tag{14}$$

$$K = \pi(D/b)\beta(o)(\alpha - D/4b) \quad \text{for } b > D/2\alpha \tag{15}$$

$$K = \pi\beta(o)\alpha^2 \qquad \text{for } b \leq D/2\alpha \tag{16}$$

This result is in the same form as Equations 2 and 3. Consequently the effects of the forward-scatter error are those shown in Equations 8 and 9. The geometrical constant K is approximately the fractional error in the extinction coefficient measurement.

The forward-scatter error can be evaluated using the constants of the RVR calibrator: f = 256mm, d = 2.38 mm, α = 0.0046 radians and D = 0.34 feet. The limiting baseline between the two parts of Equation 15 is $D/2 = 37$ feet. The value of $\beta(o)$ is taken to be 50 on the basis of the measurements in Section 2. The resulting forward-scatter errors are shown in Table E-3 for three values of the transmissometer baseline. These errors are much smaller (factor of 30) than those generally observed for standard transmissometers with the angular field of view corresponding to the selected baseline (see Ref. 2).

This lower estimate of forward-scatter error in the RVR calibrator could be somewhat in error if the assumption of constant $\beta(\phi)$ is not correct. The transmissometer measurements used to define $\beta(o)$ accepted scattering angles up to 0.05 radians while the RVR calibrator accepts scattering only up to $\alpha = 0.005$ radians. The upper limit to this error would be the ratio of these two angles or a factor of 10. This limit would only be achieved if $\beta(\phi)$ dropped to zero above $\phi = 0.005$ radians, which is impossible physically. Thus the conclusion still holds that the RVR calibrator has much less forward-scatter error than the transmissometer and could therefore be used to measure the forward-scatter error of a transmissometer.

TABLE E-3. RVR CALIBRATOR FORWARD-SCATTER ERROR

BASELINE (feet)	D/4b	K
500	0.00017	.00047
250	0.00034	.00091
40	0.0021	.0033

4. REFERENCES

1. Middleton, W.E.K., Vision Through The Atmosphere, University of Toronto Press, Toronto, Ontario, 1952.

2. Douglas, C.S., and Booker, R.L., "Visual Range: Concepts, Instrumental Determination, and Aviation Applications," Report No. FAA-RD-77-8, 1977.

APPENDIX F

RAIN RESPONSE OF FORWARD-SCATTER VISIBILITY SENSORS

Paper presented at the Fifth Symposium on Meterological Observation and Instrumentation, April 11-15, 1983, in Toronto, Ontario, Canada, sponsored by the American Meteorological Society.

RAIN RESPONSE OF FORWARD-SCATTER VISIBILITY SENSORS

Dr. David C. Burnham
U.S. Department of Transportation
Transportation Systems Center
Cambridge, Massachusetts

1. INTRODUCTION

A usable forward-scatter visibility sensor (EG&G Model 207) was developed by the Air Force Geophysics Laboratory (AFGL) (Muench et al., 1974) and has been used in a research environment for the last decode. The goal of the work reported here was to assess the suitability of forward-scatter sensors for operational use at airports.

Forward-scatter visibility sensors are attactive as a replacement for transmissometers for a number of practical reasons: lower cost, simpler installation, less maintenance, and greater dynamic range. The practical advantages of forward-scatter sensors are obtained at the expense of two measurement limitations. First, the point measurement of a forward-scatter sensor gives a somewhat less representative measurement of visibility than the line average measured by a transmissometer. Second, the response of a forward-scatter sensor may depend upon the obstruction to vision. This second limitation is the subject of this paper.

In order for a visibility sensor based on scattered light to be successful, the amount of scattered light detected must have a consistent relationship to the extinction coefficient produced by the total amount of scattering. The concept of a forward-scatter sensor is based on the observation that the scattering in the range of 20 to 50 degrees is proportional to the extinction coefficient for many types of fogs with different particle size distributions (Waldram, 1945). The usefulness of a forward-scatter sensor for obstructions to vision other than fog (e.g., rain, snow or haze) depends upon whether the same proportionality is observed. Field measurements showed that, for the same extinction coefficient measured by a transmissiometer, the response of forward-scatter sensors to "pure" (i.e., fogless) rain was significantly greater than the response to fog.

2. FIELD MEASUREMENTS

The anomalous response of forward-scatter sensors was first noted in an examination of 69 selected reduced visibility events provided by AFGL from their Otis Air National Guard Base Weather Test Facility. The extinction coefficients measured by EG&G 207 forward-scatter sensors and a 164-meter baseline transmissometer were compared using a least-square fit method. A linear least-square fit yields three parameters which can be used to characterize the event and the relative sensor response. The form of the fit is

$$\sigma_1 = K\sigma_2 + D \qquad (1)$$

where σ_1 is the extinction coefficient measured by the test sensor (in this case the EG&G 207) and σ_2 is the extinction coefficient measured by the standard sensor (in this case the transmissometer). The constants K and D are the slope and offset respectively of the fit. Perfect agreement between the sensors corresonds to K = 1 and D = 0. The third parameter resulting from the fit is the residual error in σ_1 that is not explained by the fit. The most useful form for expressing this error is as the root-mean-square error divided by the mean value of σ_1, which will be termed the fractional residual standard deviation (RSD). Both intrinsic sensor noise and the natural variation in the extinction coefficent contribute to the fractional RSD.

Transmissometers and forward-scatter meters make different error contributions to the two parameters of the fit, K and D. The transmissometer has no significant errors in slope K but can have significant errors in D which correspond to errors in the 100-percent transmission setting. On the other hand, forward-scatter sensors have small errors in D but can have significant errors in K because of instrumental errors such as lamp intensity changes and, in the present study, because of differing responses to different obstructions to vision.

An examination of the slopes K between a forward-scatter sensor and a transmissometer for the 69 AFGL events showed a number of cases where the slope was larger than 1.3, which is significantly greater than the nominal value of 1.0. When those events with large fractional RSD were eliminated, all the remaining high slope events occurred during rain according to the Otis surface observations.

Once the anomalous rain behavior had been noted, events could be selected to identify the maximum value of the anomaly. The maximum slope should occur for rain uncontaminated by fog. Three criteria were developed to identify "pure" fogless rain:

1) Absence of vertical variation in extinction coefficient as measured by sensors mounted at different levels on a tower,
2) Relative humidity less than 100 percent, and

3) Consistency of the anomalous forward-scatter response.

Pure rain events with a significant extinction coefficent are rare. One will be presented in this report and several others were identified during the course of the study.

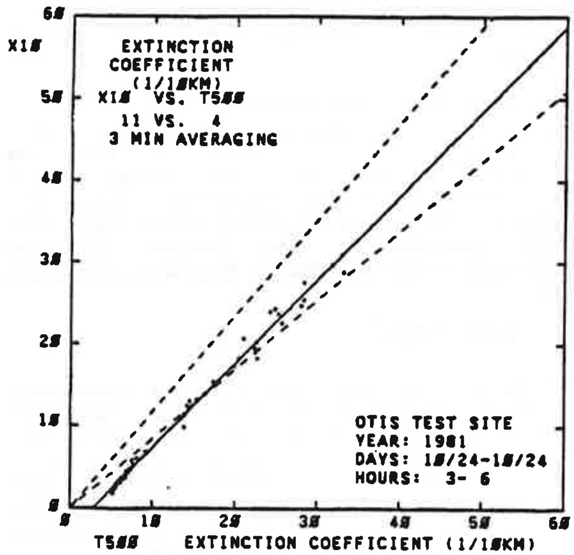

Fig. 1. Comparison of forward-scatter sensor measurements with transmissiometer measurements in fog.

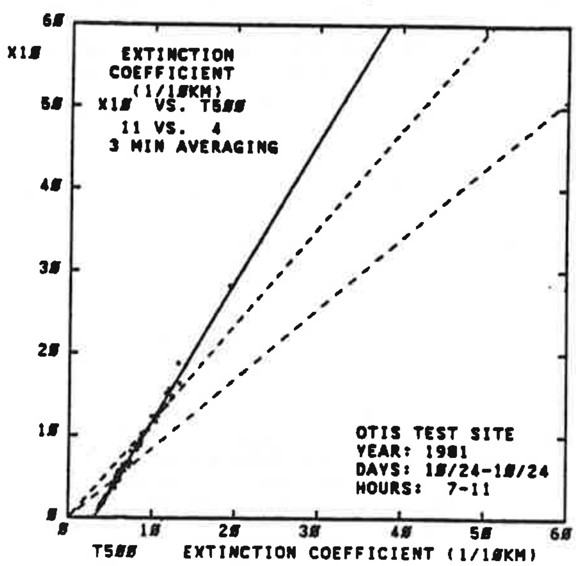

Fig. 2. Comparison of forward-scatter sensor measurements with transmissiometer measurements in pure rain.

Table 1. Least-Square Fits for Fog and Rain Events.

EVENT	SLOPE K	OFFSET D (1/10km)	FRACTIONAL RSD
FOG	1.03	-2.9	0.08
RAIN	1.70	-5.2	0.08

The rain event presented in this report was preceeded by a fog event which allowed a direct comparison of the rain and fog response with no possibility of instrument drift. Figure 1 shows a scatter plot comparing the response of an EG&G 207 sensor ("X10") to the response of the transmissometer ("T500") for a fog event. The X10 sensor was located near the center of the transmissometer baseline. The dashed lines in the figure represent disagreements between the two sensors of ±15 percent. The solid line is the least-square fit. The parameters of the fit are shown in Table 1. Figure 2 shows the same plot for the rain event which followed the fog event of Figure 1. All times are GMT. The X-axis offset is the same for both figures and corresponds to a transmissometer 100-percent setting of 96 percent. The fractional RSD is small enough for both events that the slope measurement is meaningful. The relative response of the forward-scatter sensor to rain and fog is given by the ratio of the slopes for the two events. The observed rain/fog response factor is 1.7 for these events. The other pure rain events showed similar factors.

Figures 1 and 2 show that, in fact, the rain response of a forward-scatter sensor is better defined than the fog response. In Figure 1 the fog response shows evidence for a change in slope at low extinction coefficient (high visibility) while the rain response in Figure 2 shows a consistent slope. This difference is not surprising since the angular distribution of scattered light from rain drops is probably independent of drop size and rain rate. On the other hand, the angular distribution can be expected to be different for haze than for fog. The break in the curve of Figure 1 occurs at approximately 4/10km, which corresponds to a meteorological optical range of 7 km.

3. THEORETICAL DISCUSSION

The observed difference in the rain response of transmissometers and forward-scatter sensors can be understood on the basis of a simple theoretical analysis which predicts a factor of two difference in the response. The scattering of light from spherical water drops is produced by two effects which contribute equally to the extinction of a light beam. The first effect is the direct scattering of light which hits the drop; the resulting scattered light appears at all scattering angles. The second effect is caused by diffraction of the shadow of the drop; the resulting scattered light appears only in the forward direction. The forward diffraction scattering remains undetected by a forward-scatter sensor in both fog and rain. The transmissometer, however, collects little of the forward-scattered light from fog but collects virtually all the forward-scattered light from rain. The relative response of the two sensors can therefore be expected to differ by a factor of two between fog and rain. The transmissometer measured only half the total extinction during rain. The transmissometer value is, in fact, correct since the angular resolution of the human eye also accepts virtually all the light forward-scattered by rain. This argument assumes that the angular distribution of light scattered by hitting the droplet is independent of droplet size for the scattering angles accepted by the forward-scatter sensor. The fact that the observed anomaly is somewhat less than a factor of two could be due to two effects: The fraction of direct scattered light accepted may be greater for fog droplets than for rain drops. Some of the diffraction scattering from fog may actually be accepted.

The previous discussion can be made more quantative. The shadow diffraction scattering from a disk is given (Jenkins et al., 1957) by the expressions:

$$I(\theta) = 4I_o\,(J_1(\beta)/\beta)^2 \qquad (2)$$
$$\beta = \pi\theta d/\lambda \qquad (3)$$

where λ is the wavelength, d is the diameter of the disk, θ is the scattering angle, I_o is the intensity at zero angle and J_1 is the Bessel function of first order. Equation 2 describes the familiar ring diffraction pattern of which has its first zero at $\beta = 3.83$. The central disk contains 84 percent of the total scattered energy. If one integrates Equation 2 to the point where half of the total intensity is included, one obtains the value $\beta_h = 1.69$. The half angle for the half response becomes

$$\theta_h = 0.533\,\lambda/d. \qquad (4)$$

The half angle field of view used with various transmissometer baselines is listed in Table 2. Equation 4 is used to calculate the half response droplet size.

$$d_h = 0.533\,\lambda/\theta_h \qquad (5)$$

The transmissometer will collect more than half the diffraction scattered light from droplets larger than d_h in diameter. These droplet sizes represent drizzle rather than rain.

Table 2. Transmissometer Rain Drop Response

BASELINE (ft)	HALF ANGLE FIELD OF VIEW (mrad)	HALF RESPONSE DROPLET SIZE (mm)
250	2.2	0.15
500	1.2	0.27
750	0.9	0.36
HUMAN EYE 20/40		1.0

The next question to be examined is how well the response of the transmissomter correlates with that of the human eye. Normal 20/20 daytime vision represents a resolution equivalent to that of a 2-mm aperture (Sliney et al., 1980). The angular width of lines resolved by 20/20 vision is one arc-minute. Thus the angular resolution of the eye is roughly equivalent to viewing objects with perfect resolution through a rain with 2-mm drop size. If the drop size is 1 mm, the visual acuity would be reduced to roughly 20/40. Since, for example, typical runway numerals can be read at 2.5 miles with 20/40 vision, forward scattering from rain drops larger than 1 mm would not appear to interfere with daytime aviation needs. The resolution of the eye is poorer at night than during the daytime. As long as a light source is smaller than 2.5 arc-minutes, the eye responds to it as if it were a point source (Middleton, 1952). Consequently, forward scattering from rain drops larger than about 1 mm can be expected to have little affect on night visibility.

Transmissometer measurements can thus be expected to correlate well with human vision during rain. Table 2 shows that there are drizzle conditions where the transmissometer will overestimate the visibility, e.g., for droplet sizes between 0.15 and 1.0 mm for a 250-foot baseline. The longest baseline transmissiometer correlates best with the human eye.

4. CONCLUSIONS

Transmissometers are shown to give a measurement of extinction coefficient in rain that correlates well with the response of the human eye. Forward-scatter sensors which are calibrated for fog are observed to measure abnormaly high extinction coefficients in pure rain. The operational impact of the forward-scatter sensor errors is mitigated by several factors:

1) Pure rain with significant reductions in visibility is a rare phenomenon.

2) The error is in the conservative direction in that the actual visibility will be higher than measured.

3) For many aircraft the presence of rain on the cockpit windows will tend to reduce the pilot's effective visibility.

5. REFERENCES

Jenkins, F.A., and H.E. White, 1957: Fundamentals of Optics, 3rd ed. McGraw-Hill, 637 pp.

Middleton, W. E. K., 1952: Vision Through the Atmosphere. University of Toronto Press, 250 pp.

Muench, H.S., E.Y. Moroz, and L.P. Jacobs, 1974: Development and Calibration of the forward scatter visibility Meter, Instr. Paper No. 271, AFCRL, March 1974, 37 pp.

Sliney, D., and Wolbarsht, 1980: Safety with Lasers and Other Optical Sources. Plenum Press, 1035 pp.

Waldram, J.M., 1945: Measurement of the photometric properties of the upper atmosphere. Quarterly Journal of the Royal Meteorological Society, 71, 319-336.

U.S. Department
of Transportation

**Research and
Special Programs
Administration**

Kendall Square
Cambridge, Massachusetts 02142

Postage and Fees Paid
Research and Special
Programs Administration
DOT 513

U.S. MAIL

Official Business
Penalty for Private Use $300